THE UNIVERSITY OF QUEENSLAND

AUSTRALIA

Stratigraphic architecture of Lopingian (upper Permian) strata in the Galilee Basin, NE Australia.

Laura Jayne Phillips

BSc. (Hons.) MRes.

A thesis submitted for the degree of Doctor of Philosophy at

The University of Queensland in 2017

School of Earth and Environmental Sciences

Abstract

This study reviewed the stratigraphic framework of the Koburra Trough, Galilee Basin and proposed a modified stratigraphy of the Betts Creek beds based on regional correlation of coal and interburden facies character observed in wireline log signatures, core and chip descriptions. The new stratigraphy was tested through radiogenic isotope dating of tuffs and palynology. This new framework provides the foundation for a regional palaeo-environmental model, coupled with an investigation of sediment provenance through U-Pb analysis of detrital zircons and their implications for the tectonic setting of the Galilee Basin.

Through the regional correlations of 76 public domain and 1205 proprietary geophysical wireline logs complemented by core descriptions, a series of regional coal seam correlations were developed. Using the C seam, with a distinctive tuffaceous character, as a marker horizon, the Lopingian coal seam architecture was established. The C seam is overlain by the B and A seams that merge to the north and diverge to the south above a coarsening upward sequence correlative to the Black Alley Shale. This architecture is similar to the splitting of the Fort Cooper Coal Measures into the Burngrove and Fair Hill formations in the neighbouring Bowen Basin. The C seam is underlain by three seams, D, E and F, that exhibit complex splitting patterns reflecting compensational stacking of interburden strata and coals. These form the 'Colinlea Sandstone equivalent' that, to the south, transition to the Peawaddy Formation and Catherine Sandstone. The combination of these formations elevates the Betts Creek beds to group status. From east to west the Betts Creek Group incorporates units of coal seams known as the Crossmore and Glenaras sequences. However, these seams were only found local to the Hulton-Rand Structure, and do not have an equivalent in the Koburra Trough. They were renamed the 'J and K' seams, and removed from the Betts Creek Group.

Chemical Abrasion-Isotope Dilution Thermal Ionization Mass Spectrometry (CA-IDTIMS) and palynological techniques were used to corroborate the proposed correlations. Tuffs within the C coal seams yielded zircon U-Pb dates of 254.31±0.10, 254.41±0.07 and 255.13±0.09 Ma, which are equivalent with a Lopingian date obtained from the Black Alley Shale on the Springsure Shelf, 254.08±0.06 Ma. The correspondence suggests that the C seam is an equivalent to a seam of the Fair Hill Formation in the Bowen Basin and a landward lateral equivalent of the Black Alley Shale, rather than the upper section of the 'Colinlea Sandstone equivalent'. A tuff date from the top of the B coal seam (252.81±0.07 Ma) correlates with published dates of the Yarrabee Tuff in the Bowen

Basin. This places the B seam as an equivalent to the Burngrove Formation and the overlying A seam, the only coal seam within the Bandanna Formation.

The age of the 'J and K' seams were determined with palynology and found to contain the biozone APP3.2 index species, *Praecolpatites sinuosus*, placing them in the late Cisuralian – early Guadalupian, rather than the Lopingian as previously interpreted, but above the Aramac Coal Measures. This older age has implications for understanding the mid-Permian hiatus in the Galilee Basin. With the occurrence of the APP3.2 biozone in the basin, the lacuna has decreased from 30 My to a maximum of 12-13 My, similar to the adjacent Bowen and Cooper basins, suggesting that all three basins were affected by mid-Permian tectonism.

Detailed sedimentary logging of four key wells located in the Galilee Basin provides insight into regional palaeo-environmental reconstructions. The decreases in coal seam thickness and pattern of increased splitting toward the south have been attributed to foreland loading in the Bowen Basin. The 'Colinlea Sandstone equivalent' is characterised by cyclic fluvial successions and lacustrine environments, especially toward the centre of the Koburra Trough. One large marine transgression (Black Alley Shale) is recognised in the Galilee Basin splitting the two coal-bearing sequences. This transgression is recognised on the Springsure Shelf and southern Koburra Trough, the latter of which is the northern maximum extent of the transgression. The overlying regression is represented by laterally extensive peat-forming delta plains that are characteristic of the Bandanna Formation.

Analysis of 286 concordant U-Pb ages obtained from detrital zircons was conducted as part of an investigation into the provenance of sediment in the Galilee Basin. Cisuralian samples displayed a polymodal distribution of detrital zircon U-Pb ages, with multiple peaks between 300-2000 Ma, while Lopingian samples had much more restricted detrital zircon ages of 250-320 Ma and a minor but consistent population of 1500-1600 Ma. These results suggest that the provenance of Cisuralian sediment in the Galilee Basin was a number of different sources including the nearby craton and volcanic arc, supporting an extensional tectonic setting for the basin. In contrast, the Lopingian provenance was mainly the New England Orogen, suggesting a migration to a platform basin that was combined with the adjacent retro-foreland Bowen Basin.

Declaration by author

This thesis is composed of my original work, and contains no material previously published or written by another person except where due reference has been made in the text. I have clearly stated the contribution by others to jointly-authored works that I have included in my thesis.

I have clearly stated the contribution of others to my thesis as a whole, including statistical assistance, survey design, data analysis, significant technical procedures, professional editorial advice, and any other original research work used or reported in my thesis. The content of my thesis is the result of work I have carried out since the commencement of my research higher degree candidature and does not include a substantial part of work that has been submitted to qualify for the award of any other degree or diploma in any university or other tertiary institution. I have clearly stated which parts of my thesis, if any, have been submitted to qualify for another award.

I acknowledge that an electronic copy of my thesis must be lodged with the University Library and, subject to the policy and procedures of The University of Queensland, the thesis be made available for research and study in accordance with the Copyright Act 1968 unless a period of embargo has been approved by the Dean of the Graduate School.

I acknowledge that copyright of all material contained in my thesis resides with the copyright holder(s) of that material. Where appropriate I have obtained copyright permission from the copyright holder to reproduce material in this thesis.

Publications during candidature

Peer-reviewed papers

PHILLIPS, L. J., ESTERLE, J. S. and EDWARDS, S. A., 2017, Review of Lopingian (upper Permian) stratigraphy of the Galilee Basin, Queensland, Australia, Australian Journal of Earth Sciences, 64 (3), 283-300. DOI: 10.1080/08120099.2017.1290684

PHILLIPS, L. J, EDWARDS, S. A., BIANCHI, V. and ESTERLE, J. S., 2017, Palaeo-environmental reconstruction of Lopingian (upper Permian) sediments in the Galilee Basin, Queensland, Australia. Australian Journal of Earth Sciences, 64 (5), 587-609. DOI: 10.1080/08120099.2017.1338618

PHILLIPS, L. J., CROWLEY, J., MANTLE, D., ESTERLE, J., NICOLL, R., McKELLAR, J. and WHEELER, A., In Press, U-Pb geochronology and palynology from Lopingian (upper Permian) coal measure strata of the Galilee Basin, Queensland, Australia. Australian Journal of Earth Sciences.

Conference papers

PHILLIPS, L.J., ESTERLE, J. and SLIWA, R., 2015, Rationalising coal seam stratigraphy within the Koburra Trough, Galilee Basin IN: BEESTON, J. W. (Editor): Bowen Basin Symposium 2015 – Bowen Basin and Beyond. Geological Survey of Australia Inc. Coal Geology Group and the Bowen Basin Geologists Group, Brisbane, October, 2015, 219-226

BODORKOS, S., CROWLEY, J., HOLMES, E., LAURIE, J., MANTLE, D., MCKELLAR, J., MORY, A., NICOLL, R., PHILLIPS, L., SMITH, T., STEPHENSON, M. and WOOD, G., 2016, New dates for Permian palynostratigraphic biozones in the Sydney, Gunnedah, Bowen, Galilee and Canning basins, Australia. Permophiles, 19 - 21.

Conference abstracts

PHILLIPS, L. J., ROSLIN, A. and ESTERLE J., 2014, Vertical trends in maceral composition in inertinite-rich coals: A case study from the Galilee Basin, The Society of Organic Petrology 2014, Sydney.

PHILLIPS, L.J., BIANCHI, V. and ESTERLE, J., 2016, Sedimentary trends in Late Permian Coal Measure Strata, Galilee Basin, Australian Earth Sciences Convention 2017, Adelaide.

PHILLIPS, L.J., VERDEL, C., ALLEN, C. and ESTERLE, J., 2017, Detrital zircon analysis from the Galilee Basin, Queensland, Australasian Exploration Geoscience Conference 2018, Sydney.

Publications included in this thesis

PHILLIPS, L. J., ESTERLE, J. and EDWARDS, S., 2017, Review of Lopingian (upper Permian) stratigraphy of the Galilee Basin, Queensland, Australia, Australian Journal of Earth Sciences, 64 (3), 283-300. DOI: 10.1080/08120099.2017.1290684

- incorporated as Chapter 2.

Contributor	Statement of contribution
Laura Phillips (Candidate)	Compiled well data (100%) Correlated well data (100%) Interpreted well data (100%) Wrote the manuscript (100%)
Joan Esterle	Reviewed and edited the manuscript (60%)
Sally Edwards	Reviewed and edited the manuscript (40%)

PHILLIPS, L. J., CROWLEY, J., MANTLE, D., ESTERLE, J., NICOLL, R., McKELLAR, J. and WHEELER, A., In Press, U-Pb geochronology and palynology from Lopingian (upper Permian) coal measure strata of the Galilee Basin, Queensland, Australia. Australian Journal of Earth Sciences.

- incorporated as Chapter 3.

Contributor	Statement of contribution
Laura Phillips (Candidate)	Selected samples for analysis (100%) Assisted with the geochronological analysis (20%) Wrote the manuscript (excluding the methodology) (100%)
Jim Crowley	Conducted the geochronological analysis (80%) Wrote methodology section on LA-ICPMS and CA-IDTIMS (100%) Reviewed and edited the manuscript (21%)
Daniel Mantle	Conducted the palynological analysis (100%) Wrote the palynology methods section (100%) Reviewed and edited the manuscript (21%)

Joan Esterle	Reviewed and edited the manuscript (21%)
Robert Nicoll	Reviewed and edited the manuscript (16%)
John McKellar	Reviewed and edited the manuscript (16%)
Alexander Wheeler	Reviewed and edited the manuscript (5%)

PHILLIPS, L. J., EDWARDS, S., BIANCHI, V. & ESTERLE, J., 2017, Palaeo-environmental reconstruction of Lopingian (upper Permian) sediments in the Galilee Basin, Queensland, Australia. Australian Journal of Earth Sciences. 64 (5), 587-609. DOI: 10.1080/08120099.2017.1338618

- incorporated as Chapter 4.

Contributor	Statement of contribution
Laura Phillips (Candidate)	Sedimentary logging of cores (85%) Interpretation of data (70%) Wrote the manuscript (100%)
Sally Edwards	Assisted with core logging (5%) Advised data interpretation (10%) Reviewed and edited the manuscript (40%)
Valeria Bianchi	Assisted with core logging (5%) Advised data interpretation (10%) Reviewed and edited the manuscript (35%)
Joan Esterle	Assisted with core logging (5%) Advised data interpretation (10%) Reviewed and edited the manuscript (25%)

Contributions by others to the thesis

In addition to my co-authors (outlined in previous sections), the following people have contributed to this thesis:

Professor Joan Esterle (principal supervisor), advised, commented and edited draft versions of this thesis. Professor Esterle obtained funding from the Australian Coal Association Research Program (ACARP) and the Vale-UQ Coal Geoscience Program which was used to cover research costs.

Dr. Charles Verdel (associate supervisor), advised, commented and edited draft versions of this thesis.

Dr. Jim Crowley performed and assisted with Chemical Abrasion Isotope Dilution Thermal Ionisation Mass Spectrometry (CA-IDTIMS) analyses presented in Chapter 3. Dr. Crowley wrote the LA-ICPMS and CA-IDTIMS methodology section. While the integration and interpretation was conducted by the candidate, Dr. Crowley assisted with editorial comments on the discussion.

Dr. Daniel Mantle performed the palynological methods and assisted with its interpretation presented in Chapter 3. Dr. Mantle wrote the palynology methodology section. While the integration and interpretation was conducted by the candidate, Dr. Mantle assisted with editorial comments on the discussion.

Dr. Charlotte Allen assisted with the Laser Ablation Inductively Coupled Mass Spectrometry (LA-ICPMS) analyses and subsequent data reduction presented in Chapter 5. While the integration and interpretation was conducted by the candidate, Dr. Allen assisted with editorial comments on the discussion.

Statement of parts of the thesis submitted to qualify for the award of another degree

None.

Acknowledgements

I would like to express my upmost appreciation to my principal supervisor Professor Joan Esterle who helped guide me through the past few years. Discussions with Joan were always fruitful and without her input and support, this project would not have been possible.

Dr Charles Verdel is acknowledged for his continuing support as my associate supervisor. I wish to thank my RHD committee, Professor Greg Webb, Dr Renate Sliwa and Dr Fengde Zhou, for their guidance during my candidature. In particular Renate, who was ever willing to provide her in-depth understanding towards any questions I may have.

My gratitude goes to many colleagues who have assisted with this project in various ways: Dr Robert 'Uncle Bob' Nicoll from Geoscience Australia, Dr Charlotte Allen from QUT, Dr Jim Crowley from Boise State University, Dr Dan Mantle from MGPalaeo and Sally Edwards and Dr John McKellar from GSQ.

I would like to thank the Australian Coal Association Research Program (ACARP) and the Vale-UQ Coal Geoscience Program for their continued financial support of this project. I would also like to acknowledge the Australian Academy of Science and the Australian Geoscience Council for their offer of the inaugural 34th International Geological Congress (IGC) travel grant which funded travel to Boise State University to learn state-of-the-art geochronological techniques. The University of Queensland is thanked for their financial support in the form of their international tuition fee scholarship.

Acknowledgements are extended to the companies and people within them who provided invaluable data towards this project. I am thankful for their contribution and their helpful discussions on their data.

My UQ coal colleagues and PhD peers are thanked for their on-going encouragement, motivation and for the many laughs we shared.

Last, but definitely not least, I would like to thank my family for their unwavering and long distance support from the UK and Glen for his continuing reassurance that rocks are 'cool'.

Keywords

Galilee Basin, Lopingian, stratigraphy, Betts Creek Group, Colinlea Sandstone, Bandanna Formation, Fort Cooper Coal Measures, geochronology, sedimentology, tectonics

Australian and New Zealand Standard Research Classifications (ANZSRC)

ANZSRC code: 040311, Stratigraphy, 40%
ANZSRC code: 040303, Geochronology, 30%
ANZSRC code: 040310, Sedimentology, 30%

Fields of Research (FoR) Classification

FoR code: 0403, Geology, 100%

Table of contents

List of Figures

List of Tables

List of Abbreviations used in the thesis

A – abundant

AAS – Australian Academy of Science

ACARP – Australian Coal Association Research Program

AGC – Australian Geoscience Council

API – American Petroleum Institute (units)

BAS – Black Alley Shale

BF – Bandanna Formation

BG – Burngrove Formation

'BFe' – 'Burngrove Formation equivalent'

BMR – Bureau of Mineral Resources

BR – Barcaldine Ridge

C – common

CA-IDTIMS – chemical abrasion-isotope dilution thermal ionization mass spectrometry

CL – cathodoluminescence

CSG – coal seam gas

F – frequent

FCCM – Fort Cooper Coal Measures

FCCMe – 'Fort Cooper Coal Measures equivalent'

FH – Fair Hill Formation

'FHFe' – 'Fair Hill Formation equivalent'

g/cm^3 – grams per cubic centimetre

GSQ – Geological Survey of Queensland

HBO- Hunter-Bowen Orogeny

HFSE – high field strength elements

HRS – Hulton-Rand Structure

IGC – International Geological Congress

KT – Koburra Trough

LA-ICPMS – laser ablation inductively coupled plasma mass spectrometry

LD – Lovelle Depression

MSWD – mean square of the weighted deviates

NIST – National Institute of Standards and Technology

P – present

PD – Powell Depression

QLD - Queensland

QUT – Queensland University of Technology

R – rare

REE – rare earth elements

SHRIMP – sensitive high resolution ion microprobe mass spectrometry

VR – very rare

1. Introduction

1.1. Overview

The coal and coal seam gas (CSG) exploration boom in the last decade led to a proliferation of drilling in the Galilee Basin, providing an opportunity to revisit the stratigraphy and sedimentology of this frontier basin. The Galilee Basin (Figure 1) is estimated to contain 2,208 M tonnes of thermal quality coal (Mutton, 2003), although mining has not yet commenced. It is surprising how well previous correlations have held based on sparse geophysical wireline log datasets, poor outcrops and biostratigraphy (Allen and Fielding, 2007b; Scott et al., 1995). With the proliferation of new datasets and advancement in dating techniques, an opportunity arose to test these correlations, as well as interpretations of age, tectonic setting, sedimentary provenance and depositional environment for the coal measures.

The stratigraphy of a sedimentary basin forms the framework in which to examine the lateral and vertical relationships between strata, which communicate a variety of stories, from depositional to tectonic setting of the basin. Different stratigraphic techniques (e.g. chrono-, bio- and sequence stratigraphy) combine to produce an integrated picture of basin development. Coal seams and tuffs can often be correlated over hundreds of kilometres and therefore provide a reliable tool in stratigraphic framework studies (e.g. Ayaz et al., 2015; Brakel, 1989; Esterle and Sliwa, 2002; Staines and Koppe, 1979; Warwick, 2005). Radiogenic isotope dating has been applied to test these correlations between basins in eastern Australian, as well as globally (Ayaz et al., 2016a; Nicoll et al., 2015, 2016a), and absolute dating combined with palynology is rapidly developing to recalibrate the Permian coal-bearing basins in eastern Australia (Bodorkos et al., 2016; Laurie et al., 2016; Metcalfe et al., 2015). However, using geochronological techniques alone can result in misleading correlations (Draper et al., 1997; McKay et al., 2015) and a more integrated approach is favourable.

Utilising public domain and proprietary drilling data in the Koburra Trough, this thesis examined the current stratigraphic framework of the Galilee Basin and its application, which prompted a revision based on coal seam correlations and interburden character. The project determined a consistent litho-stratigraphic framework for Lopingian (late Permian) strata that was tested through bio- and chrono-stratigraphic techniques. The resulting framework was used to interpret regional variation in depositional environments and to understand the provenance of sediment within the basin. This holistic approach towards establishing and testing stratigraphic frameworks has been

used in previous stratigraphic studies of sedimentary basins, e.g. The Karoo Basin, South Africa (e.g. Isbell et al., 2008; Rubridge et al., 2013; Smith, 1990; Ward et al., 2005), Parana Basin, Brazil (e.g. Guerra-Sommer et al., 2005; Holz et al., 2010; Horn et al., 2014), Bowen Basin, Australia (e.g. Ayaz, 2016; Esterle and Sliwa, 2002; Laurie et al, 2016; Sliwa et al., 2017) and is a useful methodology to follow for economic emergent basins, such as the Galilee Basin, where previous research is minimal (e.g. Allen and Fielding, 2007a, 2007b; Gray and Swarbrick, 1975; McKellar and Henderson, 2013; Mollan et al., 1969; Scott and Hawkins, 1992; Van Heeswijck, 2006, 2010; Vine et al., 1964, 1965).

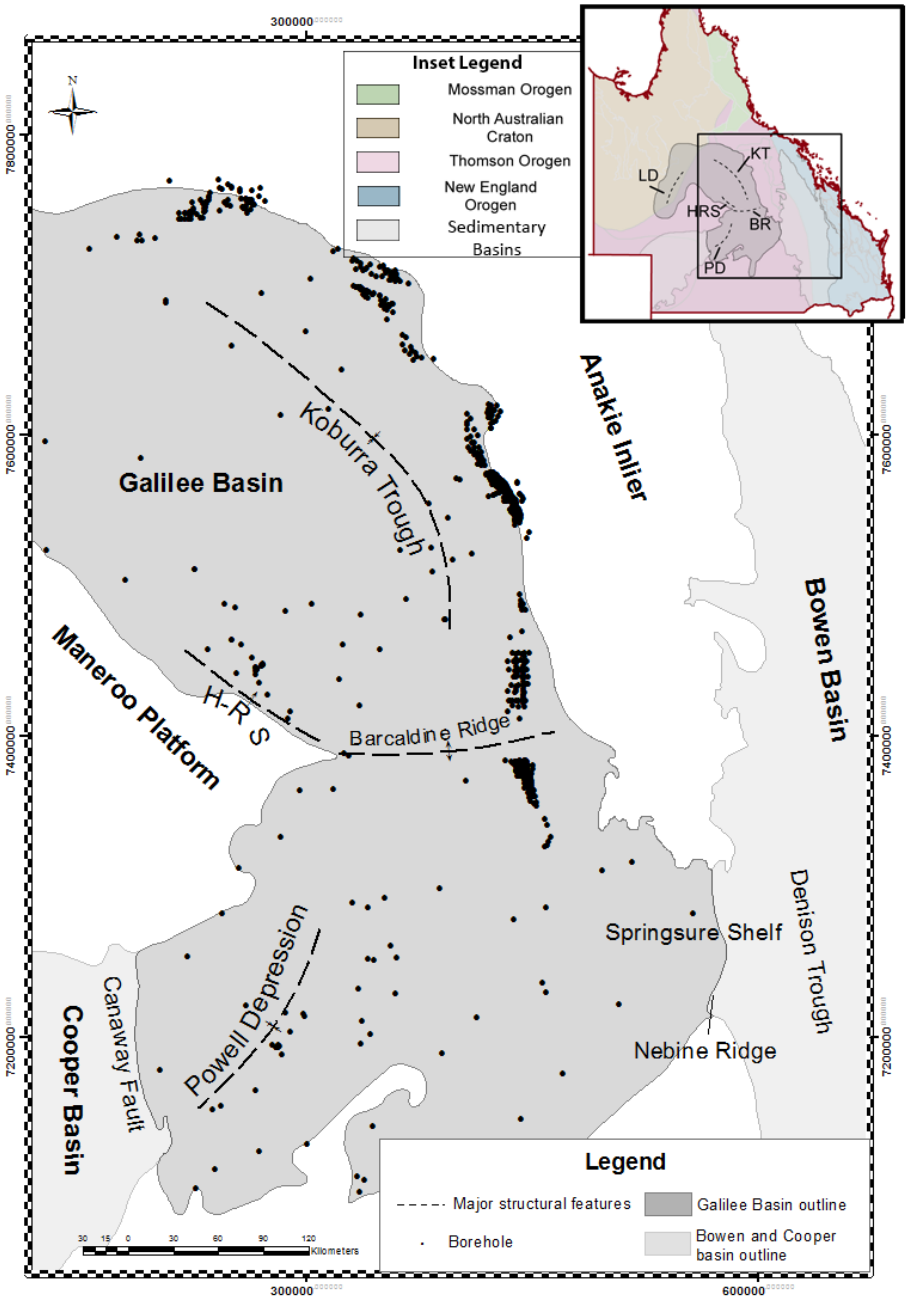

Figure 1: Map showing the location of the Galilee, Cooper and Bowen basins. Major structural trends are shown on the main map and inset map. Boreholes available for use in this study are shown. Abbreviations: KT – Koburra Trough, BR – Barcaldine Ridge, PD – Powell Depression, HRS – Hulton-Rand Structure and LD – Lovelle Depression.

1.2. Tectonic and Geological Setting

The Mississippian(?) – Pennsylvanian (mid to late Carboniferous) to late Middle Triassic Galilee Basin covers an area of 247,000 km^2 of central Queensland. It forms part of a larger Carboniferous – Triassic coal basin system located along the present day eastern margin of Australia (Figure 1). The Cooper Basin is situated to the west of the Galilee Basin, separated by the Canaway Fault, while the Springsure Shelf to the south-east provides the link between the Galilee and Bowen basins. The Galilee Basin contains three major depocentres, the Powell Depression, the Lovelle Depression and the Koburra Trough (Figure 1), in which stratigraphic thicknesses are up to 1700 m, 730 m and 2800 m, respectively (Geoscience Australia, 2016b). A large proportion of CSG exploration has concentrated in what is generally described as an east-dipping monocline. This structure is known as the Hulton-Rand Structure, and it is situated to the west of the Koburra Trough and abutting the Maneroo Platform, a crystalline basement high (Figure 1). The Galilee Basin shallowly sub-crops under minimal Cenozoic cover to the east and gently dips to the west into the Koburra Trough. Along the basin's eastern margin, the coal mining industry has taken advantage of the shallow coal seams with a flurry of exploration in recent years (Figure 1). The study area for this thesis focuses on the eastern margin of the Galilee Basin and extends westward into the Koburra Trough and the Hulton-Rand Structure. The north-eastern margin provides the northern extent of the study area, while the Springsure Shelf is the southern margin.

The general consensus for the tectonic setting of the basin is that it is an intracratonic basin (Allen and Fielding, 2007a, 2007b; Van Heeswijck, 2006) that infilled with a mix of siliclastics, coal, diamictite and tuffaceous mudstone that are time correlatives of the adjacent Bowen Basin, which, in contrast, is generally regarded as a retro-arc foreland basin (Korsch and Totterdell, 2009a). Lopingian strata in the Bowen Basin can be over 1000 m in thickness, and their correlatives in the Galilee Basin are ~200 m-thick. This condensed sequence of Lopingian coal measures in the Galilee Basin is interpreted as a result of sedimentation in a low accommodation setting (Allen and Fielding, 2007b). de Caritat and Braun (1992) suggested that the Galilee Basin was a platform basin during the Lopingian that formed in response to foreland loading in the eastern Bowen Basin. Low accommodation in the Galilee Basin was due to a decrease in subsidence rates westerly from the main thrust belt.

Tectonically eastern Australia can be split into five Palaeozoic to early Mesozoic orogenic belts collectively referred to as the Tasmanides (Glen, 2005). The sedimentary Galilee Basin is situated within the Thomson Orogen but its depositional history occurred simultaneous to the New England

Orogen to its east (inset, Figure 1). The Thomson Orogen is largely covered by thick sedimentary basins and outcrops of its basement are sparse. As a result, the geological history of the orogen is poorly understood. To the north east of the Thomson Orogen the North Australian Craton is located and to the north is the Mossman Orogen. The Thomson Orogen is split from the New England Orogen to its east by the sedimentary Bowen-Gunnedah-Sydney basin complex (inset Figure 1).

The initiation of Galilee Basin is thought to have occurred in the mid to late Carboniferous, as a result of increasing crustal convergence (Figure 2), potentially as a far field expression of the Kanimblan Orogeny (Olgers 1972; Van Heeswijck 2006, 2010; Veevers et al. 1982; Withnall et al. 1995), the last large-scale deformation event of the Delamerian and Lachlan orogens, both of which are located in New South Wales (Glen 2005; Veevers, 2006). The continental sedimentation that followed the Kanimblan orogeny is representative of a foreland regime (Van Heeswijck, 2006, 2010). Owing to slab roll back and retreat (Figure 2), the convergent margin moved eastwards of the present day margin, away from the Galilee Basin during the Carboniferous and into the Cisuralian (early Permian) (~305 Ma, Holcombe, 2013; Korsch et al., 2009b). Van Heeswijck (2010) interpreted an extensional event (Jericho Event) in the Galilee Basin that occurred at the same time as the slab movement. The new convergent tectonic setting along the east coast of Gondwana during the Permian and Triassic is the New England Orogen (Glen, 2005; Figure 2).

An initial period of extensional rifting (Denison Event ~285 Ma; Korsch et al., 2009c), in the New England Orogen during the Cisuralian saw the formation of half grabens in the Bowen Basin (e.g. Korsch et al., 2009c; Glen, 2005; Figure 2). This was expressed in the Galilee Basin as a period of tectonic dormancy (thermal sag; Van Heeswijck, 2006) where base level rose slowly and allowed the accumulation of widespread peat mires (Aramac Coal Measures) across the western part of the Galilee Basin. The mid-Permian saw the onset of the Hunter-Bowen Orogeny in the New England Orogen. A contractional event in the Bowen Basin (~280 Ma Cattle Creek Event; Korsch et al., 2009c) initiated a large period of sedimentation quiescence (Figure 2). Palynology from the borehole GSQ Springsure 17 (Filatoff and Price, 1991) on the eastern Springsure Shelf (Bowen Basin) suggests continuous deposition throughout the mid-Permian, however interpreted seismic lines from the region suggest a hiatus spanning ~3 to ~10 My occurred (Brakel et al., 2009; Korsch et al., 2009c). In the Galilee Basin, palynology and radiometric dating suggests the Cattle Creek contractional event led to a hiatus that is considered to be up to ~20 - ~30 My (e.g. Evans and Roberts, 1980; Nicoll et al., 2015, 2016a; Vine et al., 1964).

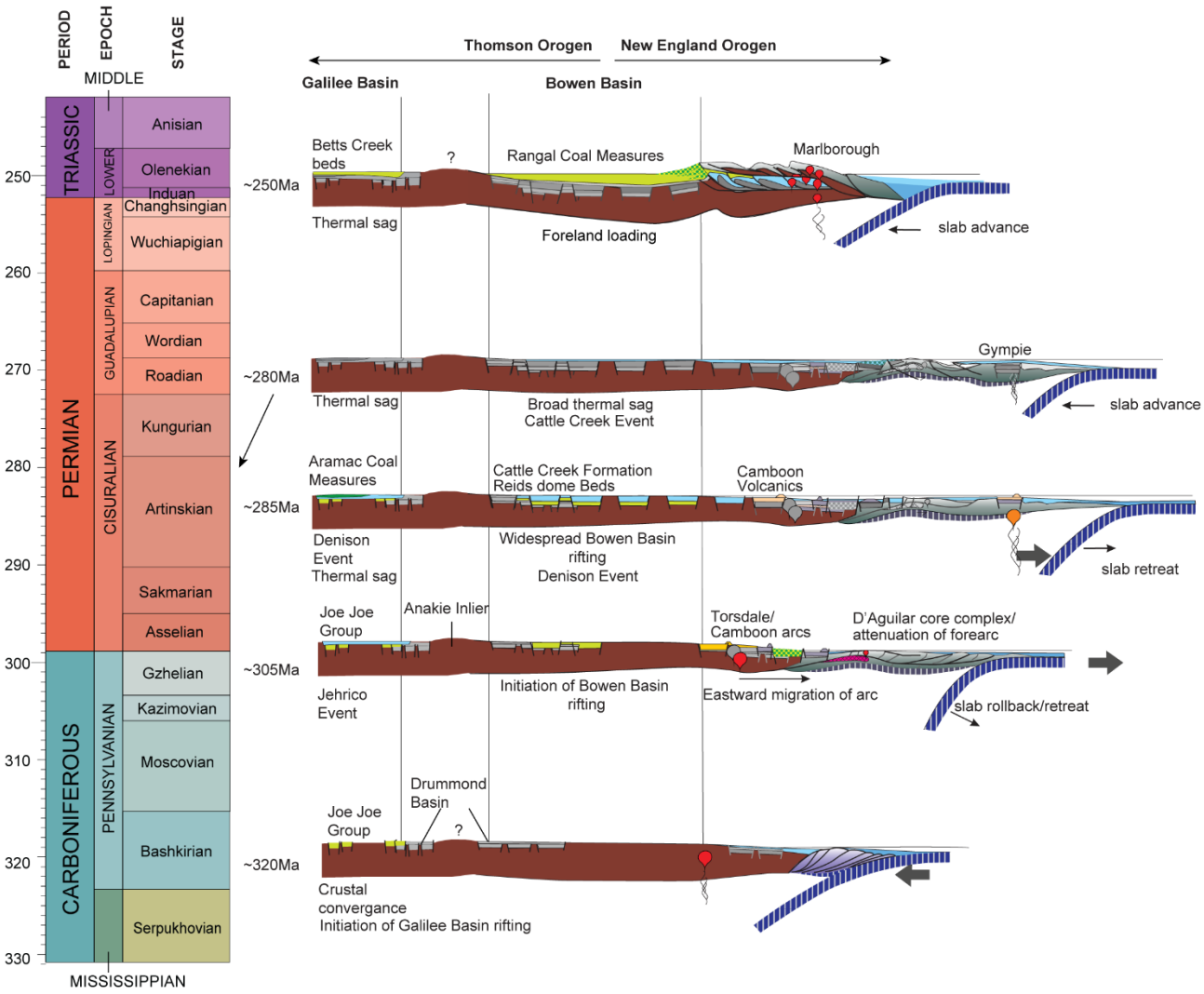

Figure 2: Schematic cross section (courtesy of R. Holcombe) modified after Sliwa et al. (2017) showing the tectonic evolution of the Galilee and Bowen basins during the Pennsylvanian – Lower Triassic. Time scale used is from Gradstein et al. (2012).

Following the hiatus, widespread peat mires developed in the Lopingian (late Permian). The resulting coal measures show merged seams in the north of the Bowen Basin that have increased splitting to the east and south (Ayaz et al., 2015; Esterle and Sliwa, 2002; Sliwa et al., 2017). This has been interpreted as a dynamic foreland loading phase in the Bowen Basin with increased subsidence to its east, towards the convergent margin (Fielding et al., 1993, 2000; Sliwa et al., 2017; Veevers, 2006; Figure 2). The stratigraphic equivalent in the Galilee Basin, the coal bearing Betts Creek beds and equivalents, show a uniform thickness and have been interpreted as a continuation of the thermal subsidence from the Cisuralian to the Lopingian (Van Heeswijck, 2006, 2010). A minor contractional event (Bellata Event; Korsch et al., 2009c) is thought to be the last contractional event in the Permian and represents a short-lived hiatus between the Permian and Triassic. However, the hiatus is not universally observed in sediments across the Galilee and Bowen basins (Brakel et al., 2009; Korsch et al., 2009c; Van Heeswijck 2010). The end of the Hunter-

Bowen Orogeny ended in the late Middle Triassic (contractional Goondiwindi Event; Korsch et al., 2009c), which saw the cessation of sedimentation in both the Galilee and Bowen basins.

1.3. Research objectives, questions and methodology

Although there is a basic understanding of the Galilee Basin, the detailed sedimentary architecture of the coal measures and spatial variation in the interburden strata that will influence the behaviour of the rock mass should these coals be exploited is poorly developed. This is important not only for mining coal, but also forecasting the potential for communication with water or gas resources in the basin (Evans and Hostetler, 2016; Evans et al., 2016). The sedimentary architecture of coal measures is commonly defined by the correlation of coal seams or groups. The coals represent periods where subsidence is in balance with peat growth, the duration of which is reflected in their thickness, areal distribution and splitting patterns. Whereas differential compaction has local to regional influence, subsidence at a basin scale is driven by the tectonics of the basin, coupled with global climatic and eustatic changes. The tectonic events in the Galilee Basin are generally tied with those affecting the adjacent Bowen Basin, but only recently has there been absolute dating of the Cisuralian units (Bodorkos et al., 2016; Nicoll et al., 2015; Nicoll et al., 2016a, 2016b) to test the biostratigraphic age relationships within and between the basins during the extensional development phase of the basins (Korsch and Totterdell, 2009b; Van Heeswijck, 2010). Moreover, there were no absolute dates in the Galilee Basin for the Lopingian that record the onset of foreland loading during the Hunter Bowen Orogeny, thus it remains unclear what affect this had on the basin.

The objective of this thesis is to re-examine the coal measure architecture and implications for palaeo-geography, timing and tectonic setting for the Lopingian age coal measures known as the Betts Creek, in light of recent exploration drilling for coal and coal seam gas. This objective required a firm stratigraphy, supported by regional marker horizons corroborated by high resolution radiogenic isotope dating and palynology. Sediment provenance, which reflects tectonic setting, was evaluated through detrital zircon analysis. The thesis is subdivided into four independent but complementary components. Each component is then subdivided into individual research questions that address the overarching objective of this thesis.

Component 1

Component 1 reviewed the existing stratigraphy and built a consistent stratigraphy that better fits and represents the Lopingian coal measure strata. The current stratigraphy is inconsistently applied as there was no regional correlation study that developed criteria for recognition of seams across the

basin. Regional and mine scale correlation of public and proprietary drilling data was conducted to provide a master framework in which sedimentary variation can be examined. The following research questions were developed for the thesis:

- What is the regional correlation of the coal seams and interburden strata in the Koburra Trough, Galilee Basin?
- Is there a consistent pattern to the coal seam splitting that can help to define areas of higher and lower accommodation?

Component 2

Component 2 tested the stratigraphic correlations, both internally and with the Bowen Basin. Radiogenic isotope dating using Chemical Abrasion-Isotope Dilution Thermal Ionization Mass Spectrometry (CA-IDTIMS) was conducted on zircons obtained from samples of Galilee Basin volcanic ash layers. Palynological analysis also helped to build a robust data set that can be applied to existing, more established biostratigraphic models. The following research questions guided component 2:

- How well are the correlations constrained through tephrochronology and palynology?
- How do the ages of the coal seams relate to the Bowen Basin through tephrochronology and palynology?
- Do the tuffaceous sediments correlate to events recorded in adjacent basins?

Component 3

The tested correlations provided the framework in which to reconstruct palaeo-environments for both siliciclastics and coal. Sedimentological facies analyses of core and petrophysical wireline logs were used to develop a model of palaeo-geographic environments for the Lopingian coal measures. The following research questions guided component 3:

- Do coal seam splitting patterns reflect changes in palaeo-environment in the interburden clastics?
- Do the environments change stratigraphically up section and/or laterally across the basin?
- Are changes in palaeo-environment ‘local’ to the Galilee Basin or correlative to regional changes and events also observed in the Bowen Basin?

Component 4

Understanding the tectonic processes that affect the deposition of strata during the Lopingian is the objective of component 4. Laser Ablation – Inductively Coupled Plasma Mass Spectrometry (LA-ICPMS) was used to obtain ages of detrital zircons from clastic interburden, and these detrital

zircon age populations are relevant to determining the provenance of sediment within the Galilee Basin. The following research questions helped to guide component 4:

- Where are the source areas for the late Permian interburden siliclastics?
- Can the provenance of the interburden help to reconstruct the tectonic setting of the Galilee Basin during the Late Permian?

1.4. Research significance

The Galilee Basin is an understudied basin, but is marked as the 'next frontier' for coal mining in Queensland. This thesis aims to provide a solid foundation for stratigraphy, sedimentology and structure of the Lopingian strata within the basin, known as the Betts Creek Beds. A consistent stratigraphy for the coal measures and clastic interburden across the basin provides a foundation for exploration. It also establishes a context for examining potential variation in the characteristics of Galilee Basin coal, which will impact on the geotechnical behaviour of any future mines, and potential for interaction with groundwater resources. The stratigraphic correlation between the Galilee and Bowen basins is tenuous, and the application of tephrochronology and palynology will support or refute current correlations.

1.5. Research outcome and structure of thesis

This thesis has been produced as a 'thesis with publications', and chapters 2-5 are presented as standalone scientific papers that arose from the above components proposed at the start of the thesis. As a result some repetition may be encountered, especially in background information and figures. The referencing style used in this thesis is APA which has the citations listed in alphabetical order, not chronological.

The first paper, titled "**Review of Lopingian (upper Permian) stratigraphy of the Galilee Basin, Queensland, Australia,**" forms the literature review component of this thesis (chapter 2). This paper collates literature from unpublished governmental reports, mining and coal seam gas reports and peer reviewed journal articles. A combination of open-file and propriety geophysical wireline log data is used to track the continuity of coal seam packages on a regional scale around the Koburra Trough of the Galilee Basin. The reasons behind the differences in regional stratigraphic nomenclature are explored. Paper 1 tested the following hypothesis:

> *H_1. The eastern and southern Bandanna and Colinlea Sandstone coal bearing formations can be correlated to coal seams within the northern Betts Creek beds.*

Through the use of wireline correlations, regional cross sections were drawn across the basin. Coal seams can be correlated from the north to south of the Galilee Basin, across the different nomenclature boundaries. During the construction of regional cross sections through the Galilee Basin and into the Bowen Basin other issues arose: (1) a series of coal seams ('J and K' seams, also known as the Crossmore and Glenaras seams) in the Hulton-Rand Structure (Rodney Creek area) had no lateral equivalents in the Koburra Trough or along the eastern margin; and (2) correlations between the Galilee and Bowen Basins stratigraphy highlighted inconsistences between putatively time-equivalent units.

A modified stratigraphic framework was proposed to remedy these discrepancies. The second paper, **"U-Pb geochronology and palynology from Lopingian (upper Permian) coal measure strata of the Galilee Basin, Queensland, Australia,"** investigates the proposed stratigraphic framework through geochronological and palynological analysis (chapter 3). Paper 2 tested the following hypotheses:

> *H_2. The proposed stratigraphy is correct.*
> *H_3. A Fort Cooper Coal Measures equivalent unit and its subdivisions, the lower Fair Hill Formation and upper Burngrove Formation, previously omitted from the stratigraphy, can be identified in the Galilee Basin strata.*
> *H_4. The western 'J and K' seams are Cisuralian (early Permian) in age, not Lopingian (late Permian) Betts Creek beds as previously cited.*

The use of radiogenic isotope dating technique, CA-IDTIMS, identified important marker horizons that confirmed the stratigraphic framework proposed in paper 1. For the Galilee Basin, the recognition of the Yarrabee Tuff, a significant horizon in the Bowen Basin, established the correct placement of the Fort Cooper Coal Measures equivalent within the stratigraphy. Palynology of the 'J and K' seams confirmed the shift from Lopingian strata to Cisuralian, with more affinity to the Aramac than the Betts Creek Group coal measures.

Using the newly established stratigraphic framework, the depositional environments that formed the coal measures were revisited in the third paper (chapter 4) "**Palaeo-environmental reconstruction of Lopingian (upper Permian) sediments in the Galilee Basin, Queensland, Australia."** Here the following hypotheses are tested:

> *H_5. The Lopingian strata of the Galilee Basin are characterised by a large transgression followed by a regression.*
> *H_6. The transgression was in a northerly direction.*

H_7. Marine environments are restricted to the central and southern parts of the Galilee Basin.

Using detailed sedimentary logging of core from four key wells from across the basin, clear regional variations in depositional environments became apparent. Increased coal seam splitting is observed toward the southern part of the basin, where coals eventually shale into a marine environment. The third paper highlights the importance of correct stratigraphic correlations when reconstructing regional depositional environments.

The fourth paper (chapter 5), **"Detrital zircon geochronology of Permian strata in the Galilee Basin, Queensland, Australia,"** explores the tectonic processes influencing the deposition of strata during the Lopingian in the Galilee Basin and integrates the new stratigraphic framework and palaeo-environmental interpretations described in papers 1, 2 and 3. Paper 4 tested the following hypotheses:

H_8. Detrital zircon populations reflect the differing tectonic setting from the Cisuralian to the Lopingian in the basin.
H_9. The Lopingian detrital zircon population will be characteristic of a passive margin setting with a minor constituent of a population representative of convergent tectonic setting.

By analysing detrital zircon populations from the clastic interburden in one key well from the Galilee Basin, preliminary concepts of the tectonic setting can be understood. Combined with absolute ages presented in paper 2, deposition of the clastic strata within the Galilee Basin showed little to no offset from the age of the detritus. This initial deposition is suggestive of the Galilee Basin being under a much larger sphere of influence from the adjacent retroarc foreland Bowen Basin throughout its development.

The sixth chapter draws together individual findings from the separate papers and presents a comprehensive synthesis for the entire study.

Chapter 2 is published in the Australian Journal of Earth Sciences (2017) as:

2. Review of Lopingian (upper Permian) stratigraphy of the Galilee Basin, Queensland, Australia

L. J. Phillips[1], J. S. Esterle[1] and S. A. Edwards[2]

[1]Department of Earth Sciences, University of Queensland, Qld 4072, Australia

[2]Geological Survey of Queensland, Department of Natural Resources and Mines, Qld 4000, Australia

2.1. Abstract

The recent increase in exploration activity in the Galilee Basin, Queensland, has highlighted inconsistencies in the usage of Lopingian (upper Permian) stratigraphic nomenclature across the basin. This study utilised peer reviewed journal, company and government publications to evaluate the current understanding of the naming conventions in use and correlated them to nomenclature in the adjacent Bowen Basin. The prominent misinterpretation is between the stratigraphic relationship and terminology of the northern and western Betts Creek beds and its eastern and southern correlatives the Bandanna Formation and Colinlea Sandstone. The correlation between the units has been assessed from a (1) lithological (2) sedimentological, and (3) coal seam architectural perspective. The Betts Creek beds appear similar to the Colinlea Sandstone in their lithology and sedimentological character, but increased drilling data suggest the original type-sections no longer fit the heterogeneous lithology of correlated strata bearing that nomenclature. Correlation across the Springsure Shelf into the Bowen Basin suggests that the Betts Creek beds and their subdivisions are in fact equivalent to the Bandanna Formation, the Fort Cooper Coal Measures (the Burngrove and Fair Hill formations) and the Moranbah Coal Measures. A revised stratigraphic column for the Galilee Basin has been proposed to reflect this, and to suggest that a new stratigraphic unit be introduced; the 'Fort Cooper Coal Measures equivalent' and its subdivisions the 'Burngrove and Fair Hill formation equivalents'.

Keywords: stratigraphy, Galilee Basin, Bowen Basin, Lopingian, Betts Creek beds, Bandanna Formation, Peawaddy Formation, Black Alley Shale, Colinlea Sandstone, Fort Cooper Coal Measures

2.2. Introduction

The intracratonic Galilee Basin covers an area of 247 000 km^2, a majority of central Queensland. It contains a Carboniferous to Triassic sedimentary sequence, and its Permian coal measures are currently being explored for their economic potential for coal and coal seam gas. Recent exploration activity in the basin has exponentially increased the availability of drill hole data. With this new data, discrepancies in the presently used stratigraphic nomenclature have been revealed, type-sections and the derived nomenclature can be amalgamated and the current lithostratigraphy can be revised. The focus of this article is on the Lopingian (upper Permian) stratigraphy in the Hulton-Rand Structure, Koburra Trough and Springsure Shelf areas of the Galilee Basin.

The Galilee Basin is part of a larger Carboniferous–Triassic basin system in eastern Australia that encompasses the intracratonic Cooper Basin to its west and the foreland Bowen Basin to its east (Figure 3). Three tectonic events have been recognised in both the Galilee and Bowen basins, albeit at slightly different times. Mechanical extension in the Carboniferous initiated the formation of some major depo-centres in the Galilee Basin such as the Koburra Trough. During the Cisuralian (early Permian) this shifted to a period of thermal subsidence in the Galilee Basin while the Bowen Basin experienced initial mechanical extension. This initial thermal subsidence interval allowed the formation of mires in the basin, now attributed to the Cisuralian (lower Permian) Aramac Coal Measures. The thermal subsidence continued into the Lopingian and Triassic of the Galilee Basin, while the Bowen Basin underwent a short interval of thermal subsidence then prolonged foreland loading until the Middle Triassic (Korsch and Totterdell, 2009b; Van Heeswijck, 2010). Sedimentation in the area between the Cooper and Galilee basins was minimal during the Lopingian as a result of activity along the Canaway Fault, which bounds the Canaway Ridge separating the two basins. The Springsure Shelf at the northern end of the Nebine Ridge connects the Bowen and Galilee basins, and allowed continuous sedimentation between both basins, enabling them to have an interlinked stratigraphy and tectonic history. Given the foreland setting of the Bowen Basin, volcanoclastic input into the basin is greater than that of the Galilee Basin (Fielding et al., 2000). The Lopingian strata of the Galilee Basin are preserved across much of the basin, and the thickest stratigraphic sections are in the Koburra Trough, which runs centrally in the north east of the basin, parallel to the eastern margin (Figure 3). Much of the Galilee Basin is overlain by the Upper Triassic–Cretaceous Eromanga Basin, with Lopingian strata only subcropping along the eastern margin, in northern drainage systems, and on the Springsure Shelf. With only limited outcrops, many type-sections have been derived from small isolated pockets in the northern and southern parts of the basin.

The aims of this paper are fivefold: (1) to clarify the lithostratigraphic and coal seam nomenclature of Lopingian strata in the Galilee Basin (Figures 4 and 5), (2) to present cross sections that intersect nomenclature boundaries to establish stratigraphic correlations between them (Figures 7 and 8), (3) to clarify the stratigraphic relationship between the Betts Creek beds, the Bandanna Formation and the Colinlea Sandstone, (4) to summarise stratigraphic relations of Lopingian age formations in the adjacent Bowen Basin, and (5) to summarise the implications of a revised stratigraphy.

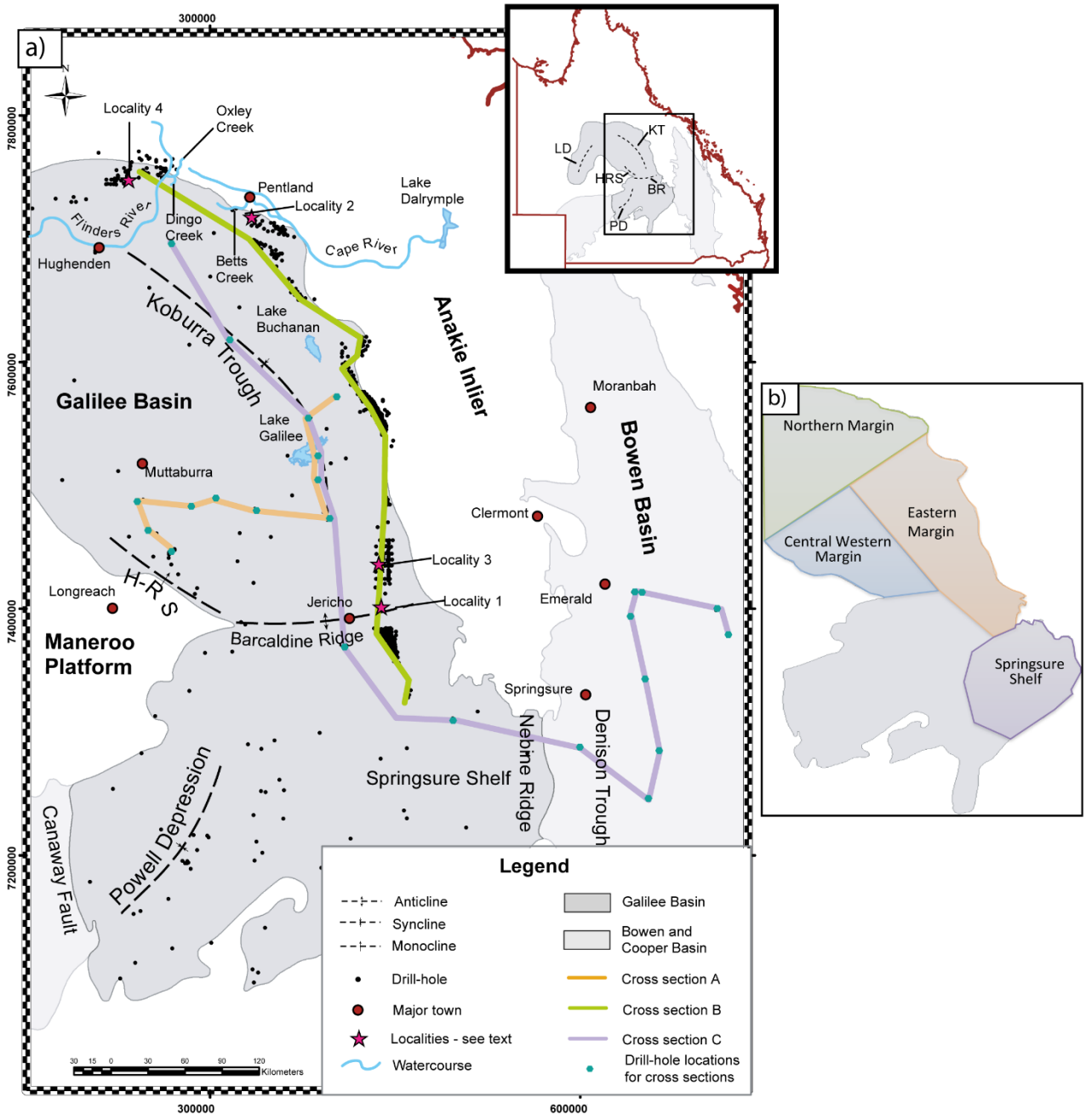

Figure 3: a) Map of the Galilee and Bowen basins, showing major structural features and borehole locations. Cross sections shown and locations mentioned in this study are also marked. Key structural features for the Galilee Basin are shown in the inset map. Abbreviations: LD, Lovelle Depression; KT, Koburra Trough; HRS, Hulton-Rand Structure; BR, Barcaldine Ridge; and PD, Powell Depression. b) Areas referred to in this study.

2.3. Development of stratigraphic nomenclature

The strata of the Galilee Basin were first documented for the Geological Survey of Queensland (GSQ) by Rands (1891). This was only by chance, because Rands was prospecting for gold. While studying the Desert Sandstone (stratigraphic nomenclature now obsolete) in the Betts Creek area (Figure 3), approximately 20 km south west of Pentland, Rands identified a bed of shale containing *Glossopteris* leaves. He did not name this bed, but commented that the presence of the *Glossopteris* leaves in the Desert Sandstone was unusual, because the formation was thought to be Cretaceous, thereby falsely placing *Glossopteris* vegetation in the late Mesozoic era (Figure 4).

Marks (1911) revisited the site reported by Rands (1891), and noted what appeared to be a conformable contact between conglomerate and underlying *Glossopteris*-rich shale beds. Marks agreed with a previous observation by Maitland (1898) of a conglomerate at the base of the Desert Sandstone, and he postulated that this shared similar lithological characteristics with the conglomerate bed above the *Glossopteris*-rich shale and was therefore correlative. Thus the *Glossopteris*-rich beds underlying the conglomerate were older than Rands (1891) had hypothesised, and Marks placed them in the Lower Cretaceous or Jurassic Blythesdale Braystone (Figure 4).

Reid (1916) re-examined the outcrops visited by Rands (1891) and Marks (1911). He noted that strata found within the Betts Creek area were a series of alternating conglomerate, sandstone, clay and coaly shale. The first mention of volcanic activity during the time of deposition was made by Reid (1916), who identified a pink tuffaceous sandstone within the beds. Reid saw a resemblance between the abundant ‘soapy’ shales at Betts Creek and those within the Upper Coal Measures (Carne, 1908) of Newcastle (New South Wales). Reid (1916) was the first to speculate that the beds located in Betts Creek were of Permian age, and he named the unit the Betts Creek Series (Figure 4). The search for coal measures was expanded from the Betts Creek locality, and Reid (1918) reported on coal measures 68 km west-north-west of Pentland at Oxley and Dingo creeks (Figure 3). Two coal seams intersected by shafts at Dingo Creek and found in outcrop in Oxley Creek were confirmed by the presence of Vertebraria and *Glossopteris* fossils (Reid, 1918) to be Permian. Reid (1918) identified a pink clay overlying the upper coal seam, but no conclusions were drawn on possible correlations between this pinkish rock and the tuffaceous sandstone described by Reid (1916), or the coal measures at the Oxley Creek/Dingo Creek and Betts Creek localities. Due to the low quality of the coal located in the area, and the significant findings of coking coal in the nearby Bowen Basin, exploration in the Pentland and Hughenden area ceased for four and a half decades.

In the interim, geological reports on the area placed the coal measures under the heading ‘Permian,’ and no units were formally named.

Northern Margin

Age	Rands (1891)	Marks (1911)	Reid (1916)	Reid (1918)	Vine et al (1964)	Gray and Swarbrick (1975)	Hawkins (1978)	Scott and Hawkins (1992)
Cretaeous	Glossopteris beds in the Desert Sandstone							
lower Cretaceous or Jurassic		Blythesdale Braystone						
upper Permian			Betts Creek Series	Oxley Creek Coal Measures	Betts Creek beds *	Undifferentiated Bandanna Formation and Colinlea Sandstone	Bandanna Correlative / Colinlea Sandstone Correlative	Betts Creek beds

* thought to be part of the Eromanga Basin

Central Western Margin

Age	Vine et al (1964)	Vine et al (1965)		Benstead (1973)	Gray and Swarbrick (1975)
upper Permian	Betts Creek beds	Betts Creek beds	Bandanna Formation / Colinlea Sandstone	Bandanna Formation	Undifferentiated Bandanna Formation and Colinlea Sandstone

Eastern Margin

Age	Vine et al (1965)			Carr (1974) and Swarbrick (1974)	(1)	Scott and Hawkins (1992)
upper Permian	Betts Creek beds	Bandanna Formation	Upper	Bandanna Formation	Bandanna Formation Correlative	Bandanna Formation
			Lower	Black Alley Shale		
		Colinlea Sandstone	Peawaddy Formation	Peawaddy Formation	Colinlea Sandstone Correlative	Colinlea Sandstone
				Colinlea Sandstone		

Springsure Shelf

Age	(2)	Mollan et al (1969)	Scott and Hawkins (1992)
upper Permian	Cheshire Formation	Blackwater Group	Bandanna Formation
		Black Alley Shale	Black Alley Shale
	Mantuan Downs Productus Bed	Peawaddy Formation	Peawaddy Formation
	Colinlea Formation	Colinlea Sandstone	Colinlea Sandstone

Figure 4: Summary of the nomenclature historically applied to the upper Permian strata of the Galilee Basin. For area descriptions, refer to Figure 3b. (1) Gray (1976); Gray and Swarbrick (1975); Hawkins (1978); (2) Shell Queensland Development Pty Ltd (1952); Schneeberger (1952); Hill (1957).

While coal exploration and discoveries ceased around the Pentland and Hughenden area after the early 20th century, continued exploration work was occurring in the adjacent Bowen Basin. Permian coal seams and their enveloping formations were mapped from Collinsville in the north to Springsure in the south. Both Schneeberger (1952) and Shell Queensland Development Pty Ltd (1952) described the stratigraphy on the western side of the Springsure Shelf (Figure 4), prior to this only the eastern side of the Springsure Shelf was described (e.g. Reid, 1930). Their stratigraphic nomenclature consisted of a threefold division for Lopingian strata: from oldest to youngest, the Colinlea Formation, the Mantuan Downs Productus Bed and the Cheshire Formation. The Colinlea Formation was interpreted as the lateral equivalent of the Catherine Sandstone, Ingelara Formation and Aldebaran Sandstone on the eastern side of the Springsure Shelf. The base of the Cheshire Formation overlies the Mantuan Downs Productus Bed, a marine fossil-rich bed, while the upper part of the Cheshire Formation consisted of Triassic strata. Hill (1957) used this nomenclature in her mapping of the Springsure geological sheet, which was influential on further exploration.

In the 1960's the Bureau of Mineral Resources (BMR) and GSQ recognised the need for more rigorous stratigraphic nomenclature and issued mapping reports and portfolios on central Queensland. Vine et al. (1964) erected the current name, the Betts Creek beds, which is used today to designate the coal-bearing Permian sequence in the northern part of the Galilee Basin (Figure 4), although, at the time, the unit was thought to be part of the overlying Eromanga Basin. Vine et al. (1964) tentatively expanded the known extent of the Betts Creek beds to the Muttaburra area in the central western part of the basin (Figures 3 and 4), because coals were intersected at similar depths to the northern area of the Galilee Basin. However, they did not discuss any correlation to Permian sedimentary rocks found by Schneeberger (1952) and others on the Springsure Shelf.

The term 'Galilee Basin' was fleetingly mentioned by Whitehouse (1955) to describe the Permian to lower Mesozoic strata west of the Bowen Basin, but it was not used in BMR and GSQ publications until Vine et al. (1965). Within their report the term is inconsistently used, and the term 'Eromanga Basin' is more frequent. Their report focused on the stratigraphy of the central area of the Galilee Basin, from Jericho in the south to Lake Buchanan in the north and Longreach in the west. Using palynological and petrographic samples collected from core, Vine et al. (1965) retained the Lopingian Betts Creek beds for the northern part of the basin (Figure 4), because poor exposure did not permit stratigraphic subdivisions similar to the Lopingian sediments on the Springsure Shelf. Vine et al. (1965) extended the southern nomenclature into the central part of the basin, along the Koburra Trough, replacing the Colinlea Formation with the Colinlea Sandstone. The term 'Peawaddy Formation' was used to describe the upper part of the Colinlea Sandstone, although the

Peawaddy Formation is equivalent to the Mantuan Productus Beds, first used by Mollan et al. (1964) for sediments on the eastern Springsure Shelf. Conformably overlying the Peawaddy Formation is the coal-bearing Bandanna Formation, a term that replaced the previously used Cheshire Formation (Figure 4). Vine et al. (1965) noted discordance between fossiliferous and palynological ages for samples from the Colinlea Sandstone. The fossiliferous ages of correlative strata in the Denison Trough of the Bowen Basin suggested late Cisuralian age, whereas palynological samples from the Jericho area suggest a Lopingian age. Three reasons were suggested for this irregularity, (1) a miscorrelation, (2) the Colinlea Sandstone is diachronous, and (3) Lopingian flora could extend down into the Cisuralian. Vine et al. (1965) suggested that the third possibility was most likely.

Whereas Vine et al. (1964, 1965) established the nomenclature for the northern and central parts of the Galilee Basin, Mollan et al. (1969) revised the Permian stratigraphy of the western side of the Springsure Shelf, bringing it into line with standard correlations from throughout the adjacent Bowen Basin (Figure 4). They renamed the Colinlea Formation of Schneeberger (1952) and Hill (1957), to the Colinlea Sandstone. It was noted that the unit was predominately comprised of quartz sandstone and the nomenclature would now be consistent with that brought in by Vine et al (1965) for the Koburra Trough. Mollan et al. (1969) suggested that it was the probable lateral equivalent of the Aldebaran Sandstone, Ingelara Formation and Catherine Sandstone. Mollan et al. (1964) proposed the name Peawaddy Formation to replace the Mantuan Downs Productus Beds on the eastern side of the Springsure Shelf. This nomenclature was used for the western side of the Springsure Shelf by Mollan et al. (1969) (Figure 4), who subdivided the Cheshire Formation of Schneeberger (1952) and Hill (1957) into the Black Alley Shale and the overlying, coal-bearing Blackwater Group. Since then the Blackwater Group nomenclature has diminished and has been replaced with ‘Bandanna Formation’ in the Galilee Basin. However, no formal publication has noted this change for the western Springsure Shelf. Nomenclature that resulted from the BMR and GSQ mapping during the 1960’s is still in use; only minor stratigraphic relationships were changed.

In the 1970’s exploration expanded within the Galilee Basin, in particular along the eastern margin. Led by A. F. Carr, the GSQ drilled 66 boreholes along the eastern margin from Lambton Meadows (see Figure 3, locality 1) in the south to Pentland (see Figure 3, locality 2) in the north (Matheson, 1987). A maximum of six coal seams were recorded and named alphabetically in stratigraphic order from youngest to oldest. This was the first naming of coal seams in the Bandanna Formation, Peawaddy Formation and the Colinlea Sandstone. Carr (1973b) was inconsistent with his naming convention, however, initially using the nomenclature described by Vine et al. (1965) for the strata

intersected in the first borehole drilled at Wendouree (see Figure 3, locality 3). A revised terminology based on strata from the Denison Trough of the Bowen Basin was used by Swarbrick (1974) in a report of the Lambton Meadows area, which had the additional unit of the Black Alley Shale. This unit replaced the lower Bandanna Formation unit of Vine et al. (1965) (Figure 4). As the drilling locations moved northward, the consistent use of nomenclature deteriorated and 'upper Permian' was eventually used to describe all Lopingian strata.

As more geological knowledge was published about the Galilee Basin during the 1970s and 80s many private companies obtained leases to explore for conventional petroleum potential. This led to an increase of available data and many GSQ publications. Benstead (1973) used palynological evidence to confirm the presence of Lopingian strata in the Muttaburra area. He used the term Bandanna Formation to encompass all Lopingian strata in the western side of the basin, ignoring the name 'Colinlea Sandstone' used by Vine et al. (1965) to describe the lower section of Lopingian strata in the area (Figure 4). Gray and Swarbrick (1975) and Gray (1976) proposed a twofold division for strata on the eastern margin of the Galilee Basin after correlating the pinch out of the Peawaddy Formation and Black Alley Shale from Carr (1973b); Mollan et al. (1969) and Swarbrick (1974) north of the Springsure Shelf. This division took the names of existing nomenclature from the southern and central parts of the basin: the older Colinlea Sandstone correlative and younger Bandanna Formation correlative (Figure 4).

A preliminary revision of a more consistent stratigraphy was presented by Scott and Hawkins (1992), based on a review of numerous borehole data from across the basin. The more unified stratigraphy was based on the original formal descriptive nomenclature of Gray and Swarbrick (1975); Mollan et al. (1969) and Vine et al. (1964) for the northern, central to eastern margin and Springsure Shelf (Figure 4). Scott and Hawkins (1992) were also the first to comment as to which coal seam were present within which formations. Keeping in line with Carr, they used alphabetical nomenclature for the coal seams along the eastern margin and within the Koburra Trough. The A and B seam belonged to the Bandanna Formation, and the C, D, E and F seams were part of the Colinlea Sandstone (Figure 5). This division of coal seams is still in use.

Two commonly cited and influential papers regarding the internal architecture of the Galilee Basin are by Allen and Fielding (2007a, 2007b). They describe the stratigraphic framework of the Betts Creek beds in the northern part of the basin, as well as sequence stratigraphic correlations with strata in the Koburra Trough, the Springsure Shelf and the Bowen Basin. They identified six third-order depositional sequences within the Betts Creek beds, which can be correlated to a similar

sequence in the Bowen Basin, thus strengthening the stratigraphic relationship between the two basins. More recently Phillips et al. (2017b) revisited these correlations in part and found the sole use of a gamma ray log[1] by Allen and Fielding (2007b) for correlation purposes resulted in the mis-identification of coal seams as distributary channels. As such, the sequence stratigraphic boundaries of Allen and Fielding (2007b) are disputed, and, if nothing else, highlights the need for additional work on Lopingian correlations between the Galilee and Bowen basins.

Although the stratigraphic nomenclature for the Galilee Basin was formalised in the 1960s, many variants have been used in publications since. The result is confusing regarding the correct nomenclature to use when referring to Lopingian strata in the Galilee Basin. As an example, reports by Hawkins (1978) and Durie et al. (1992) were focused on a similar part of the Galilee Basin. Hawkins (1978) used the two fold division, Colinlea Sandstone correlative and Bandanna Formation correlative of Gray (1976) and Gray and Swarbrick (1975), whereas Durie et al. (1992) used the Betts Creek beds nomenclature of Vine et al. (1964). The confusion is also evident from recent well-completion reports in the Galilee Basin, in which the nomenclature is consistently used inconsistently. This paper will refer to the formal stratigraphic nomenclature described by Scott and Hawkins (1992) for the northern, central to eastern margin of the Koburra Trough and Springsure Shelf.

Coal seam nomenclature

Due to the limited number of publications on formal naming of coal seams in the Galilee Basin, particularly on the central western margin of the basin where no formal publications exist, company well completion reports have been reviewed for coal seam nomenclature. Nomenclature can be individual to companies, and may not be representative of a widely used naming convention, therefore only general inferences have been made regarding the coal seam nomenclature, and the authors recognise that discrepancies may occur at a company level.

The first naming of coal seams within the Galilee Basin was by Carr during the 1970s (e.g. Carr, 1973a; Carr, 1973b; Carr, 1974a; Carr, 1974b; Carr, 1974c; Carr, 1976; Carr, 1977; Carr, 1978). He used an alphabetical naming convention for coal seams along the eastern margin: A (the youngest coal seam) through to F (the oldest Lopingian coal seam). Carr described the coal seams at ten separate locations along the ~400 km eastern margin of the basin. Most coal seams were recorded as being non-descript dull with some bright banding, thermal quality coal, except for the B and C seams, which contain distinctive ‘fawn mudstone’ lithologies. Without densely drilled boreholes or

[1] At the time of publishing gamma ray logs were all that was reliable and available to Allen and Fielding (2007b).

seismic lines along strike, these distinctive coal seams became marker horizons allowing Carr to correlate the over- and under-lying coal seams. Scott and Hawkins (1992) continued what Carr had started and produced the first north to south correlation of coal seams along the eastern margin from drilling conducted by the GSQ and reported by Carr in the 1970s. Their paper firmly established the alphabetical naming convention of the coal seams along the eastern margin that is still in use. They placed the A and B seams within the Bandanna Formation and the highly tuffaceous C seam and underlying seams within the Colinlea Sandstone. The work of Carr and Scott and Hawkins (1992) included coal seams that are within both the Betts Creek beds in the north, and the Bandanna Formation and Colinlea Sandstone in the east. While no mention was made regarding a boundary, they showed that the coal seams are laterally continuous between the formations.

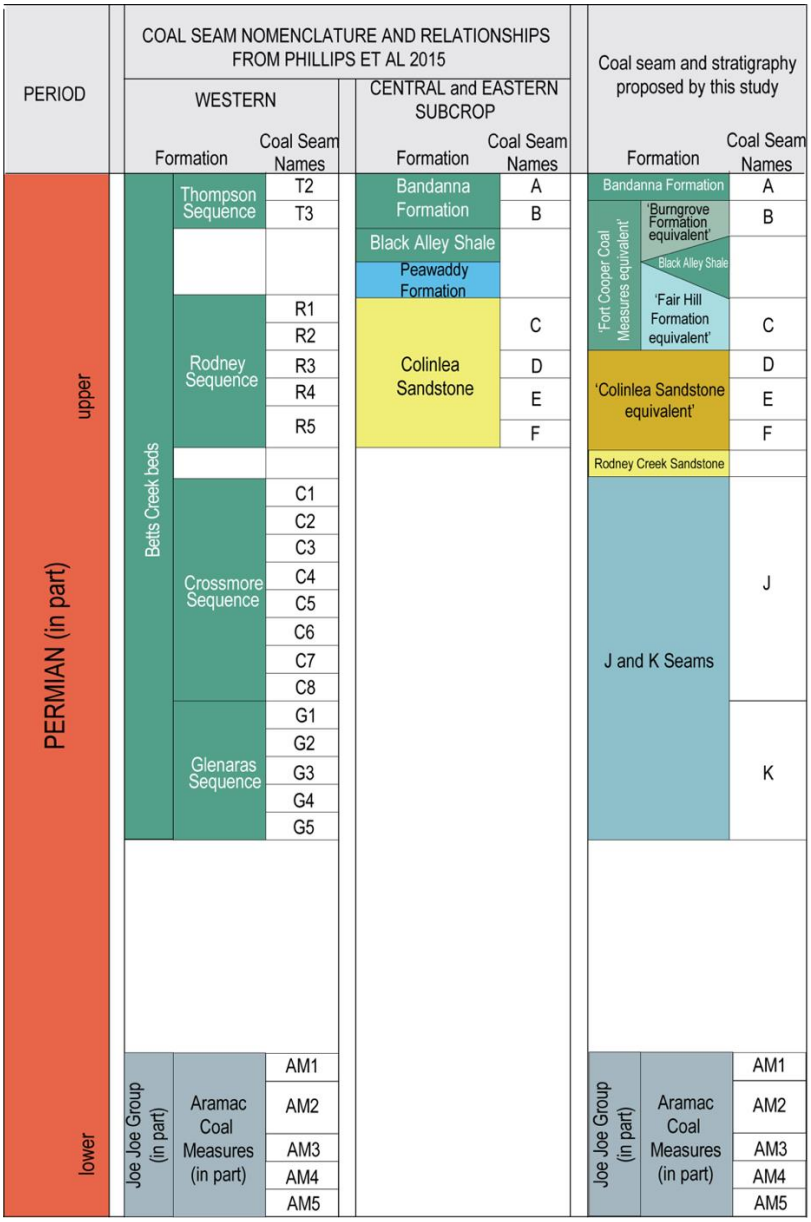

Figure 5: Coal seam nomenclature and stratigraphic relationships from Phillips et al. (2016) with proposed stratigraphic units defined in this study. Note spacing between lower and upper Permian is not to scale. See Figure 9 for proposed stratigraphy.

Vine et al. (1964) discussed the possibility of the Betts Creek beds extending to the Muttaburra area along the central western margin of the basin. Carr and Scott and Hawkins (1992) did not apply their nomenclature to the coal seams in that area, so no formal publication of coal seam nomenclature is available for the Lopingian strata of that area. Well-completion reports from the area provide insight into the coal seam nomenclature used. Despite numerous boreholes drilled along the central western margin from the 1960s to 1980s, coal seams were not named until 1994 by Enron Exploration Australia (1994) who explored the region for coal seam gas potential and used the alphabetical nomenclature similar to Carr (1973b) and Scott and Hawkins (1992) with the A seam representing the youngest coal seam within the formation through to G. They correlated these coals with those in PPS Glenaras 1 (McDonagh, 1967), a nearby borehole drilled in 1966, but did not correlate the coal seams elsewhere in the basin. In the well completion report of EEA Rodney Creek 3, Gaddy et al. (1995) had split the Betts Creek beds into four sequences, the Thomson and Rodney sequences, separated from the Crossmore and Glenaras sequences by a distinctive sand body referred to as the 'Colinlea Sandstone' in some later well completion reports. The reasoning for this split was to aid stratigraphic description as it allowed for coal seam plies to be named. The coal seam/ply within each sequence was given the first letter of the sequence in which it was located, with a number distinguishing its origin within the sequence, for example the fourth coal ply within the Rodney Sequence would be given the term R4, and the first ply within the Thomson sequence would be T1. This naming convention was used until 2008 when Holland and Bocking (2008) revised the coal seam nomenclature and termed all coal seams that were within the Lopingian R1–R8 inclusively, removing the detail of naming the coal seam plies.

Cross sections (Figures 7 and 8) were created using the gamma and density geophysical logs. The gamma log was normalised to a common baseline of 100API (shale line; Figure 6) to ensure consistency between data sets. The geophysical responses were validated against geologists' field descriptions of the core and chips. This was to QAQC the interpretation of the geophysical logs. After examination the following density and gamma cut of values were used; density cut off values for coal were set at <1.8 g/cc (coloured black on Figure 6), gamma cut off values for other lithologies were set at <100 API, as sandstone (coloured yellow on Figure 6), and those ≥100 API were classified as siltstone and finer (coloured dark turquoise on Figure 6). The coal seams were correlated based on their density signature. This was extremely useful when correlating the tuffaceous coal seams.

Using newly gathered geophysical (Figure 6) and lithological data, Phillips et al. (2015) correlated from west to east across the basin using tuffaceous coal seams as marker horizons (Figure 7). The sequences used by Gaddy et al. (1995) correlated well with units along the eastern margin of the Galilee Basin. Phillips et al. (2015) correlated the Bandanna Formation and Colinlea Sandstone along the eastern margin with the Thomson and Rodney sequences, respectively (Figure 5). The A and B coal seams within the Bandanna Formation are correlative to the T2 and T3 coals, whereas the tuffaceous C seam and underlying seams within the Colinlea Sandstone are coalesced into coal seams within the Rodney Sequence. The 'Colinlea Sandstone' unit on the central western margin did not correlate to the coal-bearing Colinlea Sandstone on the eastern margin, but Phillips et al. (2015) did not rename this unit. Herein, this unit will be called the 'Rodney Creek Sandstone' due to its geographical proximity to the Rodney Creek boreholes' (Figures 5 and 10) to avoid confusion with the coal bearing Colinlea Sandstone unit in the Koburra Trough and eastern margin. The Crossmore and Glenaras sequences on the central western margin are absent along the eastern margin, and Phillips et al. (2015) questioned their current stratigraphic placing within the Lopingian Betts Creek beds because they are only observed where the Cisuralian Aramac Coal Measures are present. Phillips et al. (2015) did not name the individual coal seams, but instead gave the coal seams within the Crossmore and Glenaras sequences a holistic terminology, the 'J and K' seams, respectively, using an alphabetical convention to follow the overlying seams.

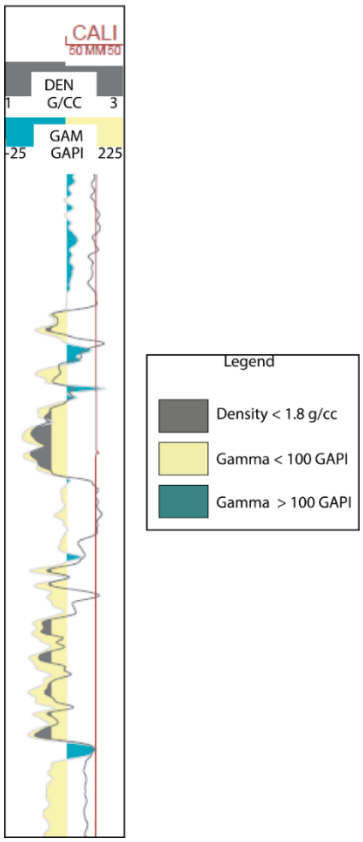

Figure 6: Example layout of wireline log used in correlations. Caliper is shown in red, Density is shown with a black line. Anything less than 1.8 g/cc has been coloured black. Gamma is shown with a grey line. The shale line has been placed at 100 GAPI, less than this is coloured yellow, greater than this is coloured dark turquoise.

2.4. Betts Creek beds vs. Colinlea Sandstone and Bandanna Formation

The stratigraphic relationship between the Betts Creek beds and the Colinlea Sandstone and Bandanna Formation is unclear and can become problematic when correlating north to south and east to west across the Koburra Trough, as no formation boundaries have been set. From previous literature, it appears that two stratigraphic terminologies developed during the evolution of nomenclature in the Galilee Basin and have been only poorly integrated even though it is now realised that they are correlative. The geographic boundary between the two nomenclatures is a blurred line and has never fully been addressed. Scott et al. (1995) drew simple maps of the extent of the different strata, but these maps lack detail. Whether the Betts Creek beds are a separate entity to the Colinlea Sandstone and Bandanna Formation, or if they represent one or both of these formations, has never been established. Allen and Fielding (2007b) suggested that sequence stratigraphic boundaries can be traced between the two nomenclature divisions, and hence that the Betts Creek beds are correlative with both the Colinlea Sandstone and Bandanna Formation. Recently new data have been acquired by Phillips et al. (2017b) that suggest the stratigraphic boundaries used by Allen and Fielding (2007b) were difficult to corroborate. Although the Colinlea Sandstone and Bandanna Formation are correlatives of the Betts Creek beds, pinpointing the interchange within the latter is illusive.

Misapplication of stratigraphic nomenclature for the Galilee Basin has led to confusion in stratigraphic relationships between Lopingian strata. In reviewing published literature three reasons as to why this misapplication occurs became apparent: (1) lithological reasoning, (2) facies reasoning and (3) coal seam reasoning.

Lithological reasoning

The misapplication of stratigraphic nomenclature for the Galilee Basin has led to naming confusion in petrographic studies wherein the same strata have been given different names in separate reports. Care has been taken when reviewing clastic petrology, using samples from locations close to type-sections in an attempt to avoid stratigraphic misinterpretation.

The type-section nominated for the Betts Creek beds near the township of Pentland has a lower part that is conglomeratic, overlain by *Glossopteris*-bearing mudstone and sandstone, with coal seams restricted to the upper part (Vine et al., 1964). The bulk of the unit is made up of kaolinitic and micaceous sandstone and has a thickness range of 46–366 m.

The type-section of Mollan et al. (1969) for the Colinlea Sandstone on the Springsure Shelf contains a conglomerate at its base that is possibly correlative to the conglomerate at the base of the Betts Creek beds. However, the type-sections are separated by a large distance (>450 km), so the correlation is questionable. It is more likely that both conglomerates represent a revival in sedimentation after the long mid-Permian hiatus (e.g. Evans and Roberts, 1980; Nicoll et al., 2015; Vine et al., 1964). The Colinlea Sandstone is largely composed of fine to medium quartz sandstone with a kaolinitic matrix (Grigorescu, 2012; Mollan et al., 1969), similar in composition to the sandstone within the Betts Creek beds (Vine et al., 1964). Vine et al. (1965) noted that palynological evidence within the Colinlea Sandstone is comparable with that from the Betts Creek beds at Hughenden and that minor argillaceous beds increase in proportion within the Colinlea Sandstone towards the north into the Betts Creek beds.

The Bandanna Formation (Blackwater Group of Mollan et al., 1969) type-locality on the Springsure Shelf contains coal seams, similar to the architecture proposed by Vine et al. (1965) of the coal seams within the type-section of the Betts Creek beds (Vine et al., 1964). Mineralogically, the Bandanna Formation commonly contains calcareous minerals (Grigorescu, 2012; Mollan et al., 1969) as well as minor illite, hematite and zeolite (Grigorescu, 2012), while the Betts Creek beds are kaolinite and illite-rich (Hawkins and Carmichael, 1987).

While the Betts Creek beds are noted to be petrologically similar to the Colinlea Sandstone, comparisons have been drawn between the architecture of the beds and that of the Bandanna Formation. A reason for this disagreement could be found in early descriptions of the formations, primarily the absence of coal in the Colinlea Sandstone (Mollan et al., 1969; Vine et al., 1965) and the description of coals only in the Bandanna Formation (Mollan et al., 1969; Vine et al., 1965). Nevertheless, under the most recent nomenclature (Scott and Hawkins, 1992) the Colinlea Sandstone covers four major coal seams, C through to F. This raises the question of whether the Scott and Hawkins (1992) Colinlea Sandstone on the eastern margin of the Galilee Basin is the same as that described by Mollan et al. (1969) on the Springsure Shelf, or the possible lateral equivalent of another formation on the shelf.

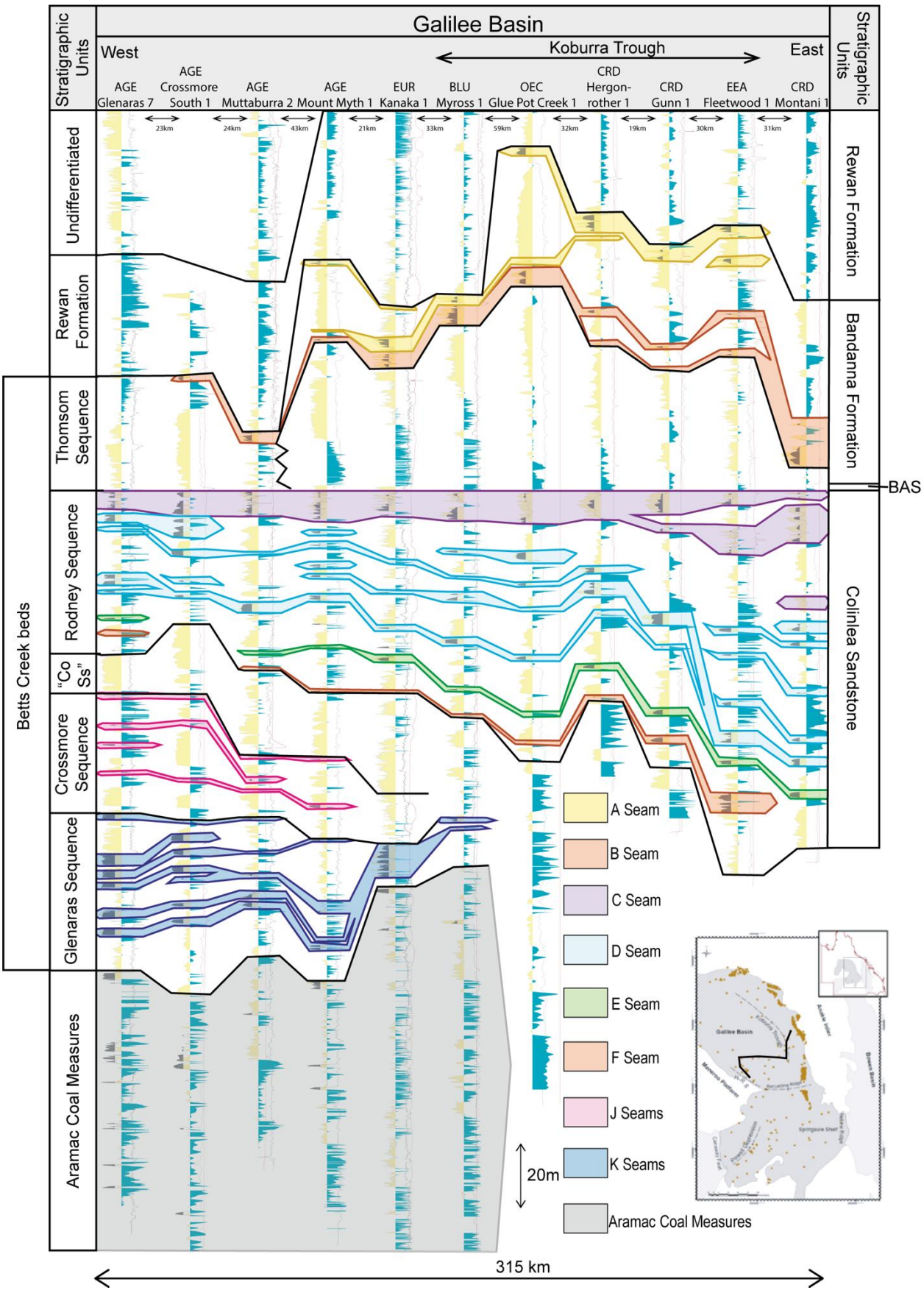

Figure 7: Cross section A. Correlation from west to east across the Galilee Basin. See Figure 3 and insert for cross-section location. Note boreholes are not equidistance from each other. Abbreviations: 'Co Ss', 'Colinlea Sandstone'; BAS, Black Alley Shale. Modified from Phillips et al. (2017b).

Facies reasoning

Initially, the interpretation of the Betts Creek beds in the north as piedmont deposits (Vine et al. (1964), allowed for the local change in facies, as adjacent environments within such deposits are highly variable and independent of one another. More recently, an alluvial/coastal plain setting was interpreted by Allen and Fielding (2007a, 2007b) for an outcrop of the Betts Creek beds near the township of Hughenden (see Figure 3, locality 4). The Colinlea Sandstone was originally thought to have been deposited in an alluvial-plain setting (Hawkins, 1978; Mollan et al., 1969), similar to that of the Betts Creek beds in the north, with a more westerly source (Hawkins, 1978). Recent revisits of palaeo-geography by (Fielding et al., 2000) suggest that the Colinlea Sandstone was a coastal plain setting, perhaps a logical southerly adjacent environment to the northerly Betts Creek beds alluvial plain. It is agreed that the Bandanna Formation represents a deltaic environment (Allen and Fielding, 2007b; Fielding et al., 2000; Hawkins, 1978), sometimes referred to as paludal (Mollan et al., 1969).

The palaeo-environmental differences from north to south within the Galilee Basin can be highlighted through the major facies changes within Lopingian strata, particularly along the eastern margin. Using wireline logs (Figure 6), correlations from Phillips et al. (2017b) (Figure 8) document this lateral variability of clastic facies, as well as the continuity of coal beds in this area. The correlation, flattened on the tuffaceous C seam, shows the Colinlea Sandstone beneath this datum and the Bandanna Formation and Peawaddy Formation/Black Alley Shale equivalents above it. The cross section spans the length of the eastern margin from the north to the south, and therefore should cross the arbitrary boundary across which naming conventions change. Towards the northern end of the cross section the Betts Creek beds should prevail and towards the south the Colinlea Sandstone, Peawaddy Formation, Black Alley Shale and Bandanna Formations should exist.

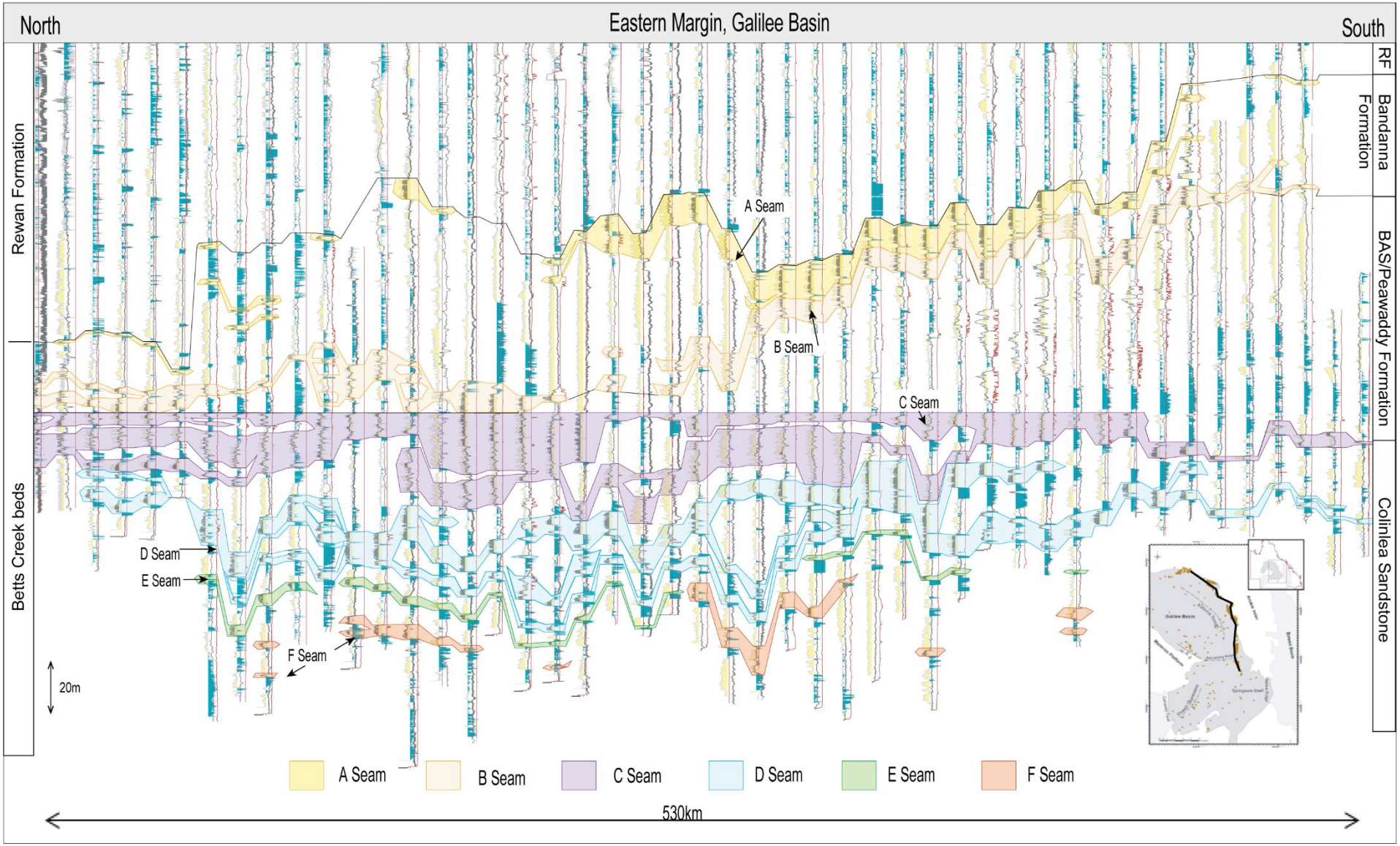

Figure 8: Cross section B. Correlation along the eastern margin, see Figure 3 and inset map for cross section location. Note boreholes are not equidistance from each other. Abbreviations: RF, Rewan Formation; BAS, Black Alley Shale. Modified from Phillips et al. (2017b).

Figure 8 illustrates that the lower section of the alluvially-formed Betts Creek beds is dominated by sandstone channels (Allen and Fielding, 2007a) and coals with only a minor component of fine-grained lithologies. This architecture is consistent southward through the Colinlea Sandstone, where coal seams coalesce then eventually split and thin onto the Springsure Shelf, where fine-grained lithologies, potentially marine influenced, are the dominant strata. The upper section of the Betts Creek beds is the inverse: flood basin-derived (Allen and Fielding, 2007a), fine-grained lithologies are prevalent with only thin and commonly absent coal seams. The coal seams within this upper unit coalesce southward into the Bandanna Formation, overlying the expanding Peawaddy Formation and dark anoxic Black Alley Shale toward the south, a distinct coarsening upward trend that has been well documented by previous researchers (Gray and Swarbrick, 1975; Hawkins and Green, 1993; Scott and Hawkins, 1992). The low gamma-ray signature inferred to be sandstone-dominant lithologies of the southern Bandanna Formation contrast with high gamma signature, finer grained inferred lithologies in the upper section of the northern Betts Creek beds. This is in contrast to the comments of Vine et al. (1965) who argued that the Betts Creek beds were lithologically similar to the Colinlea Sandstone and architecturally comparable to the Bandanna Formation. The more robust understanding of the formations and their lithological and architectural make-up since their type-sections were created could allow this discrepancy to be clarified.

It could be argued that the Betts Creek beds occur when the marine influenced strata from the south are no longer present and the Bandanna Formation overlies the Colinlea Sandstone (Figure 8). Marine facies were originally thought to extend to approximately 24°S (Vine, 1975), which was subsequently extended to 23.5°S (Hawkins and Green, 1993). Thus, it can be inferred that Lopingian strata north of this latitude would be considered to be the Betts Creek beds. This argument has difficulties, however, because Allen and Fielding (2007a, 2007b) interpret estuarine strata at the very north of the basin in their flood basin deposits, not far from the type-section of the Betts Creek beds. As this marine influence separates the Bandanna Formation and Colinlea Sandstone in the south, it may have a similar relationship in the north. Allen and Fielding (2007a) observed it at numerous stratigraphic horizons in a northern outcrop section, suggesting that the Lopingian included more than one marine incursion. Allen and Fielding (2007a) did not correlate these estuarine deposits in outcrop to borehole data, therefore the estuarine deposits cannot be accurately attributed to any of the fine-grained lithologies in the northern part of the cross section. Thus, it cannot be concluded if they were deposited as a time correlative to the correlated Black Alley Shale/Peawaddy Formation, the only known marine incursion in the southern part of the basin, or if they occur at another stratigraphic horizon.

Coal seam reasoning

Scott and Hawkins (1992), using Carr's data, were the first to demonstrate the impressive continuity of the coal seams and architecture along the eastern margin of the Galilee Basin as the seams encountered the marine incursion from the south. They argued that the coal-seam architecture is different between the Betts Creek beds and the Bandanna Formation and Colinlea Sandstone. However, the relative location of this transition is open to interpretation. If using the naming convention laid out by Scott and Hawkins (1992), whereby the tuffaceous B coal seam provides the base of the Bandanna Formation and the tuffaceous C coal seam, the roof of the underlying Colinlea Sandstone (Figure 5), the separation of the Betts Creek beds may be simple. Due to the coalescing of the tuffaceous B and C seam in the north of the basin (Figure 8), it can be difficult to distinguish the exact point where the two subdivisions of the Betts Creek beds can be made.

Comparing the Betts Creek beds along the central western margin with the Bandanna Formation and Colinlea Sandstone along the eastern margin using the tuffaceous C seam as a marker horizon, Phillips et al. (2015) recognised both the Bandanna Formation and the Colinlea Sandstone subdivisions within the Betts Creek beds (Figure 7). They also identified a possible miscorrelation. Coal seams underlying the 'Rodney Creek Sandstone' along the central western margin had previously been considered to be Lopingian Betts Creek beds with no lateral equivalent on the eastern side of the basin, and thus no correlatives to the Betts Creek beds in the north of the basin. The age of these extra coal seams, termed the 'J and K' seams (Phillips et al, 2015; Figure 7) is not clear. Nevertheless, they represent a poorly constrained stratigraphy that has been built upon very few data points and extended basin wide. Therefore, only the upper sections (Thomson and Rodney sequences) of the Betts Creek beds on the western central margin are correlatable with the Bandanna Formation and Colinlea Sandstone and to the Betts Creek beds in the north.

Correlations between the Betts Creek beds and their correlatives have been approached in two ways. The first approach is by determining the units' lithological (e.g. Hawkins and Carmichael, 1987; Vine et al., 1964) and facies (e.g. Allen and Fielding, 2007a) characteristics, whereby the Betts Creek beds have a unique lithological make up. Therefore, the Betts Creek beds could be considered as a separate entity. Without detailed and densely sampled petrographic analysis it can be challenging to pinpoint the exact change between these two formations. Secondly, the lateral continuity of coal seams allows for a robust correlation between these two nomenclatures (Phillips et al., 2017b) and supports the idea that the Betts Creek beds can be subdivided into two subunits, the Bandanna Formation and Colinlea Sandstone.

2.5. Stratigraphic relationship with the Bowen Basin

The tie between the Galilee Basin and the Bowen Basin occurs across the Springsure Shelf, over the Nebine Ridge and into the Denison Trough. The Springsure Shelf is an area that is sparsely drilled, but is thought to have existed as a topographic high, relative to surrounding areas, until the latest Lopingian (Allen and Fielding, 2007b), therefore allowing sediments to pass between the two basins, causing them to have an interlinked stratigraphic history. Marker coal horizons are few and sporadic on the shelf, resulting in initial correlations based on sparsely placed outcrops on both sides of the shelf. The following units are recognised on the shelf, and a brief explanation is provided of their lateral equivalents elsewhere within the Bowen Basin. For a more robust review of the stratigraphy of the Bowen Basin, the reader is referred to Draper (2013).

Colinlea Sandstone

The Colinlea Sandstone is correlated with the package (from oldest to youngest) of the upper Aldebaran Sandstone, Freitag Formation, Ingelara Formation and Catherine Sandstone on the Springsure Shelf and Denison Trough of the Bowen Basin (Allen and Fielding, 2007b; McKellar and Henderson, 2013); the Aldebaran Sandstone and the Frietag Formation are only observed in these areas of the Bowen Basin. Within the Bowen Basin the marine Ingelara Formation is known as the Maria (Prouza and Park, 1973) and Blenheim formations (Jensen et al., 1966), displaying shallower marine environments as it transitions northward. The Catherine Sandstone passes laterally into the marine Flat Top Formation (Olgers et al., 1966) and the coal-bearing German Creek Formation (Prouza and Park, 1973) in the Denison Trough and Comet Ridge, which become the lower part of the Moranbah Coal Measures (Koppe, 1978) in the northern Bowen Basin. These are therefore thought to be the correlatives to the coal measures found within the Colinlea Sandstone along the eastern margin of the Galilee Basin. Recent geochronological analysis of the Moranbah Coal Measures has established an age for them of no younger than 256 Ma (Nicoll et al., 2015).

Peawaddy Formation

The Peawaddy Formation has been subdivided into lower and upper units in the Denison Trough. The lower section of the Peawaddy Formation interfingers with the marine MacMillan Formation (Prouza and Park, 1973) in the Bowen Basin, correlatable with the upper section of the Moranbah Coal Measures in the northern part of the basin. The upper section of the Peawaddy Formation in the Denison Trough is correlatable with the highly tuffaceous and coal-bearing Fair Hill Formation (Prouza and Park, 1973), the basal section of the Fort Cooper Coal Measures (Anderson, 1985; Ayaz et al., 2015; Draper, 2013; Jensen, 1971; Figure 9) in the Bowen Basin.

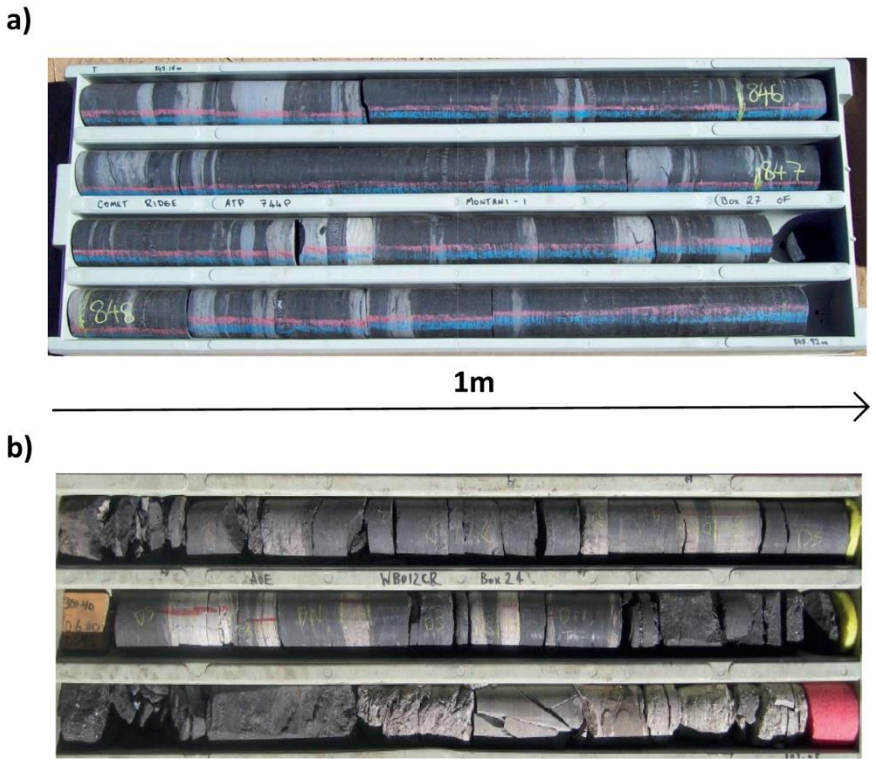

Figure 9: Photographs of a) tuffaceous horizons in the C Seam from the Galilee Basin (Comet Ridge, 2010) and b) tuffaceous horizons within the Fort Cooper Coal Measures, Bowen Basin (Ayaz, 2016).

Black Alley Shale

The Black Alley Shale overlies the Peawaddy Formation and is traceable from the Galilee Basin (where it separates the Colinlea Sandstone and the Bandanna Formation) into the southern Bowen Basin, which separates the Fair Hill Formation (Anderson, 1985; Ayaz et al., 2015) from the overlying Burngrove Formation (Malone et al., 1969).The Black Alley Shale pinches out northward in the Bowen Basin as the coal-bearing succession merge into the Fort Cooper Coal Measures. The Fort Cooper Coal Measures are associated with abundant tuffaceous layers within their coals (Figure 9). These have been dated by Ayaz et al. (2016a) using the CA-IDTIMS technique, with an age range of 252.58 ± 0.23 to 254.03 ± 0.26 Ma. This stratigraphic unit is absent from the Galilee Basin, because the Black Alley Shale and Peawaddy Formation pinch out and do not have a named correlative.

Bandanna Formation

The Yarrabee Tuff, a thick tuffaceous horizon that has been used as a correlation tool by Anderson (1985) and Ayaz et al. (2015), separates the Fort Cooper Coal Measures from overlying tuffaceous free units. Overlying the Yarrabee Tuff is the final prograding Rangal–Baralaba–Bandanna coal measures (Malone et al., 1969; Olgers et al., 1966; Phillips, 1960) that are correlative to the uppermost Bandanna coal measures in the Galilee Basin.

2.6. Proposed revision of Galilee Basin stratigraphy

This study has reviewed stratigraphic units in both the Galilee and Bowen basins and their relationships with one another. The Bowen Basin has a more refined stratigraphic nomenclature, because of the numerous studies conducted there, particularly since mining began. On the other hand, the Galilee Basin, where only sporadic exploration has been done until recent years, has a simple, yet inconsistently used, stratigraphic nomenclature. The low accommodation, slow depositional and high erosional rates associated with intracratonic basins may have made it difficult to identify units in comparison to the thick succession of Lopingian strata within the Bowen Basin. Nevertheless, with the newly acquired data and observations from the Galilee Basin, this study proposes an informal stratigraphic nomenclature that reflects possible lateral equivalence to units in the Bowen Basin (Figure 10). With further work, these informal units may be formalised as new formations.

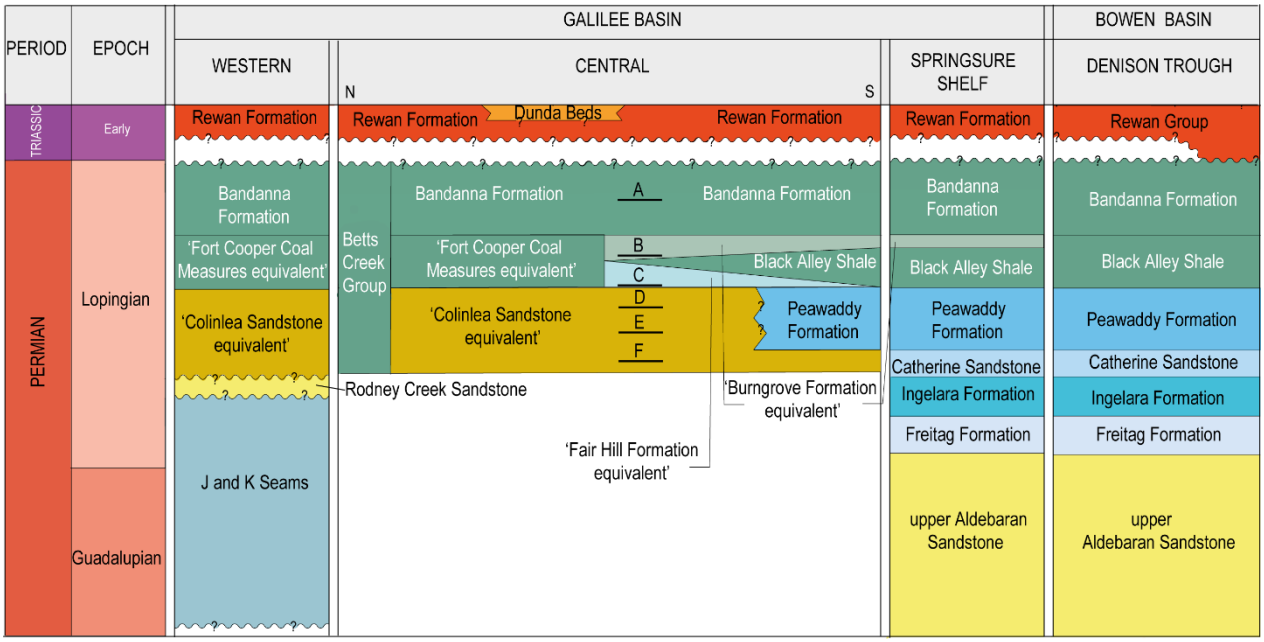

Figure 10: New proposed stratigraphy for the Galilee Basin, with lateral stratigraphic units in the Denison Trough, Bowen Basin. Underlined letters represent coal seams located in their respective proposed formations. Note that placement of coal seams is not exact.

It is also proposed the Betts Creek beds be upgraded to the rank of Group because it can be subdivided using coal seam correlations (Figure 10).

The Colinlea Sandstone within the Galilee Basin is now referred to as the 'Colinlea Sandstone equivalent' (Figure 10), because the Colinlea Sandstone as originally defined is a coal free, quartz-rich sandstone (Mollan et al., 1969). When extrapolated along the eastern margin, the rocks become more heterogeneous and coal bearing (seams D to F) and Mollan et al.'s. (1969) description is no

longer appropriate. The ‘Colinlea Sandstone equivalent’ interfingers with the Peawaddy Formation towards the southern part of the Galilee Basin as well as the Catherine Sandstone on the Springsure Shelf. In a similar manner, these are, lateral equivalents of the Moranbah Coal Measures within the Bowen Basin (Figures 10 and 11).

Two new informal units (the ‘Fair Hill Formation equivalent’ and the ‘Burngrove Formation equivalent’) have been proposed. These lie below and above the Black Alley Shale, respectively (Figures 10 and 11). The lowermost of the new formations to be proposed is the ‘Fair Hill Formation equivalent’, which contains the tuffaceous C seam and is correlatable to the tuffaceous coal seams within the Fair Hill Formation of the Bowen Basin. Overlying the Black Alley Shale is the ‘Burngrove Formation equivalent’, which contains the B seam. This unit is correlatable to the coal seams within the Burngrove Formation of the Bowen Basin (Figure 11). Where these units are no longer split by the Black Alley Shale (Figure 8) and are coalesced, the informal name of the ‘Fort Cooper Coal Measures equivalent’ has been proposed (Figure 10). These revisions now align with the stratigraphic relationships of the Fort Cooper Coal Measures in the Bowen Basin.

The Bandanna Formation retains the A seam and is the lateral equivalent to the Rangal–Baralaba–Bandanna coal measures in the Bowen Basin (Figures 10 and 11).

The new proposed stratigraphy has been applied to a correlation between the Galilee and Bowen basins (Figure 11). The correlation has been flattened to the top of the C seam, so it is comparable to the correlations of Phillips et al. (2015, 2017b). The interpretation is described herein.

The characteristic wireline signatures for blocky sandstone, overlain by interbedded sandstone and siltstone and fine-grained marine sediments representing the Aldebaran Sandstone, Freitag Formation and the marine Ingelara Formation, respectively, are clearly defined in the Denison Trough. These units decrease in thickness on the Springsure Shelf toward the west and are last observed in the GSQ Tambo 3 well (Figure 11). The distinct wireline- log signatures in the Aldebaran Sandstone, Freitag Formation and Ingelara Formation do not carry into the Galilee Basin past the Springsure Shelf, strengthening the hypothesis that the ‘Colinlea Sandstone equivalent’ is correlatable to the Peawaddy Formation and Catherine Sandstone. If this theory were correct, which can be tested through geochronology, deposition occurred along the eastern margin later than previously thought, extending the age of the mid-Permian hiatus in this area.

As noted above, the ‘Colinlea Sandstone equivalent’ interfingers with the Peawaddy Formation and the Catherine Sandstone on the Springsure Shelf. In the Denison Trough, the Peawaddy Formation and Catherine Sandstone pass into the fine-grained marine MacMillan Formation, Flat Top Formation and German Creek Formation/Moranbah Coal Measures (Figure 11).

The tuffaceous C seam, which can be traced to the very north of the Galilee Basin, correlates in the Bowen Basin with the tuffaceous Fair Hill Formation in the Denison Trough and Comet Ridge. Overlying this, the fine-grained Black Alley Shale pinches out to the west and east of the Springsure Shelf (Figure 11). A distinct deltaic coarsening upward sequence, punctuated by coal seams, conformably overlies the Black Alley Shale in both basins. In the Bowen Basin, this sequence, referred to as the Burngrove Formation, can be correlated to the ‘Burngrove Formation equivalent’ in the Galilee Basin. The foreland setting of the Bowen Basin provides increased accommodation space causing coal seam splitting, generating numerous coal seams within the Fort Cooper Coal Measures (Fair Hill and Burngrove formations), which are correlated to the B and C seams in the Galilee Basin.

No Yarrabee Tuff equivalent can be observed in the wireline logs of the Galilee Basin, possibly due to being farther away from volcanic sources proximal to the Bowen Basin. The condensed Bandanna Formation conformably overlying the Burngrove Formation and its equivalent is the last unit within the Lopingian strata (Figure 11). The coarsening upward sequence exhibited by the Bandanna Formation on either side of the shelf, as well as its relatively tuffaceous-free coal measures, suggests the two formations have a similar palaeo-environmental setting.

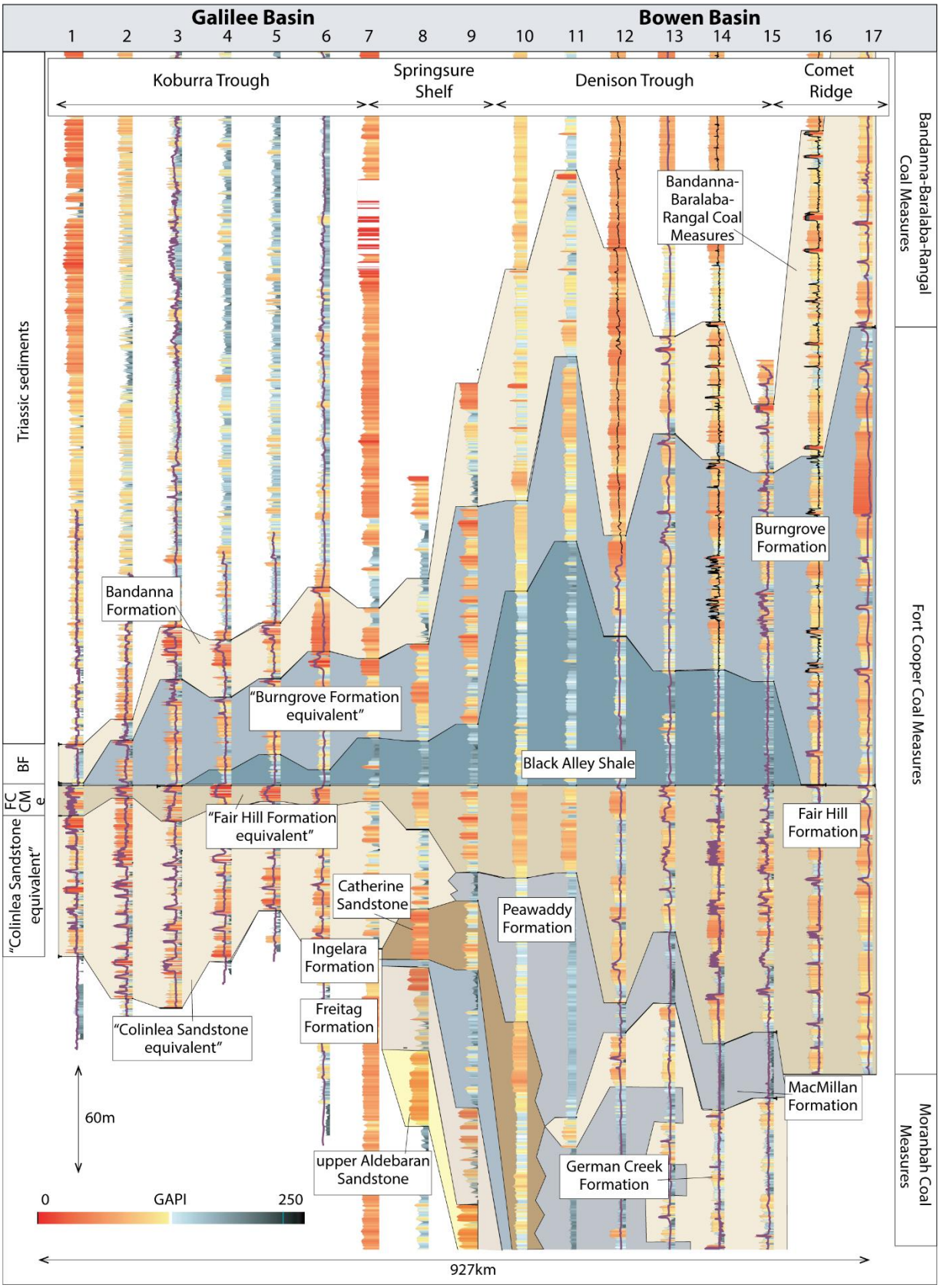

Figure 11: Cross section C. Correlations into the Bowen Basin with traced new formation boundaries. Flattened on the base of the Black Alley Shale. See Figure 3 for cross section location. Abbreviations: BF, Bandanna Formation; FCCMe, 'Fort Cooper Coal Measures equivalent'. Borehole name: 1, OER Bullock 1; 2, EEA Aberfoyle 1A; 3, EEA Fleetwood 1; 4, CRD Gunn 1; 5, CRD Hergenrother 1; 6 ,OEC Glue Pot Creek 1; 7, AOD Jericho 1; 8, GSQ Tambo 3; 9, GSQ Springsure 11; 10, PEC Warrinilla North 1; 11, AFO Rolleston 1; 12, SGO Zerogen 1; 13, SSL Yamala 2;14, MIH Emerald 3; 15, QGC Wyuna 1; 16, QGC Duckworth 11; 17, QGC Dingonose 14. Modified from Phillips and Ayaz (2015).

2.7. Summary and conclusions

The discovery of coal beds near the towns of Hughenden and Pentland in central Queensland in the late 19th century was the start of a long history of coal discoveries that eventually led to the delineation of the Galilee Basin. The Lopingian stratigraphy within the basin has been developed in two discrete areas that are separated by over 450 km. In the north, the Betts Creek beds incorporate the whole of the Lopingian strata, whereas as discussed above, the stratigraphy of the southern area can be subdivided into the Colinlea Sandstone and Bandanna Formation, split by the Peawaddy Formation and Black Alley Shale that pinch out to the north. No formal stratigraphy has been defined for the eastern and central western areas of the basin, so nomenclature has been extrapolated from both the north and the south, causing multiple cross overs in naming conventions. Coal seam nomenclature used by previous workers across the basin was also found to be inconsistent. In this study, cross sections constructed from north to south along the eastern margin, as well as west to east, transecting inferred unit boundaries, demonstrate that coal seams can be correlated regionally (Figures 7 and 8), and that sub-division of the Betts Creek beds is possible.

The Betts Creek beds were initially established to describe the coal measures within the northern part of the basin. This study has shown that the Betts Creek beds can be subdivided into its eastern and southern correlatives, the Bandanna Formation, Black Alley Shale, Peawaddy Formation and the Colinlea Sandstone. Therefore, it is proposed that it be upgraded in status to the Betts Creek Group. A case for revising the nomenclature is made for the Colinlea Sandstone, which was originally described in its type-section as quartz-rich sandstone. Now the term is more commonly applied to rocks that contain a number of coal seams in the Galilee Basin. Therefore, it is suggested a new name be given to these ‘Colinlea Sandstone equivalents’ along the eastern margin of the basin and a type-section that better fits their lithology be allocated (Figure 10).

Stratigraphic relationships with the Bowen Basin have been discussed, and the absence of stratigraphic units within the Galilee Basins stratigraphy has become apparent. The tuffaceous Fort Cooper Coal Measures have not been represented within the Galilee Basins stratigraphy despite highly tuffaceous coal seams being described.

To remedy the current confusion (Figure 10), two informal stratigraphic units that have equivalents in the Bowen Basin have been proposed: the ‘Fair Hill Formation equivalent’ and the ‘Burngrove Formation equivalent’. The ‘Fair Hill Formation equivalent’ includes the tuffaceous C coal seam, and shales into the Black Alley Shale towards the southern part of the Galilee Basin. Overlying the Black Alley Shale, the ‘Burngrove Formation equivalent’ includes the B coal seam.

A cross section drawn between the Galilee and Bowen basins using this informal stratigraphy (Figure 11) demonstrates that gamma responses tie well between the two basins. The authors acknowledge that further investigation into this stratigraphy is needed. The following research is suggested to test the informal stratigraphy that has been proposed in this study:

1. Tephrochronological analysis is needed on volcanic ash deposits within the coal seams to constrain stratigraphic units proposed. This would complement work conducted by Ayaz et al. (2016a); Laurie et al. (2016); Metcalfe et al. (2015) and Nicoll et al. (2015) on similar deposits in the Bowen Basin.
2. Palynological studies would enhance tephrochronological work and provide a link to other Permian basins worldwide.
3. Sedimentological work could be conducted in key areas around the basin to assist with determination of stratigraphic relationships, in particular the interfingering between the 'Colinlea Sandstone equivalent' and the Peawaddy Formation. Sedimentological work would also complement correlations produced by Allen and Fielding (2007b), which could confirm or refute their proposed sequence boundaries.
4. Provenance work would determine source areas for sediments. This would aim to clarify the difference in nomenclature, especially along the eastern boundary.

2.8. Acknowledgements

The authors of this paper would like to thank the Australian Coal Association Research Program (ACARP), grant number C22028, for funding. The Geological Survey of Queensland (GSQ) assisted greatly with locating historical documents while industry provided many data points. Helpful early reviews from Dr Charlie Verdel and Mr Matthias Klawitter improved the manuscript. The Australian Stratigraphic Commission is thanked for their discussions around stratigraphy, in particular Mr Ian Withnall and Dr Paul Blake. The manuscript greatly benefited from reviews from Mr Tim Evans and an anonymous reviewer. Chapter 2, '**Review of Lopingian (upper Permian) stratigraphy of the Galilee Basin, Queensland, Australia**,' has been published with the permission of the Geological Society of Australia.

Chapter 3 has been accepted (in press) in the Australian Journal of Earth Sciences (2017) as:

3. U-Pb geochronology and palynology from Lopingian (upper Permian) coal measure strata of the Galilee Basin, Queensland, Australia.

L. J. Phillips[1], J. Crowley[2], D. Mantle[3], J. S. Esterle[1], R. Nicoll[4], J. L. McKellar[5] and A. Wheeler[1]

[1] School of Earth and Environmental Sciences, University of Queensland
[2] Department of Geosciences, Boise State University
[3]MGPalaeo, Perth
[4]Geoscience Australia, Canberra
[5]Department of Natural Resources and Mines, Geological Survey of Queensland, Brisbane

3.1. Abstract

This study presents the first CA-IDTIMS U-Pb zircon ages from tuffs in Lopingian (upper Permian) strata of the Galilee Basin, Queensland, and reassigns the A and B seams to the Bandanna and 'Burngrove equivalent' formations, respectively. Five Lopingian tuffs were dated: four from CRD Montani 1 well, including one from the 'Burngrove Formation equivalent' (252.81 ± 0.07 Ma, approximately the age of the Yarrabee Tuff in the Bowen Basin) and three from the 'Fair Hill Formation equivalent' (254.32 ± 0.10, 254.41 ± 0.07 and 255.13 ± 0.09 Ma). A tuff from the Black Alley Shale in GSQ Tambo 1-1A well yielded a date of 254.09 ± 0.06 Ma. All three units are constituents of the Betts Creek Group, here formally elevated in nomenclatural status from the Betts Creek beds. On the western margin of the basin, the Betts Creek Group thins, and the 'J and K' seams (formerly known as the Crossmore and Glenaras sequence, respectively) in GSQ Muttaburra 1 well have been interpreted through palynology as Cisuralian-early Guadalupian (spore-pollen assemblage APP3.2). This corroborates the exclusion of the 'J and K' seams from the overlying Lopingian Betts Creek Group (spore-pollen assemblage APP5), and the underlying early to mid Cisuralian Aramac Coal Measures (spore-pollen assemblage APP2.2), which represent the uppermost unit of the Joe Joe Group. It is proposed that the 'J and K' seams occur locally in a depression created by the Hulton-Rand Structure. The recognition of these APP3.2 strata suggests that the mid-Permian hiatus is reduced to 12-13 My from 30 My (where the 'J and K' seams are absent). The results of the radiogenic isotope dating and palynological analysis in the Galilee Basin support the proposed, albeit informal stratigraphy.

Key words: CA-IDTIMS, Geochronology, Palynology, Galilee Basin, Bowen Basin, Lopingian, Stratigraphy

3.2. Introduction

Integrated geochronological and palynological studies help to establish unambiguous stratigraphic relationships, both within and between sedimentary basins, and especially in non-marine sediments that show high lateral facies variability (e.g. Marzoli et al., 2004; Metcalfe et al., 2015; Santos et al., 2006). Ambiguity in Lopingian (upper Permian) coal seam correlations across the Koburra Trough, Galilee Basin, led Phillips et al. (2017c) to propose revision and formal nomenclatural elevation of the embracing Betts Creek beds to group status, a recommendation here undertaken (Figures 12 and 13). The Betts Creek Group (beds) has been referred to as a condensed section and, based on compression flora (e.g. *Glossopteris*) and palynology, is a collective correlative of the Lopingian Moranbah, Fort Cooper and Rangal coal measures in the northern Bowen Basin and their stratigraphic equivalents in other regions of the basin. When lithostratigraphically correlated from the Galilee to the Bowen basin, not all coal groups intersected by drilling fitted neatly into the Lopingian strata. The aim of this study was to test the revised correlations for the Betts Creek Group using palynology and high-precision chemical abrasion-isotope dilution thermal ionization mass spectrometry (CA-IDTIMS) U-Pb zircon dating of volcanic ash layers. In particular, from east to west in the basin, where the 'J and K' seams (previously known as the Glenaras and Crossmore sequences, respectively, Phillips et al., 2015), had more similarities with the older Aramac Coal Measures. Of the several evolving palynostratigraphic schemes proposed for the Permian successions of Queensland (e.g. Evans, 1967; Paten, 1969; Price, 1976; Price et al., 1985), the commonly used alphanumeric zonal nomenclature of Price (1997) is followed here. No radiogenic isotope dating had previously been conducted on the Lopingian strata from the Galilee Basin, although CA-IDTIMS ages have been recently obtained from the Cisuralian section therein (Nicoll et al., 2015, 2016a, 2016b).

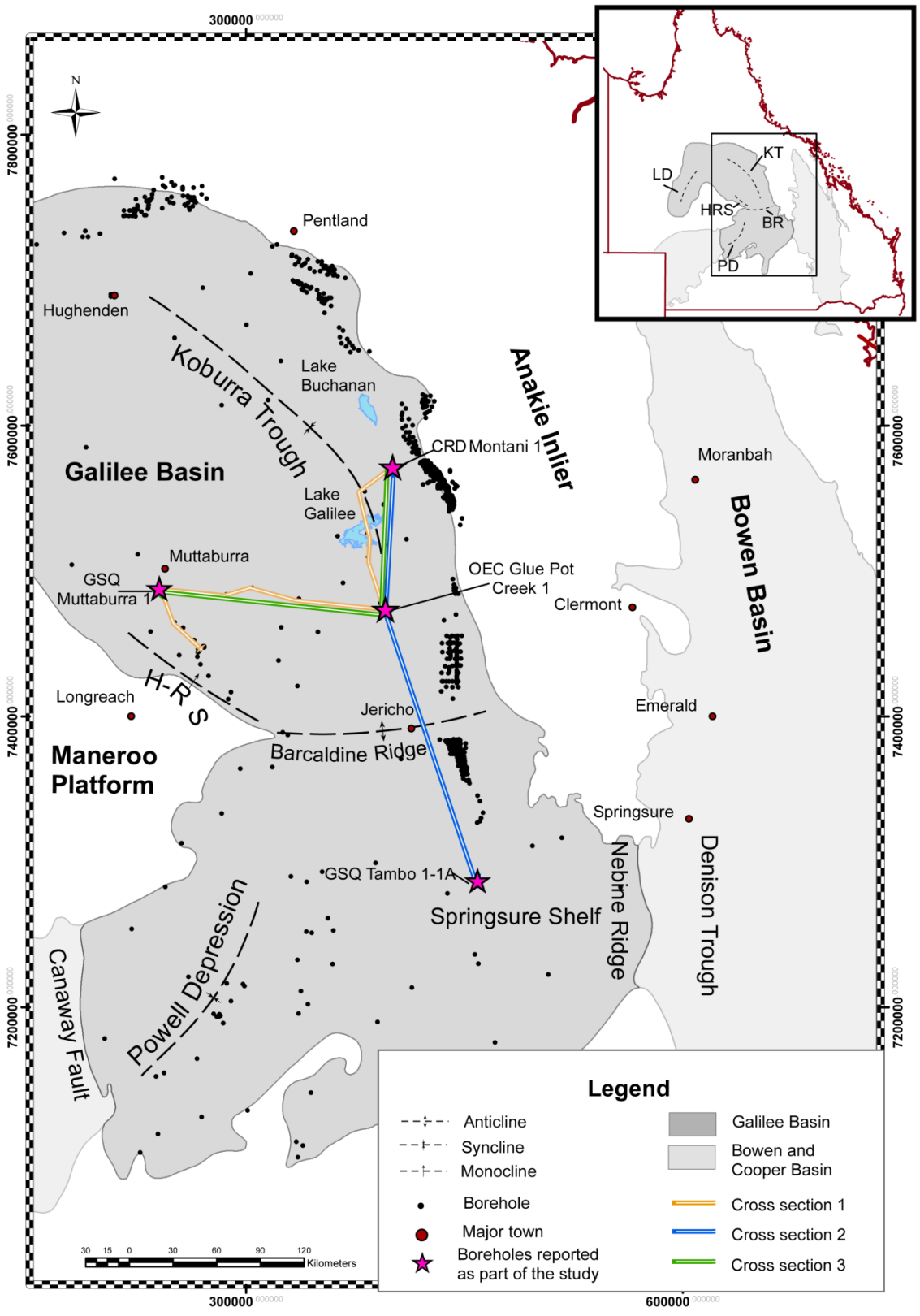

Figure 12: Map of the Galilee and Bowen Basins, showing major structural features and borehole locations. Cross section presented in this study is shown. Key structural features for the Galilee Basin are shown in the inset map. Abbreviations: LD – Lovelle Depression, KT – Koburra Trough, HRS – Hulton-Rand Structure, BR – Barcaldine Ridge and PD – Powell Depression.

3.3. Geological setting

The intracratonic Galilee Basin (Figure 12) covers 247,000 km^2 of central Queensland, Australia. The strata in the basin range from the latest Mississippian(?) – Pennsylvanian (mid to late Carboniferous) to late Middle Triassic (Figure 13) and are part of the larger late Paleozoic – early Mesozoic sedimentary basin system that encompassed much of Queensland and New South Wales. The Canaway Ridge, to the south-west, separates the Galilee Basin from the Cooper Basin, and to the south-east, the Nebine Ridge separates the Galilee Basin from the Bowen Basin (Figure 12). During the Permian, sedimentation extended across the Nebine Ridge (central Springsure Shelf) from the Bowen Basin into the Galilee Basin. Contrastingly, interpreted seismic lines (Hoffman, 1988) and geophysical wireline logs (McKellar, 2013) suggest that the Canaway Ridge was generally an active barrier to sedimentation between the Galilee and Cooper basins.

There are three main depocentres in the sickle-shaped Galilee Basin: the Lovelle Depression (in the north-west), the Koburra Trough (in the north-east), and the Powell Depression (in the south) (Figure 12). This paper deals with the basin's north-eastern region, which is partly bordered by metasedimentary rocks and granites of the Maneroo Platform to the south-west. Although the sediment pile can be up to 2866 m thick (FPN Koburra 1), it is highly variable and averages 800 m basin-wide (McKellar and Henderson, 2013).

3.4. Current stratigraphic framework of the Permian

Lithostratigraphy

Late Mississippian(?) to Cisuralian strata in the Galilee Basin are collectively known as the Joe Joe Group, and they are at their thickest in the Koburra Trough (1781 m; Gray and Swarbrick, 1975). The Joe Joe Group comprises four formations (oldest to youngest): the Lake Galilee Sandstone, Jericho Formation (including the Oakleigh Siltstone Member), Jochmus Formation (including the Edie Tuff Member) and the Aramac Coal Measures (Figure 13). The Lake Galilee Sandstone is confined to the northernmost area of the western Springsure Shelf and the Koburra Trough and the Jericho Formation is absent from the Lovelle Depression. The Jochmus Formation is observed in the north-western, north-eastern and northernmost southern areas of the basin and the Aramac Coal Measures are restricted to the north-western and central-western parts of the basin (Scott et al., 1995).

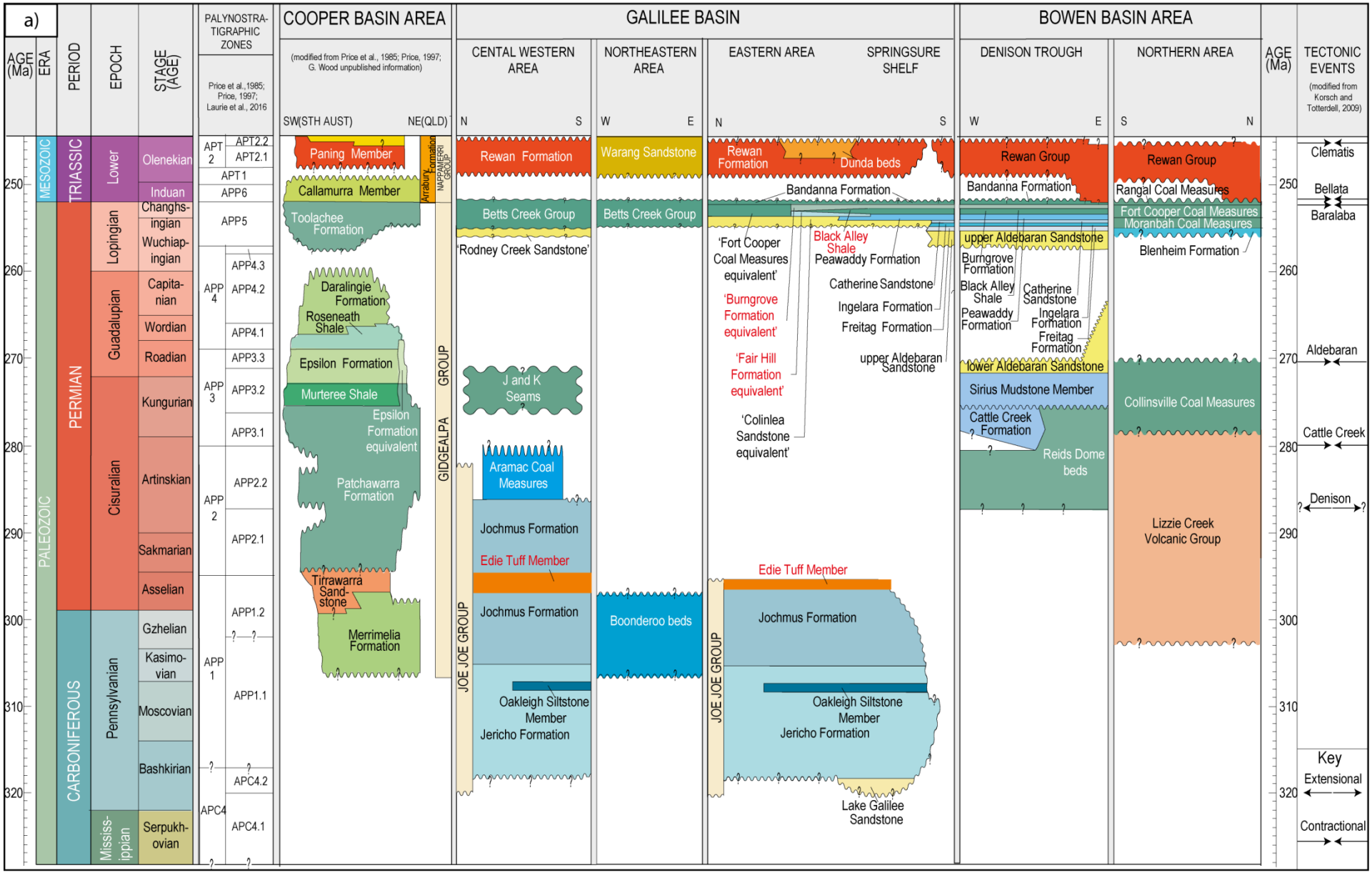
a)
AGE (Ma)
ERA
PERIOD
EPOCH
STAGE (AGE)
PALYNOSTRA-TIGRAPHIC ZONES
Price et al.,1985; Price, 1997; Laurie et al., 2016
COOPER BASIN AREA
(modified from Price et al., 1985; Price, 1997; G. Wood unpublished information)
SW(STH AUST)
NE(QLD)
GALILEE BASIN
CENTAL WESTERN AREA
NORTHEASTERN AREA
EASTERN AREA
SPRINGSURE SHELF
N
S
W
E
BOWEN BASIN AREA
DENISON TROUGH
NORTHERN AREA
TECTONIC EVENTS
(modified from Korsch and Totterdell, 2009)
MESOZOIC
PALEOZOIC
TRIASSIC
PERMIAN
CARBONIFEROUS
Lower
Lopingian
Guadalupian
Cisuralian
Pennsylvanian
Mississ-ippian
Olenekian
Induan
Changhs-ingian
Wuchiap-ingian
Capita-nian
Wordian
Roadian
Kungurian
Artinskian
Sakmarian
Asselian
Gzhelian
Kasimo-vian
Moscovian
Bashkirian
Serpukh-ovian
APT 2
APT2.2
APT2.1
APT1
APP6
APP5
APP 4
APP4.3
APP4.2
APP4.1
APP 3
APP3.3
APP3.2
APP3.1
APP 2
APP2.2
APP2.1
APP 1
APP1.2
APP1.1
APC4
APC4.2
APC4.1
Paning Member
Callamurra Member
Toolachee Formation
Arraluru Formation
NAPPAMERRI GROUP
GIDGEALPA GROUP
Daralingie Formation
Roseneath Shale
Epsilon Formation
Murteree Shale
Epsilon Formation equivalent
Patchawarra Formation
Tirrawarra Sand-stone
Merrimelia Formation
Rewan Formation
Betts Creek Group
'Rodney Creek Sandstone'
J and K Seams
Aramac Coal Measures
Jochmus Formation
Edie Tuff Member
Jochmus Formation
Oakleigh Siltstone Member
Jericho Formation
JOE JOE GROUP
Warang Sandstone
Betts Creek Group
Boonderoo beds
Rewan Formation
Dunda beds
Bandanna Formation
'Fort Cooper Coal Measures equivalent'
'Burngrove Formation equivalent'
'Fair Hill Formation equivalent'
'Colinlea Sandstone equivalent'
Black Alley Shale
Peawaddy Formation
Catherine Sandstone
Ingelara Formation
Freitag Formation
upper Aldebaran Sandstone
Edie Tuff Member
Jochmus Formation
Oakleigh Siltstone Member
Jericho Formation
Lake Galilee Sandstone
JOE JOE GROUP
Rewan Group
Bandanna Formation
upper Aldebaran Sandstone
Burngrove Formation
Black Alley Shale
Peawaddy Formation
Catherine Sandstone
Ingelara Formation
Freitag Formation
lower Aldebaran Sandstone
Sirius Mudstone Member
Cattle Creek Formation
Reids Dome beds
Rewan Group
Rangal Coal Measures
Fort Cooper Coal Measures
Moranbah Coal Measures
Blenheim Formation
Collinsville Coal Measures
Lizzie Creek Volcanic Group
AGE (Ma)
250
260
270
280
290
300
310
320
Clematis
Bellata
Baralaba
Aldebaran
Cattle Creek
Denison
Key
Extensional
Contractional

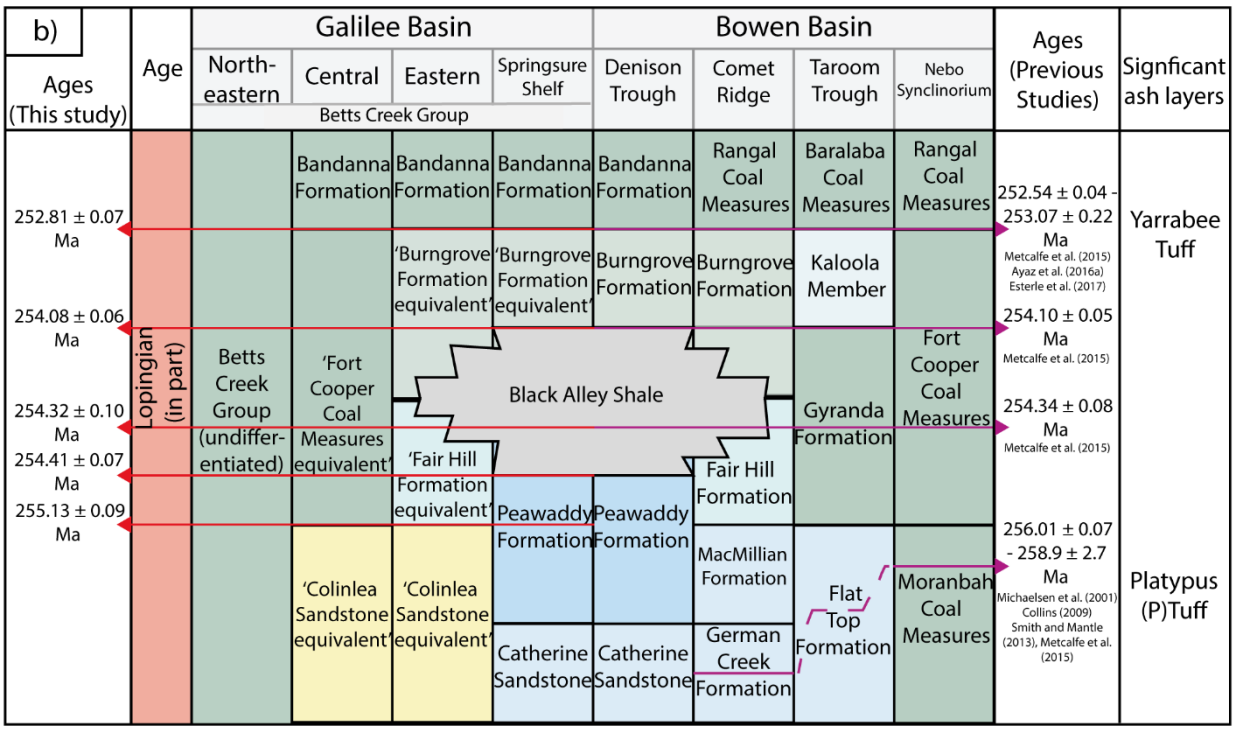

Figure 13: a) Stratigraphy of the Galilee, Bowen and Cooper Basins used in this study (modified from McKellar and Henderson, 2013). Stratigraphic names in red text represent units CA-IDTIMS dated as part of this study. Palynology modified from Laurie et al. (2016); Price et al. (1985); Price (1997). Stratigraphy modified from Draper (2013); McKellar and Henderson (2013); Phillips et al. (2017c); Price et al. (1985); Price (1997). Tectonic events modified from Korsch and Totterdell (2009b). b) Detailed late Permian stratigraphy of the Galilee and Bowen Basins. Previously published dates are shown with relation to their significant ash layers and stratigraphic position in the Bowen Basin to the right (modified from Ayaz et al., 2016a). Dates from this study and their stratigraphic relationship in the Galilee Basin are shown on the left. For ages and sample numbers shown in figure see Appendix 8.5.

Due to the differential development of Lopingian lithostratigraphic nomenclature across the Galilee Basin, different names have been applied to the same unit. To avoid confusion, the present study will refer to the Lopingian stratigraphy of Phillips et al. (2017c), shown in Figure 13b. The 'Rodney Creek Sandstone' is only observed in the central-western margin of the basin, abutting the Maneroo Platform. It is correlative to the Ingelara Formation on the Springsure Shelf. Overlying this, the Betts Creek Group (Figure 13), which is here formally elevated in status[2] from the previous terminology of the Betts Creek beds (e.g. Scott and Hawkins, 1992; Vine et al., 1964) can be subdivided through coal seam correlation (Phillips et al., 2017b) into the (ascending stratigraphically): The 'Colinlea Sandstone equivalent', the 'Fort Cooper Coal Measures equivalent' and the Bandanna Formation. The 'Colinlea Sandstone equivalent', which contains coal seams, is recognised in the Koburra Trough and along the eastern margin of the basin. As implied, it is

[2]The elevation in nomenclatural status was proposed by Phillips et al., (2017). Considering the Field Geologist's guide to Lithostratigraphic Nomenclature in Australia (Staines, 1985), beds, formations and groups are defined as follows: 'beds' are the smallest lithostratigraphic unit and are distinguishable individual layers. When combined they are upgraded to a 'Formation'. If a number of formations have unifying features, the stratigraphic nomenclature can be upgraded to 'Group'. For the Betts Creek Group, the reason for rank elevations from beds to Group is based on identification in the attendant succession of the coal bearing formations in the Bandanna Formation, 'Fort Cooper Coal Measures equivalent' and 'Colinlea Sandstone equivalent' (descending stratigraphic order). As these formations/formation equivalents are here recognised in the Betts Creek beds, the unit is no longer poorly defined, although the formation-equivalent units therein are in need of formal recognition and description.

considered to be an equivalent of the Colinlea Sandstone (Mollan et al., 1969) on the Springsure Shelf. The Colinlea Sandstone is stratigraphically equivalent to the Catherine Sandstone and Peawaddy Formation of the Denison Trough in the Bowen Basin (Figure 13).

Overlying this, the characteristically tuffaceous 'Fort Cooper Coal Measures equivalent' is recognised in the west and north of the Galilee Basin. Towards the south of the basin and onto the Springsure Shelf, the 'Fort Cooper Coal Measures equivalent' can be split into the lower 'Fair Hill Formation equivalent' and the upper 'Burngrove Formation equivalent'. The 'Fair Hill Formation' interfingers with the marine Black Alley Shale on the Springsure Shelf. The Black Alley Shale has been mapped transgressing north into the Galilee Basin (Allen and Fielding, 2007b; Phillips et al., 2017c; Scott et al., 1995) and pinches out between the 'Fair Hill Formation equivalent' and the 'Burngrove Formation equivalent' (Figure 13). Overlying the 'Burngrove Formation equivalent', the Bandanna Formation is recognised across the basin. The Lopingian strata have a cumulative thickness of approximately 200 m (Australia Pacific LNG, 2010; EEAPL, 1993), whereas the Bowen Basin correlatives have a thickness of >1 km.

Using the tuffaceous 'Fair Hill Formation equivalent' seam as a marker horizon, west-to-east cross sections of geophysical wireline logs (Phillips et al., 2015, 2017b) showed a possible discrepancy along the central-western margin in coal seam nomenclature and age. Phillips et al. (2015, 2017b) identified the 'J and K' seams (Figures 13 and 15), which, in the main, had been placed in the Lopingian Betts Creek Group (e.g. AGL Energy, 2012; Galilee Energy Limited, 2001; Holland and Bocking, 2008). These coal seams overly the Cisuralian Aramac Coal Measures and do not have correlatives on the eastern margin (Figure 15). Original palynological analysis of GSQ Muttaburra 1 (McKellar, 1991), a stratigraphic borehole drilled on the central-western margin, assigned strata identified as the 'J and K' seams by Phillips et al. (2017b), to the Cisuralian Aramac Coal Measures. This age has not been ascribed to other wells in the area and the age and lateral continuity of these seams is still unclear (Phillips et al., 2015).

Chronostratigraphy

All geochronological dates presented in this study are given at 2σ unless otherwise stated. No previous geochronological data exist for the Lopingian strata of the Galilee Basin. Radiogenic isotope ages for formations from the adjacent Bowen Basin are discussed (Figure 13b). A significant marker horizon in the Moranbah Coal Measures of the Bowen Basin, the Platypus (P) Tuff, was initially dated by Sensitive High Resolution Ion Microprobe (SHRIMP) mass spectrometry at 258.9 ± 2.7 Ma (1σ) (Michaelsen et al., 2001) and 257 ± 1.5 Ma (1σ) (Collins,

2009) and then by CA-IDTIMS at 256.01 ± 0.07 Ma (Metcalfe et al., 2015; Smith and Mantle, 2013).

A number of ashes in the Black Alley Shale in the Bowen Basin were dated by Metcalfe et al. (2015). A sample towards the base yielded an age of 254.34 ± 0.08 Ma, and one from the top yielded an age of 254.10 ± 0.05 Ma (Figure 13b). Ayaz et al. (2016a) dated a series of ashes in the tuffaceous Fort Cooper Coal Measures and its subdivisions, the Burngrove and Fair Hill formations in the Bowen Basin, using CA-IDTIMS. These were dated at 252.85 ± 0.16 to 254.03 ± 0.03 Ma, providing additional age constraints to the Fort Cooper Coal Measures. The Yarrabee Tuff is a large regional marker horizon that stratigraphically separates the underlying Fort Cooper Coal Measures and the overlying Bandanna-Rangal-Baralaba Coal Measures. Several studies have dated this ash due to its regional significance and have provided ages of 252.54 ± 0.04 Ma (Metcalfe et al., 2015), 252.69 ± 0.16 - 253.07 ± 0.22 Ma (Ayaz et al., 2016a) and 252.85 ± 0.07 - 252.92 ± 0.07 Ma (Esterle et al., 2017; Figure 13b).

Regional ash layer marker horizons in other Australian basins were dated by Metcalfe et al. (2015). The Nobbys Tuff from near the base of the Newcastle Coal Measures in the Newcastle and Hunter coalfields of the Sydney Basin is a 0.5-25 m (Geoscience Australia, 2016a) thick ash layer that is dated at 255.02 ± 0.03 and 255.26 ± 0.07 Ma (Metcalfe et al., 2015). The Awaba Tuff in the Sydney Basin is a regionally extensive ash layer near the top of the Newcastle Coal Measures that is dated at 253.14 ± 0.04, 253.21 ± 0.06 and 253.25 ± 0.04 Ma (Metcalfe et al., 2015). The Awaba and Yarrabee tuffs represent a short-lived period of volcanic activity during the Changhsingian along eastern Australia.

Palynostratigraphy

An initial review of the palynology of the Galilee Basin was conducted by Norvick (1974) using Evans' (1967, 1969) zonal scheme. However, the palynostratigraphic assessment undertaken herein utilises the widely applied zonal scheme devised by Price (1997). This hierarchical scheme is constructed using the first appearance datums of distinctive and wide-ranging eastern Australian taxa, with less distinctive, rarer or more localised marker taxa retained as subzone indicators. Further, recent work conducted by Geoscience Australia (Bodorkos et al., 2016; Laurie et al., 2016; Nicoll et al., 2015) has recalibrated Price's palynozones against the Geologic Time Scale (Gradstein et al., 2012) using CA-IDTIMS methodology (Figure 14). Compared to the previous calibration by Mantle et al. (2010), which was undertaken with limited constraints on the numerical values assigned to zonal boundaries, some of the adjustments made are significant and have implications for regional modelling of depositional rates, and both pan-Australian and international correlations.

The present study applies the new calibration of Price's zones (Bodorkos et al., 2016; Laurie et al., 2016) to the Galilee Basin (Figure 14).

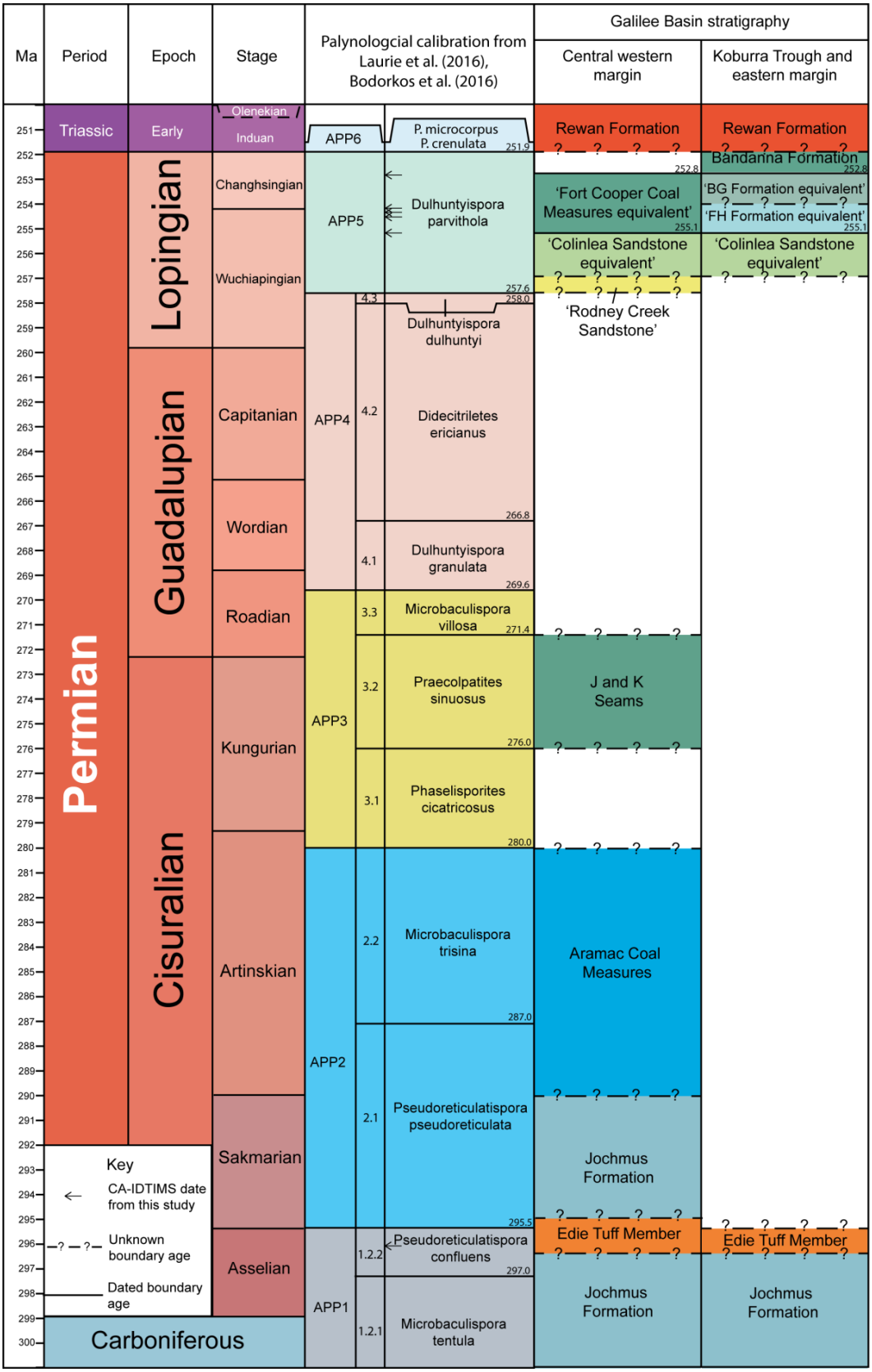

Figure 14: Palynostratigraphic column for the Galilee Basin with nomenclature used in this study (modified from Bodorkos et al., 2016). Revised calibration of palynostratigraphy from Bodorkos et al. (2016) and Laurie et al. (2016). APP6 abbreviations: *Protohaploxypinus microcorpus* and *Playfordiaspora crenulata*. Arrows indicate a CA-IDTIMS date obtained in this study. Galilee Basin stratigraphy abbreviations: BG – Burngrove and FH – Fair Hill.

The late Mississippian(?) – Cisuralian Joe Joe Group (including the Jochmus Formation, Edie Tuff Member and Aramac Coal Measures, Figures 13a, 14 and 15) in the Galilee Basin is placed within the APP1 and APP2 palynological zones (Nicoll et al., 2015, 2016b; Figures 13a and 14). A major unconformity has been interpreted above the Joe Joe Group, with a hiatus encompassing the APP3 and APP4 palynological zones. A possible exception being the enigmatic Weston beds, observed in a single well (HPP Weston 1) in the Lovelle Depression, which are assigned to APP4.1 (Price, 1974, 1997). The Lopingian Epoch is considered to span approximately 8 My and contains three palynostratigraphic units: part of APP4.2 (*Didecitriletes ericianus* Zone), APP4.3 (*Dulhuntyispora dulhuntyi* Zone) and APP5 (*Dulhuntyispora parvithola* Zone) (Laurie et al., 2016; Metcalfe et al., 2015; Figure 13). Unit APP5 comprises a series of subzones, which are often only locally recognisable and have been inconsistently applied in the past. The *Micrhystridium evansii* acme event of the Gunnedah and Bowen basins represents a regional marine incursion into the eastern Australian Permian basins within APP5 (Price, 1997; Smith and Mantle, 2013). Stratigraphically, the acme sits between the Peawaddy Formation and the overlying Black Alley Shale in the Bowen Basin. With the use of palynology and geochronology Laurie et al. (2016), provisionally placed the event at 255 Ma. The appearance of this acme, limited to marine conditions, is not applicable for correlations where terrestrial environments prevailed. The Betts Creek Group and subdivisions lie within the APP5 zone (McKellar and Henderson, 2013; Figures 13 and 14). By utilising chrono- and biostratigraphic analyses of samples obtained from the Galilee Basin, this study will be able to confirm or refute the current lithostratigraphic correlations, as discussed above.

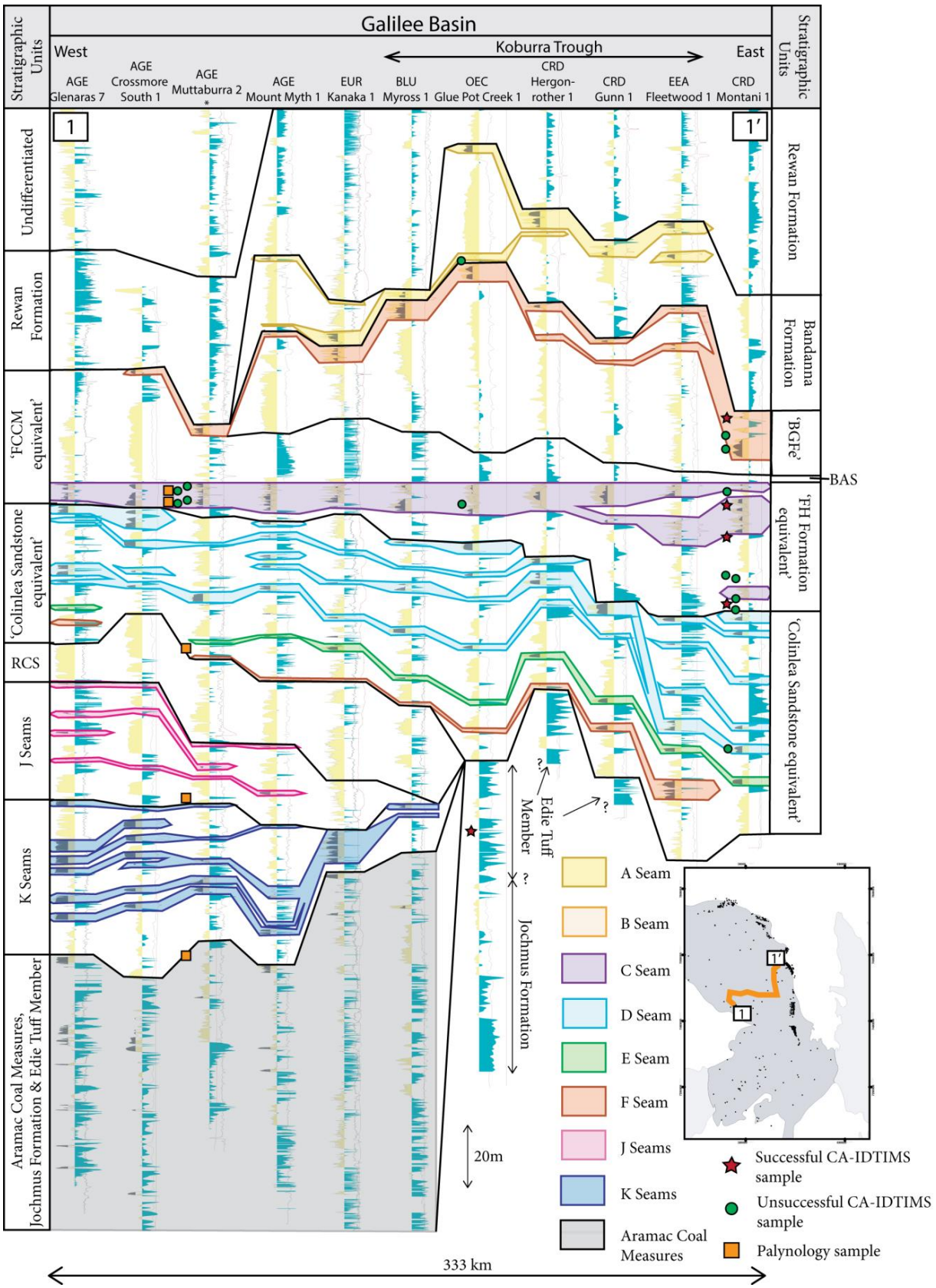

Figure 15: Correlation from west to east across the Galilee Basin (modified from Phillips et al., 2015, 2017b, 2017c). See Figure 12 and insert for cross section location. Red stars represent sample locations that yielded sufficient zircons for CA-IDTMS analysis. Green circles represent sample locations that did not yield sufficient zircons for CA-IDTMS analysis. Orange squares represent palynology sample locations. * note that GSQ Muttaburra 1 is not shown in the cross section. Sample locations from GSQ Muttaburra 1 are correlated to AGE Muttaburra 2, a well 10 kms to its east. Abbreviations: BGFe – 'Burngrove Formation equivalent' BAS – Black Alley Shale, FH – Fair Hill and RCS – 'Rodney Creek Sandstone'.

3.5. Sampling and Methods

Detailed sedimentological logging in four key wells, GSQ Muttaburra 1, GSQ Tambo 1-1A, OEC Glue Pot Creek 1 and CRD Montani 1 (Figure 12), identified volcanic ash layers and organic mudstones through the Permian sequences. The strategy of the study was to choose drill holes across the study area to obtain a wide regional coverage. In total, 24 ash layers were sampled for CA-IDTIMS (See Appendix 8.6): four from GSQ Muttaburra 1, five from GSQ Tambo 1-1A, three from OEC Glue Pot Creek 1 and twelve from CRD Montani 1.

Six samples yielded sufficient zircons for CA-IDTIMS analyses. For palynological analysis, five organic-rich mudstone samples from GSQ Muttaburra 1 were processed. The palynological slides from the previous study (McKellar, 1991) of this stratigraphic drill hole were also re-examined, and new slides were made from the palynological residues kept by the Geological Survey of Queensland from McKellar's (1991) study.

LA-ICPMS methods

Zircon grains were separated from ashes using an ultrasonic method (Hoke et al., 2014) and annealed at 900ºC for 60 hours in a muffle furnace. Randomly selected grains were mounted in epoxy and polished until their centres were exposed. Cathodoluminescence (CL) (Figure 16) images were obtained with a JEOL JSM-1300 scanning electron microscope and Gatan MiniCL. Zircon was analysed by laser ablation inductively coupled plasma mass spectrometry (LA-ICPMS) using a ThermoElectron X-Series II quadrupole ICPMS and New Wave Research UP-213 Nd:YAG UV (213 nm) laser ablation system. In-house analytical protocols, standard materials, and data reduction software were used for acquisition and calibration of U-Pb dates and a suite of high field strength elements (HFSE) and rare earth elements (REE). Zircon was ablated with a laser spot of 25 µm wide using fluence and pulse rates of 5 J/cm^2 and 10 Hz, respectively, during a 45 second analysis (15 sec gas blank, 30 sec ablation) that excavated a pit ~25 µm deep. Ablated material was carried by a 1.2 L/min He gas stream to the nebulizer flow of the plasma. Quadrupole dwell times were 5 ms for Si and Zr, 200 ms for ^{49}Ti and ^{207}Pb, 80 ms for ^{206}Pb, 40 ms for ^{202}Hg, ^{204}Pb, ^{208}Pb, ^{232}Th, and ^{238}U and 10 ms for all other HFSE and REE; total sweep duration is 950 ms. Background count rates for each analyte were obtained prior to each spot analysis and subtracted from the raw count rate for each analyte. For concentration calculations, background-subtracted count rates for each analyte were internally normalized to ^{29}Si and calibrated with respect to NIST SRM-610 and -612 glasses as the primary standards. Ablations pits that appear to have intersected glass or mineral inclusions were identified based on Ti and P signal excursions, and associated sweeps were discarded. U-Pb dates from these analyses are considered valid if the U-Pb ratios appear to have

been unaffected by the inclusions. Signals at mass 204 were normally indistinguishable from zero following subtraction of mercury backgrounds measured during the gas blank (<1000 cps ^{202}Hg), and thus dates are reported without common Pb correction. Rare analyses that appear contaminated by common Pb were rejected based on mass 204 greater than baseline. Temperature was calculated from the Ti-in-zircon thermometer (Watson et al., 2006). Because there are no constraints on the activity of TiO_2 in the source rocks, an average value in crustal rocks of 0.8 was used.

Data were collected in one experiment in June 2016. For U-Pb and $^{207}Pb/^{206}Pb$ dates, instrumental fractionation of the background-subtracted ratios was corrected and dates were calibrated with respect to interspersed measurements of zircon standards and reference materials. The primary standard Plešovice zircon (Sláma et al., 2008) was used to monitor time-dependent instrumental fractionation based on two analyses for every 10 analyses of unknown zircon. A secondary correction to the $^{206}Pb/^{238}U$ dates was made based on results from the zircon standards Seiland (530 Ma, unpublished data, Boise State University) and Zirconia (327 Ma, unpublished data, Boise State University), which were treated as unknowns and measured once for every 10 analyses of unknown zircon. These results showed a linear age bias of several percent that is related to the ^{206}Pb count rate. The secondary correction is thought to mitigate matrix-dependent variations due to contrasting compositions and ablation characteristics between the Plešovice zircon and other standards (and unknowns).

Radiogenic isotope ratio and age error propagation for all analyses includes uncertainty contributions from counting statistics and background subtraction. The error on the weighted mean calculation includes uncertainties from the standard calibration during the experiment. These uncertainties are the local standard deviations of the polynomial fits to the interspersed primary standard measurements versus time for the time-dependent, relatively larger U/Pb fractionation factor, and the standard errors of the means of the consistently time-invariant and smaller $^{207}Pb/^{206}Pb$ fractionation factor. These uncertainties are 1.7% (2 σ) for $^{206}Pb/^{238}U$ and 1.3% (2σ) for $^{207}Pb/^{206}Pb$. Age interpretations are based $^{206}Pb/^{238}U$ dates. Errors on the dates from individual analyses are given at 2σ.

CA-IDTIMS U-Pb Geochronology Methods

U-Pb dates were obtained by the CA-IDTIMS method from analyses composed of single zircon grains (Table 2), modified after Mattinson (2005). Zircon was separated from ashes and imaged with CL as described above. Zircon was removed from the epoxy mounts for dating based on CL images, with grains that appear to have inherited cores being avoided, and put into 3 ml Teflon PFA beakers, rinsed with 3.5 M HNO_3 and ultrapure H_2O before being loaded into 300 µl Teflon PFA

microcapsules. Fifteen microcapsules were placed in a large-capacity Parr vessel and the grains partially dissolved in 120 µl of 29 M HF for 12 hours at 180°C. The contents of the microcapsules were returned to 3 ml Teflon PFA beakers, HF removed, and the residual grains immersed in 3.5 M HNO_3, cleaned in an ultrasonic bath for an hour, and fluxed on a hotplate at 80°C for an hour. This chemical abrasion process is to ensure that any domains that may have suffered Pb loss are removed. The HNO_3 was removed and grains were rinsed twice in ultrapure H_2O before being reloaded into the 300 µl Teflon PFA microcapsules (rinsed and fluxed in 6 M HCl during sonication and washing of the grains) and spiked with the EARTHTIME mixed ^{233}U-^{235}U-^{205}Pb tracer solution. Zircon was dissolved in Parr vessels in 120 µl of 29 M HF with a trace of 3.5 M HNO_3 at 220°C for 48 hours, dried to fluorides, and re-dissolved in 6 M HCl at 180°C overnight. U and Pb were separated from the zircon matrix using an HCl-based anion-exchange chromatographic procedure (Krogh, 1973), eluted together and dried with 2 µl of 0.05 N H_3PO_4.

Pb and U were loaded on a single outgassed Re filament in 5 µl of a silica-gel/phosphoric acid mixture (Gerstenberger and Haase, 1997), and U and Pb isotopic measurements made on a GV Isoprobe-T multicollector thermal ionization mass spectrometer equipped with an ion-counting Daly detector. Pb isotopes were measured by peak-jumping all isotopes on the Daly detector for 100 to 160 cycles, and corrected for 0.16 ± 0.03%/a.m.u. (1 sigma error) mass fractionation. Transitory isobaric interferences due to high-molecular weight organics, particularly on ^{204}Pb and ^{207}Pb, disappeared within approximately 30 cycles, while ionization efficiency averaged 10^4 cps/pg of each Pb isotope. Linearity (to $\geq 1.4 \times 10^6$ cps) and the associated deadtime correction of the Daly detector were monitored by repeated analyses of NBS982, and have been constant since installation. Uranium was analyzed as UO_2^+ ions in static Faraday mode on 10^{12} ohm resistors for 200-300 cycles, and corrected for isobaric interference of $^{233}U^{18}O^{16}O$ on $^{235}U^{16}O^{16}O$ with an $^{18}O/^{16}O$ of 0.00206. Ionization efficiency averaged 20 mV/ng of each U isotope. U mass fractionation was corrected using the known $^{233}U/^{235}U$ ratio of the EARTHTIME tracer solution.

CA-IDTIMS U-Pb dates and uncertainties were calculated using the algorithms of Schmitz and Schoene (2007), EARTHTIME ET535 tracer solution (Condon et al., 2015) with calibration of $^{235}U/^{205}Pb$ = 100.233, $^{233}U/^{235}U$ = 0.99506, and $^{205}Pb/^{204}Pb$ = 11268, and U decay constants recommended by Jaffey et al. (1971). $^{206}Pb/^{238}U$ ratios and dates were corrected for initial ^{230}Th disequilibrium using a Th/U[magma] = 3.0 ± 0.3 using the algorithms of Crowley et al. (2007), resulting in an increase in the $^{206}Pb/^{238}U$ dates of ~0.09 Ma. All common Pb in analyses was attributed to laboratory blank and subtracted based on the measured laboratory Pb isotopic composition and associated uncertainty. U blanks are estimated at 0.05 pg.

Ages of ash layer deposition are interpreted from $^{206}Pb/^{238}U$ dates. Weighted mean dates are calculated from equivalent dates (probability of fit >0.05) using Isoplot 3.0 (Ludwig, 2003). Errors on the weighted mean dates are given as ± x / y / z, where x is the internal error based on analytical uncertainties only, including counting statistics, subtraction of tracer solution, and blank and initial common Pb subtraction, y includes the tracer calibration uncertainty propagated in quadrature, and z includes the ^{238}U decay constant uncertainty propagated in quadrature. Internal errors should be considered when comparing our dates with $^{206}Pb/^{238}U$ dates from other laboratories that used the same EARTHTIME tracer solution or a tracer solution that was cross-calibrated using EARTHTIME gravimetric standards. Errors including the uncertainty in the tracer calibration should be considered when comparing our dates with those derived from other geochronological methods using the U-Pb decay scheme (e.g. laser ablation ICPMS). Errors including uncertainties in the tracer calibration and ^{238}U decay constant (Jaffey et al., 1971) should be considered when comparing our dates with those derived from other decay schemes (e.g. $^{40}Ar/^{39}Ar$, ^{187}Re-^{187}Os). Errors for weighted mean dates and dates from individual grains are given at 2σ.

Palynological methods

The five new samples from GSQ Muttaburra 1 were processed for palynological analysis using the standard preparatory techniques outlined by Phipps and Playford (1984) and Wood et al. (1996). The samples, weighing between 40 and 80 g, were scrubbed and washed to remove any drilling additives or modern spore-pollen contaminants. They were then crushed to a 2–5 mm diameter grit and immersed in 100 ml of hydrochloric acid (32%) to remove any calcareous minerals. The hydrochloric acid reactions were found not to be particularly vigorous, and only a short maceration time (approximately 30 minutes) was required for each sample, which were then left in 100 ml of cold hydrofluoric acid (48%) for 24 hours to remove the majority of the siliciclastic minerals. Following neutralisation, the samples were washed through hydrochloric acid to remove any fluorides that may have formed, prior to heavy mineral separation using zinc bromide (specific gravity 2.1). The resulting float was again neutralised before filtering through 10 µm and 100 µm nylon sieves to remove fine organic particles and coarser woody fragments, respectively. The kerogen fraction was subjected to a moderately short oxidation (30 sec) in nitric acid (69%), followed by a final neutralisation and mounting of the residue on glass slides for microscopic analysis.

Five samples (960.65 m 1055.02 m, 1063.66 m, 1074.98 m, 1081.65 m), which were documented in the original stratigraphic drilling report for GSQ Muttaburra 1 (McKellar, 1991), were also re-examined here. To obtain semi-quantitative assemblage compositions, one hundred palynomorphs were counted from each of the newly processed and the five original samples. The remainder of the

assemblages were then scanned to locate further marker taxa falling outside of these counts. The recorded palynofloras were assessed against the zonal scheme of Price (1997) and the results of these analyses are summarised in Table 3; selected taxa are illustrated in Figure 18.

3.6. Results

LA-ICPMS results

CL imaging shows dark and light grains in sample MON_48 (821.58 m). To determine if there was a drastic age difference between the CL dark and CL light grains, LA-ICPMS was performed. Nineteen grains were analysed, the 12 youngest of which are equivalent in age with weighted mean of 259 ± 5 Ma (MSWD = 1.5, probability of fit = 0.11). Older dates are 274 ± 13 to 501 ± 21 Ma (Table 1). There is no statistically significant age difference in the youngest population between the CL dark and CL light grains, therefore, both groups underwent CA-IDTIMS.

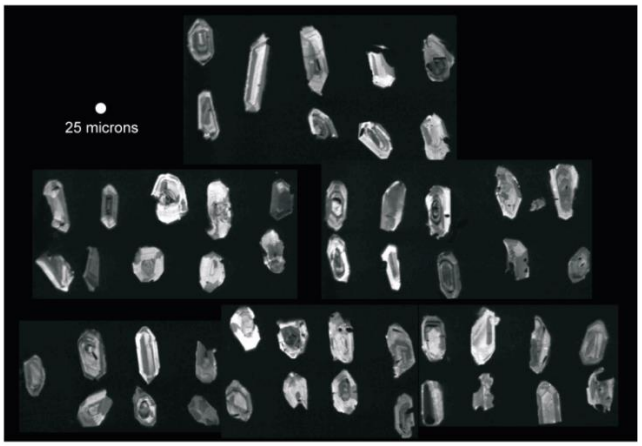

Figure 16: Cathodoluminescence (CL) images of zircons from sample MON_45, (829.19 m).

	Corrected isotope ratios							Dates (Ma)						
Analysis	207Pb* 235U*	±2s (%)	206Pb* 238U	±2s (%)	error corr.	207Pb* 206Pb*	±2s (%)	207Pb* 206Pb*	±2s (Ma)	207Pb* 235U	±2s (Ma)	206Pb* 238U*	±2s (Ma)	% disc.
MON_48 S 17	0.6339	7.62	0.0809	4.40	0.55	0.0568	6.22	486	137	499	30	501	21	-3
MON_48 M 9	0.4025	4.10	0.0547	2.96	0.65	0.0534	2.83	347	64	343	12	343	10	1
MON_48 S 28	0.3756	10.19	0.0530	6.20	0.59	0.0514	8.09	259	186	324	28	333	20	-29
MON_48 S 33	0.4221	9.82	0.0470	3.13	0.29	0.0651	9.31	777	196	358	30	296	9	62
MON_48 M 8	0.3326	13.17	0.0456	5.18	0.38	0.0529	12.10	324	275	292	33	288	15	11
MON_48 M 10	0.3161	5.50	0.0451	3.95	0.68	0.0508	3.82	232	88	279	13	284	11	-22
MON_48 L 1	0.2795	12.49	0.0435	4.97	0.38	0.0466	11.46	31	275	250	28	274	13	-778
MON_48 M 6	0.3149	8.99	0.0429	5.19	0.56	0.0533	7.34	341	166	278	22	**270**	**14**	21
MON_48 M 7	0.3405	8.26	0.0427	4.70	0.55	0.0578	6.79	522	149	298	21	**270**	**12**	48
MON_48 S 15	0.3312	15.14	0.0427	4.80	0.31	0.0562	14.36	462	318	291	38	**270**	**13**	42
MON_48 S 13	0.3615	16.57	0.0420	4.60	0.27	0.0624	15.92	688	340	313	45	**265**	**12**	61
MON_48 M 4	0.2906	9.84	0.0416	5.00	0.49	0.0507	8.48	226	196	259	22	**263**	**13**	-16
MON_48 M 2	0.3547	9.65	0.0415	4.06	0.40	0.0620	8.76	675	187	308	26	**262**	**10**	61
MON_48 M 12	0.3062	8.95	0.0412	4.32	0.46	0.0539	7.84	365	177	271	21	**261**	**11**	29
MON_48 M 11	0.2777	11.14	0.0407	4.04	0.34	0.0495	10.39	170	243	249	25	**257**	**10**	-51
MON_48 S 32	0.2756	6.74	0.0404	2.78	0.36	0.0494	6.14	168	143	247	15	**256**	**7**	-52
MON_48 M 3	0.3016	5.82	0.0402	3.53	0.56	0.0544	4.63	389	104	268	14	**254**	**9**	35
MON_48 S 30	0.2821	12.51	0.0402	3.50	0.26	0.0509	12.00	238	277	252	28	**254**	**9**	-7
MON_48 S 31	0.3599	7.41	0.0401	2.70	0.32	0.0651	6.90	776	145	312	20	**254**	**7**	67
								Weighted mean date (Ma), error includes standard calibration uncertainty and is at 2 sigma.				**259**	**5**	

Experiment on June 4, 2016
Isotope ratio and date errors do not include systematic calibration errors of 1.32% (207Pb/206Pb), 1.68% (206Pb/238U) (2 sigma).
Trace element concentrations were deleted from analyses known to have intersected inclusions of other minerals based on P and Ti.
Ablation used a laser spot size of 25 microns, and a laser firing repetition rate of 10 Hz.
Activity of TiO2 for Ti-in-Zircon temperature calculation is 0.8.
Dates shown in bold were used in weighted mean calculation, the results of which are shown.

Table 1: LA – ICPMS isotopic U-Pb data. For full elemental composition see Appendix 8.7.

CA-IDTIMS results

Figure 17 and Table 2 present the CA-IDTIMS results. Six to eight grains were included in calculating the mean weighted depositional age. These grains were chosen based on (1) grains that yield equivalent dates are those that formed immediately before eruption and (2) the youngest grains are closest to the eruption age and older grains are detrital or inherited.'

Nine zircon grains from OEC Glue Pot Creek 1 (824.60 m, sample GPC_37) were analyzed, the seven youngest of which yielded a weighted mean date of 296.09 ± 0.07 / 0.16 / 0.35 Ma (MSWD = 1.5, probability of fit = 0.19). This is the interpreted deposition age. Two other grains that yielded dates of 296.42 ± 0.18 and 303.75 ± 0.19 Ma are interpreted as containing inherited components or to be detrital.

Seven zircon grains from CRD Montani 1, at a depth of 851.47 m (sample MON_31) were analyzed, the six youngest of which yielded a weighted mean date of 255.13 ± 0.09 / 0.15 / 0.31 Ma (MSWD = 0.8, probability of fit = 0.55). This is the interpreted deposition age. A grain that yielded a date of 256.82 ± 0.21 Ma is interpreted as containing an inherited component or to be detrital.

Nine zircon grains from CRD Montani 1, at a depth of 829.19 m (sample MON_45) were analyzed, the eight youngest of which yielded a weighted mean date of 254.41 ± 0.07 / 0.14 / 0.31 Ma (MSWD = 1.8, probability of fit = 0.08). This is the interpreted deposition age. A grain that yielded a date of 283.64 ± 0.19 Ma is interpreted as containing an inherited component or to be detrital.

Nine zircon grains from CRD Montani 1, at a depth of 821.58 m (sample MON_48) were analyzed, the six youngest of which yielded a weighted mean date of 254.32 ± 0.10 / 0.16 / 0.31 Ma (MSWD = 1.9, probability of fit = 0.09). This is the interpreted deposition age. Three other grains that yielded dates of 261.76 ± 0.17 to 265.26 ± 0.37 Ma are interpreted as containing inherited components or to be detrital.

Seven zircon grains from CRD Montani 1, at a depth of 796.77 (sample MON_60) were analyzed, the six youngest of which yielded a weighted mean date of 252.81 ± 0.07 / 0.14 / 0.30 Ma (MSWD = 1.1, probability of fit = 0.35). This is the interpreted deposition age. A grain that yielded a date of 253.99 ± 0.17 Ma is interpreted as containing an inherited component or to be detrital.

Seven zircon grains from GSQ Tambo 1-1A, at a depth of 810.25 m (sample TAM_29) were analyzed and yielded a weighted mean date of 254.08 ± 0.06 / 0.14 / 0.30 Ma (MSWD = 1.4, probability of fit = 0.21). This is the interpreted deposition age.

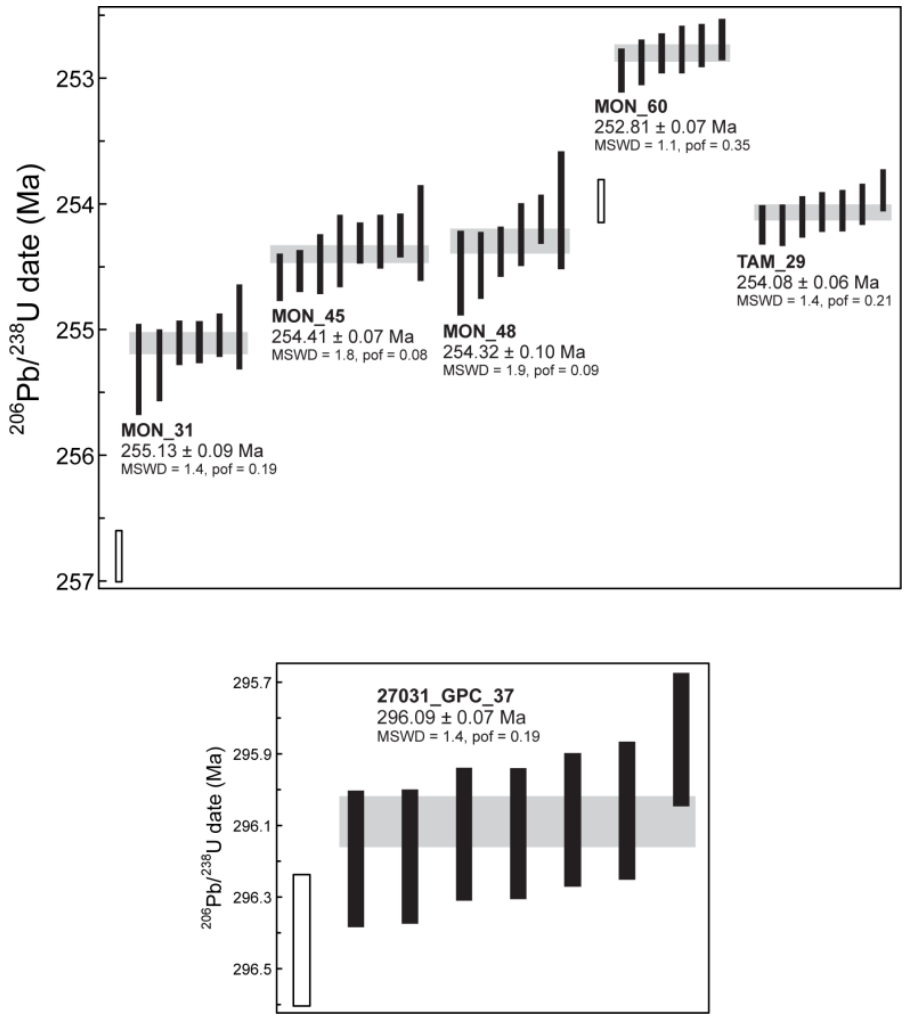

Figure 17: Plot of 206Pb/238U dates from single grains and fragments of zircon analysed by CA-IDTIMS. Plotted with Isoplot 3.0 (Ludwig, 2003). Error bars are at the 2 sigma confidence interval. A weighted mean date is shown and represented by the grey boxes behind the error bars. One older date from MON_45 (829.19 m) and three older dates from MON_48 (821.58 m) are not shown. Two older dates from GPC_37 (824.60 m) are not shown.

							Radiogenic Isotope Ratios								Isotopic Dates					
Sample	$\frac{Th}{U}$	$^{206}Pb^*$ x10^{-13} mol	mol % $^{206}Pb^*$	$\frac{Pb^*}{Pb_c}$	Pb_c (pg)	$\frac{^{206}Pb}{^{204}Pb}$	$\frac{^{208}Pb}{^{206}Pb}$	$\frac{^{207}Pb}{^{206}Pb}$	% err	$\frac{^{207}Pb}{^{235}U}$	% err	$\frac{^{206}Pb}{^{238}U}$	% err	corr. coef.	$\frac{^{207}Pb}{^{206}Pb}$	±	$\frac{^{207}Pb}{^{235}U}$	±	$\frac{^{206}Pb}{^{238}U}$	±
(a)	(b)	(c)	(c)	(c)	(c)	(d)	(e)	(e)	(f)	(e)	(f)	(e)	(f)		(g)	(f)	(g)	(f)	(g)	(f)
GPC_37																				
z1	0.784	1.7371	99.84%	202	0.23	11306	0.248	0.052227	0.076	0.338202	0.134	0.046965	0.064	0.945	295.37	1.74	295.81	0.34	295.86	0.19
z2	0.638	1.2690	99.84%	195	0.17	11310	0.202	0.052467	0.077	0.349023	0.135	0.048246	0.065	0.947	305.82	1.75	303.99	0.36	303.75	0.19
z3	0.898	1.1464	99.85%	224	0.14	12188	0.284	0.052276	0.068	0.338823	0.132	0.047008	0.063	1.002	297.49	1.56	296.28	0.34	296.13	0.18
z4	0.736	1.7778	99.87%	242	0.19	13706	0.233	0.052309	0.076	0.339040	0.134	0.047008	0.064	0.943	298.93	1.74	296.44	0.34	296.13	0.19
z5	0.728	1.5843	99.88%	265	0.16	15015	0.230	0.052340	0.071	0.339587	0.130	0.047056	0.063	0.966	300.28	1.62	296.86	0.34	296.42	0.18
z6	0.710	0.6987	99.62%	84	0.22	4808	0.225	0.052317	0.109	0.339015	0.162	0.046998	0.067	0.870	299.29	2.50	296.43	0.42	296.06	0.19
z7	0.737	1.2310	99.66%	93	0.35	5262	0.233	0.052181	0.096	0.338291	0.152	0.047019	0.066	0.916	293.34	2.18	295.88	0.39	296.20	0.19
z8	0.802	1.6394	99.58%	77	0.57	4324	0.254	0.052369	0.081	0.339381	0.141	0.047002	0.065	0.963	301.55	1.84	296.70	0.36	296.09	0.19
z9	1.077	0.8197	99.80%	173	0.14	9031	0.341	0.052380	0.092	0.339572	0.147	0.047019	0.065	0.909	302.02	2.10	296.85	0.38	296.19	0.19
MON_31																				
z1	0.589	0.9637	99.69%	100	0.25	5878	0.187	0.051314	0.114	0.285614	0.165	0.040368	0.067	0.840	254.97	2.63	255.10	0.37	255.12	0.17
z4	0.663	0.3537	99.34%	47	0.20	2717	0.210	0.051240	0.209	0.285208	0.251	0.040369	0.071	0.683	251.65	4.80	254.78	0.56	255.12	0.18
z5	0.780	0.0676	96.22%	8	0.22	477	0.247	0.050905	1.105	0.283582	1.187	0.040403	0.145	0.608	236.54	25.50	253.50	2.66	255.33	0.36
z6	0.562	0.1715	95.67%	7	0.64	418	0.178	0.051118	1.103	0.284381	1.198	0.040348	0.135	0.734	246.16	25.39	254.13	2.69	254.99	0.34
z7	0.485	0.5567	99.18%	36	0.38	2188	0.154	0.051174	0.215	0.284770	0.259	0.040359	0.070	0.715	248.67	4.95	254.43	0.58	255.06	0.18
z8	0.568	0.1329	97.99%	15	0.23	896	0.180	0.051523	0.586	0.286986	0.656	0.040398	0.114	0.666	264.29	13.45	256.18	1.49	255.30	0.29
z10	0.533	0.2147	98.91%	28	0.20	1658	0.169	0.051274	0.291	0.287336	0.336	0.040644	0.082	0.636	253.16	6.68	256.46	0.76	256.82	0.21
MON_45																				
z1	0.631	0.2079	95.80%	7	0.76	431	0.200	0.051192	0.931	0.283942	1.005	0.040228	0.154	0.538	249.47	21.43	253.78	2.26	254.25	0.38
z5	0.850	0.5248	98.16%	18	0.81	988	0.269	0.051250	0.394	0.284431	0.447	0.040251	0.115	0.563	252.11	9.05	254.17	1.00	254.39	0.29
z6	0.784	0.3965	98.43%	20	0.53	1147	0.249	0.051195	0.466	0.284041	0.513	0.040239	0.086	0.605	249.64	10.72	253.86	1.15	254.31	0.21
z9	0.674	0.6371	99.58%	75	0.22	4307	0.214	0.051382	0.148	0.285346	0.195	0.040277	0.067	0.796	258.02	3.39	254.89	0.44	254.55	0.17
z10	0.652	0.3414	99.28%	43	0.20	2519	0.207	0.051167	0.207	0.283897	0.255	0.040241	0.066	0.789	248.37	4.77	253.74	0.57	254.33	0.17
z11	0.696	0.3243	99.27%	43	0.20	2468	0.221	0.051338	0.253	0.285155	0.293	0.040285	0.075	0.617	256.02	5.82	254.74	0.66	254.60	0.19
z12	0.944	0.3125	99.22%	43	0.20	2309	0.299	0.051240	0.220	0.284231	0.264	0.040231	0.070	0.710	251.63	5.06	254.01	0.59	254.27	0.17
z13	0.100	0.3582	99.14%	31	0.26	2107	0.032	0.052095	0.219	0.323094	0.263	0.044982	0.070	0.713	289.56	4.99	284.28	0.65	283.64	0.19
z14	0.753	0.1574	96.51%	9	0.47	518	0.239	0.051361	0.825	0.285164	0.894	0.040268	0.096	0.748	257.06	18.95	254.75	2.01	254.49	0.24

Sample	Th/U	$^{206}Pb^*$ x10^{-13} mol	mol % $^{206}Pb^*$	Pb^*/Pb_c	Pb_c (pg)	$^{206}Pb/^{204}Pb$	$^{208}Pb/^{206}Pb$	$^{207}Pb/^{206}Pb$	% err	$^{207}Pb/^{235}U$	% err	$^{206}Pb/^{238}U$	% err	corr. coef.	$^{207}Pb/^{206}Pb$	±	$^{207}Pb/^{235}U$	±	$^{206}Pb/^{238}U$	±
(a)	(b)	(c)	(c)	(c)	(c)	(d)	(e)	(e)	(f)	(e)	(f)	(e)	(f)		(g)	(f)	(g)	(f)	(g)	(f)
MON_48																				
z1	0.713	0.7511	99.41%	54	0.37	3059	0.226	0.051504	0.167	0.294292	0.211	0.041442	0.068	0.746	263.45	3.83	261.93	0.49	261.76	0.17
z2	0.665	0.0612	93.90%	5	0.33	296	0.211	0.051127	1.723	0.283376	1.841	0.040199	0.188	0.659	246.56	39.66	253.33	4.13	254.06	0.47
z3	0.633	0.3247	98.15%	17	0.51	975	0.201	0.051544	0.477	0.285771	0.526	0.040210	0.078	0.676	265.23	10.95	255.22	1.19	254.14	0.19
z4	0.606	0.2004	97.48%	12	0.43	716	0.192	0.051061	0.865	0.283511	0.929	0.040270	0.107	0.634	243.59	19.92	253.44	2.08	254.50	0.27
z5	0.621	0.1452	98.41%	19	0.20	1132	0.197	0.051213	0.428	0.284071	0.482	0.040230	0.101	0.604	250.41	9.85	253.88	1.08	254.26	0.25
z6	0.726	0.1695	98.08%	16	0.28	940	0.230	0.051285	0.486	0.284628	0.540	0.040252	0.081	0.713	253.66	11.18	254.32	1.22	254.39	0.20
z7	0.629	0.1084	96.84%	10	0.29	571	0.199	0.051330	0.825	0.285071	0.897	0.040279	0.136	0.583	255.66	18.97	254.67	2.02	254.56	0.34
z8	0.855	0.2614	98.66%	24	0.29	1351	0.271	0.051286	0.389	0.297045	0.451	0.042007	0.142	0.563	253.72	8.95	264.09	1.05	265.26	0.37
z9	0.804	0.1920	97.79%	14	0.36	817	0.255	0.051398	0.603	0.295820	0.659	0.041743	0.105	0.592	258.71	13.85	263.13	1.53	263.63	0.27
MON_60																				
z1	0.867	0.5470	99.64%	91	0.17	4980	0.275	0.051230	0.128	0.282396	0.177	0.039979	0.066	0.824	251.18	2.94	252.56	0.39	252.70	0.16
z2	0.869	0.5785	99.42%	57	0.28	3150	0.276	0.051368	0.190	0.283368	0.228	0.040009	0.074	0.635	257.38	4.36	253.33	0.51	252.89	0.18
z3	0.732	0.3902	99.34%	48	0.22	2733	0.232	0.051183	0.172	0.282191	0.223	0.039987	0.070	0.804	249.07	3.95	252.39	0.50	252.75	0.17
z5	1.044	0.4316	98.00%	17	0.73	913	0.331	0.051335	0.337	0.283068	0.383	0.039993	0.077	0.663	255.88	7.75	253.09	0.86	252.79	0.19
z6	0.910	0.3710	99.45%	61	0.17	3295	0.289	0.051248	0.169	0.283958	0.214	0.040186	0.069	0.745	251.98	3.89	253.79	0.48	253.99	0.17
z7	0.833	0.8025	99.61%	85	0.26	4697	0.264	0.051234	0.092	0.282546	0.151	0.039997	0.064	0.954	251.38	2.11	252.68	0.34	252.81	0.16
z8	0.731	0.4989	99.18%	39	0.34	2219	0.232	0.051317	0.172	0.283159	0.219	0.040019	0.070	0.762	255.09	3.95	253.16	0.49	252.95	0.17
TAM_29																				
z1	0.596	1.5571	99.73%	112	0.36	6571	0.189	0.051339	0.105	0.284373	0.156	0.040173	0.067	0.851	256.09	2.41	254.12	0.35	253.91	0.17
z2	0.773	0.6184	99.63%	86	0.19	4840	0.245	0.051272	0.111	0.284198	0.170	0.040201	0.064	0.944	253.07	2.56	253.98	0.38	254.08	0.16
z3	0.540	0.6392	99.61%	78	0.21	4621	0.171	0.051348	0.133	0.284665	0.182	0.040207	0.067	0.815	256.50	3.07	254.35	0.41	254.12	0.17
z4	0.648	1.0964	99.57%	73	0.39	4224	0.205	0.051233	0.112	0.284097	0.166	0.040218	0.066	0.887	251.32	2.58	253.90	0.37	254.18	0.17
z5	0.614	2.0433	99.87%	244	0.22	14207	0.195	0.051431	0.067	0.285009	0.130	0.040191	0.066	0.979	260.21	1.54	254.62	0.29	254.02	0.16
z6	0.613	1.9191	99.76%	131	0.38	7665	0.194	0.051332	0.043	0.284646	0.123	0.040218	0.064	1.109	255.75	0.99	254.34	0.28	254.18	0.16
z7	0.623	0.4011	99.13%	35	0.29	2072	0.197	0.051198	0.204	0.283772	0.251	0.040199	0.066	0.788	249.73	4.69	253.65	0.56	254.07	0.16

(a) z1, z2, etc. are labels for analyses composed of single zircon grains that were annealed and chemically abraded (Mattinson, 2005). Labels in bold denote analyses used in weighted mean calculations.

(b) Model Th/U ratio calculated from radiogenic 208Pb/206Pb ratio and 207Pb/235U date.

(c) Pb* and Pbc are radiogenic and common Pb, respectively. mol % ^{206}Pb* is with respect to radiogenic and blank Pb.
(d) Measured ratio corrected for spike and fractionation only. Fractionation correction is 0.16 ± 0.03 (1 sigma) %/amu (atomic mass unit) for single-collector Daly analyses, based on analysis of EARTHTIME 202Pb-205Pb tracer solution.

(e) Corrected for fractionation and spike. Common Pb in zircon analyses is assigned to procedural blank with composition of 206Pb/204Pb = 18.04 ± 0.61%; 207Pb/204Pb = 15.54 ± 0.52%; 208Pb/204Pb = 37.69 ± 0.63% (1 sigma).
206Pb/238U and 207Pb/206Pb ratios corrected for initial disequilibrium in 230Th/238U using Th/U [magma] = 3.0 ± 0.3 (1 sigma).

(f) Errors are 2 sigma, propagated using algorithms of Schmitz and Schoene (2007) and Crowley et al. (2007).

(g) Calculations based on the decay constants of Jaffey et al. (1971). 206Pb/238U and 207Pb/206Pb dates corrected for initial disequilibrium in 230Th/238U using Th/U [magma] = 3.0 ± 0.3 (1 sigma).

Table 2: CA-IDTIMS U-Pb isotopic data.

Palynology

Palynological analyses (Table 3) of carbonaceous mudstone samples from GSQ Muttaburra 1 identified poorly preserved to well-preserved, yellow-brown palynomorphs (Figure 18). There was a moderate to very high diversity of spore-pollen grains, whereas microplankton never exceeded 6% of the microfossils found in one sample. All samples were interpreted to have a non-marine depositional setting as they do not contain marine dinoflagellate cysts (Appendix 8.9). Key findings are:

- The key datums identified in the assemblage recovered from 1101.09 m in the Aramac Coal Measures are very rare *Microbaculispora trisina,* frequent *M. tentula* and *Plicatipollenites* spp. and common *Horriditriletes tereteangulatus* (Table 3). Although no younger marker taxa were identified, an age of APP2.2 or younger is interpreted as McKellar (1991) recorded questionable specimens of both *Phaselisporites cicatricosus* (the APP3.1 marker taxon) and *Praecolpatites sinuosus* (the APP3.2 marker) in the underlying sample at 1193.62m.
- The regular occurrences of *Praecolpatites sinuosus*, in the absence of younger marker taxa, in assemblages from 1081.63, 1074.98, 1063.66, 1055.02, 1054.68 and 1046.86 m, indicate an age of APP3.2 for the middle of the 'J and K' seams (Table 3).
- Above the 'J and K' seams, the palynoflora from 1032.23 m (McKellar, 1991), in the basal 'Colinlea Sandstone equivalent' contains *Didecitriletes ericianus*, the index for APP4.2 (Price, 1997). However, McKellar (1991) interpreted an age of APP4.2–APP5 as the presence of *Brevitriletes hennellyi*, *Polypodiisporites* sp. cf. *P. mutabalis* and the high abundance of disaccate pollen are more typical of APP5, despite the lack of the associated zonal marker taxon, *Dulhuntyispora parvithola*.
- Samples from depths 982.88, 980.07, 975.78, 973.86 and 966.50 m (McKellar, 1991) in the 'Fort Cooper Coal Measures equivalent', contained *Dulhuntyispora parvithola* and ?*Microreticulatisporites bitriangularis*. This indicates an age of APP5 for the 'Fort Cooper Coal Measures equivalent'.
- A single sample (960.65 m McKellar, 1991) from the Rewan Formation yielded a diverse assemblage including rare *Protohaploxypinus microcorpus*, *Triplexisporites playfordii*, *Triquitrites proratus*, *Limatulasporites limatulus*, *Lunatisporites noviaulensis*, frequent *Brevitriletes hennellyi* and *Playfordiaspora crenulata* and common *Lundbladispora* spp. This combination of taxa indicates APP6 that is now considered to be earliest Triassic (Laurie et al., 2016), rather than latest Permian, as previously calibrated to the geologic timescale (Mantle et al., 2010). In the original drilling report for GSQ Muttaburra 1, Brain et

al. (1991) contrastingly picked the top of the Betts Creek beds (Group) and the base of the Rewan Formation at 950.05 m, thus associating this APP6 palynoflora with the Permian Betts Creek Group, rather than the Triassic Rewan Formation. Given the recent evidence that APP6 is earliest Triassic in age (Laurie et al., 2016), the boundary between the Permian Betts Creek Group and overlying Triassic Rewan Formation should be placed stratigraphically lower than 960.65 m in GSQ Muttaburra 1. However, the exact location of this boundary is unknown.

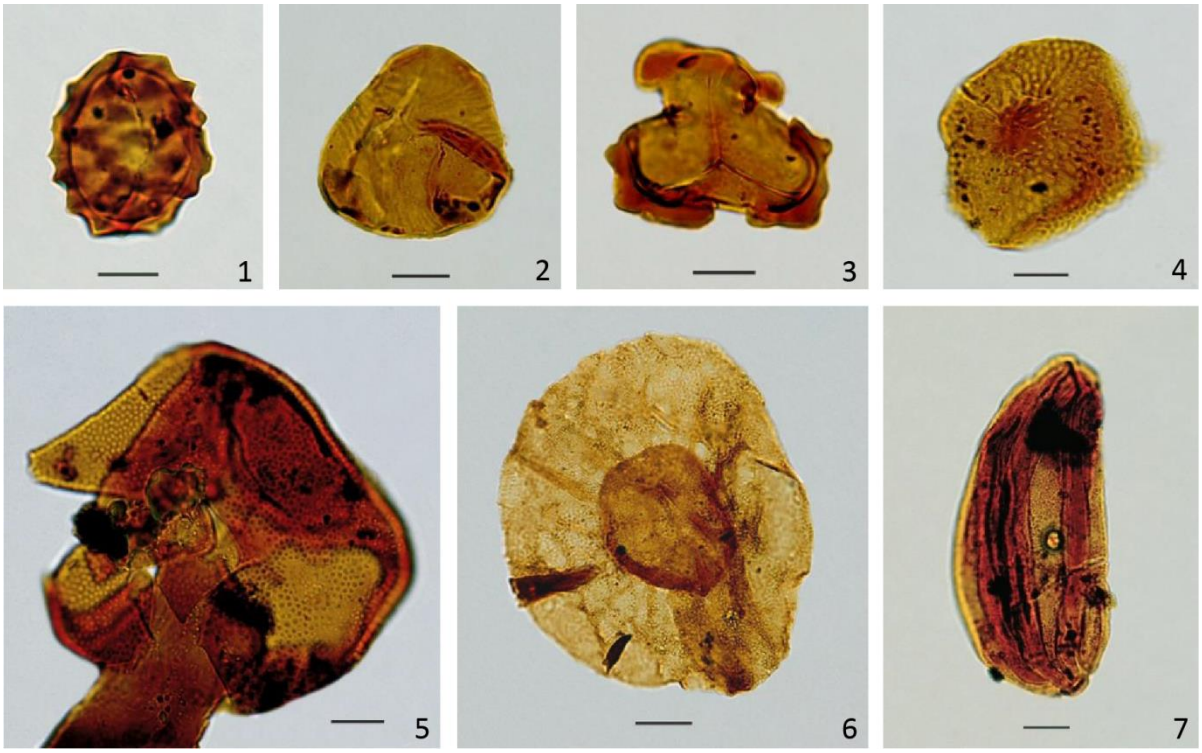

Figure 18: The scale bar is 10 microns in all images. 1) *Phaselisporites cicatricosus* (Balme and Hennelly) Price 1983. Sample: 1055.02m Muttaburra-1, slide 1. Proximal focus. EF coordinates V15/0. 2) *Triplexisporites playfordii* (de Jersey and Hamilton) Foster 1979. Sample: 960.65m Muttaburra-1, slide 1. Proximal focus. EF coordinates O15/1. 3) *Triquitrites proratus* Balme 1970. Sample: 960.65m Muttaburra-1, slide 1. Proximal focus. EF coordinates F29/3. 4) *Dulhuntyispora parvithola* (Balme and Hennelly) Potonié 1960. Sample: 962.0m Muttaburra-1, slide 1. Proximal focus on exoexinal blister of spore fragment. EF coordinates M13/2. 5) *Microbaculispora trisina* (Balme and Hennelly) Anderson 1977. Sample: 1055.02m Muttaburra-1, slide 1. Distal focus of crushed specimen. EF coordinates X35/0. 6) *Playfordiaspora crenulata* (Wilson) Foster 1979. Sample: 960.65m Muttaburra-1, slide 2. Proximal focus. EF coordinates O17/2. 7) *Praecolpatites sinuosus* (Balme and Hennelly) Bharadwaj and Srivastava 1969. Sample: 1055.02m Muttaburra-1, slide 1. Polar focus. EF coordinates N38/2.

FORMATION	TOP DEPTH [mbRT]	BASE DEPTH [mbRT]	SAMPLE TYPE	MICROFOSSIL YIELD	PRESERVATION	DIVERSITY (1)		SPORE & POLLEN ZONE / SUBZONE (Price 1997)	ENVIRONMENT (2)	KEY DATUMS	SOURCE
						MICROPLANK.	SPORE-POLLEN				
Rewan Formation	960.65	960.65	Core	High	Good	Very Low	Very High	APP6	Non-marine	P. microcorpus (R), T. playfordii (R), T. proratus (VR), B. hennellyi F),(R ay. crenulata (F), D. parvithola (R), L. limatula (R), L. noviaulensis (R), and common Lundbladispora spp. and large striate bisaccates.	McKellar (1991) and further slides prepared from residues and re-logged herein.
'Fort Cooper Coal Measures equivalent'	966.50	966.50	Core	High	Fair-Good	No new counts		APP5	Non-marine	D. parvithola (P)	McKellar (1991). Slides were unavailable for re-logging or photography.
	973.86	973.86	Core	Moderate-High	Fair	No new counts		APP5	Non-marine	D. parvithola (P)	McKellar (1991). Slides were unavailable for re-logging or photography.
	975.78	975.84	Core	Very High	Good-Fair	Very Low	Very High	APP5	Non-marine	B. cornutus (R), B. hennellyi (R), L. iphilegna (VR), Indospora baculata (VR), Praecolpatites ovatus (VR)	Processed and analysed herein.
	980.07	980.07	Core	Moderate-High	Fair	No new counts		APP5	Non-marine	D. parvithola (P)	McKellar (1991). Slides were unavailable for re-logging or photography.
	982.88	982.95	Core	Low	Fair	Very Low	High	APP5	Non-marine	D. parvithola (VR), ?M. bitriangularis (VR), M. trisina (VR), M. cf. villosa (VR)	Processed and analysed herein.
'Colinlea Sandstone equivalent'	1030.65	1030.72	Core	High	Fair	Very Low	Very High	APP4.2-APP5	Non-marine	D. ericianus (VR), M. villosa (VR), M. trisinus (VR), M. tentula (F), I. clara (R), P. cicatricosus (R), P. sinuosus (R -F)	Processed and analysed herein.
	1032.23	1032.23	Core	Moderate	Fair	No new counts		APP4.2-APP5 (probably APP5)	Non-marine (lacustrine influence)	B. gliksoniae (P), B. sp. cf. T. secatus (P), D. ericianus (P) and D. inornata (P).	McKellar (1991). Slides were unavailable for re-logging or photography
J and k Seams	1046.86	1046.86	Core	Moderate-High	Fair	No new counts		APP3.2.1.2-APP5 (probably APP5)	Non-marine (lacustrine influence)	M. sp. cf. M. indica (P), B. hennellyi (P), P. sp. cf. P. mutabilis (P), and R. diversiformis (P).	McKellar (1991). Slides were unavailable for re-logging or photography
	1054.68	1054.79	Core	High	Poor	Very Low	High	APP3.2	Non-marine	P. sinuosus (VR), M. tentula (F), D. townrowii (VR), M. trisina (R), mid nodosa (F), L. directus (C), Plicatipollenites spp. (F)	Processed and analysed herein.
	1055.02	1055.02	Core	High	Good-Fair	Very Low	Very High	APP3.2	Non-marine	P. sinuosus (VR), P. cicatricosus (R), M. trisina (C), M. tentula (C), M. micronodosa (F), P. pseudoreticulata (R), R. diversiformis (R), P. spinosa (VR), S. fusus (VR)	McKellar (1991) and further slides prepared from residues and re-logged herein.
	1063.66	1063.66	Core	Moderate	Fair	Very Low	Very High	APP3.2	Non-marine	P. sinuosus (VR), P. cicatricosus (VR), M. trisina (R), M. tentula (C), M. micronodosa (R), P. pseudoreticulata (R), R. diversiformis (R), S. fusus (VR)	McKellar (1991) and further slides prepared from residues and re-logged herein.
	1074.98	1074.98	Core	High	Good-Fair	Very Low	Very High	APP3.2	Non-marine	P. sinuosus (VR), P. hamatus (VR), M. trisina (R), M. tentula (C), M. micronodosa (R), P. pseudoreticulata (R), R. diversiformis (R), S. fusus (VR)	McKellar (1991) and further slides prepared from residues and re-logged herein.
	1081.63	1081.63	Core	High	Good-Fair	Very Low	Very High	APP3.2	Non-marine	P. sinuosus (VR), M. trisina (R), M. micronodosa (F)	McKellar (1991) and further slides prepared from residues and re-logged herein.
Aramac Coal Measures	1101.09	1101.17	Core	Low	Fair	Very Low	Moderate	APP2.2 or younger	Non-marine	M. trisina (VR), M. tentula (F), ?G. parvus (VR), Plicatipollenites spp. (F), H. tereteangulatus (C)	Processed and analysed herein.
	1193.62	1193.62	Core	Moderate-High	Good-Fair	No new counts		APP2.2–(?) APP3.1	Non-marine (lacustrine influence)	M. trisinus (P), P. cicatricosus (single questionable specimen), Botryococcus spp. (P), Maculatisporites spp. (P), Q. horridus (P), B. scissa (P), Tetraporina spp. (P)	McKellar (1991). Slides were unavailable for re-logging or photography

Table 3: Summary table of palynology results from the original GSQ Muttaburra 1 palynology report by McKellar (1991) as well as samples analysed in this study. Parentheses in key the datum column are abbreviated from: P – present (abundance unknown), VR – very rare, R – rare, F – frequent, C – common and A – abundant indicating the abundance of the key taxa within the sample. For details on (1) diversity and (2) environment see Appendix 8.9.

3.7. Implications for stratigraphy

Determining the age of the 'J and K' seams

No tuffaceous material was observed in the 'J and K' seams, therefore palynology has been used to determine the age of the 'J and K' seams. The presence of rare *Microbaculispora trisina* at 1101.09 m and 1193.62 m (Table 3) in GSQ Muttaburra 1 suggests a palynostratigraphic zone no older than APP2.2 (which is Artinskian and has a provisional age range from 280 to 287 Ma (Bodorkos et al., 2016; Figures 14 and 20) for the Aramac Coal Measures in the uppermost Joe Joe Group. CA-IDTIMS dates obtained from the Aramac Coal Measures by Nicoll et al. (2016a, 2016b) yielded ages of 282.72 ± 0.07 and 282.41 ± 0.08 Ma, which corroborate the APP2.2 age of the Aramac Coal Measures as assigned by McKellar (1991).

In GSQ Muttaburra 1, the 'J and K' seams (Phillips et al., 2017b, 2017c) were placed in the upper Aramac Coal Measures, based on the palynological assessment of McKellar (1991) who largely assigned this part of the succession to palynological unit APP3.1 of lower Permian (Cisuralian) age. The exception being a sample from the top of the 'J and K' seams (1046.86 m), where McKellar (1991) assigned an APP3.2.1.2 – APP5 age. Despite this, in subsequent well completion reports, the 'J and K' seams have been placed in the Lopingian Betts Creek Group.

A palynological sample from the 'J and K' seams (1054.79 m) contains *Praecolpatites sinuosus*, the index taxa for APP3.2. Reassessment of McKellar's (1991) GSQ Muttaburra 1 palynological samples confirmed that his *Praecolpatites sinuosus* records from 1046.86 m to 1081.63 m related to *Praecolpatites sinuosus 'corona'*[3]. These records, along with the lack of younger marker taxa, place the 'J and K' seams into the late Cisuralian – early Guadalupian. A newly processed sample from 1054.79 m in GSQ Muttaburra 1 was also found to contain rare *Praecolpatites sinuosus 'corona'* and thus further confirming the recognition of APP3.2 across the 'J and K' seams (Table 3, Figure 20).

[3] Although this species represented the designated index for unit 'APP3.2' (e.g. Price et al., 1985; specified as *Praecolpatites sinuosus* sp. 21), its biostratigraphic importance was not recorded by McKellar (1991). This is because of records of other varieties of the species from stratigraphically older units (such as the Reids Dome beds) in the adjacent Bowen Basin (e.g. Rigby and Hekel, 1977), although this was unstated in the original palynological report. Nonetheless, the reliability of *Praecolpatites sinuosus* 'corona' (sp. 21) has been subsequently confirmed as the index for unit APP3.2 (Price, 1997). Further, examination of new slides made from McKellar's (1991) palynological residues from his samples in the 1055.02–1081.63 m interval showed that the form reported by him as *Praecolpatites sinuosus* is of the *corona* 'variety', permitting reassignment of his samples to palynological unit APP3.2 (Table 3).

If the ‘J and K’ seams represent an upper section of the Aramac Coal Measures, or are a distinct stratigraphic unit separated from the underlying Aramac Coal Measures by a hiatus remains undetermined. Although the results in this study point towards the existence of a hiatus between the two units, further palynological sampling and sedimentary logging of core where both, the ‘J and K’ seams, as well as the Aramac Coal Measures exist, would better define their stratigraphic relationship (Figure 14).

Recognition of unit APP3.2 and its association with the ‘J and K’ seams also has implications for better assessing the time period embraced by the mid-Permian hiatus in the Galilee Basin. Nicoll et al. (2015) indicated a 30 My hiatus between strata assigned to the Artinskian and Wuchiapingian in the basin, but, with the occurrence of APP3.2 age rocks, the hiatus on the central-western margin of the Galilee Basin is shorter by 12-13 Ma than previously estimated (Figures 13a and 14), and similar to the adjacent Bowen Basin (Draper, 2013; McKellar and Henderson, 2013; Nicoll et al., 2015). This suggests that the Aldebaran contraction event (Figure 13a) of the Bowen Basin (Korsch and Totterdell, 2009b) had a similar effect on sedimentation in the Galilee Basin.

Galilee Basin correlations

No zircon bearing samples were recovered from the sediments of the ‘J and K’ seams, the ‘Rodney Creek Sandstone’ or the ‘Colinlea Sandstone equivalent’. The radiogenic isotope ages obtained in this study from the Permian strata of the Galilee Basin reveal two age groups (Figure 17, Table 2), Asselian (Cisuralian) and Wuchiapingian to Changhsingian (Lopingian) (Gradstein et al., 2012). The Asselian age is given to the Edie Tuff Member of the Jochmus Formation in the upper part of the Joe Joe Group on the eastern margin of the Galilee Basin. The Wuchiapingian to Changhsingian ages are given to the Betts Creek Group along the eastern margin and the Springsure Shelf.

Sample GPC_37 (OEC Glue Pot Creek 1, 824.60 m) from the Koburra Trough yielded an Asselian age of 296.09 ± 0.07 Ma (Figures 14 and 19). The result is surprising as the well completion report recorded this section of core as the Lopingian Betts Creek Group (Australia Pacific LNG, 2010). During the sampling procedure it was noted that the strata surrounding sample GPC_37 (OEC, Glue Pot Creek 1, 824.60 m) contained a distinctive red mineral. This red mineralisation is associated with the Edie Tuff Member (Gray and Swarbrick, 1975) and given the Cisuralian age of sample GPC_37 (OEC Glue Pot Creek 1, 824.60 m) the Edie Tuff Member in OEC Glue Pot Creek 1 has been recognised and placed between the depths 803 – 839.50 m (Figures 19 and 20). Therefore, sample GPC_37 was obtained from approximately the lower third of the member intersected in OEC Glue Pot Creek 1. Recently, an ash layer from the top of the Edie Tuff Member in OEC Glue Pot Creek 1 (803 m) was dated at 295.65 ± 0.07 Ma (R. Nicoll pers. comm.). Previous sampling of

two ash layers from near the top of the Edie Tuff Member in GSQ Muttaburra 1 (west of OEC Glue Pot Creek 1, Figure 12), reported by Nicoll et al. (2015), were dated as 294.80 ± 0.08 and 294.91 ± 0.09 Ma (Figure 20), approximately 850,000 years younger than the ash layer sampled at the top of the Edie Tuff Member in OEC Glue Pot Creek 1. This disparity in age suggests the eastern side of the Galilee Basin was more deeply eroded than the western margin prior to later Permian deposition.

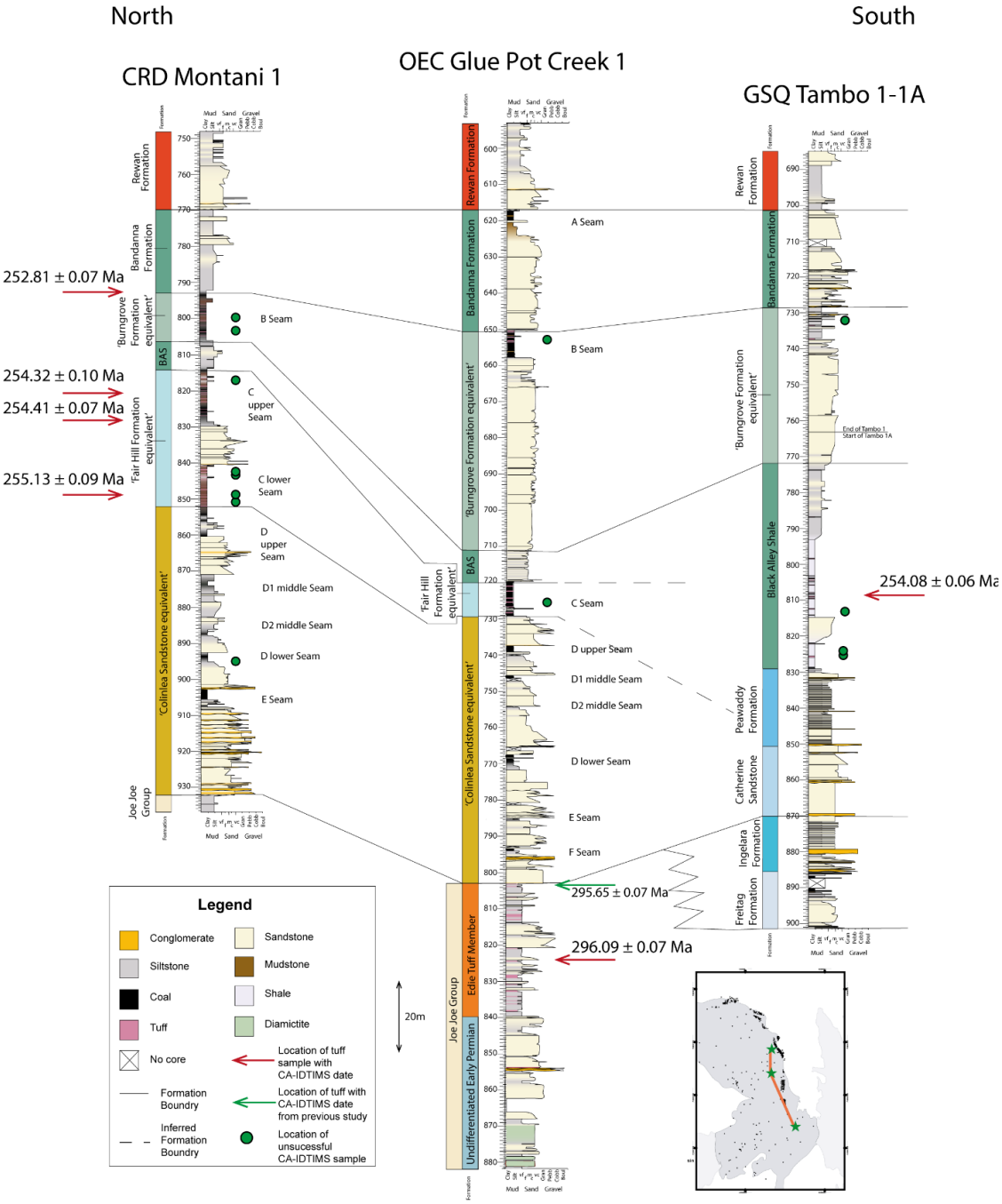

Figure 19: Sedimentary logging and correlation of three boreholes used in this study, CRD Montani 1, OCE Glue Pot Creek 1 and GSQ Tambo 1-1A, north to south in the basin with CA-IDTIMS dates superimposed. Green arrow shows previous CA-IDTIMS date from R. Nicoll (pers. comm.). See Figure 12 and inset map for cross section location.

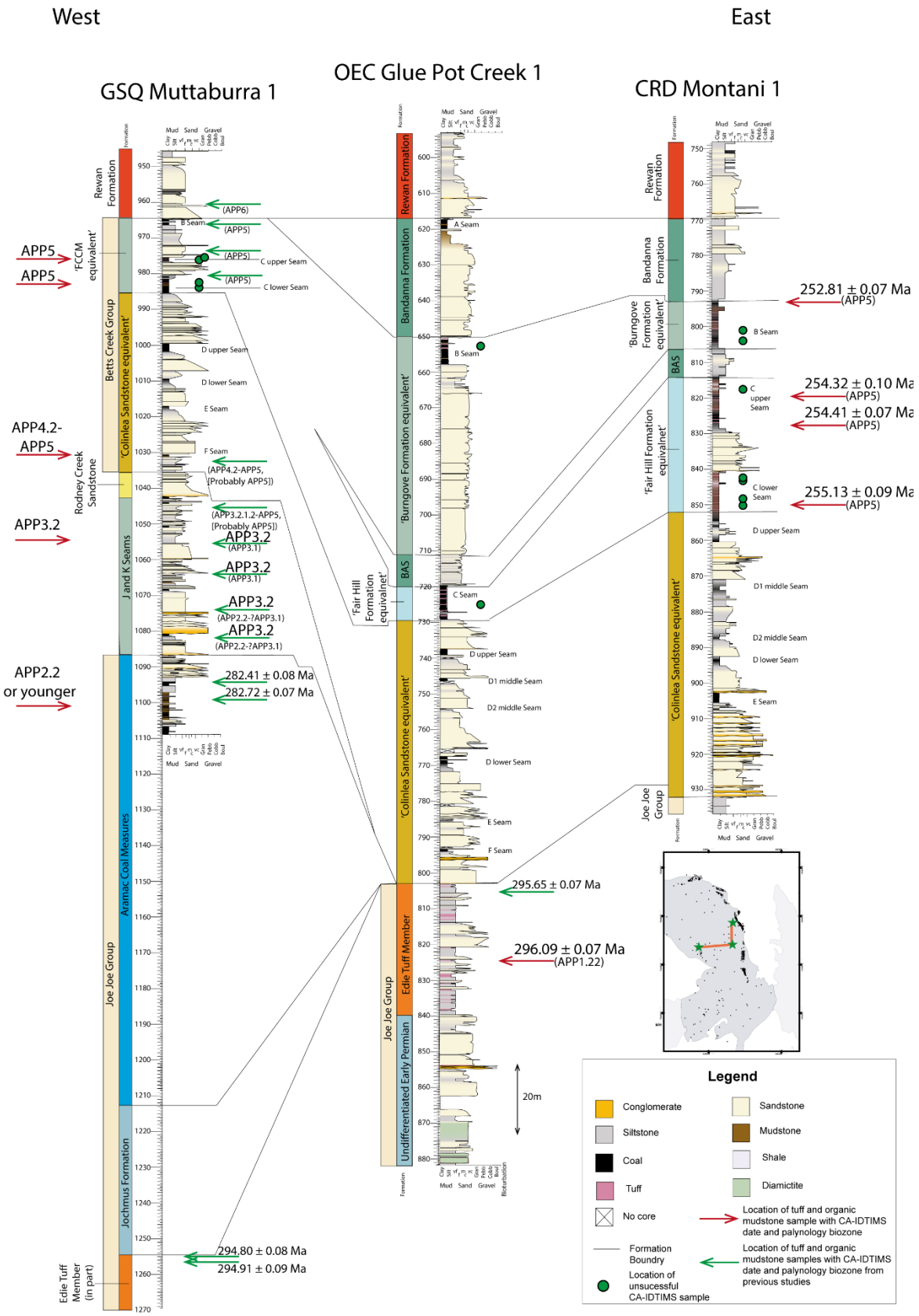

Figure 20: Correlation of three boreholes used in this study, GSQ Muttaburra 1, OCE Glue Pot Creek 1 and CRD Montani 1, west to east across the basin. GSQ Muttabura 1 was not fully logged. Formation boundaries for unlogged section derived from well completion report (Brain et al., 1991). Palynology and CA-IDTIMS results from this study are superimposed with red arrows. Green arrows show previous CA-IDTIMS dates from Nicoll et al. (2015) and R. Nicoll (pers. comm.) and palynology biozones from McKellar (1991). Re-analysed biozones from McKellar (1991) are shown above the green arrow. See inset map and Figure 12 for cross section location. Abbreviations: FCCM – 'Fort Cooper Coal Measures equivalent'.

Ages from the Black Alley Shale (254.08 ± 0.06 Ma from TAM_29, 810.25 m) in GSQ Tambo 1-1A and the upper 'Fair Hill Formation equivalent' (254.32 ± 0.10 Ma from MON_48, 821.58 m) in CRD Montani 1 differ by at least 0.08 Ma (Figure 19). This slight variance supports the interpretation that the C seam in CRD Montani 1 (MON_48, 821.58 m) is representative of a landward facies of the Black Alley Shale (Phillips et al., 2017c). In the Bowen Basin, Metcalfe et al. (2015) suggested an age range of 254.43 to 254.1 Ma for the Black Alley Shale, an age range that nearly encompass both of the above dates, thus affirming the suggested correlation.

Phillips et al. (2015, 2017b, 2017c) correlated the 'Fort Cooper Coal Measures equivalent' in GSQ Muttaburra 1 across into the Koburra Trough (Figures 12 and 15). With an APP5 age assigned to the 'Fort Cooper Coal Measures' in GSQ Muttaburra 1 (Table 3), and Lopingian CA-IDTIMS dates obtained from the Koburra Trough (Figures 17 and 19), the correlations between the west and east of the basin are supported (Figures 15 and 20).

Correlation between the Galilee and Bowen basins

The 254.08 ± 0.06 Ma age from an ash layer in the Black Alley Shale (TAM_29, 810.25 m) of the Galilee Basin (Figures 17 and 19; Table 2) is statistically indistinguishable from the 254.10 ± 0.05 Ma age retrieved from an ash layer at the top of the Black Alley Shale in the Bowen Basin (Metcalfe et al., 2015). This age correspondence reinforces the correlation between the stratigraphic units in both basins.

Previous correlations of the C seam, formally part of the Colinlea Sandstone (Scott and Hawkins, 1992), were interpreted to be lateral time equivalents to the upper section of the Moranbah Coal Measures in the Bowen Basin. However, the age of an ash layer from the Black Alley Shale (254.08 ± 0.06 Ma from TAM_29, 810.25 m) and the ages obtained from ash layers in the C seam in CRD Montani 1 (254.41 ± 0.07 and 254.31 ± 0.10 Ma from MON_45, 829.19 m and MON_48, 821.58 m, respectively) suggest that the C seam is a landward facies of the Black Alley Shale (Figure 19). This interpretation is strengthened by the similarity in ages between the base of the C Seam (255.13 ± 0.09 Ma, MON_31, 851.47 m) and the provisional 255 Ma age assigned to the acme event at the Peawaddy Formation/Black Alley Shale boundary in the Bowen Basin (Laurie et al., 2016). Therefore, the C seam in the Galilee Basin is correlatable to the Black Alley Shale in the Bowen Basin. Extending this interpretation northwards in the Bowen Basin, the C Seam is equivalent to the Fair Hill Formation and the lower part of the Fort Cooper Coal Measures (Figure 13b), a stratigraphic relationship that was proposed by Phillips et al. (2017c) in their revised intra basin correlation. Thus, the age of the ash layers in the C seam supports the stratigraphic correlations of Phillips et al. (2017c) and refutes previous correlations that the C seam was the lateral equivalent of

the Moranbah Coal Measures (256.01 ± 0.07 Ma - 258.9 ± 2.7 Ma (1σ), Collins, 2009; Metcalfe et al., 2015; Michaelsen et al., 2001; Smith and Mantle, 2013) in the Bowen Basin (Scott and Hawkins, 1992).

An ash layer from the upper section of the tuffaceous 'Burngrove Formation equivalent' which provides the boundary with the overlying Bandanna Formation was deposited at 252.81 ± 0.07 Ma (MON_60, 796.77 m) (Figures 17 and 19; Table 2). This age is slightly younger than published ages from the Awaba Tuff of the Sydney Basin (Metcalfe et al., 2015) and marginally older than the youngest tuff in the Bulli Coal Seam from the Newcastle Coal Measures (252.60 ± 0.04 Ma; Metcalfe et al., 2015). The proposed stratigraphy of Phillips et al. (2017c) suggests that the tuffaceous B and C coal seams of the Galilee Basin should be a separate formation, similar to that of the tuffaceous Fort Cooper Coal Measures which underlie the Yarrabee Tuff in the Bowen Basin (Figures 13b and 19). Nevertheless, without the presence of the Yarrabee Tuff in the Galilee Basin, the separation could only be speculation. The age of the ash layer at the top of the 'Burngrove Formation equivalent' in CRD Montani 1, 252.81 ± 0.07 Ma, is statistically indistinguishable from ages of the Yarrabee Tuff in the Bowen Basin, 252.54 ± 0.04 Ma to 253.07 ± 0.22 Ma (Metcalfe et al., 2015). Thus, the ash layer at the top of the 'Burngrove Formation equivalent' is interpreted to be the Yarrabee Tuff equivalent, therefore confirming the proposed division of the Bandanna Formation and underlying 'Burngrove Formation equivalent' in the Galilee Basin (Phillips et al., 2017c; Figures 13b and 19).

Correlation with other basins

In the Sydney Basin, the section from the Greta Coal Measures (Rowan Formation) to the top of the Wittingham Coal Measures contains moderately abundant ash layers associated with coal beds and have provided CA-IDTIMS dates ranging from 272 to 257 Ma (Laurie et al., 2016). However, no isotopic ages were obtained in the present study from the characteristically tuffaceous units (the 'Fort Cooper Coal Measures equivalent') in the Galilee Basin for correlation with the cited Sydney Basin dates. The maximum isotopic age obtained from the 'Fort Cooper Coal Measures equivalent' is 255.13 ± 0.09 Ma (CRD Montani 1, MON_31, 851.47 m) which is younger than isotopic ages derived from the Greta to Wittingham coal measures interval in the Sydney Basin, thus placing the 'Fort Cooper Coal Measures equivalent' stratigraphically higher. The Nobbys Tuff, located in the lower Newcastle Coal Measures, of the Sydney Basin, has been dated at 255.02 ± 0.03 Ma (Metcalfe et al., 2015). This date closely corresponds to the 255.13 ± 0.09 Ma age from near the base of the 'Fair Hill Formation equivalent' in CRD Montani 1 (MON_31, 851.47 m). These statistically indistinguishable ages correlate with one another meaning the ash layer at the base of

the ‘Fair Hill Formation equivalent’ is a lateral equivalent to the Nobbys Tuff in the Newcastle Coal Measures.

Assignment of the ‘J and K’ seams to APP3.2 (Kungurian-Roadian) points to their correlation with: (1) the Epsilon Formation of the Cooper Basin (Hall et al., 2015) (Figure 13); (2) the Collinsville Coal Measures of the Bowen Basin (Draper, 2013) (Figure 13); (3) the Blair Athol Coal Measures, Bowen Basin (encompassing an ‘upper stage 4a’ palynoflora ≈ APP3.2; see Price, 1997) (Foster, 1979); (4) the upper part of the coal-bearing Maules Creek Formation, Gunnedah Basin (encompassing APP3.2.1; Wood, 2013), and (5) the Greta Coal Measures, Sydney Basin (Balme and Hennelly, 1956; Boyd and Leckie, 2000).

In Permian basins in eastern Australia there appears to be unconformities within the upper section of APP2; between the Cattle Creek Formation and overlying Reids Dome beds in the Bowen Basin (Korsch and Totterdell, 2009b); in the upper Patachawarra Formation in the Cooper Basin (G. Wood. pers. comm. 2016; Figure 13a) and between the Goonbri Formation and overlying Maules Creek Formation in the Gunnedah Basin (G. Wood pers. comm. 2016). With sparse lower Permian palynological sampling across all eastern Australian basins it is not clear if this hiatus extends into APP3.1, such that it would encompass the apparent (APP3.1) unconformity between the Aramac Coal Measures and overlying ‘J and K’ seams in the Galilee Basin.

Radiogenic isotope dating is currently underway in a number of Gondwanan and Laurasian basins, for example, in the South African Karoo Basin, (Bangert et al., 1999; Rubidge et al., 2013), the Brazilian Parana Basin, (Guerra-Sommer et al., 2005) and the Russian southern Urals (Schmitz and Davydov, 2012). By combining the dates obtained as part of this study with other Gondwanan and Laurasian dates, a better understanding of the development of continental palaeo-geography can be achieved.

3.8. Ash fall source

López-Gamundí (2006) suggested the Cisuralian volcanic source that resulted in abundant tuffaceous strata in the Karoo and Parana basins can be found in the northern Patagonian region. This is distal from the depocentres of the eastern Australian basins; therefore another source would need to be found. Nicoll et al. (2016a) hypothesised that a potential source of volcanic ash in the Cisuralian Galilee Basin could be the nearby Camboon Volcanics, flooring parts of the Bowen Basin. SHRIMP dating of the Camboon Volcanics has produced ages of 295.20 ± 6.2 and 297.10 ±

3.3 Ma (Fanning et al., 2009; Nicoll et al., 2015), which overlap with the 296.09 ± 0.07 Ma (GPC_37, 824.60m) age from the Edie Tuff Member in OEC Glue Pot Creek 1 (Table 2).

The Awaba Tuff (Sydney Basin) shows an intermediate geochemical composition (Grevenitz et al., 2003), whereas the Yarrabee Tuff has a felsic composition (Fricker, 2016). The latter author suggested that, considering their compositional differences and similar ages, they represent a plinian eruption with mafic and intermediate materials erupting first while the more fractionated Yarrabee Tuff erupted slightly later. In addition, the Awaba Tuff's thickness in comparison to the relatively thinner Yarrabee Tuff, indicates that a more southerly volcanic source is likely. While this evidence points to a New South Wales volcanic source, recent dating of volcanics closer to, and in, Queensland has produced Lopingian ages. The Dundee Rhyodacite, located in northern New South Wales, which has been dated at 254.3 ± 0.3 Ma (Brownlow and Cross, 2010), is similar to the date obtained in this study from the top of the 'Fair Hill Formation equivalent' (Figures 13b and 19). The Wallangarra Volcanics, located in northern New South Wales, are indistinguishable in age (253.8 ± 2.4 Ma; Cross et al., 2009; Geoscience Australia, 2016a) and could be synchronous with any of the volcanic ash deposits preserved in the 'Fair Hill and Burngrove formation equivalents' (Figures 13b and 19). Campbell et al. (2015) recently dated the Texas Orocline Gibraltar Ignimbrite at 251.6 ± 3.2 Ma, located on the New South Wales – Queensland border and is considered by this study as a possible volcanic source of the Yarrabee Tuff in the Galilee and Bowen basins.

3.9. Conclusions

This study set out to test the stratigraphic framework presented for the Galilee Basin by Phillips et al. (2017c). Firstly, this study aimed to determine a Cisuralian or Lopingian palynological age for the 'J and K' seams on the central-western margin. Palynological analyses yielded APP3.2 assemblages, placing the 'J and K' seams in the late Cisuralian and early Guadalupian (Figures 13 and 14), similar to the original palynological report by McKellar (1991), whose assignment of the 'J and K' seams to the Cisuralian Aramac Coal Measures was not followed by most exploration companies in the Galilee Basin (e.g. Holland and Bocking, 2008). This change from the Lopingian to late Cisuralian-early Guadalupian expands the timing of known sediment deposition in the central-western part of the Galilee Basin and delays the onset of the mid-Permian hiatus in the Galilee Basin to the early Guadalupian, thus shortening the hiatus by 12-13 My.

Secondly, this study tested the stratigraphic relationship between the Galilee Basin and the adjacent Bowen Basin. Six volcanic ash samples yielded good zircons for CA-IDTIMS dating (Table 2). The youngest age, 252.81 ± 0.07 Ma (MON_60, 796.77 m), is equivalent to the age of the significant

marker horizon between the Fort Cooper Coal Measures and overlying Rangal-Bandanna-Baralaba coal measures in the Bowen Basin, the Yarrabee Tuff. Previous to this study, no Yarrabee Tuff equivalent had been recorded in the Galilee Basin and the importance of it as a stratigraphic marker horizon was not known. With the recognition of it in the Galilee Basin, the proposed splitting of the Bandanna Formation and the tuff-rich lower section of it, the 'Fort Cooper Coal Measures equivalent' of Phillips et al. (2017c) is confirmed (Figure 13b). The dates obtained from the tuffaceous C seam ('Fair Hill Formation equivalent') in CRD Montani 1 (254.32 ± 0.10 Ma from MON_48, 821.58 m and 254.41 ± 0.07 Ma from MON_45, 829.19 m) and the date from the Black Alley Shale in GSQ Tambo 1-1A (254.08 ± 0.06 Ma from TAM_29, 810.25 m) have been interpreted to be correlative (Figure 19). Resulting from this, the C seam is interpreted as a landward facies of the marine Black Alley Shale. This stratigraphic relationship was proposed by Phillips et al. (2017c) through the correlation of geophysical wireline logs between the Galilee and Bowen basins. At present no dates from the Bowen Basin are statistically indistinguishable from the 255.13 ± 0.09 Ma date obtained from the base of the 'Fair Hill Formation equivalent' in CRD Montani 1 (MON_31, 851.47 m). However, the date is interpreted to be correlative to a 255.02 ± 0.03 Ma (Metcalfe et al., 2015) date from Nobbys Tuff in the Sydney Basin. Thus, widespread volcanism associated with ash layers in New South Wales and in Queensland was occurring along the eastern margin of Australia during the Lopingian.

The oldest date obtained in this study, 296.09 ± 0.07 Ma, from OEC Glue Pot Creek 1, identified a Cisuralian age for these strata and allowed the identification of the Edie Tuff Member in this well.

3.10. Acknowledgements

The authors thank the Australian Coal Association Research Program (ACARP), grant number C22028, and the Vale UQ Coal Geoscience Program for funding. The inaugural 34th International Geological Congress (IGC) travel grant awarded by the Australian Geoscience Council (AGC) and the Australian Academy of Science (AAS) allowed travel to Boise State University. Dr. Syeda Areeba Ayaz is thanked for her helpful early reviews. Debra Pierce is thanked for mineral separation and Geoff Wood for his contribution to this manuscript. Dr. John Laurie provided many helpful and insightful reviews that greatly improved this manuscript.

Chapter 4 is published in the Australian Journal of Earth Sciences (2017) as

4. Palaeo-environmental reconstruction of Lopingian (upper Permian) sediments in the Galilee Basin, Queensland, Australia

L. J. Phillips[1], S. A. Edwards[2], V. Bianchi[1] and J. S. Esterle[1]

[1]School of Earth and Environmental Sciences, University of Queensland, St. Lucia, 4072

[2]Geological Survey of Queensland, Department of Natural Resources and Mines, Brisbane, 4000

4.1. Abstract

The recent review of the Lopingian (upper Permian) stratigraphic framework of the Galilee Basin, prompted a reconsideration of the palaeo-environments of deposition. This study interpreted the distribution of sedimentary facies from geophysical logs across the basin complemented by detailed logging from four key wells (GSQ Tambo 1-1A, OEC Glue Pot Creek 1, CRD Montani 1 and GSQ Muttaburra 1). Seven facies associations were identified: terrestrial fluvial, floodplain, lacustrine, and mire; and paralic to marine estuarine shoreline, delta, and restricted marine. Coal measures (mire facies) are best developed in the north-eastern margin of the basin, whereas the southern Springsure Shelf was dominated by marine conditions throughout the Lopingian, only developing terrestrial facies towards the very latest Lopingian. The 'Colinlea Sandstone equivalent' was deposited in a fluvial system, with tidal influence exhibited in the southern part of the basin, which decreases further north as lacustrine environments become common. The regional transgression represented by the Black Alley Shale, can be mapped into the central part of the basin, but based on new exploration data its northern extent is more limited than previously thought. The 'Burngrove Formation equivalent' and Bandanna Formation represent a southerly prograding fluvial-deltaic system during the regional regression in the latter part of the Lopingian.

Key words: Galilee Basin, stratigraphy, Lopingian, palaeo-environment, correlation, facies associations, Bowen Basin

4.2. Introduction

Recent exploration drilling in the Galilee Basin provides an opportunity to test the current stratigraphy and sedimentary interpretations of the Lopingian (upper Permian) coal measures that will potentially provide 2,208 M tonnes of thermal coal (Mutton, 2003) in the coming decades. Seminal early correlations and sedimentological studies worked on the limited outcrop and drilling data (e.g. Allen and Fielding, 2007b; Gray and Swarbrick, 1975; Hawkins, 1976; Hawkins, 1978; Hawkins and Green, 1993; Scott and Hawkins, 1992). Phillips et al. (2017b, 2017c) compiled open file and proprietary drilling data and suggested changes to the stratigraphy based on regional correlation of coals and tuff. Using that regional stratigraphic framework, the aim of this paper is to revisit interpretations of depositional environments within the Koburra Trough in the Galilee Basin and onto the southern Springsure Shelf (Allen and Fielding, 2007b; Fielding et al., 2000; Hawkins, 1976; Figure 21).

4.3. Geological setting

The Galilee Basin is a large intracratonic basin that covers an area of 247 000 km^2 (Figure 21). It is part of a larger Carboniferous–Triassic basin system in eastern Australia that encompasses the intracratonic Cooper Basin to its west and the foreland Bowen Basin to its east (Figure 21). It is bounded by the crystalline Maneroo Platform basement high to the west, with the Hulton-Rand Structure (H-RS) acting as the basin boundary. The Springsure Shelf at the northern end of the Nebine Ridge connects the Bowen and Galilee basins, and allowed continuous sedimentation between both basins, enabling them to have an interlinked stratigraphy and tectonic history. The Canaway Fault bounds the Canaway Ridge, which separates the Galilee and the Cooper basins. Various tectonic settings have been suggested for the origins of the Galilee Basin, from being the result of an incipient coupled or double orocline, a pericratonic basin and a foreland basin (de Caritat and Braun, 1992; Evans and Roberts, 1980; Veevers et al., 1982). It is now generally accepted that the tectonic setting is that of an intracratonic basin (Allen and Fielding, 2007a, 2007b; Van Heeswijck, 2010). There are three main depocentres in the basin; the Lovelle Depression in the north west; the Koburra Trough in the north-east and the Powell Depression in the south (Figure 21), with maximum initial thicknesses of 630 m, 2800 m and 1700 m, respectively (Stewart, 2013). The study area (Figure 21) is defined to the east and west by the basin margins (i.e. eastern Permian subcrop to the Hulton-Rand Structure and Maneroo Platform) and to the north and south by the basin's northern margin (northern Koburra Trough) and the Springsure Shelf.

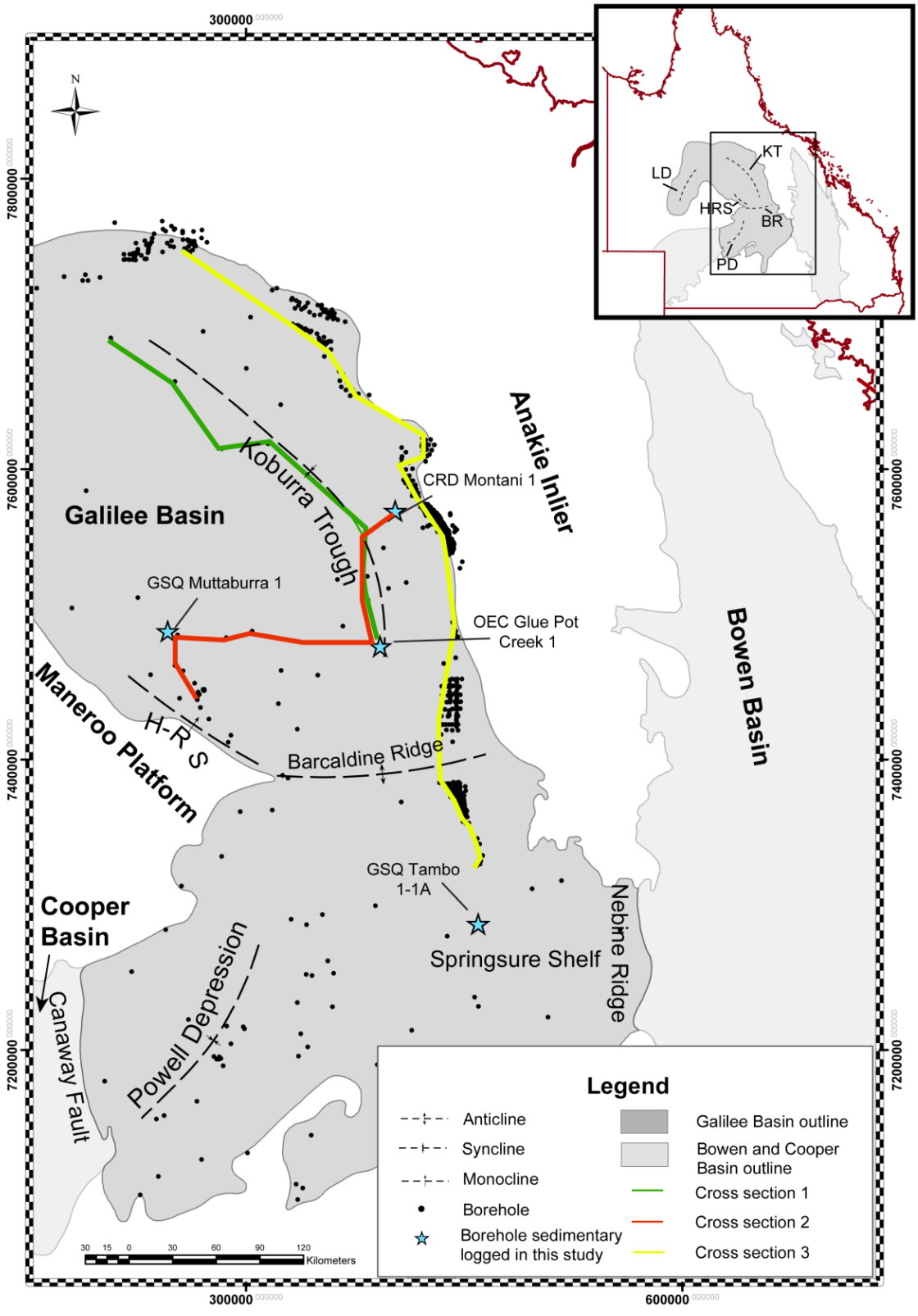

Figure 21: Map of central and eastern parts of the Galilee Basin, showing the locations of borehole data relative to major features in the Galilee Basin. Cross sections used in this study are highlighted in green (Figure 29), red (Figure 30) and yellow (Figure 31). Starred boreholes indicate cores logged for sedimentary and facies analysis as part of this study. Inset map shows major structural features. LD, Lovelle Depression; KT, Koburra Trough; BR, Barcaldine Ridge; PD, Powell Depression; and HRS, Hulton-Rand Structure.

4.4. Syntectonic history

The Galilee Basin formed coevally with the Bowen Basin and as such has experienced many of the same tectonic events (Figure 22), albeit experiencing less subsidence and deformation. Evans and Roberts (1980) and Van Heeswijck (2004, 2010) interpreted three basin phases between the late Carboniferous and Middle Triassic, comprising of mechanical extension, thermal subsidence and then protracted thermal subsidence at the time the Bowen Basin was undergoing foreland loading and thrusting (Fielding et al., 2000; Korsch and Totterdell, 2009b).

The initiation of the Galilee Basin is believed to have occurred during the mechanical extension (Jericho Event) of the underlying Devonian–Carboniferous Drummond Basin during the Pennsylvanian period (Stewart, 2013). The Joe Joe Group was deposited during this time with the upper section of the group including coal measures. The Aramac Coal Measures are not widespread and are local to the Lovelle Depression and Hulton-Rand Structure in the Galilee Basin.

Following accumulation of the Aramac Coal Measures, a sedimentation hiatus occurred (Nicoll et al., 2015; Van Heeswijck 2010; Figure 22). Uncertainty surrounds the reason behind this pause. Evans and Roberts (1980) suggested that the Galilee Basin underwent gentle uplift and erosion, during east–west compression (Hawkins and Green, 1993). No evidence of erosion is observed in seismic profiles (Van Heeswijck, 2010), so it is more likely that reduced rates of sedimentation and subsidence occurred.

The resumption of deposition in the Galilee Basin during the Lopingian has not been attributed to any tectonic event, but is commonly correlated to strata in the Denison Trough that coincide with the contractional Aldebaran Event (Korsch and Totterdell 2009b; Van Heeswijck 2010; Figure 22). An extended period of thermal subsidence in the Galilee Basin allowed the deposition of the Betts Creek Group, across all parts of the basin. These deposits were formed in a range of transgressive and regressive system tracts (Allen and Fielding, 2007a, 2007b) that Van Heeswijck (2010) attributes to the contractional Bellata Event in the Bowen Basin (Figure 22). Reasons for the transgression and regression are still speculative. Previous workers suggested it was caused through tectonic processes (Fielding et al., 2000; Korsch and Totterdell, 2009b) but it also coincides with the gradual decrease in glacial episodes during the Lopingian (Fielding et al., 2008). Waschbusch et al. (2009) observed that during the same time frame, the southern part of the Bowen Basin was undergoing static flexural foreland loading. Based on increased thickening of the Betts Creek Group, Van Heeswijck (2010) interpreted increased subsidence, possibly responding to the foreland loading, in the southern Galilee Basin. Phillips et al. (2017b) corroborated this with the observation

of coal seams splitting towards the southern part of the basin. Thermal subsidence continued into the Triassic, with the deposition of the Rewan Formation, Clematis Sandstone, Moolayember Formation and their time equivalents.

4.5. Current Lopingian stratigraphic framework

Phillips et al. (2017c) recently modified the Galilee Basin stratigraphy (Figures 22 and 23) and its correlation with the adjacent Bowen Basin, based on geophysical log signatures and subsequent corroboration by CA-IDTIMS dates of tuffs from core by Phillips et al. (In Press). Their interpretation added two additional stratigraphic units along the eastern margin and in the Koburra Trough as well as one new unit in the Hulton-Rand Structure. For a more comprehensive review of the stratigraphy the reader is referred to Phillips et al. (2017c).

The Lopingian in the Galilee Basin, consists of the Betts Creek Group that is subdivided along the eastern margin and within the Koburra Trough into the basal 'Colinlea Sandstone equivalent', the tuffaceous coal bearing 'Fair Hill Formation equivalent', the coal-free Black Alley Shale, another tuffaceous coal-bearing unit, the 'Burngrove Formation equivalent' and the Bandanna Formation – the youngest Permian-aged coal measure (Figures 22 and 23). The naming convention for the Lopingian coal seams are A (Bandanna Formation), B ('Burngrove Formation equivalent'), C ('Fair Hill Formation equivalent'), D, E and F ('Colinlea Sandstone equivalent') (Phillips et al., 2017c; Scott and Hawkins, 1992).

The tie between the Galilee Basin and the Denison Trough is across the Springsure Shelf, which is sparsely drilled and thought to have existed as a relative topographic high, still allowing sediments to pass between the basins, until the latest Lopingian (Allen and Fielding, 2007b; Figure 21).

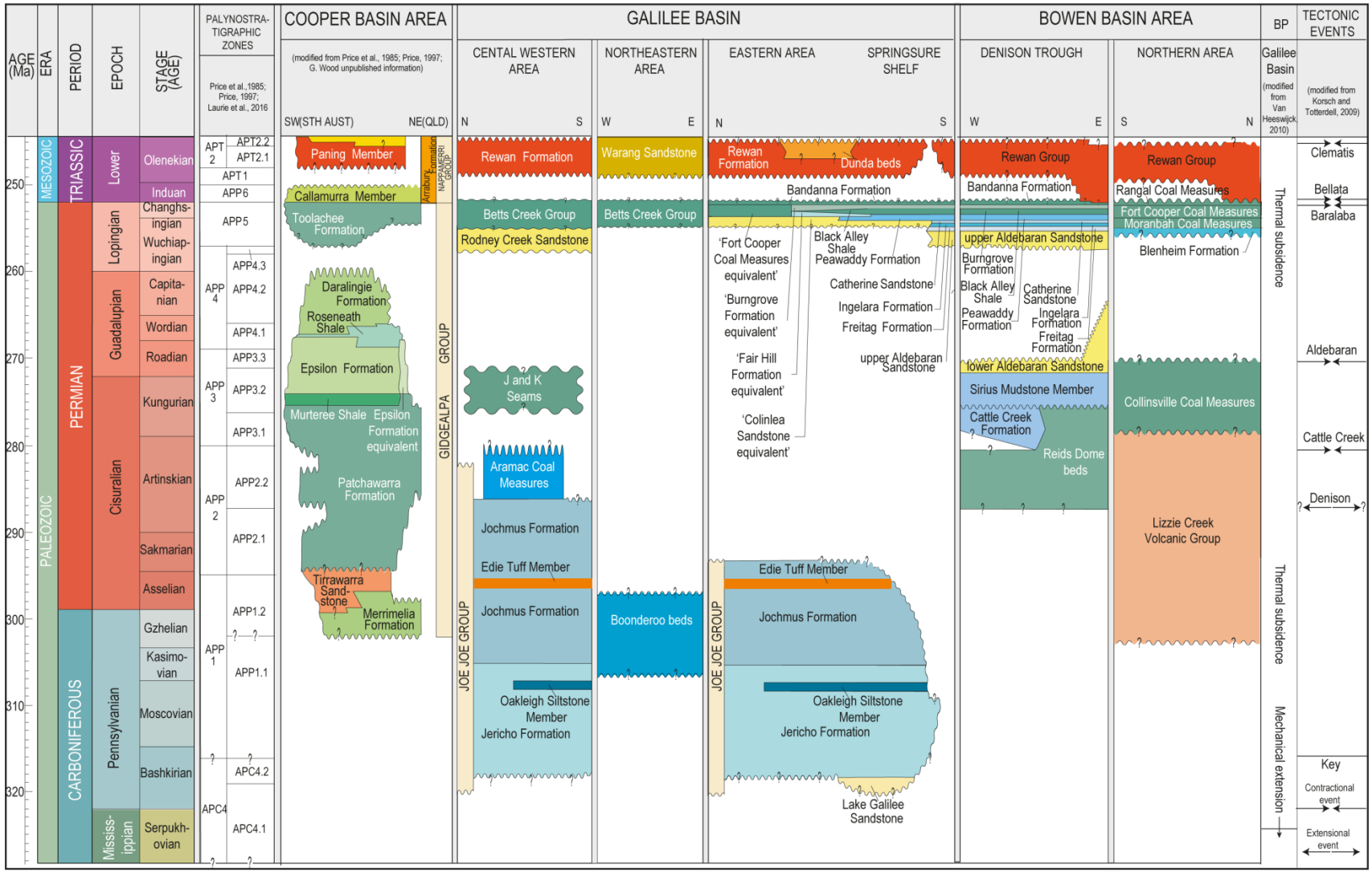

Figure 22: Stratigraphic nomenclature of the Galilee, Bowen and Cooper basins used in this study (modified from McKellar and Henderson, 2013). Timescale from Gradstein et al. (2012). Palynology modified from Laurie et al. (2016); Price et al. (1985); Price (1997). Stratigraphy modified from Draper (2013); McKellar and Henderson (2013); Phillips et al. (2017c); Price et al. (1985); Price (1997). Galilee basin phases (BP) modified from Van Heeswijck (2010). Tectonic events modified from Korsch and Totterdell (2009b). Tectonic arrows represent extensional (outward facing arrows) and contractional (inside facing arrows) events.

4.6. Depositional environments throughout the Lopingian in the Galilee Basin

Based on biostratigraphic work by Norvick (1981) and sedimentary analysis of outcrop and core (Allen and Fielding, 2007a, 2007b) the coal measures are generally interpreted to have formed in sub-aerially exposed alluvial settings with different energy regimes. The coal-free siltstone dominated formations are interpreted to have formed as open to restricted marine and lake units, bounded by paralic units varying from deltaic to coastal origins. The sequence is generally devoid of marine sediments apart from localised regions over the Springsure Shelf and Nebine Ridge. Marine sediments are specific to the Peawaddy Formation and Black Alley Shale, where there was a connection to the marine incursions during the thermal subsidence period, observed in the Bowen Basin (Allen and Fielding, 2007a, 2007b; Evans, 1980; Vine, 1975).

The deposition of the Betts Creek Group located in the north of the study area was originally related to a eustatic sea-level rise that caused low-energy alluvial sediments to be deposited across the basin (Evans and Roberts, 1980). However, subsequent work by Allen and Fielding (2007a, 2007b) recognised both coastal and alluvial plain environments in the Betts Creek Group with estuarine facies observed in a northern outcrop.

The 'Colinlea Sandstone equivalent' (previously Colinlea Sandstone and thought to have occurred in the southern part of the study area) is dominated by quartz-rich sandstone (Grigorescu, 2012). The sandstones are interpreted to have formed on an alluvial plain, where rivers flowed in a southerly and easterly direction (Scott et al., 1995), and which were occasionally able to support peat swamps (Hawkins, 1978). Allen and Fielding (2007a, 2007b) interpreted the lower Betts Creek Group as having tidally influenced sandstones, capped by estuarine deposits, thus suggesting influence of a transgression can be seen towards the north of the Galilee Basin.

The Peawaddy Formation on the Springsure Shelf of the Galilee Basin is considered by Phillips et al. (2017c) to be the southern equivalent of the 'Colinlea Sandstone equivalent'. The Peawaddy Formation has similar origins to its lateral correlative in the Bowen Basin. It is thought to be the onset of greater sediment accumulation than accommodation in the Bowen Basin, during the Lopingian, with sediment dispersal patterns from east to west across the Nebine Ridge into the Galilee Basin (Fielding et al., 2000). Scott et al. (1995) comment on its rich sandstone makeup, while Allen and Fielding (2007b) remark that it is comprised of higher concentrations of mud and siltstone with small-scale coarsening-upwards sequences. The Peawaddy Formation is terminated

by a coquinite, thought to be the lateral equivalent of the Mantuan Productus beds in the Bowen Basin (Draper, 2013). The presence of small coarsening-upwards sequences within the Peawaddy Formation (Allen and Fielding, 2007b) is suggestive of fluctuating base levels.

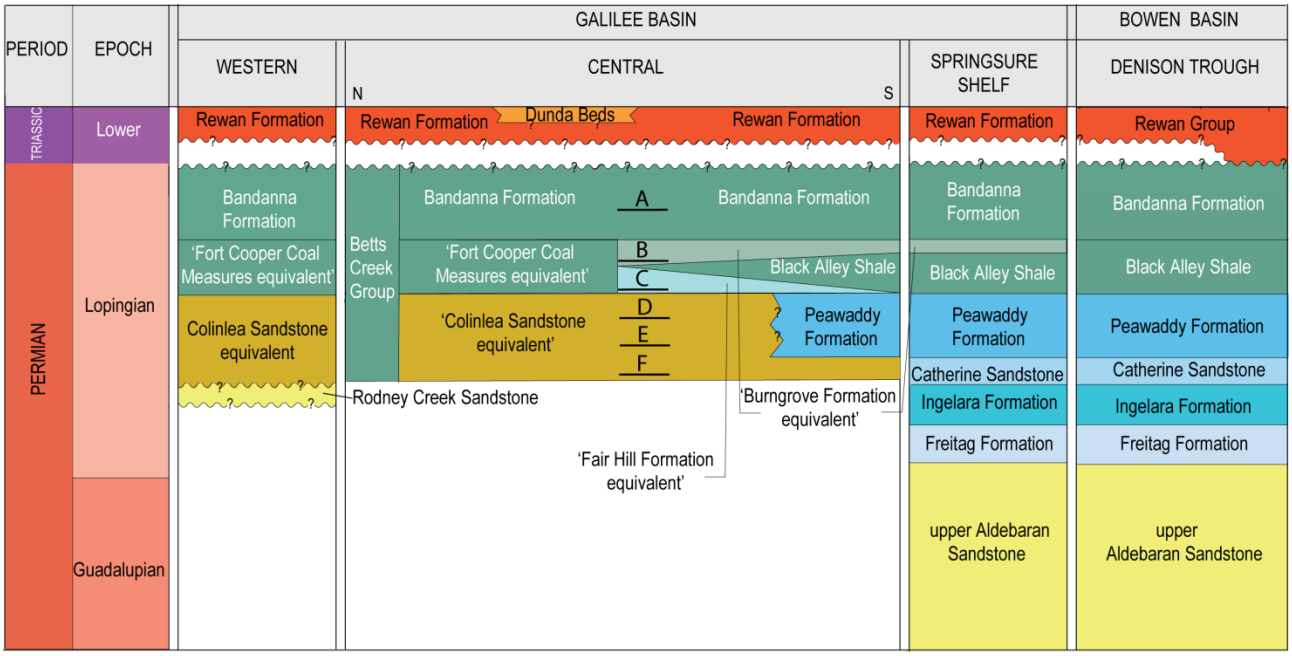

Figure 23: Lithostratigraphic nomenclature used in this study after Phillips et al. (2017c), with relative units in the Bowen Basin (Draper, 2013). Underlined letters represent coal seams located in their respective formations. Note that placement of coal seams is not exact.

Overlying the 'Colinlea Sandstone equivalent', the 'Fair Hill Formation equivalent' was identified as a separate formation in the Galilee Basin by Phillips et al. (2017c) (Figures 22 and 23). Previously the tuffaceous C seam, now within the 'Fair Hill Formation', was interpreted as the upper section of the 'Colinlea Sandstone equivalent' (Scott and Hawkins, 1992). No other volcanic activity is seen within the unit and it was interpreted to have formed in a coastal and alluvial plain setting (Allen and Fielding, 2007b).

On the Springsure Shelf overlying the Peawaddy Formation is the Black Alley Shale (Figure 23), which contains dark shales punctuated with tuffaceous material, interpreted to have formed in a transgressive setting (Mollan et al., 1969). Correlations by Allen and Fielding (2007b); Phillips et al. (2017b, 2017c) and Scott and Hawkins (1992) show the extent of incursion of the water body into the basin. A highly bioturbated interval overlying the C coal seam has been identified and forms the base of a coarsening-upwards sequence, that includes the upper section of the Black Alley Shale and lower section of the overlying formation (Blanco, 2010). Blanco (2010) attributed this to a prograding deltaic sequence from the north towards the Springsure Shelf.

The advancement of terrestrial environments towards the Springsure Shelf allowed the formation of peat swamps once more in a coastal/alluvial plain environment, identified as the 'Burngrove Formation equivalent' and Bandanna Formation. Previously the 'Burngrove Formation equivalent' was the tuffaceous lower section of the Bandanna Formation, but was re-assigned by Phillips et al. (2017c). Many of the sediments typical of the Bandanna Formation, massive to thickly bedded labile sandstone interbedded with mudstones and siltstones, are indicative of a meandering stream system (Allen and Fielding, 2007b; Grigorescu, 2012; Hawkins, 1978; Hawkins and Green, 1993; Wells, 1968).

To date, depositional interpretations have been suggested for Lopingian strata of the Galilee Basin based on localised studies of outcrop and core. With the revised stratigraphy and coal seam correlations between the Galilee and Bowen basins, afforded by recent exploration drilling for coal and coal-seam gas (Phillips et al., 2017c), it is timely to revisit palaeo-environmental interpretations on a regional scale.

4.7. Methodology

Four strategically located cores across the basin, GSQ Tambo 1-1A, OEC Glue Pot Creek 1, CRD Montani 1 and GSQ Muttaburra 1 (Figure 21) were logged as part of this study. These wells represent the change from alluvial to paralic and offshore facies described in the literature and observed in the wireline-log signatures. Each core was logged to analyse sedimentary facies in the siliciclastic interburdens between coal seams and lithofacies were ascertained. The lithofacies were grouped according to grain-size relationships and sedimentary structures observed in the core, used to interpret the depositional environments. Accompanying wireline logs signatures were assigned to the depositional environments. This allowed the correlation of interpreted depositional environments along wireline geophysical cross sections by Phillips et al. (2017b), traversing the basin.

4.8. Facies associations

Fourteen individual facies were identified from detailed sedimentary analysis of the four drill cores. These facies are summarised in Table 4 with corresponding photographs. Seven facies associations (Table 5) were identified from the individual facies and their apparent sequences in the cores. These associations have been interpreted to be seven different terrestrial and marine depositional environments: floodplains, lakes, mires, river channels, estuarine shoreline, deltas, and restricted marine (similar to Allen and Fielding, 2007a, 2007b).

Facies	Lithology	Sedimentary Structures	Fauna and Flora	Interpretation	Photograph of facies in core
1	Matrix supported conglomerate	Rounded pebbles, slight imbrication, normal grading of pebbles, flooring erosional scours		Fluvial Thalweg	
2	Medium to coarse grained sandstone	Medium to low angle cross bedding confined in erosional scours		Channel fill, prograding fluvial bars	
3	Fine grained sandstone	Low anglecross bedding with carbonaceous laminae, occasional climbing ripples	Some plant material in laminae	Lateral accretion bars (point bar), occasionally reworked	
4	Fine grained sandstone	Low angle to horizontal bedding to lamination, abundant horizons of siderite nodules		Frequently exposed sand bars	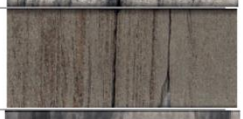
5	Very fine sand, siltstone	Slight wavy bedding, disturbed structures	Rare horizontal burrows, root penetration	Overbank/floodplain deposits	
6	Siltstone, mudstone	Mostly structureless, water escape features, oxidised bands		Distal overbank/ponded floodplain	
7	Mudstone and siltstone, occasional tuffaceous and carbonaceous material	Horizontal lamination	Plant material	Vegetated, high water table	
8	Coal, tuffaceous material		Plant material	Marsh, swamp deposits	
9	Matrix supported conglomerate	Sub angular pebbles		Alluvial fan, storm deposits	
10	Interbedded fine grained sandstone, mudstone	Mud drapes (?doublets), wavy and flaser bedding, occasional oil staining, sulphur staining	Rare horizontal burrows in mud drapes	Intertidal flats	
11	Medium to coarse grained sandstone	Well sorted, clean sand, mainly structureless with very rare siltstone laminae		Wave influenced subaqueous sand bar	
12	Very fine sand, siltstone	Horizontal to wavy lamination	Abundant horizontal and vertical bioturbation	Pro delta	
13	Very fine sand, siltstone	Slumping, siderite staining		Delta slope	
14	Coquinite, shale	Shale is the matrix	Shell fragments and rare unbroken specimens	Marine shelf	
15	Black shale, tuffaceous material	Structureless		Anoxic water body/basin	

Table 4: Individual facies and their interpretation from sedimentary logged cores in this study.

Facies Associations	Individual facies that are commonly sequenced	Interpreted depositional environment
A	1, 2, 3 capped by association B	Fluvial
B	5, 6, 7, capped by association D or C	Floodplain
C	7, commonly overlying association C or D	Lacustrine
D	7, 8, eroded by association A	Mire
E	9, 10, 13	Estuarine shoreline
F	11, 12, 4	Delta
G	14	Restricted marine

Table 5: Facies associations compiled of individual facies and their interpreted depositional setting.

Terrestrial

Fluvial facies

Facies 1, 2 and 3 (Table 4) are commonly associated with each other in the cores, with facies 3 being substituted for facies 4 in places. The rounded matrix supported conglomerates of facies 1 form the base of the fining-upwards sequences. This is followed by coarse to medium grained low angle cross-bedded sandstones of facies 2. Commonly overlying facies 2 is low angle cross bedded fine-grained sandstone with carbonaceous siltstone laminae (facies 3) that in places show signs of rhythmic deposition. The typical fining-upwards sequence has been interpreted as being deposited in a predominately fluvial environment (Bridge, 2003). However, the presence of rhythmic lamination and small-scale mud drapes could suggest a tidal influence within a fluvial setting. (Dalrymple et al., 1992; Dalrymple and Choi, 2007). This is not unreasonable given the proposed low gradient of the basin and recent evidence that tidal influence may be recognised landward for further distances (Blum and Törnqvist, 2000; Fielding, 2015).

The geophysical signature of interpreted fluvial facies is a bell shape with a low gamma signature (approximately 40 API) at the base gradually increasing to above 100 API when abundant laminae are present. Density values range from 2.2 to 2.6 g/cm^3.

Floodplain facies

Overlying the fluvial facies, facies 5 and 6 (Table 4) are typically detected. They may occur individually or as a combination. Facies 5 contains very fine sands to siltstone lithologies, while facies 6 contains siltstone and mudstone lithologies where facies 5 contains disturbance of strata, only rare faunal bioturbation is seen. Facies 6 contains more pronounced bedding and lamination, with occasional oxidised surfaces. The presence of water escape features in facies 6 suggests that sediments were water saturated before the next layer was deposited. Facies 5 and 6 have been interpreted as floodplain deposits.

The flood plain facies have a high gamma signature, commonly in excess of 200 API and a density value of 2.3 to 2.4 g/cm^3.

Ponded floodplain/lacustrine

Facies 7 (Table 4) is comprised of siltstone and mudstone with variable carbonaceous content. Deposits are organised in horizontal bedding and in places no structures are visible. Common organic material can be found in the form of plant remains. In certain horizons the facies is interrupted by clay-rich tuffaceous material. The bounding relationship between facies 7 and typically fluvial facies 2, 3 and 4 interbedded with facies 8 (Table 4), suggests a low-energy ponded terrestrial environment (Picard and High, 1972). A terrestrial environment is favoured over marine due to the presence of horizontal lamination and lack of sands within the facies attributed to mud flocculation. Facies 7 has been interpreted as being deposited in a standing body of water (lake) that was in close proximity to vegetated areas that occasionally became emergent. The alternating shades of grey could indicate fluctuations of the water table, allowing some areas to be inundated with water and minerals, resulting in a lighter sediment colour.

Due to the high clay content, the facies has a high-gamma signature, in excess of 180 API and commonly over 200 API. When tuffaceous material is present this increases. The density has a range of 2.15 to 2.3 g/cm^3 depending on the organic content, with higher organic contents having lower density values.

Mire facies

Facies 8 (Table 4) comprises coal. In places bright coal bands are observed. However, dull, mineral-rich coal is predominant. Commonly coal is observed overlying channel over-bank deposits (facies 5 and 6) and is interbedded with facies 7 and tuffaceous material. Coal seams range from 1–6 m in thickness. The minimal presence of bright bands can either suggest that big trees were lacking and herbaceous material prevailed (Blanco, 2010; Stopes, 1919) or the low accommodation setting allowed for extensive oxidation of the peats (Hunt and Smyth, 1989). The high mineral matter and carbonaceous mud and siltstone suggest that water tables were high and could not support large tree growth. This may be indicative of low lying mires that were frequently exposed and experienced episodic flooding events.

Owing to the high carbon content of the coals the gamma signatures are low, approximately 40 API, however the high mineral matter and sedimentary rock lithologies within the coal seams causes the coals to have a wide density range from 1.5 to 1.8 g/cm^3.

Marine

Estuarine shoreline

Flaser to wavy bedded alternating fine-grained sandstone and siltstone, which is in places horizontally bioturbated, make up facies 10. This deposition of alternating grain sizes and clay doublets is attributed to the ebb and flood tides which is typical in a marine sequence (Reineck and Wunderlich, 1968). Thus, the rare presence of horizontal bioturbation and well developed alternation of grain size in facies 10 has been interpreted to be inter to subtidal flat deposits (Daidu et al., 2013; Dalrymple et al., 1992; Reineck and Wunderlich, 1968). However, the presence of matrix supported sub-angular conglomerates (facies 9) that interrupt facies 10 (Table 4) represent a common feature in this succession. The conglomerates consist of polymictic pebbles surrounded by a sandy matrix. The observed coarse material requires deposition in much higher energy environments. However a consistently higher energy environment, where occurs the constant reworking of sediments by tides and waves, would have rounded the clasts, similar to that observed in facies 1. This is not seen as facies 9 is characterised by sub-angular clasts. Fan deltas shedding sediment from a nearby palaeo-high is a plausible explanation (Postma, 1990). However, a typical fan delta sequence is not preserved, so it is suggested that during higher energy storm events coarser grained sediments (i.e. from the fan deltas) could be transported and deposited in this restricted marine system. The presence of reworked fan deposits during high-energy events suggests that the depositional environment was within an estuarine setting with intermittent wave influence, which reworked the fan deposits above the storm-weather wave base. Unfortunately, data are sparse in this area, and it is not possible to reconcile.

Clean, well-sorted, medium to coarse grained sandstone, which display very rare siltstone laminae, represent facies 11. The cleanliness of the sandstone coupled with the well-sorted nature of the sediments suggests a continuous reworking of sediments prior to deposition. Facies 11 has been interpreted as a wave influenced sandbar (deVries Klein, 1970), which under- and overlays the facies 10.

Facies 14 (Table 4) is a coquinite composed of mainly shell fragments (>90%) with rare intact specimens (<10%) and has only been observed in one place in GSQ Tambo 1-1A (Figure 28). The shell fragments are not orientated, and comprise articulated and disarticulated valves (some closed in life position) in a matrix of black shale. Although this facies may not be typical of an estuarine succession (Bridge and Droser, 1985), the presence of the coquinite solely in the southern part of the basin is significant and further adds emphasis to a marine interpretation. The presence of disarticulated and articulated mollusc shells, suggests transportation from a nearby source (Jeffery

and Aigner, 1982; Johnson, 1960). The disarticulated valves are an expression of wave action, possibly tempestites (Johnson, 1989).

The presence of deposits (facies 10 and 11) influenced by wave processes in close stratigraphic relationships to estuarine deposits (facies 9) suggest that the environment was in proximity to the outer side of an estuarine funnel, where fetch is bigger and effects of storm events can be found.

No geophysical log is available for GSQ Tambo 1-1A and so no geophysical signature can be ascertained for facies 9, 10, 11 and 14.

Delta

Abundant vertical and horizontal bioturbation and laminated very fine sandstone and siltstone observed in facies 12 (Table 4) suggest a nutrient-rich, low energy environment, which had a low but constant rate of sediment deposition (supply). Overlying facies 12, facies 13 (Table 4) exhibits large-scale slumping and soft sediment deformation with an overall increase in grain size, transitioning into the fine-grained sandstone of facies 4. This coarsening-upwards sequence with a highly bioturbated base is indicative of a deltaic succession with facies 12 representing the more distal pro delta and facies 13 a relatively proximal and more dynamic delta slope (Galloway, 1975). The coarsening-upwards sequences range in size from 10 m to >70 m, where the smaller sequences represent mouth bars within a larger deltaic system. The lack of carbonaceous material and presence of siderite nodules in facies 4 (Table 4) suggest a delta-front setting where different water chemistries intermixed which promoted the precipitation of iron oxides (Berner, 1981).

The coarsening-upwards sequence is displayed in wireline by a decrease in gamma values with the base approximately 140 API decreasing to 80 API or lower, dependant on the sand to mud ratio.

Restricted marine

Facies 15 (Table 4) is a black shale where any floral or faunal evidence is absent. No sedimentary structures are observed at the base of the facies but towards the top, slight horizontal lamination is observed. The lack of sedimentary structures show no/little movement of sediments, thus is suggestive that the shale was either deposited in deep water or a water body that become restricted and anoxic (Heckel, 1972). The facies are frequently interrupted with tuffaceous material suggesting a restricted water body environment, as volcanic ash would likely be dispersed in a deep-marine environment below the storm-weather wave base. Strengthening this interpretation is

the association with the coquinite facies (facies 14) beneath, and deltaic facies (facies 12 and 13) above.

No geophysical log is available for GSQ Tambo 1-1A. However, the fine-grained material would be represented on a geophysical log by a high gamma value, ~180 API and a density value of 2.4–2.5 g/cm^3.

4.9. Palaeo-environmental reconstruction

Lithological and palaeo-environmental description of the Catherine Sandstone, Ingelara Formation, Freitag Formation, Aldebaran Sandstone and 'Rodney Creek Sandstone'

Sedimentary logging of GSQ Tambo 1-1A (Figure 28) identified the Catherine Sandstone, Ingelara Formation and Freitag Formation, having previously all been recognised as the one unit, the Colinlea Sandstone (Wallin, 1975). Distinct depositional environments for the Catherine Sandstone, Ingelara Formation and Freitag Formation are restricted to the Springsure Shelf of the Galilee Basin (Figures 21, 22 and 23). The Aldebaran Sandstone was not intersected.

The Freitag Formation (Figures 22 and 23) was only partly intersected on the Springsure Shelf and contains a series of tidally influenced fluvial channels and over-bank deposits capped by a 3.5 m thick coal seam. This is consistent with the adjacent interpretation described by Fielding et al. (2000) and Fielding et al. (2007) of the Freitag Formation in the Denison Trough of the Bowen Basin representing deposition on a coastal plain to shallow marine setting. From this study, it is not known if the coal seam intersected on the Springsure Shelf is correlatable to other coal seams, or if more exist below. However, other boreholes in the vicinity (e.g. GSQ Tambo 3; Gray, 1976) report having only one coal seam in this stratigraphic horizon.

Overlying the fluvial channels, coastal facies (facies 9, 10 and 11) are exhibited in GSQ Tambo 1-1A (Figure 28). These are correlative to the transgressive marine incursion represented by the Ingelara Formation in the Denison Trough. The Ingelara Formation in this well contains middle to subtidal flats, (facies 10; Daidu et al., 2013), that fluctuate in depth indicators and which are occasionally inundated with the sub-angular matrix supported conglomerates (facies 9). The conglomerates in the Ingelara Formation appear to be abrupt suggesting they were sharply brought from an unknown source into the system by storm events. The occurrence of these conglomerates in a tidal setting may be triggered by external forces, which require future investigation. Hummocky cross stratifications may be expected in this setting however, none were observed. The preservation

of such structures may be minimal due to the low storm aggradation rates (Dumas and Arnott, 2006). Therefore, the depositional environment could have been below the fair-wave base and above the storm-wave base (Dumas and Arnott, 2006). The palaeo-environment of the Ingelara Formation in the Galilee Basin is part of a wave-influenced estuary, with tidal-dominated deposits disturbed by storms. The Catherine Sandstone is characterised by clean, well-sorted, structureless sandstones (facies 11), indicative of intense reworking. The cleanliness and well-sorted nature of the thick Catherine Sandstone on the Springsure Shelf suggest winnowing of sands and is interpreted as deposition in an upper shoreface environment. A suitable depositional environment for these upper shoreface deposits, given the underlying tidal flats, may be sand bars or deltaic wedges, which fan easterly into the Denison Trough (Fielding et al., 2000; Mollan et al., 1969). These deposits could be reshaped through the interplay between tide and wave action in the form of rip or longshore currents (MacMahan et al., 2006). To achieve this environment the system is still in transgression, passing through to the outer part of the estuary system.

Towards the central western margin, the 'Rodney Creek Sandstone' (Figure 23) has been identified in GSQ Muttaburra 1 (Figure 25). This unit is only observed in this area and is characterised by a mixture of facies. The base of the unit exhibits conglomerates (facies 1) that fine upwards to sandstones with low-angle carbonaceous laminae (facies 3). Flaser and wavy bedding (facies 10) overlie this, fining upwards to black shales (facies 15). This sequential order (facies 3, 10 and 15) has been interpreted as a tidal channel or tidally influenced meander deposits, occurring in an estuarine environment (Dalrymple et al. 1992) that potentially have been abandoned and plugged by the adjacent offshore facies (facies 10 and 11). It is interpreted that the 'Rodney Creek Sandstone' is a condensed section of the transgressive system tracts on the Springsure Shelf.

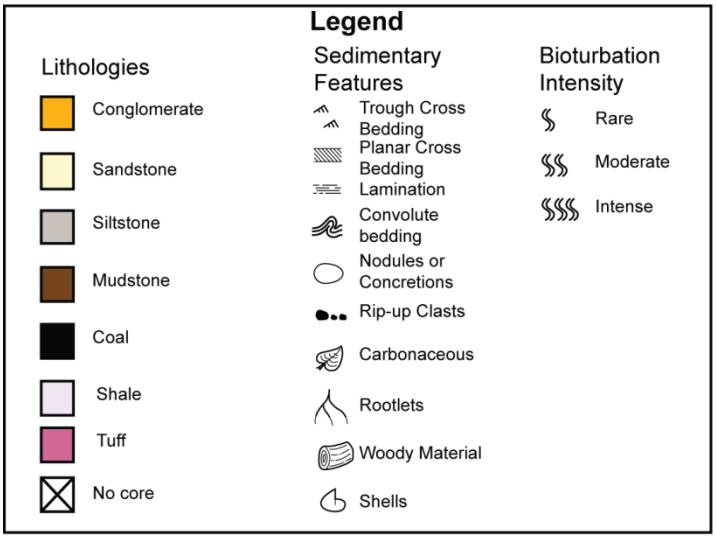

Figure 24: Legend used in sedimentary logs.

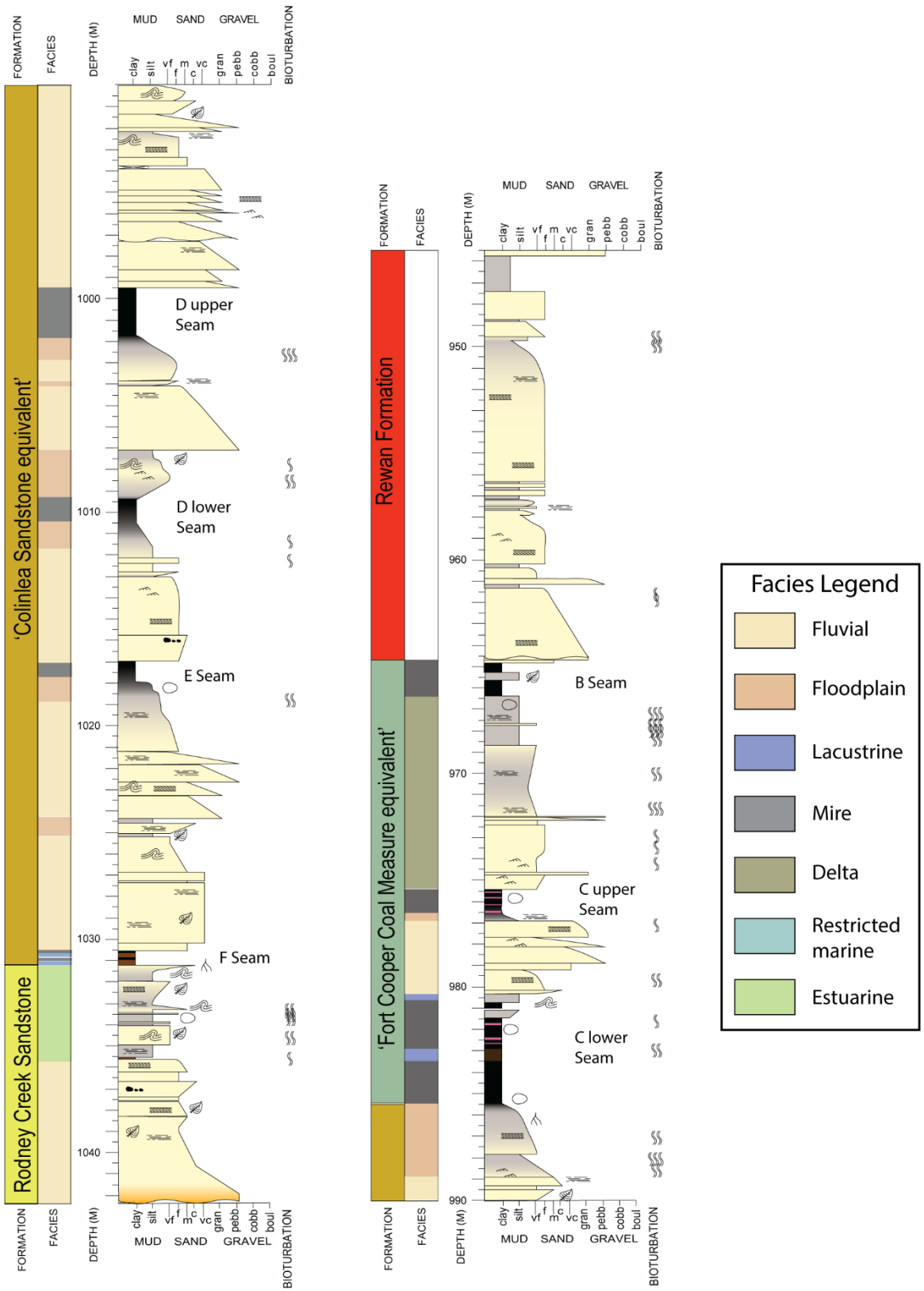

Figure 25: Sedimentary log of GSQ Muttaburra 1. Depth is in metres from top of hole. For facies legend see inset. For lithology legend see Figure 24. For borehole location see Figure 21.

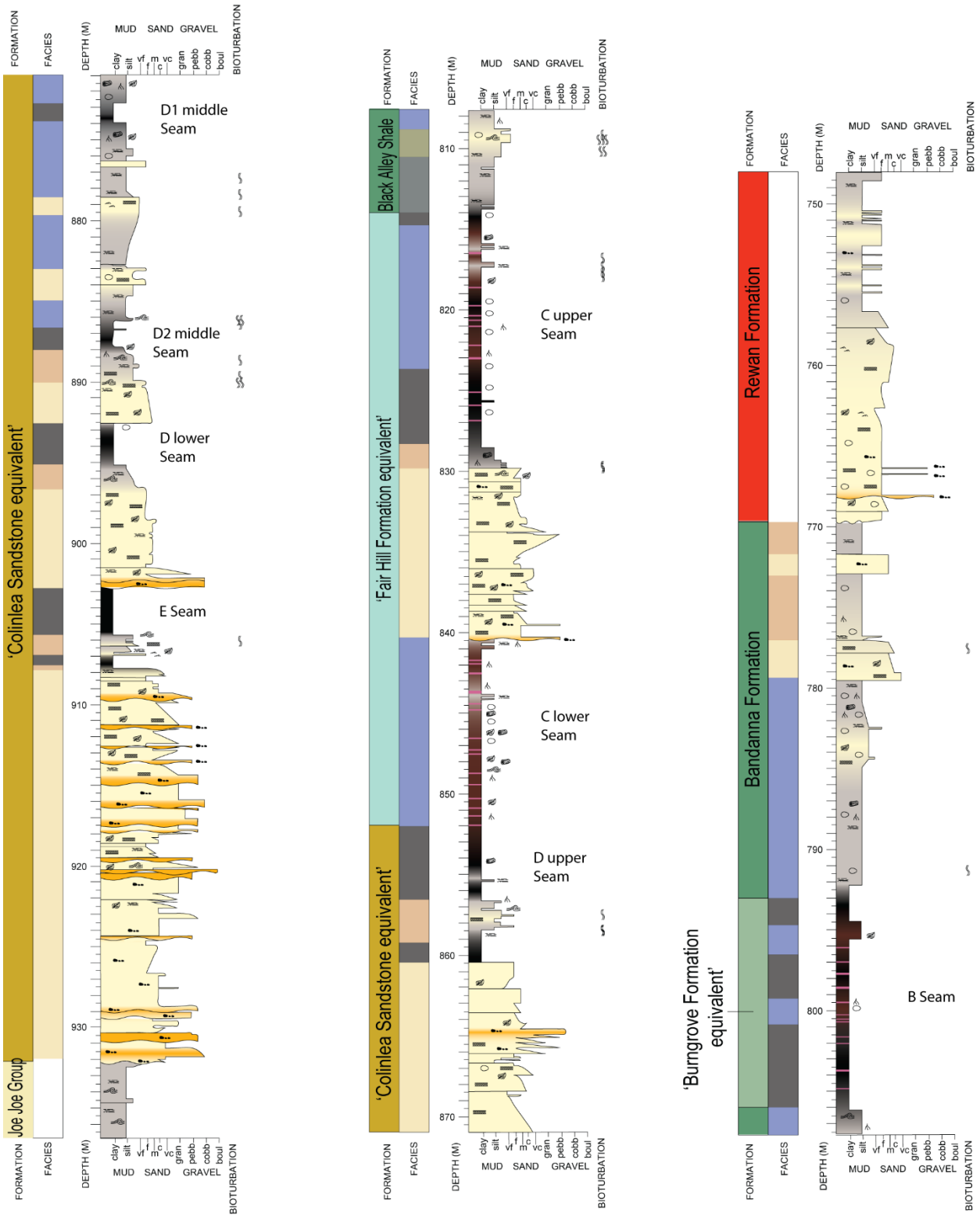

Figure 26: Sedimentary log of CRD Montani. Depth is in metres from top of hole. For facies legend see Figure 25. For lithology legend see Figure 24. For borehole locations see Figure 21.

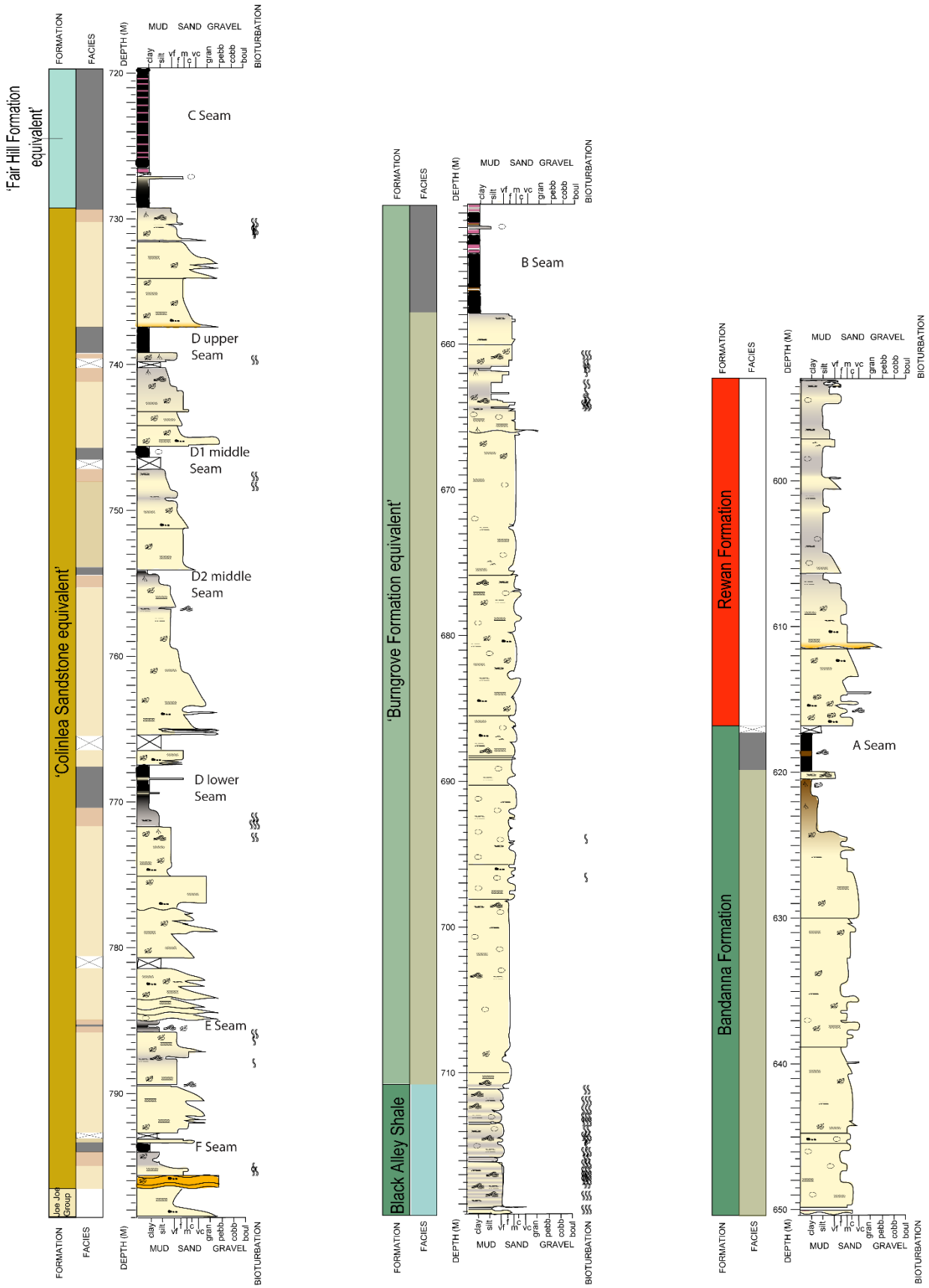

Figure 27: Sedimentary log of OCE Glue Pot Creek 1. Depth is in metres from top of hole. For facies legend see Figure 25. For lithology legend see Figure 24. For borehole location see Figure 21.

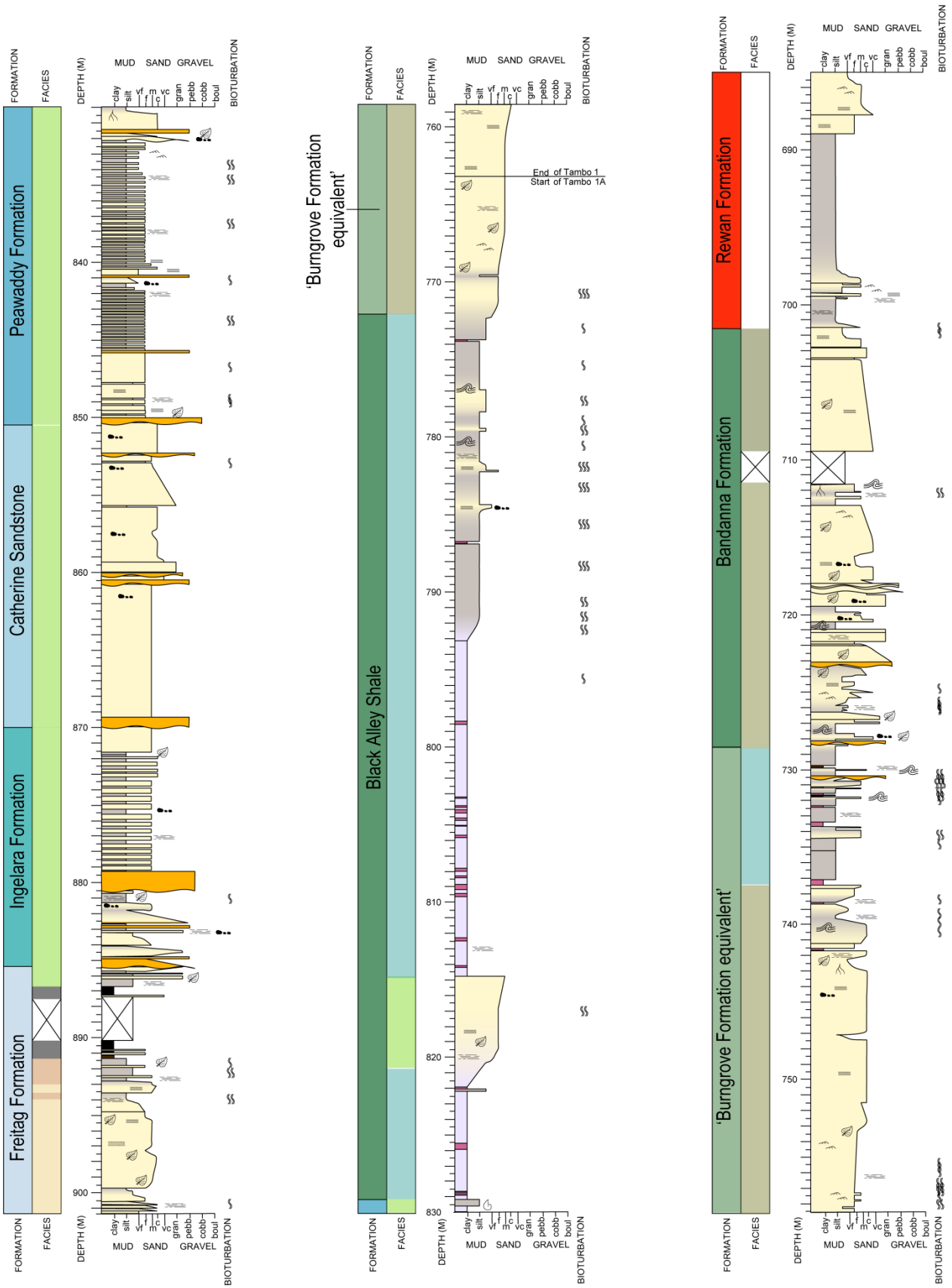

Figure 28: Sedimentary log of GSQ Tambo 1-1A. Depth is in metres from top of hole. For facies legend see Figure 25. For lithology legend see Figure 24. For borehole location see Figure 21.

Peawaddy Formation and 'Colinlea Sandstone equivalent'

Lithological description and interpretation of the Peawaddy Formation

Of the four study wells, the Peawaddy Formation was only intercepted in GSQ Tambo 1-1A, located on the Springsure Shelf where it is 21 m thick (Figure 28). It is characterised by interbedded fine-grained sandstone and mudstone drapes. In places the mudstone drapes exhibit horizontal burrows (facies 10; Table 4).The wavy and flaser bedding of the Peawaddy Formation is indicative of a tidal flat palaeo-environmental interpretation (Reineck and Wunderlich, 1968), similar to that of the Ingelara Formation. The tidal flat resemblance between the two formations is suggestive of a larger marine/brackish water body to the east situated in the Denison Trough of the Bowen Basin (Figure 32). The exception being the absence of the storm conglomerates in the Peawaddy Formation. The fan deltas providing the source for these conglomerates may not have been preserved, or were located elsewhere. The top of the sequence exhibits a fining-upwards sequence capped by a shelly interval, which may be traceable and has previously provided a datum across the Springsure Shelf (Gray, 1976). This coquinite is equivalent to the Mantuan Productus beds in the Bowen Basin (Mollan et al., 1969). The presence of the shelly interval represents a move from deposition above the storm-wave base at the base of the Peawaddy Formation, to near or below the storm-wave base at the top of the formation, where calm stable conditions were preferable to marine fauna. This is evidenced in GSQ Tambo 1-1A by some shells being preserved in life form (valves closed and articulated) after low intensity storm events.

Lithological description and interpretation of the 'Colinlea Sandstone equivalent'

North of the Springsure Shelf, the Peawaddy Formation interfingers with the minimally tidally influenced 'Colinlea Sandstone equivalent' (Figures 29 and 32), which generally thickens from 40–60 m in the west and south; and to 70 m in the north and east of the basin. The 'Colinlea Sandstone equivalent' contains a series of fining-upwards sequences comprising of facies 1, 2 and 3 capped by coal (facies 8). This represents the transition from a fluvial environment to a vegetated overbank environment, and marks the terrestrial and lateral facies variation to the shoreline environment (Peawaddy Formation) interpreted on the Springsure Shelf.

In OEC Glue Pot Creek 1 (Figure 27) each fining-upwards cycle gets thinner towards the top of the formation (Figure 29). The quickening of channel avulsion reflects an increase in meander sinuosity due to the filling of accommodation space. An alternative explanation could be given by backing up of fluvial facies during the transgression. Given that in the south of the basin the lateral equivalent of the 'Colinlea Sandstone equivalent' is the transgressive shoreline Peawaddy Formation (Figure

23), the shorter cycles are interpreted as the mouth of the river being encroached due to sea-level rise.

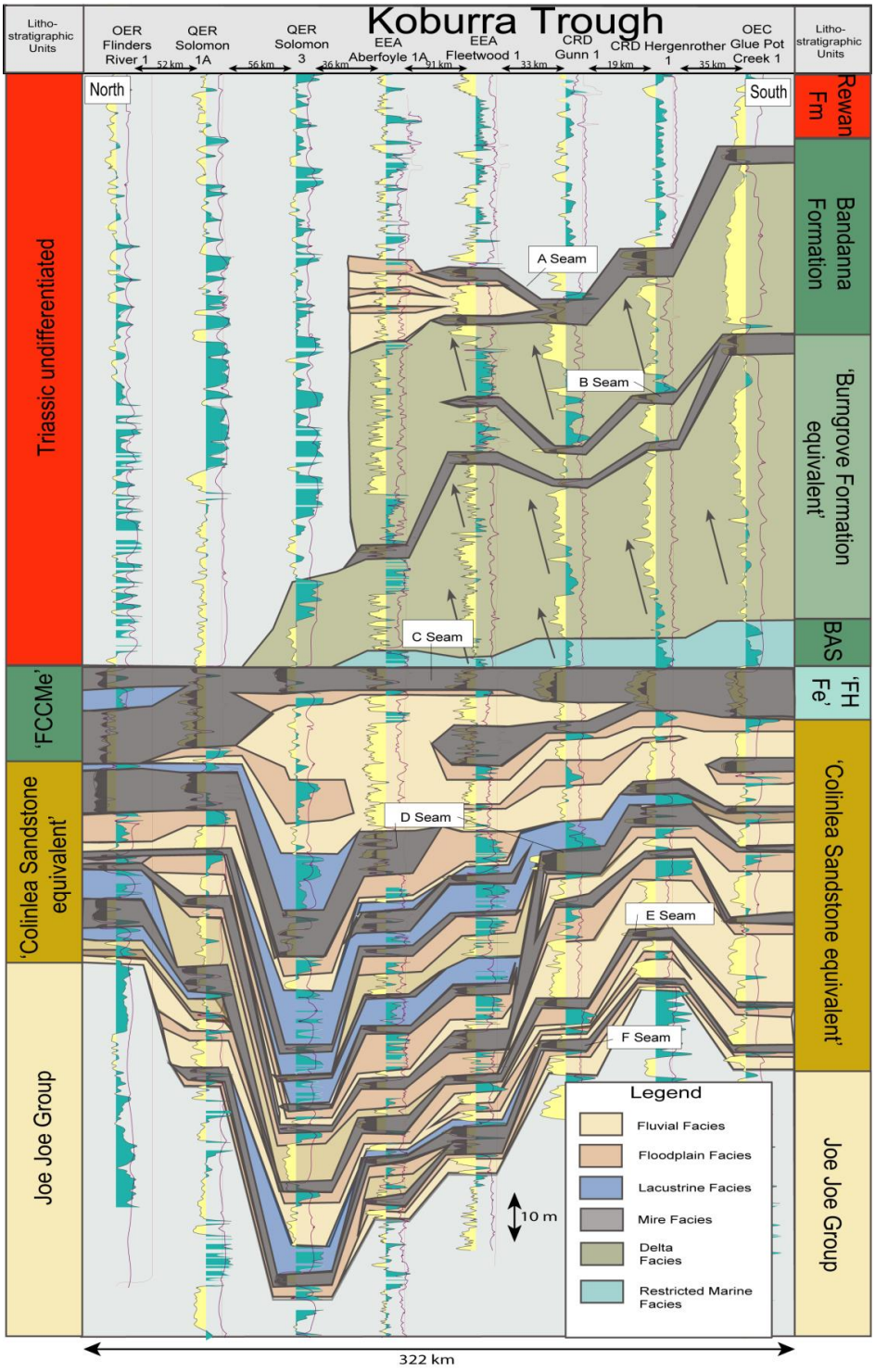

Figure 29: Koburra Trough correlation with overlain facies interpretations. Arrows represent a grain size coarsening up sequence that is recorded between the boundaries of the Black Alley Shale and overlying 'Burngrove Formation equivalent'. The sequence is attributed to a prograding delta. Wire line logs used are gamma (yellow represents <100 API, green represents >100 API), density (<1.8 g/cc coloured black) and caliper (red line). See Figure 21 for cross-section location. Abbreviations; FM – Formation, BAS – Black Alley Shale, 'FHFe' – 'Fair Hill Formation equivalent', 'FCCMe' – 'Fort Cooper Coal Measures equivalent'. Note wells are not equally spaced.

The presence of small rhythmic climbing ripples encased in mud drapes towards the top of the fining-upwards sequences shows that the river systems have a tidal signature (Choi, 2010). Recent studies suggest tidal influence can be exhibited further upstream than previously thought (Blum and Törnqvist, 2000; Fielding, 2015) and the flat, cratonic setting of the Galilee Basin may have facilitated such an influence hundreds of kilometres into the basin from the marine environment.

Westwards in the basin (Figures 25 and 30) tidally influenced fluvial and floodplain facies are dominant. The presence of flaser-bedded sandstones incorporated into the fining-upwards cycles in GSQ Muttaburra 1 (Figure 25) suggest the tidal influence was greater in the central western part of the Galilee Basin than the eastern section. Considering that the south-eastern Galilee Basin has recorded intense wave reworking, the western and the eastern areas might experience similar tidal influences. However, in the eastern side of the basin this tidal influence has not been preserved, possibly due to the continuous combing from wave action.

Moving northward through the 'Colinlea Sandstone equivalent' the tidally influenced fining-upwards sequences decrease and water saturated/lacustrine environments prevail (Figures 29, 30 and 31). This was also described by Edwards et al. (2008) in well EEA Fleetwood 1A, approximately 26 km from CRD Montani 1 (Figures 21, 26, 29 and 30). Little is known regarding local tectonics of the Galilee Basin but the presence of limited lacustrine environments suggests local controls on subsidence rates. It is unclear if these waterbodies contained fresh or brackish water. Outside of the northern part of the study area, Allen and Fielding (2007b) suggested that alluvial plains existed during the deposition of the Colinlea Sandstone (referred to as the 'Colinlea Sandstone equivalent' in this paper) within the Betts Creek beds (Group), strengthening the idea that little to no marine influence was exerted in the central to northern part of the basin during this time.

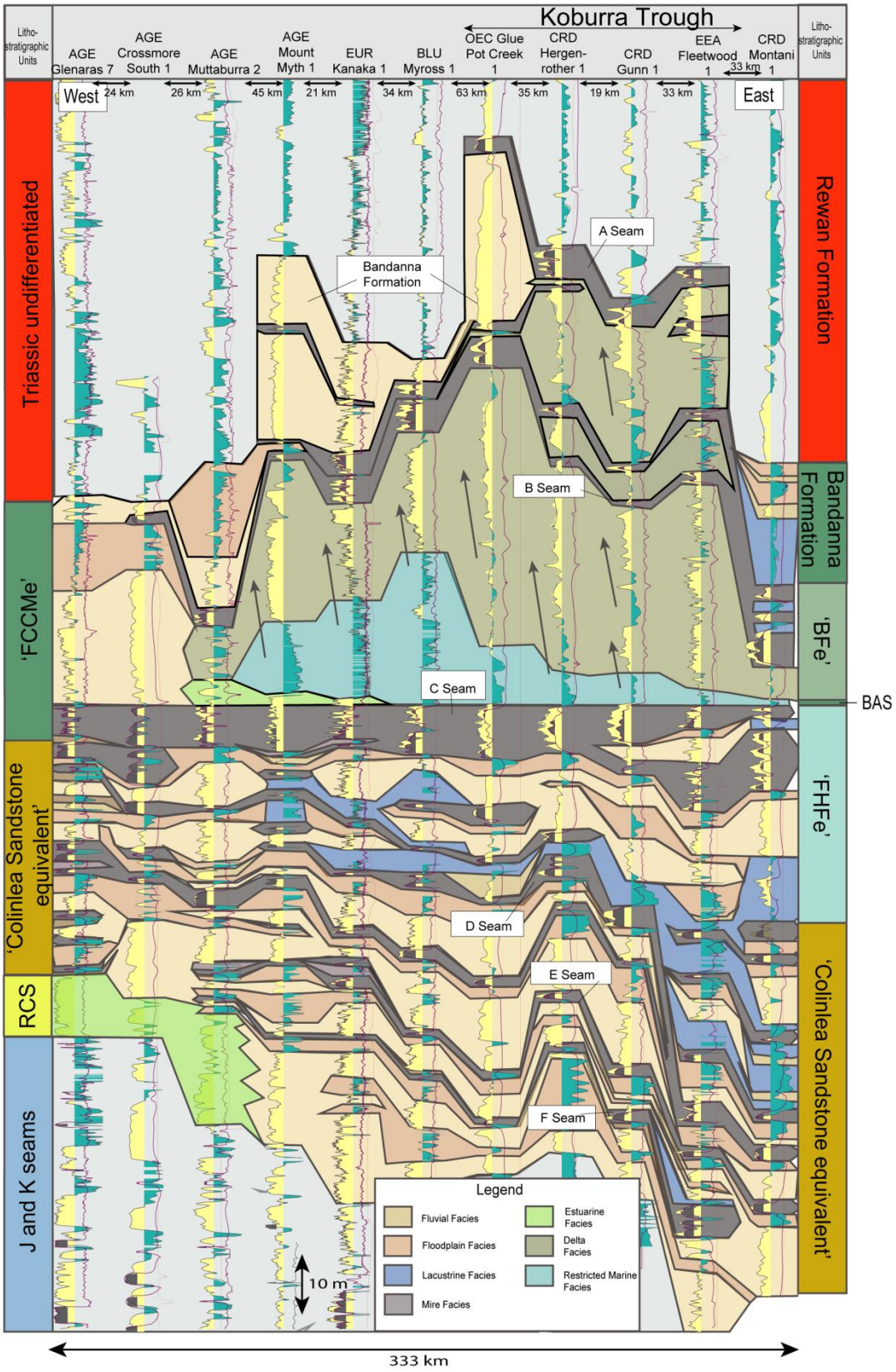

Figure 30: West to east correlation with overlain facies interpretations. See Figure 21 for cross-section location. Arrows represent a grain size coarsening up sequence that is recorded between the boundaries of the Black Alley Shale and overlying 'Burngrove Formation equivalent'. The sequence is attributed to a prograding delta. Wire line logs used are gamma (yellow represents <100 API, green represents >100 API), density (<1.8 g/cc coloured black) and caliper (red line). Abbreviations; 'BFe' – 'Burngrove Formation equivalent', BAS – Black Alley Shale, 'FHFe' – 'Fair Hill Formation equivalent', RCS – 'Rodney Creek Sandstone', ' FCCMe' – 'Fort Cooper Coal Measures equivalent'. Note wells are not equally spaced.

Combined palaeo-environmental description of the Peawaddy Formation and 'Colinlea Sandstone equivalent'

The thickness of the 'Colinlea Sandstone equivalent' and its Springsure Shelf correlative, the Peawaddy Formation, decreases from north to south. The central eastern part of the basin (OEC Glue Pot Creek 1) predominately displays fluvial facies that are capped with coal (Figure 27) and interpreted to be avulsion of river systems. The upper section of the 'Colinlea Sandstone equivalent' in CRD Montani 1 (Figure 26) shows lacustrine facies that can be interpolated across other wells in close vicinity (Figure 30). The lacustrine environments were at times able to support mire growth suggesting water-table levels were highly variable on a localised scale. Reasons for this variability are unknown at this stage, and further investigations are needed to determine the causes. These lacustrine environments are not represented in the southern and western parts of the Koburra Trough where cyclic fluvial and mire depositional systems prevail. The cyclicity combined with the interpreted low gradient of the basin, suggests a meandering fluvial system that avulses over time. The thickness between each cycle diminishes upwards stratigraphically, perhaps indicating a meandering river system, which with increasing avulsion as the marine body transgresses into the basin, forms a distributive delta plain. Due to the proximity of the marine body, the meandering river channels and the developing distributaries across the delta plain, a proximal fluvial-dominated coastline can be interpreted (Dalrymple et al., 1992; Figure 32). Deposits ascribed as transitional between the shoreline to the marine body are expressed in the Peawaddy Formation on the Springsure Shelf (Figure 32).

'Fair Hill Formation equivalent' and Black Alley Shale

Lithological description and interpretation of the 'Fair Hill Formation equivalent'

The 'Fair Hill Formation equivalent' is characterised by highly tuffaceous coals of the C coal seam. The 'Fair Hill equivalent' thins towards the west and towards the south, where it shales out into the Black Alley Shale (). The coals within the 'Fair Hill Formation equivalent' are relatively clastic rich and dull in comparison to coals located in the underlying 'Colinlea Sandstone equivalent' (Figures 25, 26 and 27) perhaps indicating an increase in groundwater level within the mire environment. Within the carbonaceous mudstone and siltstone observed within the coals in CRD Montani 1, siderite nodules are observed. In the north of the study area, the coal seams are split by sandstone units. These sandstone units are interpreted as tributaries upriver from the marine incursion to the south. A mire depositional environment is favourable for the preservation of volcanic ash fall, which the C seam has in abundance.

Lithological description and interpretation of the Black Alley Shale

The Black Alley Shale can be mapped across much of the basin (Figures 29, 30, 31 and 32) and is thickest (~20 m) on the Springsure Shelf. The thickness distribution is in contrast to the northern lateral equivalent, the 'Fair Hill Formation equivalent'. The Black Alley Shale underlies the 'Burngrove Formation equivalent'. The facies within the Black Alley Shale change laterally north to south. The calm and quiet waters have allowed the deposition of numerous volcanic ash layer horizons within the Black Alley Shale on the Springsure Shelf. Overlying facies 10, a highly bioturbated, horizontal to wavy laminated, interbedded fine-grained sandstone and mudstone unit (facies 12) has been observed on the Springsure Shelf and is interpreted as the pro delta (Galloway, 1975). Soft sediment deformation within interbedded fine sandstone and siltstone represent the delta slope (facies 13; Martinsen, 1989) to the underlying prodelta. This facies is most characteristic in OEC Glue Pot Creek 1. Facies 10 (interbedded fine-grained sandstone and mudstone of the intertidal flats environment) is not observed in OEC Glue Pot Creek 1 or CRD Montani 1 and facies 12 (very fine sand and siltstones of a pro delta environment) and facies 13 (very fine sand and siltstones of a delta slope) are not observed in CRD Montani 1 (Figures 26 and 27). This spatial variation of the facies within the Black Alley Shale indicates that the marine transgression was from a southerly source. The absence of facies 10 and 11 from the northern-most sedimentary logged bore hole in the study area, CRD Montani 1 (Figure 26), suggests that the marine transgression was not long lived in the area or did not reach this far north. It appears that the Black Alley Shale in CRD Montani 1 (Figure 26) is representative of lower delta-plain mudflats (Galloway, 1975).

The Black Alley Shale pinches out in the central western side of the Galilee Basin (region represented by GSQ Muttaburra 1, Figure 25). The absence of the Black Alley Shale unit is replaced with the 'Fort Cooper Coal Measures equivalent', which encompasses the under and overlying 'Fair Hill and Burngrove formation equivalents' when not separated by the Black Alley Shale (Figure 23).

Combined palaeo-environmental description of the 'Fair Hill Formation equivalent' and the Black Alley Shale

The Black Alley Shale represents a major transgression into the Galilee Basin from the southern Bowen Basin across the Nebine Ridge. The southernmost part of the basin is dominated by a water body transgressing northwards while the equivalent terrestrial facies show widespread mires with times of elevated water table. The water table rise may be the result of the approaching transgressive Black Alley Shale, which saturates the mires creating large bodies of water, and restricting vegetation growth, in particular that of large trees. The coal seams within the 'Fair Hill

Formation equivalent' decrease in thickness towards the south and are replaced by shale demonstrating the extent (and depth) of the water body. Both environments are optimum for the preservation of tuffaceous material and this is abundant in both areas demonstrating active volcanism during this time. These tuffs have been CA-IDTIMS dated and are correlative (Phillips et al., In Press), allowing for the assurance that the Black Alley Shale and 'Fair Hill Formation equivalent' are lateral equivalents of one another. A coastal setting is interpreted for the 'Fair Hill Formation equivalent' with water-logged mires that become vegetated periodically. The absence of flora or fauna and the characteristic dark massive shale (facies 10; Table 4) of the Black Alley Shale on the Springsure Shelf suggests that the transgressive marine system became restricted and anoxic.

Lithological description and interpretation of the 'Fort Cooper Coal Measures equivalent'

In the very north of the study area and to the central western margin, the 'Fort Cooper Coal Measures equivalent' is the combination of the 'Fair Hill Formation equivalent' and the 'Burngrove Formation equivalent'. This unit only exists when the Black Alley Shale is absent, allowing the B and C seams to coalesce, such as occurs in the north and west of the basin (Figures 25, 29, 30 and 31). At locations directly adjacent to the Black Alley Shale (well EEA Fleetwood 1), marine trace fossils (*Rosselia*, *Planolites*, *Phycosiphon* [*Helminthopsis*] and *Teichichnus*) can be observed (Edwards et al., 2008; Figure 26). Further north, outside of the study area, coal seams amalgamate in the 'Fort Cooper Coal Measures equivalent' unit (Figure 31a), which suggests that the area was stable and a palaeo-geographic high at the time of deposition. This allowed a large accumulation of peat without the influx of sediment from fluvial systems.

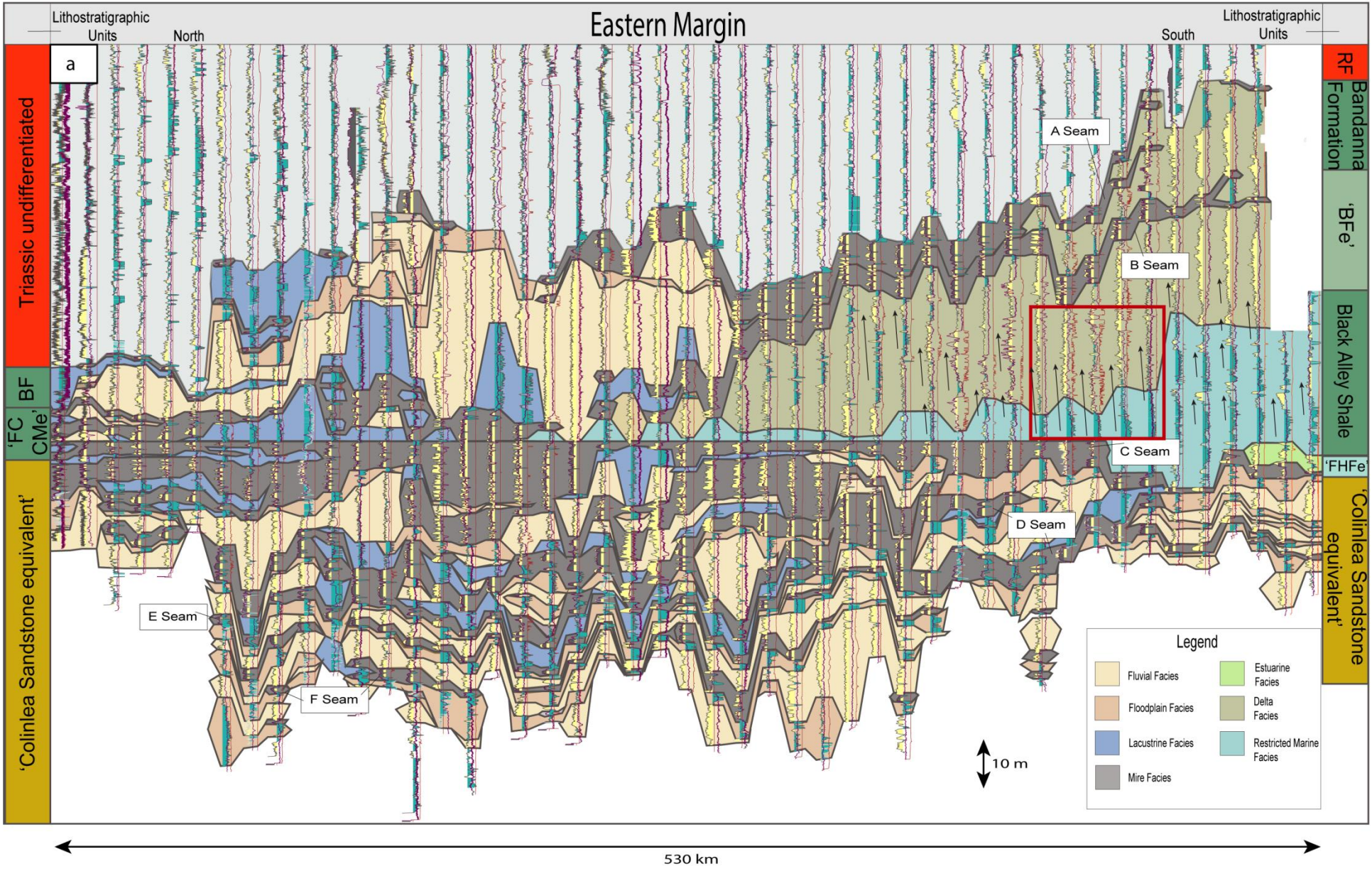
Eastern Margin
Lithostratigraphic Units
North
South
Lithostratigraphic Units
a
Triassic undifferentiated
'FC CMe' BF
'Colinlea Sandstone equivalent'
RF
Bandanna Formation
'BFe'
Black Alley Shale
'FHFe'
'Colinlea Sandstone equivalent'
A Seam
B Seam
C Seam
D Seam
E Seam
F Seam
10 m
Legend
Fluvial Facies
Floodplain Facies
Lacustrine Facies
Mire Facies
Estuarine Facies
Delta Facies
Restricted Marine Facies
530 km

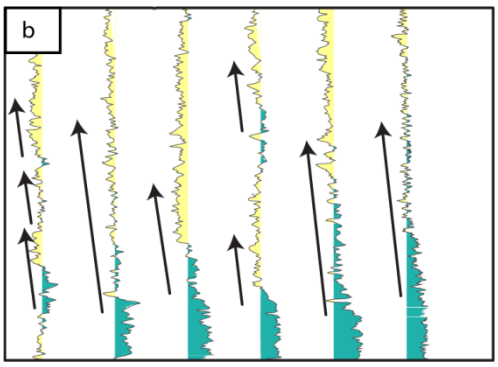

Figure 31: (a) Eastern margin correlation (modified from Phillips et al., 2017c), with overlain facies interpretations. See Figure 21 for cross-section location. Arrows represent a grain size coarsening up sequence that is recorded between the boundaries of the Black Alley Shale and overlying 'Burngrove Formation equivalent'. The sequence is attributed to a prograding delta. This is enlarged in the inset box. Wire line logs used are gamma (yellow represents <100 API, green represents >100 API), density (<1.8 g/cc coloured black) and caliper (red line). (b) Close up view of the coarsening-upwards sequence, as shown by the direction of the arrow, taken from the inset in Figure 31a. Only gamma log is shown. Abbreviations: 'FCCMe', 'Fort Cooper Coal Measures equivalent'; BF, Bandanna Formation; 'BFe', 'Burngrove Formation equivalent'; BAS, Black Alley Shale; and 'FHFe', 'Fair Hill Formation equivalent'. Note wells are not equally spaced.

'Burngrove Formation equivalent' and Bandanna Formation

Lithological description and interpretation of the 'Burngrove Formation equivalent'

The 'Burngrove Formation equivalent' is the upper part of the coarsening-upwards sequence that starts from the base of the Black Alley Shale (Figure 31b). The 'Burngrove Formation equivalent' is associated with fine sandstones that host low angle to horizontal bedding and lamination (facies 4) and contains abundant sideritic horizons and thickens towards the south. The coarsening-upwards sequence defined in OEC Glue Pot Creek 1 (Figure 27) and GSQ Tambo 1-1A (Figure 28) is observed to be stacked in the geophysical log cross section (Figure 31) when propagated northwards. Capping the coarsening-upwards sequence on the Springsure Shelf are finely laminated dark shales that are interbedded with tuffaceous material. The anoxic shale is only found on the Springsure Shelf and is suggestive of the anoxic event being local to the Springsure Shelf, unlike the regional anoxic event associated with the underlying Black Alley Shale. North of the Springsure Shelf, the 'Burngrove Formation equivalent' is capped by a tuffaceous coal seam (B seam). Given its stratigraphic position and its lithological content, the 'Burngrove Formation equivalent' is interpreted as the delta front transitioning into the lower delta plain, which became vegetated as sea level dropped. The stacking of the coarsening-upwards sequences in the Koburra Trough and along the eastern margin (Figures 29 and 31) is interpreted as deltaic foresets suggesting they were prograding southwards. Localised areas in the Springsure Shelf occasionally became restricted and anoxic.

The ‘Burngrove Formation equivalent’ is not observed along the central–western margin where the B and C seams are coalesced into the same package. Here the ‘Fort Cooper Coal Measures equivalent’ is substituted.

Lithological description and interpretation of the Bandanna Formation

The Bandanna Formation is highly lithologically variable across the basin. Towards the southern part of the basin and on the Springsure Shelf it is associated with fining-upwards sequences. These sequences contain coarse clean sands at the base-grading upwards to fine sands with carbonaceous laminae. In places capping these sequences are thin 5 cm siltstone units. This has been interpreted as a lower delta plain setting.

These facies contrast markedly to those observed in the centre of the basin where one large fining-upwards sequence (up to 30 m thick) is observed. The base of the coarsening-upwards sequence exhibits sideritic nodule horizons that decrease in abundance up sequence. The sandstones are massive to thickly bedded, with some low-angle or horizontal bedding observed. The top of the sequence displays an extremely weathered 2.5 m mudstone horizon, which is overlain by a coal seam (A seam). The weathering consists of an exposure surface expressed by highly fractured brown to dark brown mud and the presence of roots.

The Bandanna Formation in the northern section of the study area is characterised by fine-grained, horizontally laminated strata (facies 7) (Figure 26) where sporadic, iron stained horizons are observed. No coal is observed in the Bandanna Formation in CRD Montani 1 (Figure 26), located in the north-eastern basin margin.

The splitting and coalescing of the A seam observed in geophysical cross sections from the Galilee Basin (Figures 29 and 31) coupled with the observed lithological variation suggest that the Bandanna Formation was deposited under a variety of different palaeo-environments. In the south of the basin, the Bandanna Formation is interpreted as being partly deposited in a delta plain with avulsing distributary channels. Upstream of the lower delta plain, the upper delta plain was vegetated and in geophysical cross section where the A and B coal seams are coalesced, the environment appears stable and very similar to that of when the underlying ‘Burngrove Formation equivalent’ was deposited. In the northern margin of the basin, the Bandanna Formation is characterised by a low gamma signature, commonly interpreted as sandstone and suggests that these are river channels that are feeding the southern delta.

The Bandanna Formation is relatively free of tuffaceous material, which allows it to be distinguished from the underlying tuff-rich 'Burngrove Formation equivalent', despite the two having similar palaeo-environments and facies relations.

Combined palaeo-environmental description of the 'Burngrove Formation equivalent' and the Bandanna Formation

During the deposition of the 'Burngrove Formation equivalent' and the Bandanna Formation the Galilee Basin was largely dominated by a delta. The regression has been inferred to be southerly moving as stacked coarsening-upwards sequences interpreted to be delta foresets, can be observed in Figures 29 and 30. The prograding delta created a suitable environment for vegetation growth as coal seams B and A can be correlated from north to south of the basin. During the deposition of the B seam, volcanic activity was prevalent with volcanic ash preserved in the numerous tuffaceous horizons found within the 'Burngrove Formation equivalent'. This differs to conditions during the Bandanna Formation deposition, with the A seam being readily distinguishable from the B seam by a sharp decrease in tuffaceous material. The upper delta plain did not extend to cover the southern Springsure Shelf, which remained marine throughout the deposition of the 'Burngrove Formation equivalent', expressed by the local anoxic event on the Springsure Shelf, and Bandanna Formation, lower delta plain.

4.10. Summary and conclusions

The aim of this study was to revisit the interpretation of depositional environments for Lopingian strata in the Galilee Basin given the revised stratigraphy. Using both open file and proprietary data, regional detailed palaeo-environment reconstructions have been drawn for the Lopingian (Figure 32).

Interpretations from this study interpret sedimentation in the Galilee Basin to have resulted from an elongated restricted fluvial to marine environment, in particular estuarine deposition. The estuary is dominated not only by fluvial processes, but also by tidal influences. Due to the low gradient of the basin, tidal influences have been recorded landward within the fluvial deposits, confirming the marine transgression fully developed during the Black Alley Shale. Despite the restricted geography thought for the Galilee Basin, the outer eastern shoulder of the estuary (proximal to the Springsure Shelf) does not preserve an intense tidal signature, but shows wave reworking and storm deposits. This leads to an interpretation of an 'open' landscape morphology, ideal for the development of long fetch. The presence and absence of angular conglomerates on the Springsure Shelf during the Lopingian is suggestive that a local intermittent sediment supply is recorded during this time.

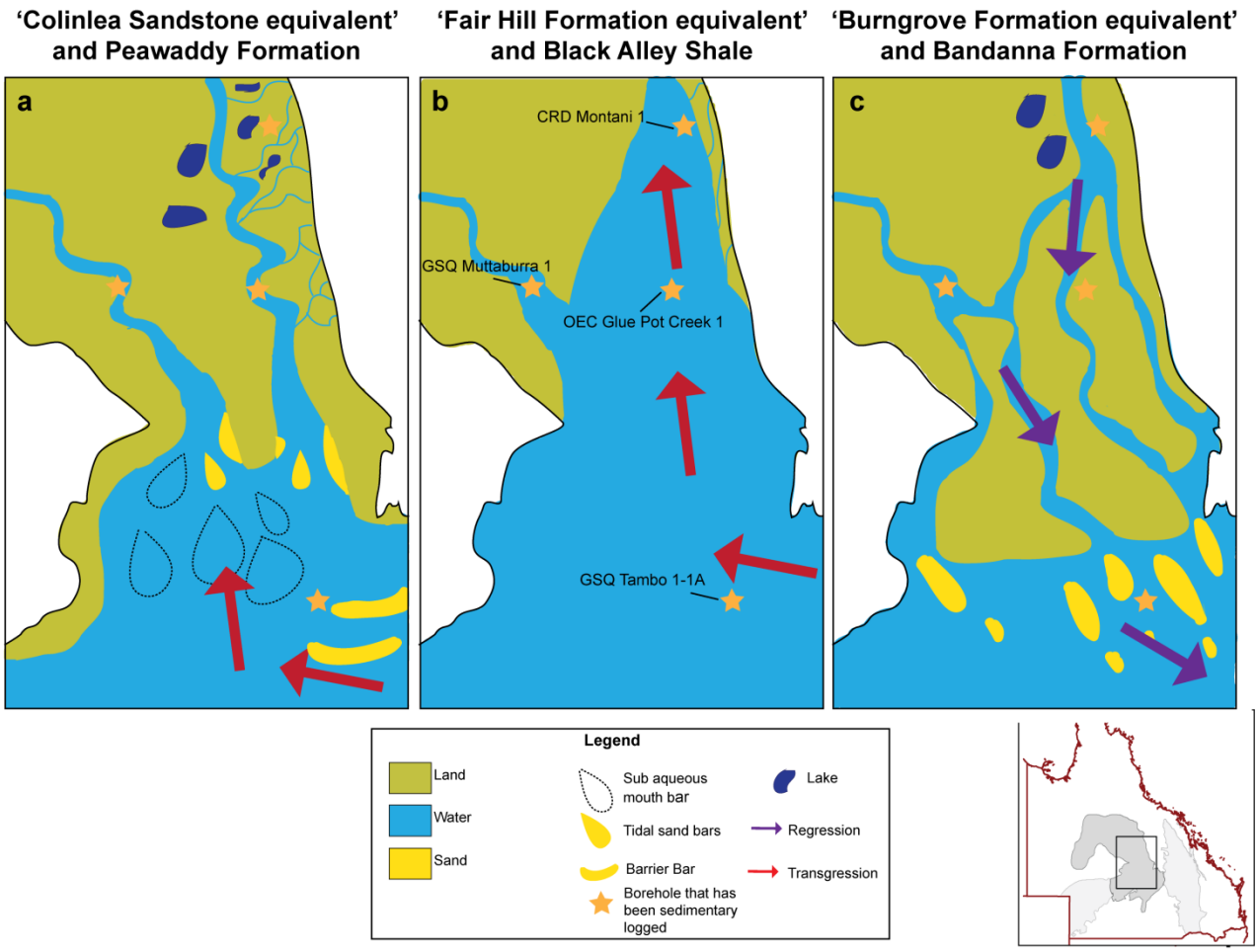

Figure 32: Interpreted palaeo-environments of (a) the 'Colinlea Sandstone equivalent' and Peawaddy Formation. Formations are time equivalent of one another. Maximum extent of land can be constrained within 50 kms north of GSQ Tambo 1-1A to the southern end of cross section 3 (Figure 31a) (b) the 'Fair Hill Formation equivalent' the Black Alley Shale. Formations are time equivalent of one another. (c) the 'Burngrove Formation equivalent' and Bandanna Formation. Formations are not time equivalent but experience similar reconstructed palaeo-environments, progradation. For borehole names see Figure 32b. Inset map shows palaeo-environment reconstruction location.

The terrestrial Freitag Formation, tidal Ingelara Formation and coastal Catherine Sandstone are only observed on the Springsure Shelf (e.g. GSQ Tambo 1-1A, Figure 28), suggesting that the earliest Lopingian marine transgression did not fully enter the Galilee Basin. Overlying these formations, the Peawaddy Formation is interpreted as tidal flats and the lateral and downstream marine facies of the terrestrial 'Colinlea Sandstone equivalent', the first Lopingian strata seen in the Koburra Trough. The southern and central western parts of the 'Colinlea Sandstone equivalent' displays classic fluvial and over bank fining-upwards sequences, all of which are capped by coal. The decrease in thickness of each fining-upwards cycle suggests a more frequent channel avulsion on a distributive delta plain, in response to the transgression leading to deposition of the Peawaddy Formation. In the northern region of the study area, localised subsidence promoted fluctuations in groundwater level resulting in the formation of lacustrine/water saturated environments, which occasionally dried out sufficiently to become vegetated.

During deposition of the Black Alley Shale and overlying the Peawaddy Formation, conditions become anoxic as the marine transgression into the basin continued. The presence of volcanic ash layers within the Black Alley Shale allows correlation with the tuffaceous coal seams in the 'Fair Hill Formation equivalent'. These coal seams are observed to thin and become increasingly shalier towards the southern Black Alley Shale, implying that the two environments were coeval.

The regression after deposition of the Black Alley Shale saw the deposition of the 'Burngrove Formation equivalent' as a prograding delta. The distinctive coarsening-upwards sequences within the 'Burngrove Formation equivalent' can be seen stacked from north to south in cross section providing evidence of a southerly delta progradation. When the environment was favourable, i.e. mires or quiet restricted bays in the lower delta plain, volcanic ash layers settled and were preserved indicating that volcanic activity was continuous from the 'Fair Hill Formation equivalent' and Black Alley Shale through to the deposition of the 'Burngrove Formation equivalent'.

The Bandanna Formation is interpreted to be a continuation of deltaic sedimentation. However, it is distinguishable from the underlying 'Burngrove Formation equivalent' by a sharp decrease in volcanic ash layers. The northern and central parts of the Galilee Basin study area display upper delta plain facies, while the southern study region and Springsure Shelf area are dominated by lower delta plain facies.

Results from this study do not make the stimulus for the large regional transgression and regression any clearer. Nonetheless, palaeo-environmental models constructed in this study complement Lopingian models from the adjacent Bowen Basin and can be used to further research into the causes of this relative sea-level change.

4.11. Acknowledgements

The authors of this paper would like to thank the Australian Coal Association Research Program, grant number C22028, for funding, and the Vale-UQ Coal Geosciences Program. The Geological Survey of Queensland's Exploration Data Centre in Zillmere, Brisbane, is thanked for use of their facilities and assistance while viewing drill core. Dr Renate Sliwa is thanked for her helpful review of an early draft of the manuscript. Dr. Mike Martin and an anonymous reviewer greatly helped to improve the quality of this manuscript. Chapter 4, '**Palaeo-environmental reconstruction of Lopingian (upper Permian) sediments in the Galilee Basin, Queensland, Australia,**' has been published with the permission of the Geological Society of Australia.

Chapter 5 is submitted to the Australian Journal of Earth Sciences to be published as:

5. Detrital zircon U-Pb geochronology of Permian strata in the Galilee Basin, Queensland, Australia

L. J. Phillips[1], C. Verdel[1], C. M. Allen[2] and J. S. Esterle[1]

[1] School of Earth and Environmental Sciences, University of Queensland, Brisbane, QLD, Australia
[2] School of Earth, Environmental and Biological Sciences, Queensland University of Technology, Brisbane, QLD, Australia

5.1. Abstract

The late Carboniferous to Triassic tectonic history of eastern Australia includes important periods of regional-scale crustal extension and contraction. Evidence for these periods of tectonism is recorded by the extensive Late Carboniferous to Triassic basin system of eastern Australia. In this study we investigate the use of U-Pb dating of detrital zircons in reconstructing the tectonic development of one of these basins, the eastern Galilee Basin of Queensland. U-Pb detrital zircon ages were obtained from samples of stratigraphically well-constrained Cisuralian and Lopingian (early and late Permian, respectively) sandstone in the Galilee Basin. Detrital zircons in these sandstones are dominated by a population with ages in the range of 250-300 Ma, and ages from the youngest detrital zircons closely approximate depositional ages. We attribute these two fundamental findings to (1) appreciable derivation of detrital zircons in the Galilee Basin from the New England Orogen of easternmost Australia, and (2) (near) syn-depositional magmatism. Furthermore, Cisuralian sandstone of the Galilee Basin contains significantly more >300 Ma detrital zircons than Lopingian sandstone. The transition in detrital zircon population, which is bracketed between 296 and 252 Ma based on previous high-precision radiogenic isotope ages from Permian ash beds in the Galilee Basin, corresponds with the Hunter-Bowen Orogeny and reflects a change in the Galilee Basin from an earlier extensional setting to a later foreland basin environment. During the Lopingian foreland basin phase, the individual depocentres of the Galilee and Bowen basins were linked to form a single and enormous foreland basin that covered >300,000 km^2 in central and eastern Queensland.

Keywords: Galilee Basin, geochronology, detrital zircon, New England Orogen, Thomson Orogen, tectonics

5.2. Introduction

The Carboniferous to Middle Triassic Galilee Basin (Figure 33) of central Queensland is commonly inferred to have formed in a low-accommodation, intracratonic setting (Allen and Fielding, 2007b; Van Heeswijck, 2006, 2010). This basin is linked, however, both stratigraphically and spatially, with the adjoining Bowen Basin (Figure 33), and the development of the Bowen Basin was clearly related to both extensional and contractional tectonism during west-dipping subduction along the east Australian margin (e.g. Korsch and Totterdell, 2009b; Korsch et al., 2009b). The extent to which the Galilee Basin may also be related to convergent margin tectonism is unclear. One line of research for addressing this uncertainty is evaluating the provenance of Galilee Basin sediments. In this study, we combine new detrital zircon U-Pb results from Permian strata of the Galilee Basin with previous petrographic and geochemical datasets. In particular, we address the question of whether provenance shifts in the Galilee Basin may be related to the first-order, early Permian to Triassic tectonic framework of north-eastern Australia. Our results are useful for evaluating the Galilee Basin Permian stratigraphy proposed by Phillips et al. (2017c), as well as examining potential changes in provenance of the Galilee Basin during Permian time.

5.3. Geological and tectonic setting

The Galilee Basin of north-eastern Australia consists of Carboniferous to Triassic sedimentary rocks and interbedded volcanic ash layers. These strata overlie Devonian to Carboniferous sedimentary and volcanic rocks of the Drummond Basin (Figure 33), which, in turn, unconformably overlie late Neoproterozoic to Ordovician metasedimentary and intrusive rocks of the Thomson Orogen. The Charters Towers and Anakie Inlier provinces (Figure 33) are exposed portions of the Thomson Orogen 'basement' that are situated to the north-east and east of the Galilee Basin, respectively.

The development of the Bowen Basin, and also, potentially, the Galilee Basin, was closely related to important periods of tectonism in eastern Australia. Crustal extension associated with initial development of the Bowen Basin began during the late Pennsylvanian and Cisuralian (early Permian) (Korsch and Totterdell, 2009b; Korsch et al., 2009b). Extensional tectonism affecting the Bowen Basin region is thought to have ceased by ~280 Ma, marking a transition to thermal subsidence of the basin, although extension may have persisted slightly longer in some parts of the Bowen Basin (Korsch and Totterdell, 2009b). In both the Bowen and Galilee basins, Guadalupian strata are generally absent, signifying a mid-Permian period of non-deposition or erosion (Nicoll et al., 2015; Van Heeswijck, 2010). A recent palynological study suggests that local sedimentation

occurred until ~272 Ma in isolated grabens in the Galilee Basin (Phillips et al., In Press), a conclusion that reduces the duration of the depositional hiatus in the Galilee Basin.

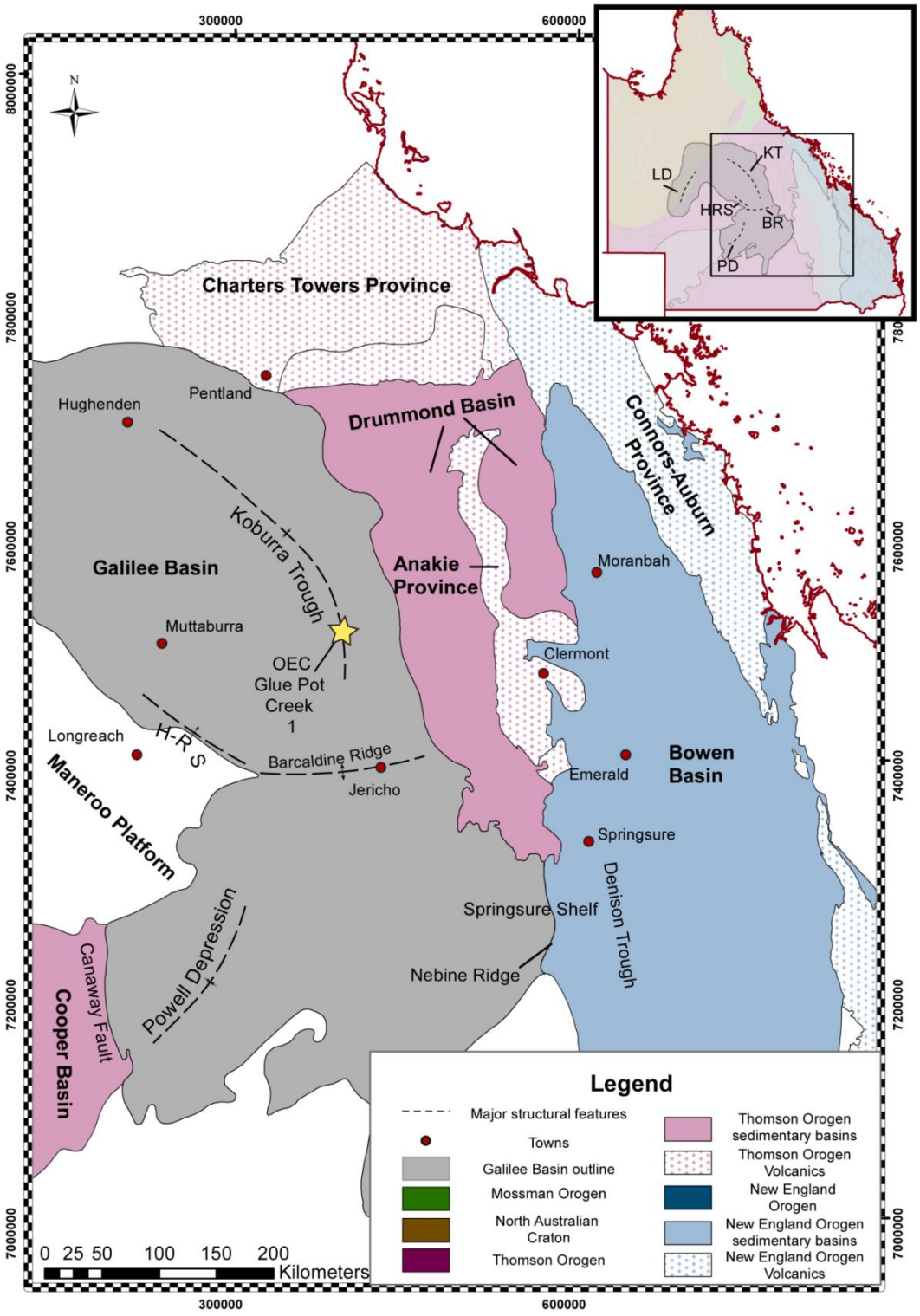

Figure 33: Map showing the Galilee Basin, key structural features, the neighbouring Thomson and New England orogens, and associated sedimentary and volcanic basins. OEC Glue Pot Creek 1 is shown by a yellow star. Inset map shows orogen locations in Queensland. Abbreviations: KT – Koburra Trough, BR – Barcaldine Ridge, PD – Powell Depression, HRS – Hulton-Rand Structure and LD – Lovelle Depression.

Both the Galilee and Bowen basins experienced renewed sedimentation during Lopingian (late Permian) time, albeit at a much greater rate in the Bowen Basin (Korsch and Totterdell, 2009b; Phillips et al., 2017c). The relatively thin (~200 m) accumulation of Lopingian sediments in the Galilee Basin has been attributed to far field expressions of dynamic loading occurring in the adjacent Bowen Basin, where, in places, Lopingian sediments are >1 km thick (de Caritat and Braun, 1992; Korsch and Totterdell, 2009b). de Caritat and Braun (1992) described the Galilee Basin as a platform basin that formed to the west of a peripheral bulge (Anakie Inlier) that separates it from a foreland basin (Bowen Basin) to the east. According to this tectonic interpretation, Lopingian strata of both the Galilee and Bowen basins are part of a large foreland basin system (e.g. DeCelles and Giles, 1996) associated with the dominantly west-vergent fold-thrust belt of the New England Orogen (Figure 33) along the easternmost part of the Australian continent. Contractile deformation and accompanying formation of this system occurred during the mid-Permian to Late Triassic (~275 to 230 Ma) Hunter Bowen Orogeny (e.g. Holcombe et al., 1997; Shaanan et al., 2015).

5.4. Stratigraphy and geochronology of the Galilee Basin

In the following description of stratigraphy, we use the updated Galilee Basin stratigraphic nomenclature of Phillips et al. (2017c). The stratigraphy of the Galilee Basin can be divided into Cisuralian and Lopingian parts that are briefly discussed below. High-precision chemical abrasion – isotope dilution thermal ionisation mass spectrometry (CA-IDTIMS) U-Pb ages from tuffaceous layers within these units are useful for inter-basinal correlation (Nicoll et al., 2015; Nicoll et al., 2016a, 2016b; Phillips et al., In Press). All dates, unless otherwise stated, discussed in this study have a 2σ error.

Cisuralian stratigraphy

The Cisuralian Joe Joe Group of the Galilee Basin consists of five formations: in ascending order, the Lake Galilee Sandstone, the Jericho Formation (including the Oakleigh Siltstone Member), the Jochmus Formation (including the Edie Tuff Member), the Aramac Coal Measures, and the combined ‘J and K’ Seams (McKellar and Henderson, 2013; Phillips et al., In Press). The Lake Galilee Sandstone is made up of silicified, very fine- to medium-grained quartz sandstone, and it is restricted to the Koburra Trough and eastern margin of the Galilee Basin (Gray and Swarbrick, 1975; Scott et al., 1995). Conformably overlying the Lake Galilee Sandstone is the widespread Jericho Formation, which is characterised by glacial sedimentary structures (Jones and Fielding, 2008) and is thought to have been deposited in an active extensional basin during Pennsylvanian

time (Jones and Truswell, 1992). A series of interbedded siltstones, mudstones, and shales in the upper part of the Jericho Formation comprise the Oakleigh Siltstone Member (Gray and Swarbrick, 1975).

Overlying the Jericho Formation is the Jochmus Formation, the majority of which is fine- to medium-grained sandstone, but the upper part of the formation consists of siltstone, mudstone, and tuff of the Edie Tuff Member. These tuffs have previously been dated using the CA-IDTIMS technique (Nicoll et al., 2015, 2016a, 2016b; Phillips et al., In Press). Nicoll et al. (2015) reported two CA-IDTIMS ages of 294.80 ± 0.08 and 294.91 ± 0.09 Ma from the upper section of the Edie Tuff Member in the GSQ Muttaburra 1 well, which is situated near the Hulton-Rand Structure (Figure 33) along the central western margin of the Galilee Basin. Two CA-IDTIMS ages have been reported from the Edie Tuff Member in the Koburra Trough: 295.65 ± 0.07 Ma from the top of the member (R. Nicoll pers. comm.) and 296.09 ± 0.07 Ma from the lower half of the unit (Phillips et al., In Press). The ~850 ky difference between the youngest age of the member on either side of the Galilee Basin suggests erosion of the upper section of the Edie Tuff Member in the Koburra Trough. Nicoll et al. (2016a) suggested that the tuffs in the Edie Tuff Member could be related to the Camboon Volcanics of the New England Orogen, which Korsch et al. (2009b) attributed to the initial, extensional stage of the Bowen Basin. The tuffs could also be related to the Lizzie Creek Volcanics (also in the New England Orogen), which contain felsic volcanic rocks, including an ignimbrite near Mackay that has been dated at 294.2 ± 2.8 Ma (1σ, Allen et al., 1998).

Overlying the Jochmus Formation are the Aramac Coal Measures, which were considered by Van Heeswijck (2006) to be the expression of the ‘thermal sag’ phase of the Galilee Basin. These coal measures are restricted to the Lovelle Depression and the Hulton-Rand Structure (Figure 33), and they consist of sandstone, siltstone, shale, and coal (Gray and Swarbrick, 1975). Tuff beds within the Aramac Coal Measures have ages of 282.72 ± 0.07 and 282.41 ± 0.08 Ma (Nicoll et al., 2016a, 2016b). The Aramac Coal Measures are overlain by the ‘J and K’ seams, which have been placed at the Cisuralian-Guadalupian boundary through palynological analysis. They consist of sandstone, siltstone, and coal (Phillips et al., In Press). Their contact with the underlying Aramac Coal Measures represents a significant depositional hiatus encompassing the APP3.1 (Price, 1997) palynological biozone in the Galilee Basin. The ‘J and K’ seams are the last records of sedimentation in the Galilee Basin prior to Lopingian time.

Lopingian stratigraphy

Lopingian strata of the eastern and central Galilee Basin are subdivided into five units. From oldest to youngest, they are the 'Colinlea Sandstone equivalent', the 'Fair Hill Formation equivalent', the Black Alley Shale, the 'Burngrove Formation equivalent', and the Bandanna Formation. Collectively these units comprise the Betts Creek Group (Phillips et al., 2017c), a nomenclature that is commonly used for the northern and western parts of the Galilee Basin. The 'Colinlea Sandstone equivalent' consists of three main coal seams (Seams D, E, and F), along with sandstone and siltstone interburden (Phillips et al., 2015, 2017b; Scott and Hawkins, 1992). The 'Fair Hill Formation equivalent' conformably overlies the 'Colinlea Sandstone equivalent', and it consists of carbonaceous mudstone and siltstone, interbedded with coal and volcanic ash layers. The main coal seam within the 'Fair Hill Formation equivalent' is the C seam (Phillips et al., 2017a, 2017c). Volcanic ash layers within the C seam have CA-IDTIMS ages of 254.31 ± 0.10, 254.41 ± 0.07, and 255.13 ± 0.09 Ma (Phillips et al., In Press). The oldest of these results suggests correlation with the Nobbys Tuff in the Sydney Basin (Metcalfe et al., 2015), and the younger results suggest correlation between the Fair Hill Formation equivalent of the Galilee Basin and the Black Alley Shale of the Bowen Basin (Metcalfe et al., 2015).

The Black Alley Shale, which overlies the 'Fair Hill Formation equivalent', was deposited during a period of marine transgression in both the Bowen and Galilee basins (Allen and Fielding, 2007b). It is a predominately structureless unit that is interbedded with volcanic ash layers (Phillips et al., 2017a), one of which produced a CA-IDTIMS age of 254.08 ± 0.06 Ma (Phillips et al., In Press). A period of regression followed deposition of the Black Alley Shale, and, during this regression, the 'Burngrove Formation equivalent' was deposited as part of a deltaic system (Allen and Fielding, 2007b; Phillips et al., 2017a). Capping this sequence is the B coal seam (Phillips et al., 2015), which includes ash horizons, the uppermost of which has an age of 252.81 ± 0.07 Ma. This upper ash horizon correlates with the Yarrabee Tuff of the Bowen Basin (Ayaz et al., 2016b; Phillips et al., In Press). In the Bowen Basin, the Yarrabee Tuff separates the underlying Burngrove Formation from the overlying Bandanna, Rangal, and Baralaba coal measures (Draper, 2013; Sliwa et al., 2017). A similar relationship occurs in the Galilee Basin, where the Bandanna Formation conformably overlies the 'Burngrove Formation equivalent'. The Bandanna Formation consists of sandstone, siltstone, and the youngest coal seam in the Galilee Basin, the A seam. It is unclear if the Triassic Rewan Formation conformably or unconformably overlies the Bandanna Formation in the Galilee Basin (McKellar and Henderson, 2013; Sliwa et al., 2017). A mudstone bed has been observed at the boundary between the Bandanna and Rewan formations in the Galilee Basin and their stratigraphic equivalents in the Bowen Basin (Michaelsen, 2002; Sliwa et al., 2017; Wilson,

2017). Although not continuous in either basin, the mudstone has been observed along the eastern margin of the Galilee Basin and the western margin of the Bowen Basin (Sliwa et al., 2017; Wilson, 2017).

Van Heeswijck (2010) concluded that all units within the Lopingian and Early Triassic stratigraphy of the Galilee Basin were deposited during an extended period of thermal subsidence of the Galilee Basin after the mid-Permian hiatus. However, the evidence of variable palaeo-environments recorded by each lithostratigraphic unit in the Galilee Basin (Phillips et al., 2017a) during this time period is suggestive of a much more complex tectonic setting.

5.5. Previous provenance studies

Limited research into sediment provenance has been conducted previously in the Galilee Basin. These studies have been mainly based on petrographic examination and can be divided into two geographic areas in the northern and southern parts of the basin. Petrographic analysis of the Cisuralian Joe Joe Group from the northern part of the basin revealed a composition of predominantly quartz, with a minor feldspathic component (Hawkins and Carmichael, 1987; Van Heeswijck, 2006). Quartz, feldspar, lithics (QFL) ternary plots suggest a 'recycled orogen' as a potential source for the northern Galilee Basin Cisuralian sediments (Van Heeswijck, 2006), and the presence of feldspar could indicate a minor component derived from a volcanic source (Hawkins and Carmichael, 1987). These sources were interpreted to be the Thomson Orogen to the west and the Carboniferous – Permian Kennedy Igneous Province to the east (Van Heeswijck, 2006; Figure 33).

The Joe Joe Group on the Springsure Shelf is also composed, predominantly, of quartz, with limited, but recognisable amounts of feldspar (Grigorescu, 2012). Mollan et al. (1969) noted that lithic fragments within the Joe Joe Group consist of fine-grained volcanic and metasedimentary rocks. The provenance of the Joe Joe Group has been linked to a number of sources, including the Neoproterozoic to early Paleozoic Anakie Metamorphics of the Anakie Inlier and the Devonian Dunstable Volcanics and other volcanic rocks within the Drummond Basin (Mollan et al., 1969; Figure 33).

Similar to the underlying Cisuralian formations, the Lopingian Betts Creek Group is predominately quartzose, although it contains more volcanolithics than underlying strata (Hawkins, 1976; Hawkins and Carmichael, 1987; Van Heeswijck, 2006). Van Heeswijck (2006) attributed the provenance to the same recycled orogenic sources as the underlying Joe Joe Group (namely, the Thomson Orogen

to the west and the Kennedy Igneous Province to the east). Hawkins and Carmichael (1987) interpreted the source areas to be granitic and metamorphic in composition. Possible sources to the east of the Galilee Basin include the Anakie Metamorphics and volcanic rocks exposed along the eastern margin of the Drummond Basin. The Ordovician-Silurian Ravenswood Granodiorite of the Charters Towers Province is a possible source to the north-east of the Galilee Basin (Figure 33).

The Colinlea Sandstone (the lateral equivalent of the 'Colinlea Sandstone equivalent' in the Koburra Trough and eastern margin of the Galilee Basin, and the lower section of the Betts Creek Group to the north) on the Springsure Shelf is predominately composed of quartz, and basal conglomerates contain chert, volcanic rocks, and subordinate quartzite (Mollan et al., 1969; Bastian, 1965). The lower part of the Colinlea Sandstone is feldspar deficient, but the upper part contains substantially more feldspar (Bastian, 1965; Mollan et al., 1969). Bastian (1965) suggested that the lower part of the Colinlea Sandstone was derived from the Anakie Inlier to the north and north-east of the Springsure Shelf, whereas the upper part was derived from a more feldspathic westerly source. In contrast, palaeo-current indicators suggest a source to the west and south-west for the lower part of the Colinlea Sandstone, transitioning to an easterly source for the upper part (Mollan et al., 1969).

The Bandanna Formation is the youngest Lopingian formation on the Springsure Shelf. It is equivalent to the upper part of the Betts Creek Group and it has a highly variable composition (Grigorescu, 2012). Although quartz is the major constituent, both plagioclase and K-feldspar are common. A significant amount of zeolite has been described from one sample from the Springsure Shelf. In conjunction with the presence of large amount of feldspar, this observation suggests a volcanic source (Grigorescu, 2012).

In summary, it is clear from previous studies that a variety of metamorphic, volcanic, and sedimentary sources contributed sediment to the Galilee Basin. To the extent that these various sources have distinctive zircon U-Pb ages, geochronological analysis of detrital zircons in sandstone of the Galilee Basin, aligned with previous petrographic studies, could be useful for determining if the provenance of Galilee Basin sediments is as polymodal as previously described.

5.6. Methodology

Sample Preparation

Drillcore from OEC Glue Pot Creek 1 was chosen for detrital zircon age analysis because it includes both early and late Permian strata. Nine sandstones samples were chosen: five are Cisuralian, and four are Lopingian. The maximum sample size was 250 g, which is somewhat limiting in terms of high zircon yields. Multiple samples were chosen from each age interval to account for the small samples sizes. All samples were crushed and sieved to <600 μm, then passed over a water table to remove the less dense fraction. Four of the nine samples yielded a large volume of high density minerals. Magnetic minerals were removed from those four samples with a Frantz Magnetic Separator. Heavy mineral separates were obtained from all samples with methylene iodide. Zircon grains were handpicked from these separates and set into a non-reactive epoxy. Mounts were polished to ensure an even and exposed surface of mid sections of the zircons. Images of the mounted zircons were collected under transmitted and reflected light on a Leica DM6000M automated microscope. Mounts were then carbon coated for cathodoluminescence (CL) imaging.

Analytical methods

CL images of the mounts were collected at the Queensland University of Technology (QUT) using a Zeiss scanning electron microscope using 15 keV accelerating voltage with a VPSE G3 detector attached, where bias=0 under high vacuum conditions. U-Pb isotopic and trace element analysis was conducted on individual zircon grains with a ESI New Wave excimer laser system (193 nm) with a TV2 cell connected to an Agilent 8800 Laser Ablation Inductively Coupled Plasma Mass Spectrometer (LA-ICPMS) at QUT during two sessions on consecutive days. Thirty second gas backgrounds were followed by ablation for 30 seconds per sample with a 30 μm laser beam with a laser fluence of about 2 J/cm^2 as measured at the exit from the laser in a He atmosphere (0.6 l/min) that was introduced into the main Ar gas carrier flow to the ICPMS (1 l/min). Ablation sites were chosen away from inclusions and cracks and targeted at coherent luminescence regions within the grains. Temora 2 (TIMS $^{206}Pb/^{238}U$ age 416.78 ± 0.33 Ma; Black et al. (2004) was used as the primary reference zircon (n=24 and 11), and the Plešovice zircon (TIMS $^{206}Pb/^{238}U$ age 337.13±0.37 Ma; Sláma et al. (2008) was used as a monitor standard (n=24 and 9). The National Institute of Standards and Technology (NIST) 610 glass standard was used for calculating trace element concentrations (n=25 and 13). The set of three standards were measured at an interval between 10-12 unknowns. Data were reduced using U-Pb Geochron4 for dating and Trace elements IS for trace element composition data reduction schemes in IOLITE (Paton et al., 2010) following the overall procedure of Longerich et al. (1996). In a post-processing Excel spreadsheet, if a 208-

based common Pb correction (after Bryan et al. 2004) improved concordance over the uncorrected age, then that age was deemed 'best' and is reported. Measured ages were also filtered for exceptionally high P, La and Ti concentrations (2000, 10 and 50 ppm, respectively), and large uncertainty (20%) in the $^{207}Pb/^{235}U$ ages and removed from compilation. Kernel density estimates (KDE) and weighted mean averages were calculated and presented using DensityPlotter (Vermeesch, 2012) and IsoPlot (Ludwig, 2003), respectively.

5.7. Results

Plešovice zircon was used as a monitor standard to test for accuracy and precision. During the two analytical sessions, the Plešovice zircon produced concordant $^{206}Pb/^{238}U$ ages (no common Pb correction) of 341.6±3.5 Ma for 24 grains with MSWD of 1.3 (1 exclusion, 2 s.e.) and 334.6±4.5 Ma, with MSWD of 0.84 for 9 grains, ages that are accurate given its TIMS age of 337.13±0.37 Ma and stated uncertainties. These results give confidence that accurate results have been obtained for populations using our fits to the primary standard, Temora (down-hole fractionation, and drift over the course of the session).

U-Pb and trace element analysis was conducted on 377 zircons from nine samples of sedimentary rocks collected from Cisuralian to Lopingian sandstone from the Glue Pot Creek 1 well, Galilee Basin. Of these, 286 zircons produced concordant ages (Figure 34) and showed no sign of included phases (e.g. phosphates and opaque minerals). The morphologies of the grains were generally euhedral, although some had a more rounded texture (Figure 35a). For statistical purposes, the results from stratigraphically similar samples were combined (Table 6): GPC_02, GPC_03, and GPC_06 were combined to create composite sample GPC_A; GPC_08 and GPC_09 were combined to create GPC_B; and GPC_29, GPC_30, GPC_31, and GPC_32 were combined to create GPC_C. Individual results are shown in Figure 36 and Appendix 8.8. Results for combined samples are presented in Figure 37. Individual analytical errors presented in this study are 2σ.

Defining the depositional age

Three different techniques were used to define the depositional ages of the combined samples (Table 7). The techniques are based on those of Dickinson and Gehrels (2009), with some modifications. The youngest single grain (YSG) is the youngest age with 2σ obtained from the sample. As an estimate of the depositional age, the use of a single grain carries a high analytical and geological uncertainty (Dickinson & Gehrels, 2009). The youngest graphical peak (YPP) has been calculated from KDE plots (Vermeesch, 2012; Figure 36) when all grains within the sample are plotted. This age represents the peak of the youngest population. The youngest 2σ grain cluster

YC2σ is defined by the overlap of the upper error age of the youngest grain and the lower error age of the oldest grain in the youngest cluster. Once these ages do not overlap, then the grains are not considered as part of the youngest coherent grain cluster. Dickinson and Gehrels (2009) define this population as having three or more grains, and, for the samples used in this study, the smallest cluster contains 11 grains. The YC2σ calculation is considered the most robust calculation of maximum depositional age, however caution must be made when referring to it as a depositional age, as it can be considerably older than the age of deposition (Dickinson & Gehrels, 2009). For this study, we use the YC2σ age when referring to maximum depositional ages.

Geochronological results

LA-ICPMS zircon U-Pb ages ranging from Cambrian to Pennsylvanian make up 62.2% of the overall population from sample GPC_A (n=82; 29.3% are Pennsylvanian and 32.9% are Cambrian to Mississippian). The predominant age population is between ~288 and ~329 Ma, and there are three minor age populations of ~360 to ~450 Ma, ~500 to ~550 Ma, and ~750 to ~850 Ma (Figure 37). The YC2σ mean weighted age from GPC_A is 302.6 ± 3.0 Ma, based on 28 zircons (Upper Pennsylvanian to Cisuralian; Figure 38).

The principal detrital zircon U-Pb age group (66.4% of ages) from sample GPC_B (n=122) is Cisuralian (Figure 34). The predominant age population is between ~270 and ~310 Ma (Figure 37). The YC2σ mean weighted age of the eleven youngest grains is 270.1 ± 4.5 Ma (Figure 38).

The youngest single zircon from sample GPC_C has an age of 233 ± 13 Ma (Middle to Upper Triassic; Figure 35b). This result is problematic because the samples that comprise GPC_C were collected from beneath the A seam which is known to be Permian based on the appearance of *Dulhuntyispora parvithola*, the palynological index taxa for the Lopingian APP5 zone (Australia Pacific LNG, 2010; Figure 37). This is an example where the use of the YSG may not be appropriate for estimating depositional age because of an analytical anomaly. When used in the calculation of the YC2σ, the mean weighted age of the 42 youngest grains is 247.1 ± 1.9 Ma. When excluded, the YC2σ includes 45 youngest grains with a mean weighted age of 248.6 ± 1.9 Ma.

Sample (Combined)	Sample (individual)	Depth to (m)	Depth from (m)	Thickness (m)	Formation
GPC_A	GPC_02	853.97	854.07	0.10	Joe Joe Group
	GPC_03	840.91	841.01	0.10	
	GPC_06	818.32	818.43	0.11	
GPC_B	GPC_08	803.14	803.25	0.11	'Colinlea Sandstone equivalent'
	GPC_09	797.95	798.05	0.10	
GPC_C	GPC_29	649.16	649.25	0.09	Bandanna Formation
	GPC_30	646.84	646.97	0.13	
	GPC_31	637.34	637.44	0.10	
	GPC_32	628.94	629.04	0.10	

Table 6: Summary of samples used within this study, showing the individual and combined sample names as well as depths, thicknesses and formations of samples.

Sample (Combined)	YSG (Ma)	YPP (Ma)	YC2σ (Ma)
GPC_A	288 ± 12	306	302.6 ± 3.0
GPC_B	250 ± 12	279	270.1 ± 4.5
GPC_C	233 ± 13	244	247.1 ± 1.9
GPC_C (excluding YSG)	239 ± 12	244	248.6 ± 1.9

Table 7: Depositional ages calculated for each combined sample. Abbreviations: YSG - youngest single grain, YPP – youngest graphical age peak from a kernel density estimate plot and YC2σ – youngest 2σ grain cluster where 3 or more grain ages overlap.

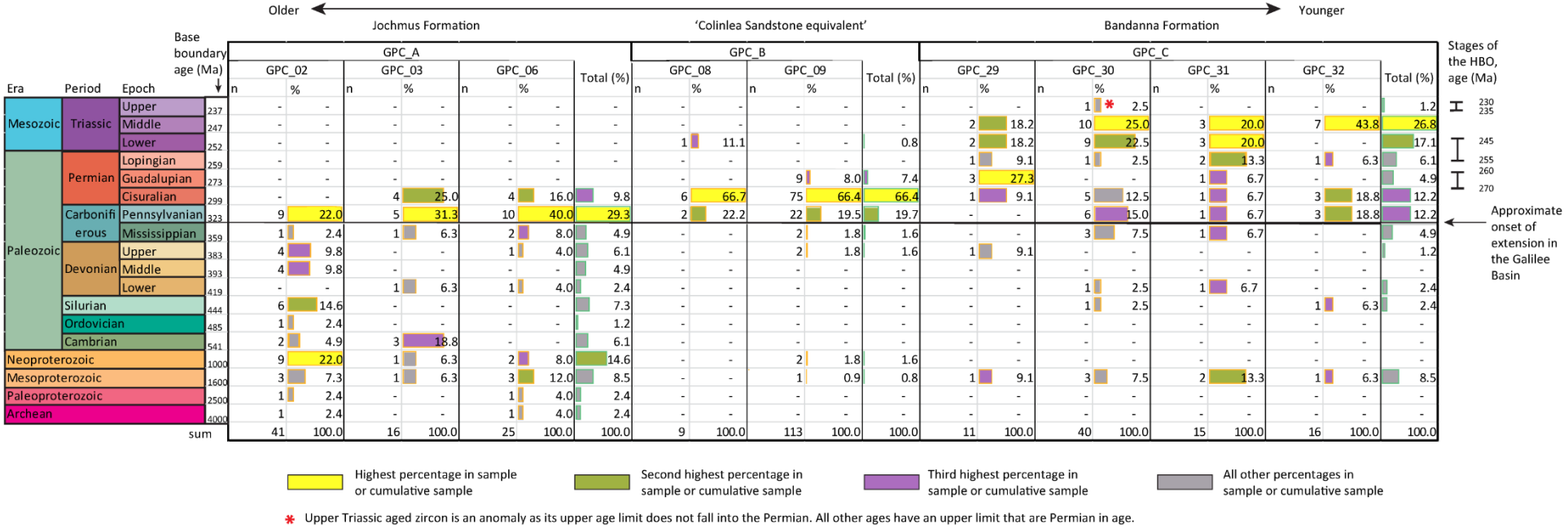

* Upper Triassic aged zircon is an anomaly as its upper age limit does not fall into the Permian. All other ages have an upper limit that are Permian in age.

Figure 34: Zircon ages for individual samples. Coloured boxes behind numerals represent the relative proportion per sample. Stages of the Hunter Bowen Orogeny modified from Hoy and Rosenbaum (2017). Abbreviations: HBO – Hunter Bowen Orogeny.

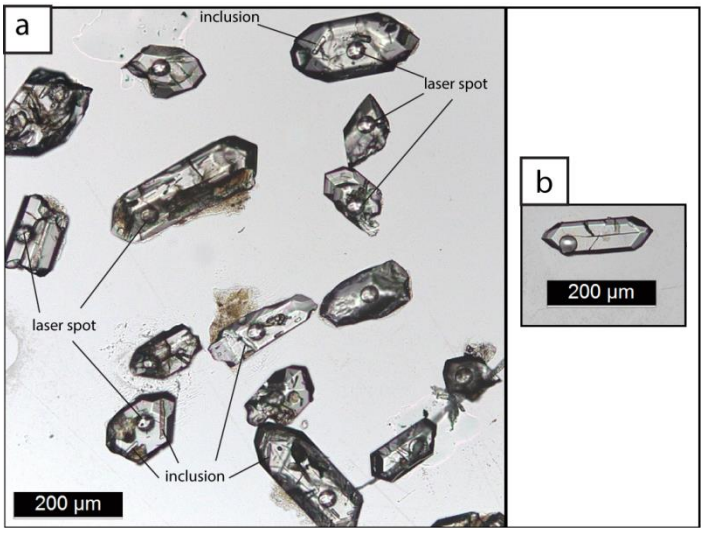

Figure 35: Plane polarised light photomicrograph showing a) the typical morphology (inclusions and euhedral shape) of zircon grains from the Galilee Basin. Laser spots are also shown. The sample is GPC_09 ('Colinlea Sandstone equivalent'). b) The excluded zircon grain from GPC_C (233 ± 13 Ma) with the laser spot.

5.8. Discussion

Comparison of detrital zircon results with depositional ages of strata in the Galilee Basin

U-Pb analysis of detrital zircons from Cisuralian strata in OEC Glue Pot Creek 1, (composite sample GPC_A) yielded a combined youngest age population of 302.6 ± 3.0 Ma from 28 zircons that overlap in age (Figure 38). This is consistent with CA-IDTIMS dates from the surrounding strata (Phillips et al., In Press, R. Nicoll pers. comm.). The oldest Lopingian samples (composite sample GPC_B), collected from the base of the 'Colinlea Sandstone equivalent', yielded a youngest mean weighted age of 270.1 ± 4.5 Ma (n=11). Although the mean weighted age of GPC_B may be indicative of a Guadalupian depositional age, palynological analysis, CA-IDTIMS ages and geophysical correlations of wells suggest that no strata of that age is present on the eastern side of the Galilee Basin (e.g. Norvick, 1981; Phillips et al., In Press; R. Nicoll pers. comms.). The lack of detrital zircons younger than 270 Ma (except for one detrital zircon grain with an age of 250 ± 12 Ma) may represent the thermal subsidence stage of the Galilee and adjacent Bowen basins (Korsch & Totterdell, 2009; Van Heeswijck, 2010), which also coincides with the depositional hiatus experienced by both basins (e.g. Nicoll et al., 2015, Phillips et al., In Press). Due to the lack of volcanic ash layers within the 'Colinlea Sandstone equivalent', no radiogenic isotope dating has been conducted on it in the Galilee Basin. A volcanic ash layer (the P-Tuff) within the Moranbah Coal Measures of the Bowen Basin has previously produced zircon Sensitive High-Resolution Ion Microprobe (SHIRMP) and CA-IDTIMS U-Pb ages of 256.0 ± 0.07 to 258.9 ± 2.7 Ma (Collins, 2009; Metcalfe et al., 2015; Michaelsen et al., 2001; Smith and Mantle, 2013). Through geophysical

correlations, the age of the P-Tuff overlaps with the age of the upper section of the 'Colinlea Sandstone equivalent'. Thus, the depositional age of the 'Colinlea Sandstone equivalent' cannot be younger than ~259 Ma. It is therefore rational to suggest that the youngest mean weighted age of 270.1 ± 4.5 Ma for GPC_B is from the lower section of 'Colinlea Sandstone equivalent' and is consistent with the correlation (Figures 37 and 38).

The youngest detrital zircons from the Lopingian Bandanna Formation (the GPC_C sample, and the youngest strata analyzed in this study), have a mean weighted age of 248.6 ± 1.9 Ma (n=45) (Figure 38). The Bandanna Formation overlies a significant volcanic marker horizon in the Galilee and Bowen basins: the Yarrabee Tuff and its equivalent. CA-IDTIMS U-Pb ages from zircons in this marker horizon, obtained from samples in both basins, are between 252.54 ± 0.04 Ma and 253.07 ± 0.22 Ma (Ayaz et al., 2016a; Esterle et al., 2017; Metcalfe et al., 2015; Phillips et al., In Press), which provide a maximum age constraint on the onset of deposition of the overlying Bandanna Formation (Figure 37). The presence of Lopingian-aged coal and the Permian-Triassic (P-T) boundary stratigraphically above the GPC_C samples provide an upper age constraint of 251.90 ± 0.02 Ma (Cohen et al., 2013; updated). Deposition of the sampled Bandanna Formation sandstone must therefore have occurred between approximately 253 and 251.9 Ma. The youngest mean weighted age of detrital zircons of 248.6 ± 1.9 Ma (n=45) (Figure 38d) is thus strictly inaccurate given the accepted stratigraphy. However, if the youngest detrital zircon age (233 ± 13 Ma; Figure 35b) is excluded[4], all other ages, given their errors, overlap the P-T boundary, which is consistent with the associated absolute ages of the Bandanna Formation.

In summary, based on prior radiogenic isotope age constraints provided by CA-IDTIMS dating of tuffs, the youngest mean weighted detrital zircon U-Pb ages from Permian strata in OEC Glue Pot Creek 1 are not significantly older than their depositional ages, a finding that points toward synchronous volcanism during the Cisuralian and Lopingian deposition of the Galilee Basin. Clear evidence of Permian volcanoes near the Galilee Basin is absent, so we suggest that the (near) syn-depositional zircons of the Galilee Basin were supplied by volcanic ash clouds. Recent detrital zircon studies from Permian sedimentary basins in the New England Orogen (Campbell et al., 2015; Hoy et al., 2014; Shaanan et al., 2015; White et al., 2016; Figures 39a and b) also revealed detrital zircons that approximate depositional ages.

[4] On examination of the grain in transmitted light the laser spot is neither situated on an inclusion nor a fracture; it is positioned at the edge of this euhedral grain and some epoxy was ablated (Figure 35).

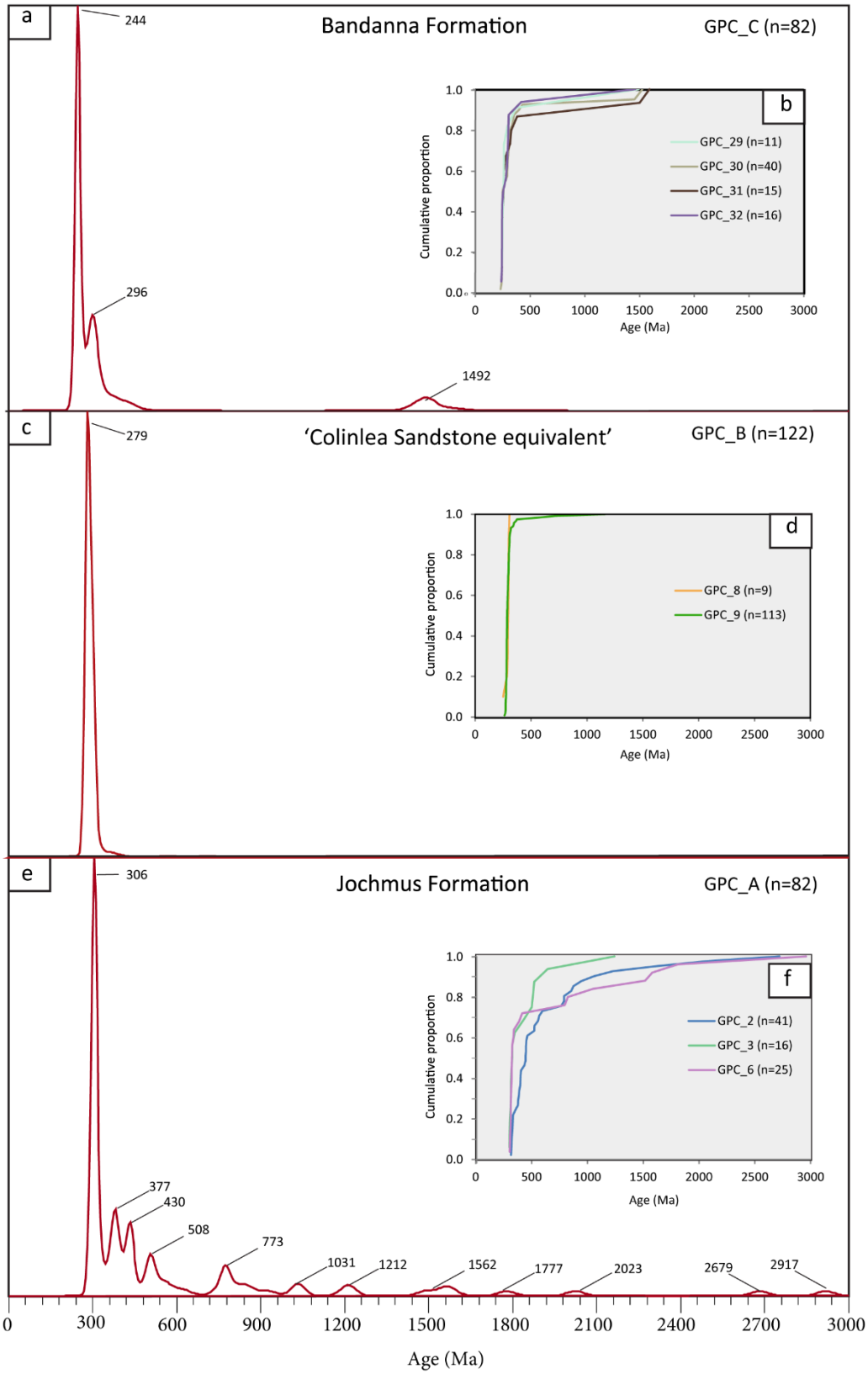

Figure 36: KDE and cumulative proportion charts for OEC Glue Pot Creek 1. Cumulative proportion charts are generated by sorting the dates within a given sample and working out their cumulative proportion between 0 and 1. This is then displayed on the chart against the dates. Vertical lines indicate a volume of dates while horizontal lines indicate an absence of dates. a) Kernel Density Estimate (KDE) for sample GPC_C from the Bandanna Formation. Peak ages are shown. b) Cumulative proportion charts for the individual samples that make up the composite sample GPC_C. c) KDE for sample GPC_B from the 'Colinlea Sandstone equivalent'. Peak ages are shown. d) Cumulative proportion charts for the individual samples that make up the composite sample GPC_B. e) KDE for sample GPC_A from the Jochmus Formation. Peak ages are shown. d) Cumulative proportion charts for the individual samples that make up the composite sample GPC_A.

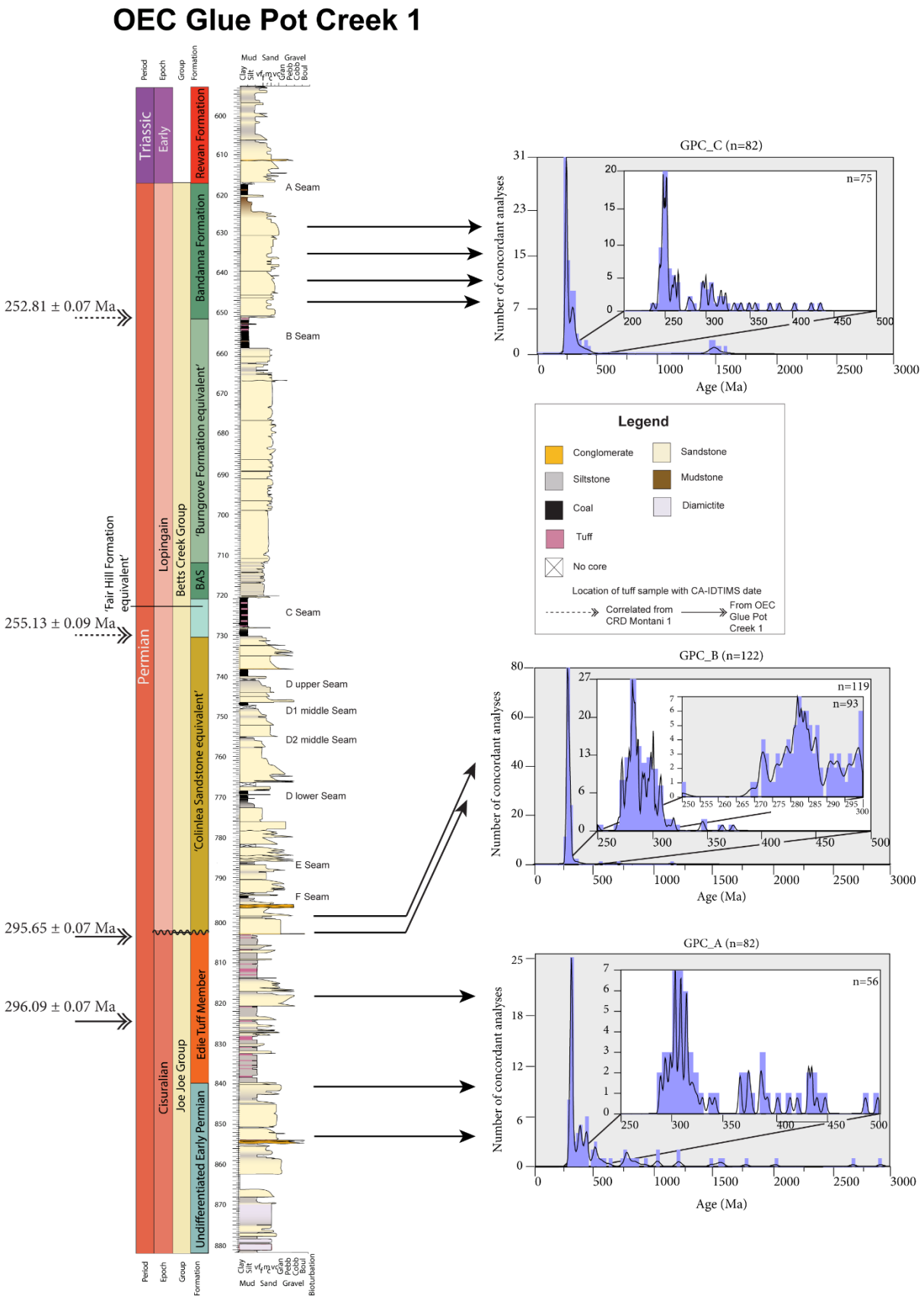

Figure 37: Sedimentary log of OEC Glue Pot Creek 1 (Phillips et al., 2017a), coupled with CA-IDTIMS dates from the Galilee Basin (Phillips et al., In Press) and R. Nicoll (pers. comm.) and combined detrital zircon histograms from this study. Each histogram also displays a Kernel Density Estimate. The time line is not to scale and the Guadalupian is represented by the squiggly line.

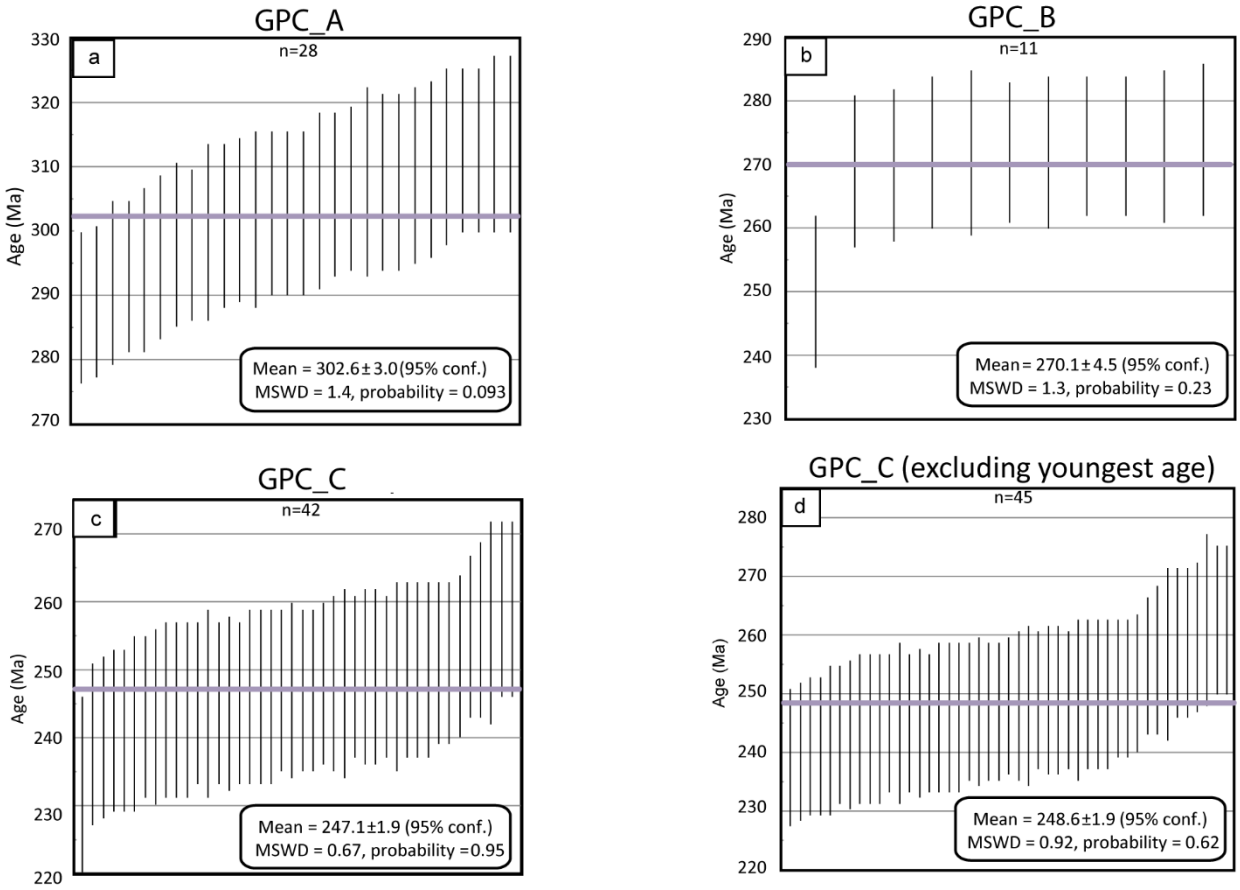

Figure 38: Mean weighted averages for a) Cisuralian sample GPC_A, b) Lopingian sample GPC_B, c) Lopingian sample GPC_C and d) Lopingian sample GPC_C (excluding the youngest detrital zircon age).

Provenance of detrital zircons in the Galilee Basin

Detrital zircons from Cisuralian strata in OEC Glue Pot Creek 1 (composite sample GPC_A) have a diverse and wide range of age populations (Figures 37 and 39a). Although there is a large component of (near) syn-depositional and relatively young grains with ages between 280 and 340 Ma, there are also less prevalent older populations with ages in the ranges of 365-388 Ma (Middle to Upper Devonian), 402-448 Ma (late Ordovician to Lower Devonian), 500-550 Ma (late Ediacaran to Cambrian), 750-850 Ma (Tonian to Cryogenian), as well as rare zircons with Mesoproterozoic and older ages. The main age peak of euhedral to subrounded zircon ages corresponds with Pennsylvanian to early Cisuralian igneous activity in the New England Orogen (Figure 39a). Felsic volcanic rocks such as the Kennedy Igneous Province and Connors Subprovince (Allen et al., 1998; Cross et al., 2009; Cross et al., 2012; Cross et al., 2016; Fanning et al., 2009), as well as siliceous intrusions (Bryan et al., 2004) that are associated with the rift system thought to have initiated deposition of the Galilee Basin (Van Heeswijck, 2010) and the Bowen-Gunnedah-Sydney Basin System (Korsch et al., 2009b), are likely sources for this relatively young zircon population.

The 750-850 Ma zircon population in the Cisuralian samples from OEC Glue Pot Creek 1 (Figure 39c) is not evident in most previous detrital zircon data from the Tasmanides, but Li et al. (2015) report a ~850 Ma peak in zircon ages from the Gympie Terrane and the New England Orogen (their summary Figure 6). The source of this population is yet to be resolved. The Proterozoic detrital zircon ages from sample GPC_A are similar to previous results from the Thomson, Delamerian, and New England orogens (Figure 39d). Although the >1500 Ma population in sample GPC_A is small (n=6), geographic proximity suggests that the Thomson Orogen is the most likely source for these zircons. Potential Thomson Orogen sources include the Anakie Province (Fergusson, 2013) and the Charters Towers Province (Hutton and Rienks, 1997; Figure 40). As both of these provinces contain meta-sedimentary strata, they may also be the origin of the metamorphic lithic fragments documented in previous petrographic studies of the Joe Joe Group (Mollan et al., 1969).

Most detrital zircons in sample GPC_B, from Lopingian strata in OEC Glue Pot Creek 1, are Pennsylvanian to late Cisuralian in age (Figures 37 and 39a, b). Similarly, sample GPC_C (from younger Lopingian strata) contains a dominant population of detrital zircons with Permian and Pennsylvanian ages, with only a minor component of early Mesoproterozoic zircons. The euhedral shape and abundant inclusions of the Lopingian zircons (Figure 35a) are consistent with the idea that many of the zircons entered the Galilee Basin through volcanic ash fall. However, not all Lopingian-aged zircons are euhedral, suggesting that some of them may have been derived from erosion of surrounding strata. Felsic volcanic rocks of the New England Orogen (Allen et al., 1998; Cross et al., 2009; Cross et al., 2012; Cross et al., 2016; Fanning et al., 2009; Nicoll et al., 2015; Phillips et al., In Press) are considered the primary contributor to the ‘Colinlea Sandstone equivalent’ and Bandanna Formation of the Galilee Basin (Figure 40b).

The ultimate provenance of early Mesoproterozoic zircons in the Bandanna Formation is unclear. A possible source is plutons from the William Supersuite (Hutton and Withnall, 2013; Page and Sun, 1998) in the North Australian Craton to the north-west of the Galilee Basin (Figure 40b). Another possible source is the Mossman Orogen, because it is the only part of the Tasmanides that contains a zircon population of similar age (Figure 39a).

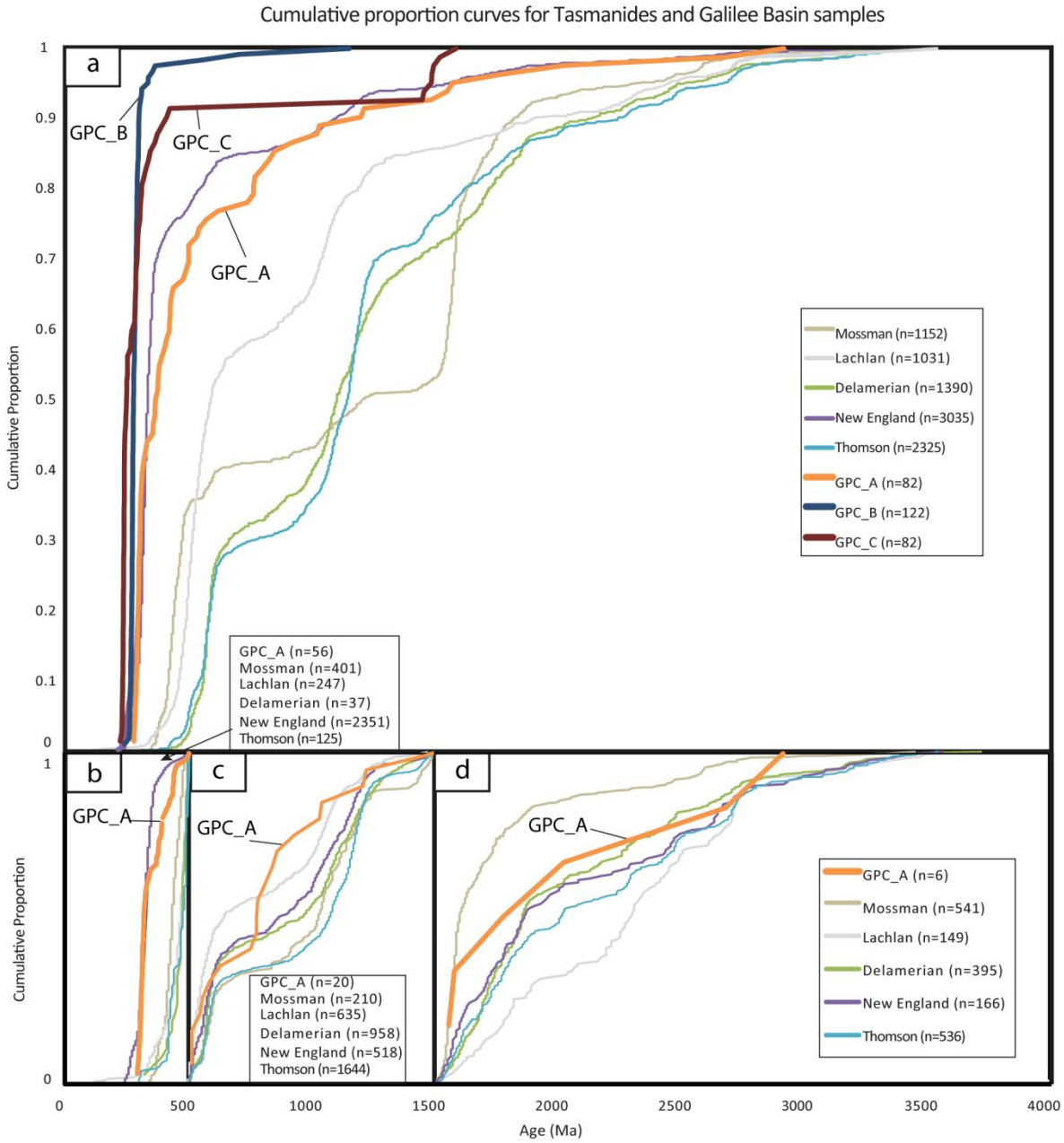

Figure 39: a) Combined Tasmanides and Galilee Basin detrital zircon data shown as cumulative proportions. b) Tasmanides and sample GPC_A cumulative proportion graph from 0-500 Ma. c) Tasmanides and sample GPC_A cumulative proportion graph from 500-1500 Ma. d) Tasmanides and sample GPC_A cumulative proportion graph of >1500 Ma detrital zircons. Tasmanides data modified from Shaanan et al. (2017). Data from: Adams et al. (2014); Adams et al. (2013); Armistead and Fraser (2015); Berry et al. (2001); Campbell et al. (2015); Cross et al. (2016); Cross et al. (2015); Fergusson and Fanning (2002); Fergusson et al. (2001); Fergusson et al. (2005); Fergusson et al. (2007); Fergusson et al. (2013b); Gibson et al. (2011); Glen et al. (2013); Henderson et al. (2011); Hoy et al. (2014); Ireland et al. (1998); Johnson et al. (2016); Keay et al. (1999); Kemp et al. (2006); Korsch et al. (2009a); Kositcin et al. (2015a); Kositcin et al. (2015b); Li et al. (2015); Meffre et al. (2007); Purdy et al. (2016); Shaanan and Rosenbaum (2016); Shaanan et al. (2015); Sircombe and McQueen (2000); Williams (2001); Geoscience Australia (2017).

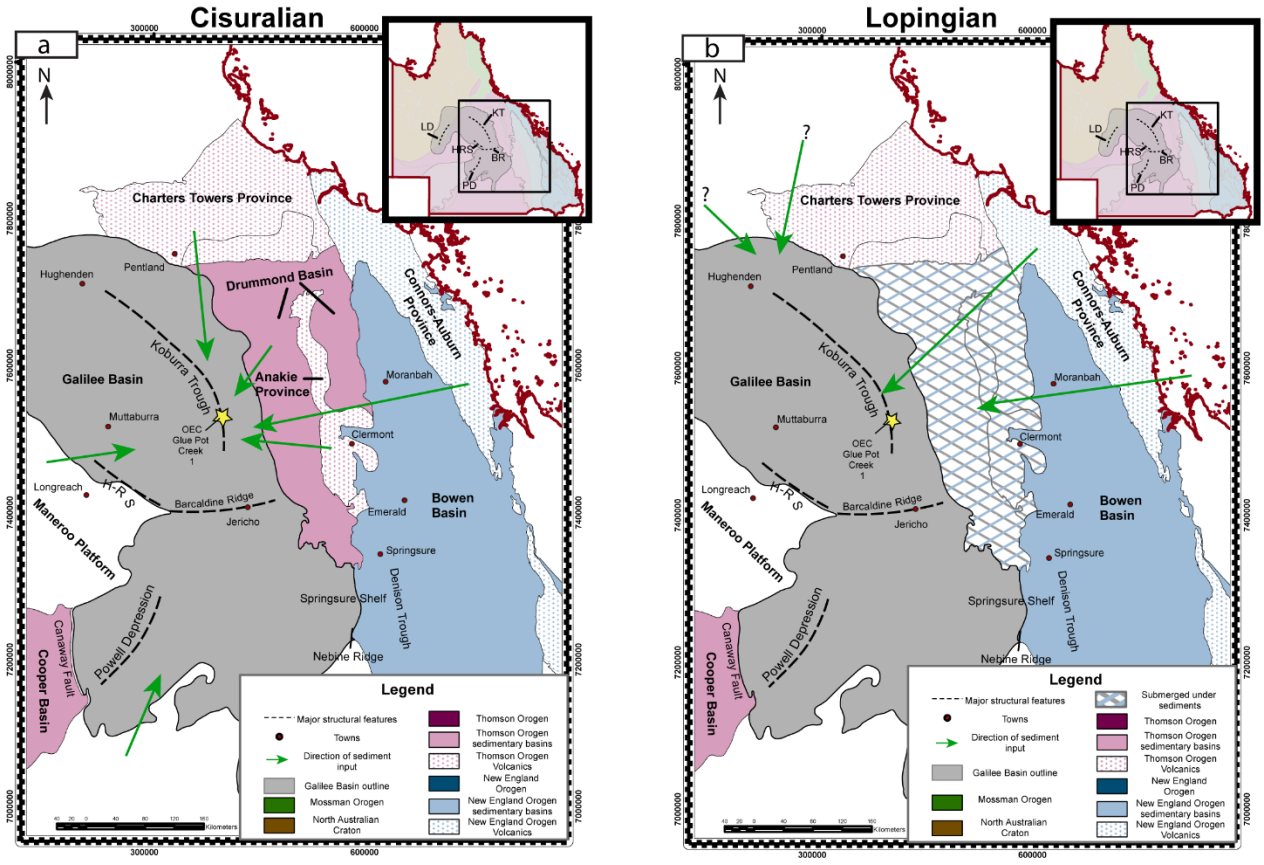

Figure 40: Map showing the potential source of detrital zircons during a) the Cisuralian and b) the Lopingian. During Lopingian time, the Drummond Basin and Anakie Province were buried, submerged creating a pathway from the Nebine Ridge northward to the Charters Towers Province between the Galilee and Bowen basins.

Implications for tectonic setting

The presence of both (near) syn-depositional and more ancient detrital zircons in the Cisuralian sample (GPC_A) from OEC Glue Pot Creek 1 suggests orogenic mixing, which is consistent with previous provenance studies of the Joe Joe Group (Van Heeswijck, 2006). This detrital signature suggests an extensional setting for the Galilee Basin during Cisuralian time, with sediments being derived from both the Thomson and New England orogens.

In contrast, the restricted range of detrital zircon ages in both Lopingian samples (GPC_B and GPC_C) suggest either a blanketing of tuffaceous material over the Cisuralian source areas or a shift of the Galilee Basin to a foreland basin setting during Lopingian time (Cawood et al., 2012). One of the main potential sources of older detrital zircons during Cisuralian deposition in the Galilee Basin was the Anakie Province (Figure 40). If this province was no longer a palaeo-high by Lopingian time, it would also no longer be a source of eroded material, including detrital zircons. Previous low-temperature thermochronology results from the Anakie Province suggest that the Anakie Province was buried during Lopingian time (Verdel et al., 2016). During this period, which coincides with the peak of Hunter-Bowen deformation, the Galilee and Bowen basins would have

been conjoined into one overall Lopingian foreland basin that received sediment shed from the fold-thrust belt of the New England Orogen (Figures 40 and 41). The rank of Lopingian coal in the Galilee and Bowen basins decreases westerly away from the maximum foreland loading in the Bowen Basin (Sliwa et al., 2017), suggesting that burial depth decreased in the same direction. The Anakie Inlier, although submerged, would have remained a basement high relative to the main depocentre of the Bowen Basin during Lopingian time. The identification of a marker mudstone horizon (Sliwa et al., 2017; Wilson, 2017) at the P-T boundary in both the Bowen and Galilee basins, which is preserved only in the vicinity of the Anakie Inlier, suggests that a large waterbody occupied the centre of the combined basin. Much of the sediment deposited from this waterbody was eroded during the subsequent exhumation of the Anakie Province, leaving only marginal remnants preserved. The conclusion that the Galilee and Bowen basins had similar palaeo-environments is consistent with previous sedimentological research (Fielding et al., 2000; Phillips et al., 2017a), and the evidence of a large combined basin supports the idea that the Galilee Basin is a platform basin related to the Bowen Basin foreland (de Caritat and Braun, 1992; Waschbusch et al., 2009).

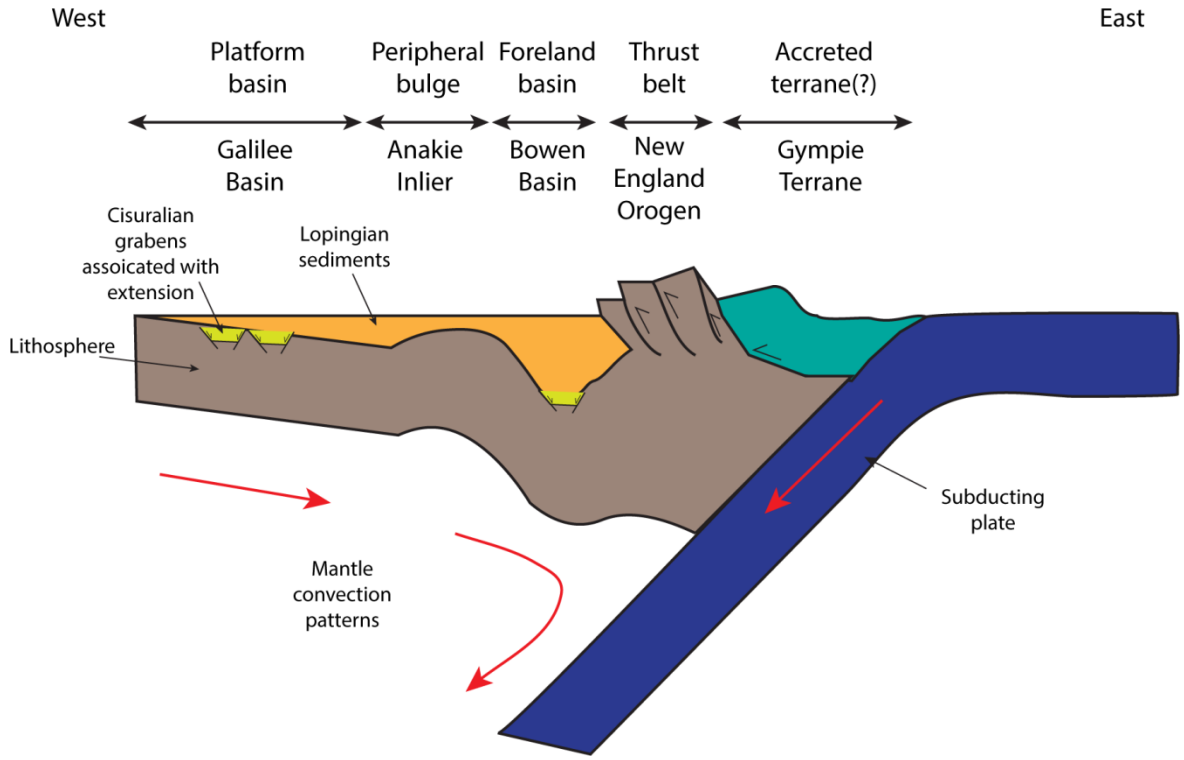

Figure 41: Schematic cross section, modified after de Caritat and Braun (1992), showing the tectonic setting of the Galilee and Bowen basins during Lopingian time.

5.9. Conclusions

We determined U-Pb ages of detrital zircons from Permian sandstone from OEC Glue Pot Creek 1, a well in the Koburra Trough of the Galilee Basin in eastern Australia. The results suggest that deposition of these sandstones was contemporaneous with volcanism along the Permian convergent margin of eastern Australia. Although (near) syn-depositional zircons were found in all samples, Cisuralian samples from the Galilee Basin contain a large population of significantly older zircons, indicating a contribution from a basement source. The transition from the detrital zircon age spectra of the Cisuralian to that of the Lopingian reflects a change in tectonic setting from an extensional to a foreland basin, a conclusion that challenges previous descriptions of the Galilee Basin as an 'intracratonic' basin. Instead, we view it as both a stratigraphic and tectonic counterpart of the neighbouring Bowen Basin.

5.10. Acknowledgements

The authors would like to thank Matthew Campbell, Mikhail Romanov, and Karine Haroumi Moromizato for technical assistance and guidance. Helpful discussions with Uri Shaanan, Derek Hoy, and Alex Slade greatly improved the manuscript. Funding was provided by the Australian Coal Association Research Program, (grant number C22028) and the Vale-UQ Coal Geoscience Program.

6. Synthesis and Conclusions

The overarching objective of this thesis was to define a regionally consistent stratigraphy of the Koburra Trough, Galilee Basin, during the Lopingian, in which the understanding of the depositional and tectonic setting might be enhanced. To achieve a consistent stratigraphy, an integrated multidisciplinary approach was undertaken. Through litho-, chrono- and bio- stratigraphy a new framework was established and provided evidence for: (1) consistency between different nomenclature usage of both coal seams and stratigraphic units, (2) re-assigned stratigraphic units within the Galilee Basin that have previously been unidentified, and (3) identification of the Yarrabee Tuff equivalent in the Galilee Basin, a significant marker horizon that can be used for inter basin correlations. With the establishment of a regionally consistent stratigraphy, the application of sedimentary, geophysical and geochronological techniques allowed (1) spatial reconstruction of temporal palaeo-environments, (2) understanding of the provenance of clastic sediments deposited in the basin and (3) insights into the changing tectonic setting of the Galilee Basin.

6.1. Stratigraphy of the Galilee Basin

Lithostratigraphy

Prior to this study, the regional Permian stratigraphy available for the Galilee Basin was inconsistently applied, and seams were poorly correlated in the Koburra Trough. A lithostratigraphic correlation was created through a compilation of propriety and open file geophysical wireline data, as presented in Chapter 2 (Phillips et al., 2017c). A lithostratigraphic correlation was generated from identifying unique coal seam signatures in geophysical logs. In the absence of seismic lines, the laterally extensive and continuous coal seams provided marker horizons to construct an almost 3D view of the subsurface.

During the process, an apparent discrepancy arose for the correlation of the Betts Creek Group from west to east. This study found that the clean and blocky ‘J and K’ seams on the western side of the study area did not have a lateral equivalent on the eastern side. When correlated across into the Bowen Basin, not only did the condensed Lopingian stratigraphy in the Galilee Basin become apparent, but mis-correlations between the basins were also observed. The tuffaceous units of the Bowen Basin, known collectively as the Fort Cooper Coal Measures, were not previously identified in the Galilee Basin. This study proposed a new stratigraphy with the newly emplaced ‘Fort Cooper Coal Measures equivalents’ and its sub divisions, the lower ‘Fair Hill Formation equivalent’ and

upper ‘Burngrove Formation equivalent’. This produced a stratigraphic framework that was the foundation for the thesis.

Chronostratigraphy

The proposed stratigraphic framework was corroborated through the CA-IDTIMS dating technique and presented in Chapter 3 (Phillips et al., In Press). One Cisuralian age was obtained from the Edie Tuff Member of the Jochmus Formation, 296.09 ± 0.07 Ma. This age corresponds with other published ages of the Edie Tuff Member (Nicoll et al., 2016b). Analysed zircons from tuffaceous layers within the C coal seam returned ages of 254.32 ± 0.10, 254.41 ± 0.07 and 255.13 ± 0.09 Ma. A similar age of 254.08 ± 0.06 Ma was obtained from a tuff towards the top of the Black Alley Shale on the Springsure Shelf. These ages are deemed to be comparable; therefore, the two units are lateral equivalents of each other. These dates also fit with published dates for the deposition of the Black Alley Shale in the Bowen Basin (Metcalfe et al., 2015). An age obtained from the top of the ‘Burngrove Formation equivalent’, 252.81 ± 0.07 Ma, is correlative to published dates of the Yarrabee Tuff in the Bowen Basin (Ayaz et al., 2016a; Esterle et al., 2017; Metcalfe et al., 2015). The identification of such a significant marker horizon in the Galilee Basin is important for inter-basin correlation, and further supports the proposed stratigraphic architecture.

Biostratigraphy

The ‘J and K’ seams, identified through geophysical wireline correlations in the Hulton-Rand monocline to the west of the study area, were found to contain the index taxa for APP3.2, *Praecolpatites sinuosus.* Given the absence of any younger species, this placed the ‘J and K’ seams in the late Cisuralian – early Guadalupian. This is the first observation of this aged stratum within the Galilee Basin and has implications on the length of mid-Permian hiatus in the basin. The length of the hiatus is now reduced to 12-13 My, which is of similar length to the hiatus experienced in the adjacent Cooper and Bowen-Gunnedah-Sydney basins, suggesting all eastern Australian Permian basins were affected by the same tectonic events. Palynological analysis of strata overlying the ‘J and K’ seam returned index taxa for APP5, *Dulhuntyispora parvithola,* stratigraphic equivalents to the Betts Creek Group, supporting the new stratigraphic framework.

6.2. Implications for stratigraphic architecture and nomenclature

This thesis has identified new stratigraphic units within the Galilee Basins Permian sequence and corroborates their placement through geochronological and palynological techniques. The identification of the localised ‘J and K’ seams as late Cisuralian – early Guadalupian supports the theory that the initiation of the Galilee Basin was due to rifting (Korsch et al., 2009b; Van

Heeswijck, 2010), which created half grabens allowing thicker and restricted deposition of Cisuralian - early Guadalupian sequences.

The relatively low accommodation space in the Galilee Basin during the Lopingian resulted in a coalesced stratigraphic architecture, which is particularly highlighted when Permian strata are correlated to the Bowen Basin. While the characteristically tuffaceous units in the Bowen Basin, the Fort Cooper Coal Measures and its subdivisions, contain numerous seams (Anderson, 1985; Ayaz et al., 2015), the newly identified equivalents in the Galilee Basin contain up to two thick tuffaceous rich coal seams. It is probable that this condensed architecture played a significant role in not recognising the Fort Cooper Coal Measures equivalent in the Galilee Basin prior to this study.

The large amount of data acquired for this thesis not only allowed for the identification of new units but also showed that there was a lateral lithostratigraphic continuity in the strata, despite how they were named. The Betts Creek Group can be split into (from lower to upper units): the 'Colinlea Sandstone equivalent', the 'Fort Cooper Coal Measures' (and its subdivisions) and the Bandanna Formation.

6.3. Palaeo-environments

The stratigraphic architecture of Lopingian strata, coupled with detailed sedimentary logging of four strategically placed wells across the study area, provided insight into the depositional sequence of the Betts Creek Groups and its subdivisions. Chapter 4 (Phillips et al., 2017a) presented time slices of the palaeo-environmental evolution between the units.

The Galilee Basin was largely terrestrial during the Lopingian, with the exception of the Springsure Shelf, which remained marine throughout. The Peawaddy Formation, located on the Springsure Shelf, is interpreted to be the downstream tidal flat equivalent of the fluvial 'Colinlea Sandstone equivalent' in the Koburra Trough, where complex coal seam splitting patterns are observed (Phillips et al., 2017b, 2017c). The Peawaddy Formation displays wave-reworking of sediments that suggest an open body of water, rather than a restricted estuarine inlet across the Nebine Ridge. The 'Colinlea Sandstone equivalent' in the Koburra Trough displays a decrease in thickness of tidally influenced fining upward sequences that are capped by coal seams. This variation is due to an increase in frequent channel avulsion on a distributive plain in response to a rise in base level. This response changes farther away from the coastline, as lacustrine environments become the dominant environment in the 'Colinlea Sandstone equivalent'. The presence of tidal sedimentary features +100km from the interpreted coastline is indicative of the low gradient and relative low

accommodation of the Galilee Basin (Allen and Fielding, 2007b) during the deposition of the 'Colinlea Sandstone equivalent'.

The increase in base level allowed the deposition of the Black Alley Shale concurrently in the Galilee and Bowen basins (Ayaz et al., 2015; Fielding et al., 2000, 2001). During this time, extensive volcanism was occurring, resulting in numerous ash layers being deposited in the marine and adjacent peat environments (Ayaz et al., 2016a; Laurie et al., 2016; Metcalfe et al., 2015; Nicoll et al., 2015). The tuffaceous C coal seam, overlying the 'Colinlea Sandstone equivalent', identified by this study as a separate formation (the 'Fair Hill Formation equivalent'), experienced increased splitting and clastic material within the seam itself toward the south as a result of the transgressing Black Alley Shale. Reconstruction of the Black Alley Shale showed that the marine transgression was restricted to the central and southern parts of the Galilee Basin, while the northern and western parts of the study area exhibited coalesced tuffaceous coal seams.

The resurgence of higher sedimentation rates in the Galilee Basin saw the regression of the Black Alley Shale and deltaic environments prevail. Nearby volcanic activity is recorded during times of depositional quiescence as tuffaceous layers within the coal seams of the 'Burngrove Formation equivalent' in the Koburra Trough. The southern equivalent on the Springsure Shelf exhibited local anoxic marine events that are also inundated with tuffaceous layers. The overlying Bandanna Formation represents upper deltaic environments with a more benign coal seam splitting pattern than the underlying fluvial 'Colinlea Sandstone equivalent' in the Koburra Trough (Phillips et al., 2017b, 2017c). The Springsure Shelf represents lower deltaic environments where coal seams were not preserved. The absence of tuffaceous material is notable and makes the Bandanna Formation identifiable from the underlying formations.

6.4. Tectonic setting

A study into the age populations of detrital zircons in sandstone samples from one key well, OEC Glue Pot Creek 1, from the Koburra Trough provide insight into the changing tectonic setting of the Galilee Basin during the Permian, as presented in Chapter 5 (Phillips et al., In Review). With in-situ volcanic activity preserved in the sediments in the form of tuffaceous layers, dating of these layers can provide constraining depositional ages for the sandstone samples obtained between them (Ayaz et al., 2016a; Laurie et al., 2016; Metcalfe et al., 2015; Nicoll et al., 2015; Phillips et al., In Press). Youngest detrital zircon age populations from the sandstone samples collected from OEC Glue Pot Creek 1 do not have a large offset from the age of the in-situ tuffaceous layers, demonstrating that syn-depositional magmatism was occurring throughout the Permian. Sandstone samples from the

Cisuralian show a range of detrital zircon age populations reflecting volcanism connected to the New England Orogen (300 – 350 Ma), as well as the Thomson Orogen (350 – 500 Ma) and Pre-Cambrian material. This orogenic recycling is indicative of an extensional tectonic setting with a range of sources. The observation of localised depositional centres outlined in Chapter 3 (Phillips et al., In Press) supports this tectonic setting.

In contrast, detrital zircons from Lopingian strata are dominated by New England Orogen related magmatic ages (250 – 350 Ma), with a very small component of Mesoproterozoic (1500 Ma) detrital zircons ages. This narrow range of age populations is consistent with a convergent tectonic setting (Cawood et al., 2012), suggesting a singular sediment source of a nearby volcanic region. The removal of Thomson Orogen material and a foreland tectonic signature are suggestive that the Anakie Inlier was eliminated as a provenance source. The idea that the Galilee Basin was a 'platform basin' during the Lopingian by de Caritat and Braun (1992), where in mantle convection patterns subside the peripheral back bulge (Anakie Inlier), is supported by the detrital zircon populations from this study. The decrease in accommodation space away from the main foreland depocentre resulted in the thinning of Lopingian strata to the west of the Galilee Basin (Chapter 3 and 4; Phillips et al., In Press; Phillips et al., 2017a). The removal (or subsidence) of the Anakie Inlier at this time (Sliwa et al., 2017; Verdel et al., 2016; Wilson, 2017) would fully combine the Galilee Basin and adjacent retro-foreland Bowen Basin, creating an enormous >300,000 km^2 basin. The large area generated by the combination of both basins would have allowed similar temporal palaeo-environments to develop within the basins (Chapter 4; Phillips et al., 2017a) and any tectonic events to have a comparable effect. Therefore, it is clear that when reviewing the components of the Lopingian stratigraphic architecture of the Galilee Basin, the interlinked relationship between the Galilee and adjacent Bowen basin during the foreland phase is one that plays a far greater role than previously thought.

6.5. Future research

This thesis presents a new stratigraphic framework for the Permian succession of the Galilee Basin, and, as a result, a better understanding of the palaeo-environments and tectonic setting of the basin during the Permian are known. However future research can be conducted that will complement the work presented in this thesis.

Extended tephrochronological research

A limited number of samples were able to be collected for CA-IDTIMS analysis due to core availability. As increased exploration drilling occurs in the basin and the availability of core rises,

there is the opportunity to obtain samples suitable for analysis. A more robust absolute age data set, accompanied by the CA-IDTIMS dates presented in Chapter 3 (Phillips et al., In Press) will help to:

- further refine the stratigraphic framework outside of the study area and into other depressions of the Galilee Basin;
- quantify sedimentation rates across the basin and compare with other basins in a similar tectonic setting; and
- integrate the coal measure stratigraphy within the Galilee Basin with other Permian Gondwanan basins, in particular the Cooper Basin to the south-west.

Biostratigraphy and palynofacies

This thesis showed the importance of palynology in the absence of radiogenic isotope dating by correcting the correlation from west to east across the study area (Chapter 3; Phillips et al. In Press). Palynology was focused on one key well, GSQ Muttaburra 1, however in future studies into the stratigraphy of the Galilee Basin, a biostratigraphic assessment is extremely important. A more encompassing study into the palynology of the Galilee Basin will help to:

- correlate the Galilee Basin with other eastern Australian Permian basins; and
- provide additional data (along with constraining absolute ages) to the recalibration of Australian palynological biozones.

Organic matter within clastic sediments can also be analysed through palynofacies analysis. This study would help to characterise potential changes in environment as well as adjacent vegetative changes. This can also be used as a proxy for climatic interpretation.

Facies analysis

The facies associations described in Chapter 4 (Phillips et al., 2017a) have been based on drill core and the interpretation of gamma and density geophysical logs. Although these associations are in line with existing palaeoenvironmental reconstructions (Allen and Fielding, 2007a, 2007b), a more robust study to confirm these reconstructions is recommended. Research into trace fossil identification can assist in confirming the marine and non-marine setting while the use of orientated down-hole imagery, such as CDI image logs, can be useful for determining bed geometries.

Coal characterisation

The lithostratigraphic correlation presented in Chapter 2 (Phillips et al., 2017c) presents an opportunity to characterise coal seams through organic petrography and coal lithotypes. This characterisation will help to ascertain areas of high and low preservation which in turn can identify the physical conditions of the swamp. This would revisit seminal work by Hunt and Smyth (1989) in the context of the palaeo-geography.

This research can supplement the sedimentary facies generated in Chapter 4 (Phillips et al., 2017a) and when coupled with carbon isotope data obtained from coal seams, potential climatic controls on the palaeo-environments can be known.

Detailed detrital zircon work

This thesis focused on the detrital zircon content from one key well, OEC Glue Pot Creek 1 (Chapter 5; Phillips et al., In Review). Further work into the provenance of the Galilee Basin should encompass additional wells with a full stratigraphic sequence sampled. A similar study should be conducted into the provenance of the Bowen Basin, with an emphasis on detailed stratigraphic sampling. This would allow for a more integrated analysis into the tectonic setting of the Galilee Basin and a greater understanding as to what role the adjacent Bowen Basin played in sediment dispersal patterns in the Galilee Basin, as well as the Cooper Basin. A detailed geochemical analysis on the trace element data and inclusions of the detrital zircons will complement provenance research and work towards potentially classifying palaeo-geographical volcanics.

The suggestions above will cement a case to formally change the stratigraphy of the Galilee Basin.

7. References

ADAMS, C. J., BRADSHAW, J. D. & IRELAND, T. R. 2014. Provenance connections between late Neoproterozoic and early Palaeozoic sedimentary basins of the Ross Sea region, Antarctica, south-east Australia and southern Zealandia. *Antarctic Science,* 26**,** 173-182.

ADAMS, C. J., KORSCH, R. J. & GRIFFIN, W. L. 2013. Provenance comparisons between the Nambucca Block, Eastern Australia and the Torlesse Composite Terrane, New Zealand: connections and implications from detrital zircon age patterns. *Australian Journal of Earth Sciences,* 60**,** 241-253.

AGL ENERGY 2012. Glenaras 7, Well Completion Report.

ALLEN, C. M., WILLIAMS, I. S., STEPHENS, C. J. & FIELDING, C. R. 1998. Granite genesis and basin formation in an extensional setting: The magmatic history of the Northernmost New England Orogen. *Australian Journal of Earth Sciences,* 45**,** 875-888.

ALLEN, J. P. & FIELDING, C. R. 2007a. Sedimentology and stratigraphic architecture of the Late Permian Betts Creek Beds, Queensland, Australia. *Sedimentary Geology,* 202**,** 5-34.

ALLEN, J. P. & FIELDING, C. R. 2007b. Sequence architecture within a low-accommodation setting: An example from the Permian of the Galilee and Bowen basins, Queensland, Australia. *AAPG Bulletin*, 91**,** 1503-1539.

ANDERSON, J. C. 1985. Geology of the Fort Cooper Coal Measures Interval. *Bowen Basin Coal Symposium* Geological Society of Australia Abstracts ed. Rockhampton, QLD: Geological Society of Australia

ARMISTEAD, S. E. & FRASER, G. L. 2015. New SHRIMP U-Pb zircon ages from the Cuttaburra and F1 prospects, southern Thomson Orogen, NSW. Canberra: Geoscience Australia.

AUSTRALIA PACIFIC LNG 2010. Glue Pot Creek 1, Well completion report.

AYAZ, S. A. 2016. *Stratigraphic arctiecture and coal charater of Late Permian Fort Cooper Coal Measures, Bowen Basin, Queensland.* PhD, University of Queensland.

AYAZ, S. A., ESTERLE, J. S. & MARTIN, M. A. 2015. Spatial variation in the stratigraphic architecture of the Fort Cooper and equivalent coal measures, Bowen Basin, Queensland. *Australian Journal of Earth Sciences***,** 1-16.

AYAZ, S. A., MARTIN, M., ESTERLE, J. S., AMELIN, Y. & NICOLL, R. S. 2016a. Age of the Yarrabee & Accessory Tuffs: Implications for the Late Permian sediment accumulation rates across the Bowen Basin. *Australian Journal of Earth Sciences,* 63**,** 843-856.

AYAZ, S. A., RODRIGUES, S., GOLDING, S. D. & ESTERLE, J. S. 2016b. Compositional variation and palaeoenvironment of the volcanolithic Fort Cooper Coal Measures, Bowen Basin, Australia. *International Journal of Coal Geology (in press)*.

BALME, B. E. & HENNELLY, J. F. P. 1956. Monolete, monocolpate and alete sporomorphs from Australian Permian sediments. *Australian Journal of Botany,* 4**,** 54-67.

BANGERT, B., STOLLHOFEN, H., LORENZ, V. & ARMSTRONG, R. 1999. The geochronology and significance of ash-fall tuffs in the glaciogenic Carboniferous-Permian Dwyka Group of Namibia and South Africa. . *Journal of African Earth Sciences* 29**,** 33–49.

BASTIAN, L. V. 1965. Petrographic notes of Permian sandstone of the Springsure 1:250000 sheet area, Queensland. *Bureau of Mineral Resources Geology and Geophysics*. Canberra, ACT: Bureau of Mineral Resources.

BENSTEAD, W. L. 1973. Galilee Basin. *In:* MINES, D. O. (ed.). Brisbane: Queensland Digital Exploration Reports (QDEX).

BERNER, R. A. 1981. A new geochemical classification of sedimentary environments. *Journal of Sedimentary Research,* 51**,** 359.

BERRY, R. F., JENNER, G. A., MEFFRE, S. & TUBRETT, M. N. 2001. A North American provenance for Neoproterozoic to Cambrian sandstones in Tasmania? *Earth and Planetary Science Letters,* 192**,** 207-222.

BLACK, L. P., KAMO, S. L., ALLEN, C. M., DAVIS, D. W., ALEINIKOFF, J. N., VALLEY, J. W., MUNDIL, R., CAMPBELL, I. H., KORSCH, R. J., WILLIAMS, I. S. & FOUDOULIS, C. 2004. Improved 206Pb/238U microprobe geochronology by the monitoring of a trace-element-related matrix effect; SHRIMP, ID–TIMS, ELA–ICP–MS and oxygen isotope documentation for a series of zircon standards. *Chemical Geology,* 205**,** 115-140.

BLANCO, E. 2010. *Coal lithotype response to chaning depositional sequences in the Betts Creek Beds, Galilee Basin.* Honours, University of Queensland.

BLUM, M. D. & TÖRNQVIST, T. E. 2000. Fluvial responses to climate and sea-level change: a review and look forward. *Sedimentology,* 47**,** 2-48.

BODORKOS, S., CROWLEY, J., HOLMES, E., LAURIE, J., MANTLE, D., MCKELLAR, J., MORY, A., NICOLL, R., PHILLIPS, L., SMITH, T., STEPHENSON, M. & WOOD, G. 2016. New dates for Permian palynostratigraphic biozones in the Sydney, Gunnedah, Bowen, Galilee and Canning basins, Australia. *Permophiles***,** 19 - 21.

BOYD, R. & LECKIE, D. 2000. Greta Coal Measures in the Muswellbrook Anticline area, New South Wales. *Australian Journal of Earth Sciences,* 47**,** 259-279.

BRAIN, T. J., MCKELLAR, J. L. & CARMICHAEL, D. C. 1991. Stratigraphic Drilling Report - GSQ Muttaburra 1 Brisbane, QLD: Geological Survey of Queensland.

BRAKEL, A. T. 1989. *Correlation of Permian coal measure sequences of eastern Australia,* Canberra, Bureau of Mineral Resources Bulletin.

BRAKEL, A. T., TOTTERDELL, J. M., WELLS, A. T. & M. G. NICOLL, M. G. 2009. Sequence stratigraphy and fill history of the Bowen Basin, Queensland, *Australian Journal of Earth Sciences,* 56, 401-432, DOI: 10.1080/08120090802698711

BRIDGE, J. 2003. *Rivers and Floodplains - Forms, Processes and Sedimentary Record,* Oxford, U.K., Blackwell Science.

BRIDGE, J. & DROSER, M. L. 1985. Unusual marginal-marine lithofacies from the Upper Devonian Catskill clastic wedge. *Geological Society of America Special Papers,* 201**,** 143-162.

BROWNLOW, J. & CROSS, A. TIMS U-Pb and Shrimp U-Pb zircon dating of the Dundee Rhyodacite, northern New England, NSW. *In:* BUCKMAN, S. & BLEVIN, P., eds. New England Orogen 2010 conference, 2010 University of New England, Armidale, New South Wales, Australia. University of New England, Armidale, 69-74.

BRYAN, S. E., ALLEN, C. M., HOLCOMBE, R. J. & FIELDING, C. R. 2004. U–Pb zircon geochronology of Late Devonian to Early Carboniferous extension-related silicic volcanism in the northern New England Fold Belt*. *Australian Journal of Earth Sciences,* 51**,** 645-664.

CAMPBELL, M., ROSENBAUM, G., SHAANAN, U., FIELDING, C. R. & ALLEN, C. 2015. The tectonic significance of lower Permian successions in the Texas Orocline (Eastern Australia). *Australian Journal of Earth Sciences,* 62**,** 789-806.

CARNE, J. E. 1908. Geology Memoir 06: Geology and Mineral resources of the western Coalfield. New South Wales Geological Survey Publication.

CARR, A. F. 1973a. Galilee Basin Exploratory Coal Drilling - Degulla Area. *In:* MINES, D. O. (ed.). Brisbane: Geological Survey of Queensland.

CARR, A. F. 1973b. Galilee Basin Exploratory Coal Drilling - Wendouree Area. Brisbane: Geological Survey of Queensland.

CARR, A. F. 1974a. Galilee Basin Exploratory Coal Drilling - Laglan Area. Brisbane: Geolgical Survey of Queensland.

CARR, A. F. 1974b. Galilee Basin Exploratory Coal Drilling - Lambton Meadows Area. Brisbane: Geological Survey of Queensland.

CARR, A. F. 1974c. Galilee Basin Exploratory Coal Drilling - Moray Downs Area. Brisbane: Geological Surevy of Queensland.

CARR, A. F. 1976. Galilee Basin Exploratory Coal Drilling - Mirtna Area. Brisbane: Geological Survey of Queensland.

CARR, A. F. 1977. Galilee Basin Exploratory Coal Drilling - View Hill Area. Brisbane: Geological Survey of Queensland.

CARR, A. F. 1978. Galilee Basin Exploratory Coal Drilling - Longton Area. Brisbane: Geological Survey of Queensland

CAWOOD, P. A., HAWKESWORTH, C. J. & DHUIME, B. 2012. Detrital zircon record and tectonic setting. *Geology,* 40**,** 875-878.

CHOI, K. 2010. Rhythmic Climbing-Ripple Cross-Lamination in Inclined Heterolithic Stratification (IHS) of a Macrotidal Estuarine Channel, Gomso Bay, West Coast of Korea. *Journal of Sedimentary Research,* 80**,** 550-561.

COHEN, K. M., FINNEY, S. C., GIBBARD, P. L. & FAN, J.-X. 2013; updated. The ICS Intrenational chronostratigraphic chart. *Episodes,* 36**,** 199-204.

COLLINS, S. 2009. *High stand or low stand: A geochemical and petrological insight into the cyclicity and depositional environment of the Wallabella Coal Member, Tinowon Formation, Bowen Basin.* BSc Honors, University of Queensland.

COMET RIDGE 2010. Montani 1. Well completion report. Queensland Digital Exploration Reports (QDEX): Queensland Government.

CONDON, D. J., SCHOENE, B., MCLEAN, N. M., BOWRING, S. A. & PARRISH, R. 2015. Metrology and traceability of U-Pb isotope dilution geochronology (EARTHTIME Tracer Calibration Part I). *Geochimica et Cosmochimica Acta* 164**,** 464-480.

CROSS, A. J., DUNKLEY, D. J., BULTITUDE, R. J., BROWN, D. D., PURDY, D. J., WITHNALL, I. W., VON GNIELINSKI, F. E. & BLAKE, P. R. 2015. Summary of results joint GSQ-GA geochronology project : Thomson Orogen, New England Orogen and Mount Isa region, 2010-2012. Brisbane, QLD: Queensland Geological Record.

CROSS, A. J., PURDY, D. J. & BULTITUDE, R. J. 2012. Summary of results - joint GSQ-GQ geochronology project: Monto and Maryborough 1:250 000 Sheet areas. Brisbane, QLD: Queensland Geological Record 2012/02.

CROSS, A. J., PURDY, D. J., BULTITUDE, R. J., BROWN, D. D. & CARR, P. A. 2016. Summary of results - joint GSQ-GA geochronology project: Thomson Orogen, New England Orogen, Mossman Orogen and Mount Isa region, 2011-2013. Brisbane,QLD: Queensland Geological Record 2016/03.

CROSS, A. J., PURDY, D. J., BULTITUDE, R. J., DHNARAM, C. R. & VON GNIELINSKI, F. E. 2009. Joint GSQ-GA NGA geochronology project New England Orogen and Drummond Basin, 2008. Brisbane, QLD: Queensland Geological Record 2009/03.

CROWLEY, J. L., SCHOENE, B. & BOWRING, S. A. 2007. U-Pb dating of zircon in the Bishop Tuff at the millennial scale. *Geology,* 35**,** 1123-1126.

DAIDU, F., YUAN, W. & MIN, L. 2013. Classifications, sedimentary features and facies associations of tidal flats. *Journal of Palaeogeography,* 2**,** 66-80.

DALRYMPLE, R. W. & CHOI, K. 2007. Morphologic and facies trends through the fluvial–marine transition in tide-dominated depositional systems: A schematic framework for environmental and sequence-stratigraphic interpretation. *Earth-Science Reviews,* 81**,** 135-174.

DALRYMPLE, R. W., ZAITLIN, B. A. & BOYD, R. 1992. Estuarine facies models; conceptual basis and stratigraphic implications. *Journal of Sedimentary Research,* 62**,** 1130-1146.

DE CARITAT, P. & BRAUN, J. 1992. Cyclic development of sedimentary basins at convergent plate margins — 1. Structural and tectono-thermal evolution of some gondwana basins of eastern Australia. *Journal of Geodynamics,* 16**,** 241-282.

DECELLES, P. G. & GILES, K. A. 1996. Foreland basin systems. *Basin Research,* 8**,** 105-123.

DEVRIES KLEIN, G. 1970. Depositional and Dispersal Dynamics of Intertidal Sand Bars. *Journal of Sedimentary Petrology,* 40**,** 1095-1127.

DICKINSON, W. R. & GEHRELS, G. E. 2009. Use of U-Pb ages of detrital zircons to infer maximum depositional age strata: A test against a Colorado Plateau Mesozoic database, *Earth and Planetary Science Letters, 288,* 115-125

DRAPER, J. J. 2013. Bowen Basin. *In:* JELL, P. A. (ed.) *Geology of Queensland.* Brisbane, QLD: Geological Survey of Queensland.

DRAPER, J. J., FIELDING, C. R., ROBERTS, J., CLAOUÉ-LONG, J. C. & FOSTER, C. B. 1997. SHRIMP zircon dating of the Permian system of eastern Australia. *Australian Journal of Earth Sciences,* 44**,** 535-538.

DUMAS, S. & ARNOTT, R. W. C. 2006. Origin of hummocky and swaley cross-stratification—The controlling influence of unidirectional current strength and aggradation rate. *Geology,* 34**,** 1073-1076.

DURIE, R. A., HAWKINS, P. J. & KUKLA, G. T. The Galilee Basin coal measures: A potential methane resource? - A case for a well planned integrated exploration and R & D programme. Coalbed Mathane Symposium, 1992 Townsville. 81-97.

EDWARDS, S., AINSWORTH, B., VAKARELOV, B. & KALDI, J. The Galilee Basin - A Potential CO2 Storage Site in Queensland. Eastern Australiasian Basins Symposium, 2008 Darling Harbour, NSW.

EEAPL 1993. Fleetwood #1 Well Report and Data.

ENRON EXPLORATION AUSTRALIA. 1994. Rodney Creek 1 Well completion Report.

ESTERLE, J., PRERORIUS, S., FRICKER, C., AYAZ, S. A., SLIWA, R., CROWLEY, J. & NICOLL, R. The Yarrabee Tuff: it really was a blast. Sydney Basin Symposium, 2017 Hunter Valley.

ESTERLE, J. & SLIWA, R. 2002. Bowen Basin Supermodel 2000. ACARP Project C9021, CSIRO Exploration & Mining.

EVANS, P. R. 1967. Upper Carboniferous and Permian palynological stages and their distributions in eastern Australia. *In:* Bureau of Mineral Resources, Geology and Geophysics

EVANS, P.R., 1969. Upper Carboniferous and Permian palynological stages and their distribution in eastern Australia. *Gondwana stratigraphy*. IUGS Symposium. Buenos Aires, 1-15 October 1967. 41-53.

EVANS, P. R. 1980. Geology of the Galilee Basin. *In:* HENDERSON, R. A. & STEPHENSON, P. J. (eds.) *The Geology and Geophysics of Northeastern Australia.* Brisbane, QLD: Geological Society of Australia, Queensland Division.

EVANS, P. R. & ROBERTS, J. 1980. Evolution of central eastern Australia during the late Palaeozoic and early Mesozoic. *Journal of the Geological Society of Australia,* 26**,** 325-340.

EVANS, T. & HOSTETLER, S. Unravelling the enigmatic Galilee Basin, insights from geological modelling for the Galilee Bioregional Assessment. *In:* FORBES, C., ed. Australian Earth Sciences Convention 2016, 2016 Adelaide. Geological Society of Australia, 128.

EVANS, T., RANSLEY, T. & HARRIS-PASCAL, C. Characterising the regional hydrogeology of the Galilee Basin and its relationship with aquifers in the Great Artesian Basin (Eromanga Basin). *In:* FORBES, C., ed. Australian Earth Sciences Convention 2016, 2016 Adelaide. Geological Society of Australia, 129.

FANNING, C. M., WITHNALL, I. W., HUTTON, L. J., BULTITUDE, R. J., VON GNIELINSKI, F. E. & RIENKS, I. P. 2009. SHRIMP U-Pb Zircon Ages From Central Queensland. *In:* WITHNALL, I. W., HUTTON, L. J., BULTITUDE, R. J., VON GNIELINSKI, F. E. & RIENKS, I. P. (eds.) *Geology of the Auburn Arch, Southern Connors Arch and Adjacent Parts of the Bowen Basin and Yarrol Province, Central Queensland.* www.qdexguest.dnrm.qld.gov.au: Department of Employment, Economic Development and Innovation.

FERGUSSON, C. L. 2013. Devonian granitoids. *In:* JELL, P. A. (ed.) *Geology of Queesland.* Brisbane, QLD: Geological Survey of Queensland.

FERGUSSON, C. L., CARR, P. F., FANNING, C. M. & GREEN, T. J. 2001. Proterozoic-Cambrian detrital zircon and monazite ages from the Anakie Inlier, central Queensland: Grenville and Pacific-Gondwana signatures. *Australian Journal of Earth Sciences,* 48**,** 857-866.

FERGUSSON, C. L. & FANNING, C. M. 2002. Late Ordovician stratigraphy, zircon provenance and tectonics, Lachlan Fold Belt, southeastern Australia*. *Australian Journal of Earth Sciences,* 49**,** 423-436.

FERGUSSON, C. L., FANNING, C. M., PHILLIPS, D. & ACKERMAN, B. R. 2005. Structure, detrital zircon U−Pb ages and 40Ar/39Ar geochronology of the Early Palaeozoic Girilambone Group, central New South Wales: subduction, contraction and extension associated with the Benambran Orogeny. *Australian Journal of Earth Sciences,* 52**,** 137-159.

FERGUSSON, C. L., HENDERSON, R. A., FANNING, C. M. & WITHNALL, I. W. 2007. Detrital zircon ages in Neoproterozoic to Ordovician siliciclastic rocks, northeastern Australia: implications for the tectonic history of the East Gondwana continental margin. *Journal of the Geological Society,* 164**,** 215-225.

FERGUSSON, C.L., HENDERSON, R.A., HUTTON, L.J., WITHNALL, I.W. 2013a, Charters Towers Province, In JELL, P. A. (Ed), 2013. Geology of Queensland, Geological Survey of Queensland, Chapter 3.3, 136-146

FERGUSSON, C. L., NUTMAN, A. P., KAMIICHI, T. & HIDAKA, H. 2013b. Evolution of a Cambrian active continental margin: The Delamerian–Lachlan connection in southeastern Australia from a zircon perspective. *Gondwana Research,* 24**,** 1051-1066.

FIELDING, C. R. 2015. Chapter 9 - A reappraisal of large, heterolithic channel fills in the upper Permian Rangal Coal Measures of the Bowen Basin, Queensland, Australia: The case for tidal influence. *In:* PHILIP J. ASHWORTH, J. L. B. & DANIEL, R. P. (eds.) *Developments in Sedimentology*. Elsevier.

FIELDING, C. R., BANN, K. L. & TRUEMAN, J. D. (eds.) 2007. *Resolving the architecture of a complex, low-accommodation unit using high-resolution sequence stratigraphy and ichnology: The late Permian Freitag Formation in the Denison Trough, Queensland, Australia*: Society for Sedimentary Geology, Short Course Notes.

FIELDING, C. R., FALKNER, A. J. & SCOTT, S. G. 1993. Fluvial response to foreland basin overfilling; the late Permian Rangal Coal Measures in the Bowen basin, Queensland, Australia. *Sedimentary Geology*, 85, 475-497.

FIELDING, C. R., FRANK, T. D., BIRGENHEIER, L. P., RYGEL, M. C., JONES, A. T. & ROBERTS, J. 2008. Stratigraphic imprint of the Late Palaeozoic Ice Age in eastern Australia: a record of alternating glacial and nonglacial climate regime. *Journal of the Geological Society,* 165**,** 129-140.

FIELDING, C. R., SLIWA, R., HOLCOMBE, R. J. & JONES, A. T. 2001. A new palaeogeographic synthesis for the Bowen, Gunnedah and Sydney basins of eastern Australia. *Petroleum Exploration Society of Australia Special Publication,* 1**,** 269-278.

FIELDING, C. R., SLIWA, R., HOLCOMBE, R. J. & KASSAN, J. A new Palaeogeographic synthesis of the Bowen Basin of Central Queensland. *In:* BEESTON, J. W., ed. Bowen Basin Symposium 2000, 2000 Rockhampton, QLD. 287-302.

FILATOFF, J. & PRICE, P. L. 1991. EPP 337 a northern Denison Trough (Springsure) palynostratigraphical reference section, Queensland Digital Exploration Reports (QDEX): Queensland Government.

FOSTER, C. B. 1979. Permian Plant Microfossils of the Blair Athol Coal Measures, Baralaba Coal Measures and Basal Rewan Formation of Queensland. Brisbane: Geological Survey of Queensland.

FRICKER, C. 2016. *Geochemical fingerprinting of the Yarrabee Tuff Bed, Bowen Basin.* Honours, University of Queensland.

GADDY, D., MCDONAGH, G. & ZEBROWITZ, M. 1995. Rodney Creek 3, Well Completion Report. Queensland Digital Exploration Reports (QDEX): Queensland Government.

GALILEE ENERGY LIMITED 2001. Rodney Creek 5, Well Completion Report.

GALLOWAY, W. E. (ed.) 1975. *Process framework for describing the morphologic and stratigraphic evolution of deltaic depositional systems,* Houston, USA: Geological Society.

GEOSCIENCE AUSTRALIA. 2016a. *Australian Stratigraphic Units Database* [Online]. http://dbforms.ga.gov.au/pls/www/geodx.strat_units.sch_full?wher=stratno=14198: Geoscience Australia. [Accessed 25th August 2016].

GEOSCIENCE AUSTRALIA. 2016b. *National Geological Provinces Online Database* [Online]. http://www.ga.gov.au/provexplorer/provinceDetails.do?eno=550790: Geoscience Australia. [Accessed 6th March 2016].

GEOSCIENCE AUSTRALIA. 2017. *Geochron Delivery* [Online]. Canberra, ACT: Geoscience Australia. Available: http://www.ga.gov.au/geochron-sapub-web/geochronology/shrimp/search.htm [Accessed 21st February 2017].

GERSTENBERGER, H. & HAASE, G. 1997. A highly effective emitter substance for mass spectrometric Pb isotope ratio determinations. *Chemical Geology,* 136**,** 309-312.

GIBSON, G. M., MORSE, M. P., IRELAND, T. R. & NAYAK, G. K. 2011. Arc–continent collision and orogenesis in western Tasmanides: Insights from reactivated basement structures and formation of an ocean–continent transform boundary off western Tasmania. *Gondwana Research,* 19**,** 608-627.

GLEN, R. A. 2005. The Tasmanides of eastern Australia. In: Vaughan, A.P.M., Leat, P.T., Pankhust, R.J. (Eds.), Terrane processes at the margins of Gondwana. *Geological Society London, Special Publications* 246, 23–96.

GLEN, R. A., CLARE A. & SPENCER, R. 1996. Extrapolating the Cobar Basin model to the regional scale: Devonian basin-formation and inversion in western New South Wales. In: COOK, W.G., FORD, A.J.H., MCDERMOTT, J.J., STANDISH, P.N., STEGMAN, C.L. & STEGMAN, T.M. (eds) The Cobar Mineral Field – 1996. Australasian Institute of Mining and Metallurgy, Melbourne, Spectrum Series 3/9, 43–83.

GLEN, R. A., KORSCH, R. J., HEGARTY, R., SAEED, A., POUDJON DJOMANI, Y., COSTELLOE, R. D. & BELOUSOVA, E. 2013. Geodynamic significance of the boundary between the Thomson Orogen and the Lachlan Orogen, northwestern New South Wales and implications for Tasmanide tectonics. *Australian Journal of Earth Sciences,* 60**,** 371-412.

GRADSTEIN, F. M., OGG, J. G., SCHMITZ, M. D. & OGG, G. M. 2012. *The Geologic Time Scale 2012,* Boston, Elsevier.

GRAY, A. R. G. 1976. Stratigraphic relationships of Late Palaeozoic sediments between Springsure and Jericho. *Queensland Government Mining Journal,* 77**,** 146-163.

GRAY, A. R. G. & SWARBRICK, C. F. J. 1975. Nomenclature of Late Palaeozoic strata in the Northeastern Galilee Basin. *Queensland Government Mining Journal,* 76**,** 344-352.

GREVENITZ, P., CARR, P. & HUTTON, A. 2003. Origin, alteration and geochemical correlation of Late Permian airfall tuffs in coal measures, Sydney Basin, Australia. *International Journal of Coal Geology,* 55**,** 27-46.

GRIGORESCU, M. 2012. Mineralogy and petrography of the southern Galilee Basin, Queensland. *In:* MINES, D. O. N. R. A. (ed.). Brisbane, QLD: Geological Survey of Queensland.

GUERRA-SOMMER, M., CAZZULO-KLEPZIG, M., FORMOSO, M. L., MENEGAT, R. & BASEI, M. A. S. New radiometric data from ash fall rocks in Candiota coal-bearing strata and the palynostratigraphic framework in southern Paraná Basin (Brazil). Gondwana 12, 2005 Mendoza, Argentina. 189.

HALL, L. S., HILL, A., TROUP, A., KORSCH, R., RADKE, B., NICOLL, R. S., PALU, T., WANG, L. & STACEY, A. 2015. Cooper Basin Architecture and Lithofacies: Regional Hydrocarbon Prospectivity of the Cooper Basin, Part 1 *In:* AUSTRALIA, G. (ed.). Canberra: Geoscience Australia.

HAWKINS, P. J. 1976. Facies Analysis and Economic Significance of Late Permian Strata in the Northern Galilee Basin. Brisbane, QLD: Queensland Government Mining Journal.

HAWKINS, P. J. 1978. Galilee Basin - Review of petroleum prospects. Brisbane, QLD: Queensland Government Mining Journal.

HAWKINS, P. J. & CARMICHAEL, D. C. 1987. Petrology and clay mineralogy of fine-grained rocks, Northern Galilee Basin. *Queensland Government Mining Journal,* 88**,** 426-435.

HAWKINS, P. J. & GREEN, P. M. 1993. Exploration results, hydrocarbon potential and future strategies for the Northern Galilee Basin. *APEA Journal,* 33**,** 280-296.

HECKEL, P. H. 1972. Recognition of ancient shallow marine environments. *In:* RIGBY, J. K. & HAMBLIN, W. K. (eds.) *Recognition of Ancient Sedimentary Environments.* Tulsa, OK: The Society of Economic Paleontologists and Mineralogists Special Publication.

HENDERSON, R. A., INNES, B. M., FERGUSSON, C. L., CRAWFORD, A. J. & WITHNALL, I. W. 2011. Collisional accretion of a Late Ordovician oceanic island arc, northern Tasman Orogenic Zone, Australia. *Australian Journal of Earth Sciences,* 58**,** 1-19.

HILL, D. 1957. Explanatory notes on the Springsure 4-mile geological sheet. *Bureau of Mineral Resources,* 5.

HOFFMAN, K. L. 1988. Revision of the limits of the Adavale Basin and Warrabin Trough, southwest Queensland. Brisbane: Geological Survey of Queensland.

HOKE, G. D., SCHMITZ, M. D. & BOWRING, S. A. 2014. An ultrasonic method for isolating nonclay components from clay-rich material. *Geochemistry, Geophysics, Geosystems,* 15**,** 492-498.

HOLCOMBE, R. J. 2013, Figure 5.145, *In* JELL, P. A. (Editor), 2013. Geology of Queensland, Geological Survey of Queensland, Chapter 5.15, 469

HOLCOMBE, R. J., STEPHENS, C. J., FIELDING, C. R., GUST, D., LITTLE, T. A., SLIWA, R., KASSAN, J., MCPHIE, J. & EWART, A. (eds.) 1997. *Tectonic evolution of the northern New England Fold Belt: the Permian-Triassic Hunter-Bowen Event,* Syndey: Special Publication - Geological Society of Australia.

HOLLAND, J. R. & BOCKING, M. A. 2008. Galilee Energy Rodney Creek 8 (GERC 8), Well Completion Report. Queensland Digital Exploration Reports (QDEX): Queensland Government.

HOLZ, M., FRANÇA, A. B., SOUZA, P. A., IANNUZZI, R. & ROHN, R., 2010. A stratigraphic chart of the Late Carboniferous/Permian succession of the eastern border of the Paraná Basin, Brazil, South America. *Journal of South American Earth Sciences*, 29, 381-399.

HORN, B. L. D., MELO, T. M., SCHULTZ, C. L., PHILIPP, R. P., KLOSS, H. P. & GOLDBERG, K., 2014. A new third-order sequence stratigraphic framework applied to the Triassic of the Paraná Basin, Rio Grande do Sul, Brazil, based on structural, stratigraphic and paleontological data. *Journal of South American Earth Sciences*, 55, 123-132.

HOY, D. & ROSENBAUM, G. 2017. Episodic behaviour of Gondwanide deformation in eastern Australia: Insights from the Gympie Terrane. *Tectonics,* 36, 1497-1520

HOY, D., ROSENBAUM, G., WORMALD, R. & SHAANAN, U. 2014. Geology and geochronology of the Emu Creek Block (northern New South Wales, Australia) and

implications for oroclinal bending in the New England Orogen. *Australian Journal of Earth Sciences,* 61**,** 1109-1124.

HUNT, J. W. & SMYTH, M. 1989. Origin of inertinite-rich coals of Australian cratonic basins. *International Journal of Coal Geology,* 11**,** 23-46.

HUTTON, L. J. & RIENKS, I. P. 1997. Geology of the Ravenswood Batholith. *In:* ENERGY, D. O. M. A. (ed.). Brisbane, QLD: Geological Survey of Queensland.

HUTTON, L. J. & WITHNALL, I. W. 2013. Northwestern Queensland (Mount Isa Province). *In:* JELL, P. A. (ed.) *Geology of Queensland.* Brisbane, QLD: Geological Survey of Queensland.

ISBELL, J. L., COLE, D. I. & CATUNEANU, O. 2008. Carboniferous-Permian glaciation in the main Karoo Basin, South Africa: Stratigraphy, depositional controls, and glacial dynamics. *Geological Society of America Special Papers*, 441, 71-82.

IRELAND, T. R., FLÖTTMANN, T., FANNING, C. M., GIBSON, G. M. & PREISS, W. V. 1998. Development of the early Paleozoic Pacific margin of Gondwana from detrital-zircon ages across the Delamerian orogen. *Geology,* 26**,** 243-246.

JAFFEY, A. H., FLYNN, K. F., GLENDENIN, L. E., BENTLEY, W. C. & ESSLING, A. M. 1971. Precision measurements of half-lives and specific activities of 235U and 238U. *Physical Review C,* 4**,** 1889-1906.

JEFFERY, D. & AIGNER, T. 1982. Storm Sedimentation in the Carboniferous Limestones Near Weston-Super-Mare (Dinantian, SW-England). *In:* EINSELE, G. & SEILACHER, A. (eds.) *Cyclic and Event Stratification.* Berlin, Heidelberg: Springer Berlin Heidelberg.

JENSEN, A. R. Regional aspects of the Upper Permian regression in the northern part of the Bowen Basin. *In:* DAVIES, A., ed. Second Bowen Basin Symposium, 1971 Brisbane. Geological Survey of Queensland Report, 7-20.

JENSEN, A. R., GREGORY, C. M. & FORBES, V. R. 1966. Geology of the Mackay 1:250,000 Sheet Queensland. *Bureau of Mineral Resources, Geology and Geophysics,* 104**,** 1-65.

JOHNSON, E. L., PHILLIPS, G. & ALLEN, C. M. 2016. Ediacaran–Cambrian basin evolution in the Koonenberry Belt (eastern Australia): Implications for the geodynamics of the Delamerian Orogen. *Gondwana Research,* 37**,** 266-284.

JOHNSON, M. E. 1989. Tempestites Recorded as Variable Pentamerus Layers in the Lower Silurian of Southern Norway. *Journal of Paleontology,* 63**,** 195-205.

JOHNSON, R. G. 1960. Models and methods for analysis of the mode of formation of fossil assemblages. *Geological Society of America Bulletin,* 71**,** 1075-1086.

JONES, A. T. & FIELDING, C. R. 2008. Sedimentary facies of a glacially influenced continental succession in the Pennsylvanian Jericho Formation, Galilee Basin, Australia. *Sedimentology,* 55**,** 531-556.

JONES, M. J. & TRUSWELL, E. M. 1992. Late Carboniferous and Early Permian palynostratigraphy of the Joe Joe Group, southern Galilee Basin, Queensland, and implications for Gondwanan stratigraphy. *Bureau of Mineral Resources Journal of Australian Geology and Geophysics,* 13**,** 143-185.

KEAY, S., STEELE, D. & COMPSTON, W. 1999. Identifying granite sources by SHRIMP U-Pb zircon geochronology: an application to the Lachlan foldbelt. *Contributions to Mineralogy and Petrology,* 137**,** 323-341.

KEMP, A. I. S., HAWKESWORTH, C. J., PATERSON, B. A. & KINNY, P. D. 2006. Episodic growth of the Gondwana supercontinent from hafnium and oxygen isotopes in zircon. *Nature,* 439**,** 580-583.

KOPPE, W. H. 1978. Review of the stratigraphy of the upper part of the Permian succession in the northern Bowen Basin. *Queensland Government Mining Journal,* 79**,** 35-45.

KORSCH, R. J., ADAMS, C. J., BLACK, L. P., FOSTER, D. A., FRASER, G. L., MURRAY, C. G., FOUDOULIS, C. & GRIFFIN, W. L. 2009a. Geochronology and provenance of the Late Paleozoic accretionary wedge and Gympie Terrane, New England Orogen, eastern Australia∗. *Australian Journal of Earth Sciences,* 56**,** 655-685.

KORSCH, R. J. & TOTTERDELL, J. M. 2009a. Evolution of the Bowen, Gunnedah and Surat Basins, eastern Australia. *Australian Journal of Earth Sciences,* 56**,** 271-272.

KORSCH, R. J. & TOTTERDELL, J. M. 2009b. Subsidence history and basin phases of the Bowen, Gunnedah and Surat Basins, eastern Australia. *Australian Journal of Earth Sciences,* 56**,** 335-353.

KORSCH, R. J., TOTTERDELL, J. M., CATHRO, D. L. & NICOLL, M. G. 2009b. Early Permian East Australian rift system. *Australian Journal of Earth Sciences,* 56**,** 381-400.

KORSCH, R. J., TOTTERDELL, J. M., FOMIN, T., & NICOLL, M. G. 2009c. Contractional structures and deformational events in the Bowen, Gunnedah and Surat Basins, eastern Australia. *Australian Journal of Earth Sciences*, 56, 477–499. doi:10.1080/0812009080269874

KOSITCIN, N., BULTITUDE, R. J., PURDY, D. J., BROWN, D. D., CARR, P. A. & LISITSIN, V. 2015a. *Summary of Results-Joint GSQ-GA Geochronology Project: Kennedy Igneous Association, Mossman Orogen, Thomson Orogen and Iron Range Province: Kennedy Igneous Association, Mossman Orogen, Thomson Orogen and Iron Range Province, 2013-2014,* Brisbane, QLD, Geological Survey of Queensland.

KOSITCIN, N., PURDY, D. J., BROWN, D. D., BULTITUDE, R. J. & CARR, P. A. 2015b. Summary of results Joint GSQ–GA geochronology project: Thomson Orogen and Hodgkinson Province, 2012–2013. Brisbane, QLD: Geological Survey of Queensland.

KROGH, T. E. 1973. A low contamination method for hydrothermal decomposition of zircon and extraction of U and Pb for isotopic age determination. *Geochimica et Cosmochimica Acta* 37**,** 485-494.

LAURIE, J. R., BODORKOS, S., NICOLL, R. S., CROWLEY, J. S., MANTLE, J. D., MORY, A. J., WOOD, G., BACKHOUSE, J., HOLMES, E. K., SMITH HOLMES, T. E. & CHAMPION, D. C. 2016. Calibrating the middle and late palynostratigraphy of Australia to the geologic time scale via U-Pb zircon CA-IDTIMS dating. *Australian Journal of Earth Sciences,* 63**,** 701-730.

LI, P., ROSENBAUM, G., YANG, J.-H. & HOY, D. 2015. Australian-derived detrital zircons in the Permian-Triassic Gympie terrane (eastern Australia): Evidence for an autochthonous origin. *Tectonics,* 34**,** 858-874.

LONGERICH, H. P., JACKSON, S. E. & GÜNTHER, D. 1996. Laser Ablation Inductively Coupled Plasma Mass Spectrometric Transient Signal Data Acquisition and Analyte Concentration Calculation* *Journal of Analytical Atomic Spectrometry,* 11**,** 899-904.

LÓPEZ-GAMUNDÍ, O. 2006. Permian plate margin volcanism and tuffs in adjacent basins of west Gondwana: Age constraints and common characteristics. *Journal of South American Earth Sciences,* 22**,** 227-238.

LUDWIG, K. R. 2003. *Users manual for isoplot 3.00,* Berkeley, CA, Berkeley Geochronology Centre.

MACMAHAN, J. H., THORNTON, E. B. & RENIERS, A. J. H. M. 2006. Rip current review. *Coastal Engineering,* 53**,** 191-208.

MAITLAND, A. G. 1898. Delimitaion of the artesian water area north of Hughenden. *Geological Surevy of Queensland Publication,* 121**,** 1-19.

MALONE, E. J., OLGERS, F. & KIRKEGAARD, A. G. 1969. *The geology of the Duaringa and Saint Lawrence 1:250,000 sheet areas, Queensland*, Austral., Bur. Miner. Resour., Geol. Geophys., Rep.

MANTLE, D., KELMAN, A. P., NICOLL, R. & LAURIE, J. 2010. Australian Biozonation Chart. *In:* AUSTRALIA, G. (ed.). Canberra.

MARKS, E. O. 1911. Carbonaceous Glossopteris-bearing strata, near Pentland. *Geological Survey of Queensland Publication,* 235**,** 21-22.

MARTINSEN, O. J. 1989. Styles of soft-sediment deformation on a Namurian (Carboniferous) delta slope, Western Irish Namurian Basin, Ireland. *Geological Society, London, Special Publications,* 41**,** 167-177.

MARZOLI, A., BERTRAND, H., KNIGHT, K. B., CIRILLI, S., BURATTI, N., VÉRATI, C., NOMADE, S., RENNE, P. R., YOUBI, N., MARTINI, R., ALLENBACH, K., NEUWERTH, R., RAPAILLE, C., ZANINETTI, L. & BELLIENI, G. 2004. Synchrony of the Central Atlantic magmatic province and the Triassic-Jurassic boundary climatic and biotic crisis. *Geology,* 32**,** 973-976.

MATHESON, S. G. 1987. Coal Exploration in the Galilee Basin - Pentland and Milray Areas. Brisbane.

MATTINSON, J. M. 2005. Zircon U-Pb chemical abrasion ("CA-TIMS") method: combined annealing and multi-step partial dissolution analysis for improved precision and accuracy of zircon ages. *Chemical Geology,* 220**,** 47-66.

MCDONAGH, G. P. 1967. Glenaras No. 1 authority to prospect 106P, Queensland, Well completion report. Brisbane: Phillips Australian Oil Company.

MCKAY, M. P., WEISLOGEL, A. L., FILDANI, A., BRUNT, R. L., HODGSON, D. M. & FLINT, S. S. 2015. U-PB zircon tuff geochronology from the Karoo Basin, South Africa: implications of zircon recycling on stratigraphic age controls. *International Geology Review,* 57**,** 393-410.

MCKELLAR, J. L. 1991. Palynostratigraphy. *In:* BRAIN, T. J., MCKELLAR, J. L. & CARMICHAEL, D. C. (eds.) *Stratigraphic Drilling Report - GSQ Muttaburra 1 1991/25.* Brisbane, QLD: Geological Survey of Queensland.

MCKELLAR, J. L. 2013. Cooper Basin. *In:* JELL, P. A. (ed.) *Geology of Queensland.* Brisbane, QLD: Geological Survey of Queensland.

MCKELLAR, J. L. & HENDERSON, R. A. 2013. Galilee Basin. *In:* JELL, P. A. (ed.) *Geology of Queensland.* Brisbane, QLD: Geological Survey of Queensland.

MEFFRE, S., SCOTT, R. J., GLEN, R. A. & SQUIRE, R. J. 2007. Re-evaluation of contact relationships between Ordovician volcanic belts and the quartz-rich turbidites of the Lachlan Orogen. *Australian Journal of Earth Sciences,* 54**,** 363-383.

METCALFE, I., CROWLEY, J. L., NICOLL, R. S. & SCHMITZ, M. 2015. High-precision U-Pb CA-TIMS calibration of Middle Permian to Lower Triassic sequences, mass extinction and extreme climate-change in eastern Australian Gondwana. *Gondwana Research*.

MICHAELSEN, P. 2002. Mass extinction of peat-forming plants and the effect on fluvial styles across the Permian-Triassic boundary, northern Bowen Basin, Australia. *Palaeogeography, Palaeoclimatology, Palaeoecology,* 179**,** 173-188.

MICHAELSEN, P., HENDERSON, R. A., CROSDALE, P. J. & FANNING, C. M. 2001. Age and significance of the Platypus Tuff Bed, a regional reference horizon in the Upper Permian Moranbah Coal Measures, north Bowen Basin. *Australian Journal of Earth Sciences* 48**,** 183 - 192.

MOLLAN, R. G., DICKINS, J. M., EXON, N. F. & KIRKEGAARD, A. G. 1969. Geology of the Springsure 1:250,000 Sheet Area, Queensland Canberra, ACT: Bureau of Mineral Resources Geology and Geophysics.

MOLLAN, R. G., KIRKEGAARD, A. G., EXON, N. F. & DICKENS, J. M. 1964. Note on the Permian Rocks of the Springsure Area and Proposal of a New Name, Peawaddy Formation. *Queensland Government Mining Journal,* 65**,** 577-581.

MUTTON, A. J. 2003. Queensland Coals 14th Edition. Brisbane, QLD: Queensland Department of Natural Resources and Mines.

NICOLL, R., MCKELLAR, J. L., AYAZ, S. A., LAURIE, J. R., ESTERLE, J., CROWLEY, J., WOOD, G. & BODORKOS, S. 2015. CA-IDTIMS dating if tuffs, calibration of palynostratigraphy and stratigraphy of Bowen and Galilee Basins. *In:* BEESTON, J. W. (ed.) *2015 Bowen Basin Symposium.* Brisbane, QLD.

NICOLL, R., MCKELLAR, J. L., CROWLEY, J., PHILLIPS, L., WOOD, G., MANTLE, D. & BODORKOS, S. Cisuralian (early Permian) stratigraphy, biostratigraphy and interbasin correlation, eastern Australia: implications for exploration. Digging Deeper 2016, 2016a Brisbane, Queensland. Geological Survey of Queensland.

NICOLL, R., MCKELLAR, J. L., CROWLEY, J., PHILLIPS, L., WOOD, G., MANTLE, D. & BODORKOS, S. Cisuralian stratigraphy, biostratigraphy and interbasin correlation, eastern Australia: implications for exploration. Australian Earth Sciences Convention, 2016b Adelaide, Australia.

NORVICK, M. 1974. Permian and Late Carboniferious Palynostratigraphy of the Galilee Basin, Queensland. Bureau of Mineral Resources, Record 1974/141. Canberra, 1-161.

OLGERS, F. 1972, Geology of the Drummond Basin, Queensland, *Bulletin of the Bureau of Mineral Resources, Australia*, 132, 1–76.

OLGERS, F., WEBB, A. W., SMIT, J. A. J. & COXHEAD, B. A. 1966. *Geology of the Baralaba 1:250,000 sheet area, Queensland*, Australian Geological Survey Organisation, Canberra, ACT, Australia.

PAGE, R. W. & SUN, S. S. 1998. Aspects of geochronology and crustal evolution in the Eastern Fold Belt, Mt Isa Inlier. *Australian Journal of Earth Sciences,* 45**,** 343-361.

PATEN, R. J. 1969. Palynologic contributions to petroleum exploration in the Permian formations of the Cooper Basin. *APEA Journal,* 9**,** 79-87.

PATON, C., WOODHEAD, J. D., HELLSTROM, J. C., HERGT, J. M., GREIG, A. & MAAS, R. 2010. Improved laser ablation U-Pb zircon geochronology through robust downhole fractionation correction. *Geochemistry, Geophysics, Geosystems,* 11**,** n/a-n/a.

PHILLIPS, K. 1960. VII Permian. *Journal of the Geological Society of Australia,* 7**,** 183-249.

PHILLIPS, L. & AYAZ, S. A. Late Permian Stratigraphy of the Bowen - Galilee Basins. Poster Presentation. Bowen Basin Symposium 2015 Brisbane.

PHILLIPS, L., CROWLEY, J., MANTLE, D., ESTERLE, J., NICOLL, R., MCKELLAR, J. & WHEELER, A. In Press. U-Pb geochronology and palynology from late Permian strata of the Galilee Basin, Queensland, Australia. *Australian Journal of Earth Sciences*.

PHILLIPS, L., EDWARDS, S., BIANCHI, V. & ESTERLE, J. 2017a. Palaeoenvironmental reconstruction of Lopingian (upper Permian) sediments in the Galilee Basin, Queensland, Australia. *Australian Journal of Earth Sciences*.

PHILLIPS, L., ESTERLE, J. & SLIWA, R. 2015. Rationalising the Late Permian Coal Stratigraphy of the Koburra Trough, Galilee Basin. *In:* BEESTON, J. W. (ed.) *2015 Bowen Basin Symposium.* Brisbane.

PHILLIPS, L., ESTERLE, J. & SLIWA, R. 2017b. Galilee Basin. *In:* ESTERLE, J. & SLIWA, R. (eds.) *Regional stratigraphic framework for the Rangal-Baralaba-Bandanna Coal Measures in the Bowen and Galilee Basins.* Brisbane: ACARP Report C2028.

PHILLIPS, L., ESTERLE, J. S. & EDWARDS, S. 2017c. Review of Lopingian (upper Permian) stratigraphy of the Galilee Basin, Queensland, Australia. *Australian Journal of Earth Sciences,* 64**,** 283-300.

PHILLIPS, L., VERDEL, C., ALLEN, C. & ESTERLE, J. In Review. Detrital zircon U-Pb geochronology of Permian strata in the Galilee Basin, Queensland, Australia. *Australian Journal of Earth Sciences*.

PHIPPS, D. & PLAYFORD, G. 1984. Laboratory techniques for extraction of palynomorphs from sediments. *Papers of the Department of Geology, University of Queensland,* 11**,** 23.

PICARD, M. D. & HIGH, L. 1972. Criteria for recognizing lacustrine rocks. *In:* RIGBY, J. K. & HAMBLIN, W. K. (eds.) *Recognition of Ancient Sedimentary Environments.* Society of Economic Paleontologists and Mineralogists Special Publication.

POSTMA, G. (ed.) 1990. *Depositional architecture and facies of river and fan deltas: a synthesis,* International association of sedimentologists Blackwell Scientific Publications.

PRICE, P.L. 1974. Palynology. *In:* WATSON, P. J. (eds.) *Well Completion Report - HPP Weston 1, QLD, A-P 166P*. Brisbane, QLD: Queensland Digital Exploration Reports (QDEX): Queensland Government.

PRICE, P. L. 1976. Permian palynology of the Bowen Basin. *In:* JENSEN, A. R., EXON, N. F., ANDERSON, J. C. & KOPPE, W. H. (eds.) *A guide to the geology ofthe Bowen and Surat Basins in Queensland.* 25th International Geological Congress.

PRICE, P. L. 1997. Permian to Jurassic palynostratigraphic nomenclature of the Bowen and Surat Basins. *In:* GREEN, P. M. (ed.) *The Surat and Bowen Basins south-east Queensland, Queensland Minerals and Energy Review Series.* Brisbane, QLD: Queensland Department of Mines and Energy.

PRICE, P. L., FILATOFF, J., WILLIAMS, A. J., PICKERING, S. A. & WOOD, G. R. 1985. Late Palaeozoic and Mesozoic palynostratigraphical units, CSR oil and gas division, Palynology Laboratory Report no 274/25. Unpublished report held by the Queensland Department of Natural Resources and Mines as CR14012.

PROUZA, V. & PARK, W. J. 1973. Revision of Permian Stratigraphy of the Emeral-German Creek-Comet Area. *Queensland Government Mining Journal,* 866**,** 433-438.

PURDY, D. J., CROSS, A. J., BROWN, D. D., CARR, P. A. & ARMSTRONG, R. A. 2016. New constraints on the origin and evolution of the Thomson Orogen and links with central Australia from isotopic studies of detrital zircons. *Gondwana Research,* 39**,** 41-56.

RANDS, W. H. 1891. Cape River Goldfield. *Geological Survey of Queensland.* Queensland Digital Exploration Reports (QDEX): Queensland Government.

REID, J. H. 1916. The Glossopteris Beds of the Betts Creek, Northern Queensland. *Geological Survey of Queensland Publication.*

REID, J. H. 1918. The Coal Measures at Oxley Creek, Hughenden District. *Geological Survey of Queensland Publication.*

REID, J. H. 1930. Geological Survey Reports. Geology of the Springsure district, Parts 1 and 2. *Queensland Government Mining Journal,* 31**,** 87-157.

RIGBY, J. F., & HEKEL, H. 1977. Palynology of the Permian sequence in the Springsure Anticline, Central Queensland. *Geological Survey of Queensland*. Queensland Digital Exploration Reports (QDEX): Queensland Government.

REINECK, H. E. & WUNDERLICH, F. 1968. CLASSIFICATION AND ORIGIN OF FLASER AND LENTICULAR BEDDING. *Sedimentology,* 11**,** 99-104.

RUBIDGE, B. S., ERWIN, D. H., RAMEZANI, J., BOWRING, S. A. & DE KLERK, W. J. 2013. High-precision temporal calibration of Late Permian vertebrate biostratigraphy: U-Pb zircon constraints from the Karoo Supergroup, South Africa. *Geology,* 41**,** 363-366.

SANTOS, R. V., SOUZA, P. A., DE ALVARENGA, C. J. S., DANTAS, E. L., PIMENTEL, M. M., DE OLIVEIRA, C. G. & DE ARAÚJO, L. M. 2006. Shrimp U–Pb zircon dating and

palynology of bentonitic layers from the Permian Irati Formation, Paraná Basin, Brazil. *Gondwana Research,* 9**,** 456-463.

SCHMITZ, M. D. & DAVYDOV, V. I. 2012. Quantitative radiometric and biostratigraphic calibration of the Pennsylvanian–Early Permian (Cisuralian) time scale and pan-Euramerican chronostratigraphic correlation. *Geological Society of America Bulletin,* 124**,** 549-577.

SCHMITZ, M. D. & SCHOENE, B. 2007. Derivation of isotope ratios, errors and error correlations for U-Pb geochronology using 205Pb-235U-(233U)-spiked isotope dilution thermal ionization mass spectrometric data. *Geochemistry, Geophysics, Geosystems (G3)* 8.

SCHNEEBERGER, W. F. 1952. Abstract of the stratigraphy of the Spingsure Area and adjacent areas (Queensland). Geoscience Australia.

SCOTT, S. G., BEESTON, J. W. & CARR, A. F. 1995. Galilee Basin. *Special Publication of the Geological Society of Australia Coal Geology,* 1**,** 341-352.

SCOTT, S. G. & HAWKINS, P. J. 1992. Coal geology of the northern Galilee Basin and its implications for coalbed methane investigations. *In:* BEAMISH, B. B. & GAMSON, P. D. (eds.) *Symposium on coal bed methane research and developments in Australia.* Townsville, QLD: James Cook University of Northern Queensland.

SHAANAN, U. & ROSENBAUM, G. 2016. Detrital zircons as palaeodrainage indicators: insights into southeastern Gondwana from Permian basins in eastern Australia. *Basin Research***,** 1-12.

SHAANAN, U., ROSENBAUM, G. & SIHOMBING, F. 2017. Continuation of the Ross-Delamerian Orogen: Insights from east Australian detrital zircon data. *Australian Journal of Earth Sciences.*

SHAANAN, U., ROSENBAUM, G. & WORMALD, R. 2015. Provenance of the Early Permian Nambucca block (eastern Australia) and implications for the role of trench retreat in accretionary orogens. *Geological Society of America Bulletin*.

SHELL QUEENSLAND DEVELOPMENT PTY LTD 1952. General Report on investigations and operations carried out by the company in the search for oil in Queensland, 1940-1951. University of Queensland Library.

SIRCOMBE, K. N. & MCQUEEN, K. G. 2000. Zircon dating of Devonian–Carboniferous rocks from the Bombala area, New South Wales. *Australian Journal of Earth Sciences,* 47**,** 1041-1051.

SLÁMA, J., KOŠLER, J., CONDON, D. J., CROWLEY, J. L., GERDES, A., HANCHAR, J. M., HORSTWOOD, M. S. A., MORRIS, G. A., NASDALA, L., NORBERG, N., SCHALTEGGER, U., SCHOENE, B., TUBRETT, M. N. & WHITEHOUSE, M. J. 2008.

Plešovice zircon — A new natural reference material for U–Pb and Hf isotopic microanalysis. *Chemical Geology,* 249**,** 1-35.

SLIWA, R., ESTERLE, J., PHILLIPS, L. & WILSON, S. 2017. Rangal Supermodel 2015: The Rangal-Baralaba-Bandanna Coal Measures in the Bowen and Galilee Basins. *In:* SLIWA, R. & ESTERLE, J. (eds.). The Australian Coal Association Research Program.

SMITH, R. M. H. 1990. A review of stratigraphy and sedimentary environments of the Karoo Basin of South Africa. *Journal of African Earth Sciences (and the Middle East),* 10, 117-137.

SMITH, T. E. & MANTLE, D. J. 2013. Late Permian palynozones and associated CA-IDTIMS dated tuffs from the Bowen Basin, Australia. Record 2013/46 Geoscience Australia, Canberra, 1-45.

STAINES, H. R. E. & KOPPE, W. H. 1979. The Geology of North Bowen Basin. *Queensland Government Mining Journal,* 80**,** 172 - 195.

STEVENS, B. 1985. Preliminary interpretation of regional basement geology in northwestern New South Wales. Quarterly Notes, *Geological Survey of New South Wales,* 6, 9–22.

STEWART, A. J. 2013. *Galilee Basin* [Online]. http://www.ga.gov.au/provexplorer/provinceDetails.do?eno=550790: Geoscience Australia. Available: http://www.ga.gov.au/provexplorer/provinceDetails.do?eno=550790 [Accessed 3rd May 2015].

STOPES, M. C. 1919. On the four visible ingredients of banded bituminous coal. *Proc. Roy. Soc. Series B,* 90.

SWARBRICK, C. F. J. 1974. Stratigraphic Drilling Report - GSQ Jericho 1. *Queensland Government Mining Journal,* 75**,** 210-215.

VAN HEESWIJCK, A. 2004. The sturcture and hydrocarbon potential of the northern Drummond Basin and northeastern Galilee Basin, central Queensland, Australia. *In:* J., B. P., JOHNS, D. R. & LANG, S. C. (eds.) *Easterm Australasian Basins Symposium II.* Adelaide, SA: Petroleum Exploration Society of Australia Special Publication.

VAN HEESWIJCK, A. 2006. *The structure, sedimentology, sequence stratigraphy and tectonics of the Northern Drummond and Galilee Basins, Central Queensland, Australia.* Phd, James Cook University.

VAN HEESWIJCK, A. 2010. Late Paleozoic to Early Mesozoic deformation in the northeastern Galilee Basin, Australia. *Australian Journal of Earth Sciences,* 57**,** 431-451.

VEEVERS, J. J. 2006. Updated Gondwana (Permian–Cretaceous) earth history of Australia. *Gondwana Research, 9*(3), 231-260.

VEEVERS, J. J., JONES, J. G. & POWELL, C. M. 1982. Tectonic Framework of Australias Sedimentary Basins. *APEA Journal,* 22**,** 283-300.

VERDEL, C., STOCKLI, D. & PURDY, D. 2016. Low-temperature thermochronology of the northern Thomson Orogen: Implications for exhumation of basement rocks in NE Australia. *Tectonophysics,* 666**,** 1-11.

VERMEESCH, P. 2012. On the visualisation of detrital age distributions. *Chemical Geology,* 312**,** 190-194.

VINE, R. R. 1975. Galilee Basin. *In:* LESLIE, R. B., EVANS, H. J. & KNIGHT, C. L. (eds.) *Economic Geology of Australia and Papua New Guinea.* Melbourne, VIC: The Australian Institue of Mining and Metallurgy.

VINE, R. R., CASEY, D. J. & JOHNSON, N. E. A. 1964. Progress Report, 1963, on the Geology of part of the north-eastern Eromanga Basin, Queensland. Bureau of Mineral Resources Geology and Geophysics.

VINE, R. R., JAUNCEY, W., CASEY, D. J. & GALLOWAY, M. C. 1965. Geology of the Longreach-Jericho-Lake Buchanan Area. Bureau of Mineral Resources Geology and Geophysics.

WALLIN, C. I. 1975. Stratigraphic Drilling Report - GSQ Tambo 1-1A. *Queensland Government Mining Journal,* 76**,** 411-415.

WARD, P. D., BOTHA, J., BUICK, R., DE KOCK, M. O., ERWIN, D. H., GARRISON, G. H., KIRSCHVINK, J. L. & SMITH, R. 2005. Abrupt and gradual extinction among Late Permian land vertebrates in the Karoo Basin, South Africa. *Science,* 307, 709-714.

WARWICK, P. D. 2005. Coal systems analysis. *Geological Society of America Special Papers,* 387

WASCHBUSCH, P., KORSCH, R. & BEAUMONT, C. 2009. Geodynamic modelling of aspects of the Bowen, Gunnedah, Surat and Eromanga Basins from the perspective of convergent margin processes. *Australian Journal of Earth Sciences,* 56**,** 309-334.

WATSON, E. B., WARK, D. A. & THOMAS, J. B. 2006. Crystallization themometers for zircon and rutile. *Contributions to Mineralogy and Petrology,* 151**,** 413-433.

WELLS, A. T. 1968. Stratigraphy and Permian Coal Measures of the Galilee Basin, Queensland. *In:* HARRINGTON, H. J. (ed.) *Permian Coals of Eastern Australia.* Bureau of Mineral Resources.

WHITE, L., ROSENBAUM, G., ALLEN, C. M. & SHAANAN, U. 2016. Orocline-driven transtensional basins: Insights from the Lower Permian Manning Basin (eastern Australia). *Tectonics,* 35**,** 690-703.

WHITEHOUSE, F. W. 1955. The Geology of the Queensland portion of the Great Artesian Basin, Appendix G. *Artesian water supplies in Queensland.*

WILLIAMS, I. S. 2001. Response of detrital zircon and monazite, and their U–Pb isotopic systems, to regional metamorphism and host-rock partial melting, Cooma Complex, southeastern Australia. *Australian Journal of Earth Sciences,* 48**,** 557-580.

WILSON, S. 2017. *Sedimentary architecture and depositional environment of the late Permian Rangal Coal Measures.* MPhil, University of Queensland.

WITHNALL, I. W., BLAKE, P. R., CROUCH, S. B. S., TENISON WOODS, K. , GRIMES, K. G., HAYWARD, M. A., LAM, J. S., GARRAD, P. & REES, I.D. 1995. Geology of the southern part of the Anakie Inlier, central Queensland, *Queensland Geology,* 7, 1–245.

WOOD, G. D. 2013. Palynostratigraphical Analysis, Bibblewindi 11C, Gunnedah Basin. Adelaide: Santos Ltd.

WOOD, G. D., GABRIEL, A. M. & LAWSON, J. C. 1996. Palynological techniques - processing and microscopy. *In:* JANSONIUS, J. & MCGREGOR, D. C. (eds.) *Palynology, Principles and Applications.* American Association of Stratigraphic Palynologists Foundation.

THE UNIVERSITY OF QUEENSLAND

AUSTRALIA

The stratigraphic architecture of Lopingian (late Permian) strata in the Galilee Basin, NE Australia.

8. Appendices

Laura Jayne Phillips

BSc. (Hons.) – Royal Holloway, University of London

MRes. – Bristol University

Appendices of a thesis submitted for the degree of Doctor of Philosophy at The University of Queensland in 2017

School of Earth and Environmental Sciences

8.1. Bowen Basin Symposium (2015) conference paper

Rationalising the Late Permian Coal Seam Stratigraphy of the Koburra Trough, Galilee Basin.

Authors: L. J. Phillips[1], J. S. Esterle[1] and R. Sliwa[2]

[1]University of Queensland, Earth Sciences, Steele Building, St. Lucia Campus, 4072

[2] Integrated Geoscience Pty Ltd, PO Box 462, Yandina, QLD, 4561

Corresponding author email: l.phillips3@uq.edu.au

Abstract

This study examines the regional variation in the coal seams of the Late Permian Betts Creek Beds in the Galilee Basin, which have implications for their equivalence in the Bowen Basin. Open file well data is correlated across the Koburra Trough, and provide a regionally consistent view of coal seams and groups. Collectively, the Bandanna Formation and Colinlea Sandstone coal measures converge to be termed the Betts Creek Beds. Individual seams within the topmost Bandanna Formation are correlated as the A and B seams. These are separated from the underlying C Seam of the Colinlea Sandstone by a thick section equivalent to the Black Alley Shale-Peawaddy Formations in the Bowen Basin. The Colinlea Sandstone contains a series of seams correlated as the C, D, E, F and G, although there are other seams that occur stratigraphically beneath this towards the centre of the trough which have been named H and I. The datum was deemed as the "C seam", which is a regionally consistent, tuffaceous seam that has visual correlatives in the Fairhill Formation of the Fort Cooper Coal Measures in the Bowen Basin. From east to west, the different coal measures show an offset stacking pattern that could reflect subsidence controlled by differential compaction or tectonics across a feature termed the "Hulton-Rand" structure. This structure has been interpreted as a monocline, and shows no evidence of faulting in the sparsely available seismic data. However, an additional sequence of coal seams attributed to the Betts Creek Beds in current formation nomenclature, named the 'J and K' seams, occur in this area. The 'J and K' seams, along with the Early Permian Aramac Coal Measures, suggest a compartmentalisation in the basin. Correlations presented in this study should be tested by biostratigraphy and tephrochronology.

KEYWORDS: Galilee Basin, Colinlea Sandstone, Bandanna Formation, Fort Cooper Coal Measures, Stratigraphy

Introduction

The Late Permian coal seams in the Galilee Basin (Figure 1) are included in the Betts Creek Beds. The stratigraphic equivalents are the Bandanna Formation and Colinlea Sandstone which are separated by the Black Alley Shale and Peawaddy Formation (Figure 2). The Colinlea Sandstone has been correlated eastward across the Springsure Shelf with the Catherine Sandstone, Ingelara Formation, Freitag Formation and the Upper Aldebaran Sandstone. In the Denison Trough the Aldebaran Sandstone to Catherine Sandstone section is thick (~1130m (Bauer and Dixon, 1981)) but its equivalent Colinlea Sandstone is thinner (up to 200m) and interpreted as a condensed section accumulated in a low accommodation setting (Allen and Fielding, 2007b). With the increased exploration for coal and coal seam gas in the Galilee Basin, there has been a proliferation of data in which to explore regional correlations. Within individual areas, there is often an inconsistent use of stratigraphic names. The objective of this study was to constrain the current stratigraphic framework using a regional correlation of coal seams across the Koburra Trough in the Galilee Basin.

Geological overview

The Galilee Basin is a large inland basin that covers an area of 247,000km2. It is part of a larger Carboniferous to Mid Triassic basin system that also contains the Cooper Basin, situated towards the south west of the Galilee Basin and the Bowen Basin to the east. The Nebine Ridge and Springsure Shelf are structural highs that separate the Galilee Basin from the Bowen Basin to the south east, while the Canaway Fault separates the Galilee from the Cooper Basin in the south west. The Galilee Basin is subdivided into three sub basins- the Koburra Trough, the Lovelle Depression and the Powell Depression. The Koburra Trough is bounded by the Maneroo Platform basement high to the west, with the Hulton-Rand Structure, occurring just to the east of the platform. The Hulton-Rand Structure is mapped as a monocline with a thicker succession of sediments on its down dip side (Van Heeswijck, 2006). Various tectonic settings have been suggested for the Galilee Basin: the result of an incipient coupled or double orocline (Evans and Roberts, 1980); a peri-cratonic basin (Veevers et al., 1982); and a foreland basin (de Caritat and Braun, 1992). It is now generally agreed that the tectonic setting is that of an intracratonic basin (Van Heeswijck, 2010, Allen and Fielding, 2007a).

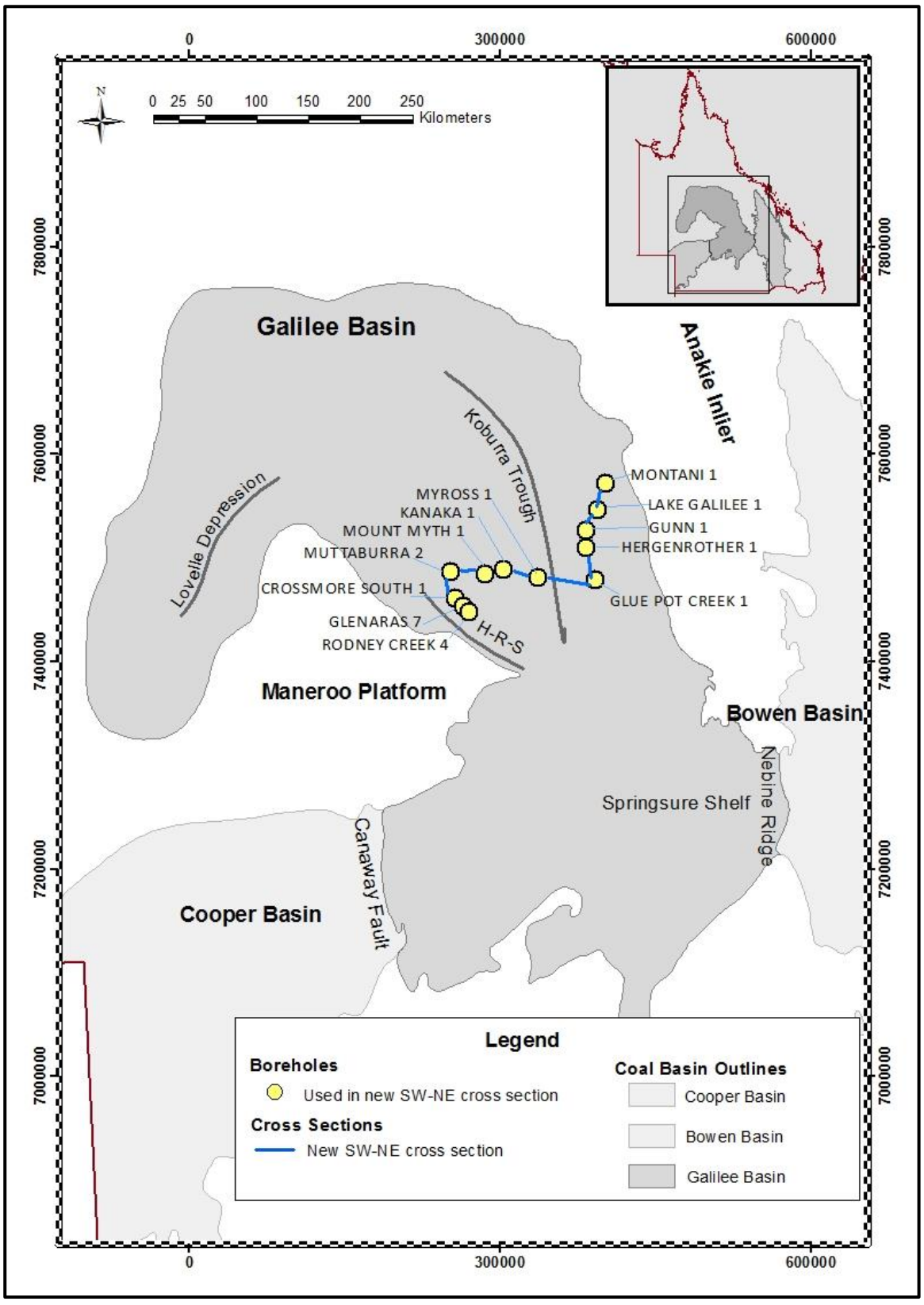

Figure 1. Map of location of the study area and boreholes used to create correlations. Main structural features are named and shown in black. H-R-S is Hulton-Rand Structure.

Current stratigraphic nomenclature

The stratigraphy of the Galilee Basin (shown in Figure 2) was first developed by Gray and Swarbrick (1975), using units defined by others (e.g. Mollan et al. (1969), Vine and Doutch (1972),

Vine (1975)). The current stratigraphy had been revised by Allen and Fielding (2007b) through correlations of geophysical wireline logs made from the Springsure Shelf up along the eastern subcrop of the Galilee Basin, with a focus on the Betts Creek Beds situated in the north.

The stratigraphy is shown in Figure 2, with the Permo-Triassic units correlated across the Springsure Shelf into the Denison Trough of the Bowen Basin. Based on palynology, the Bandanna Formation is Late APP5 Stage (Price, 1997) and correlates across the Springsure Shelf, as does the combined Black Alley Shale-Peawaddy Formation. The Colinlea Sandstone in the Galilee Basin is the condensed and coal bearing equivalent of the Catherine Sandstone, Ingelara Formation, Freitag Formation and the Upper Aldebaran Sandstone in the Denison Trough. The thickness of this unit varies from sixty eight meters to over one hundred metres depending on correlation. The Colinlea Sandstone and its equivalents were originally placed into APP3 stage (Mollan et al., 1969), however palynological analysis from QDM Aramac 1 and Hexam 1 boreholes (Swarbrick and Wallin, 1976) places the Colinlea Sandstone in the APP5 stage.

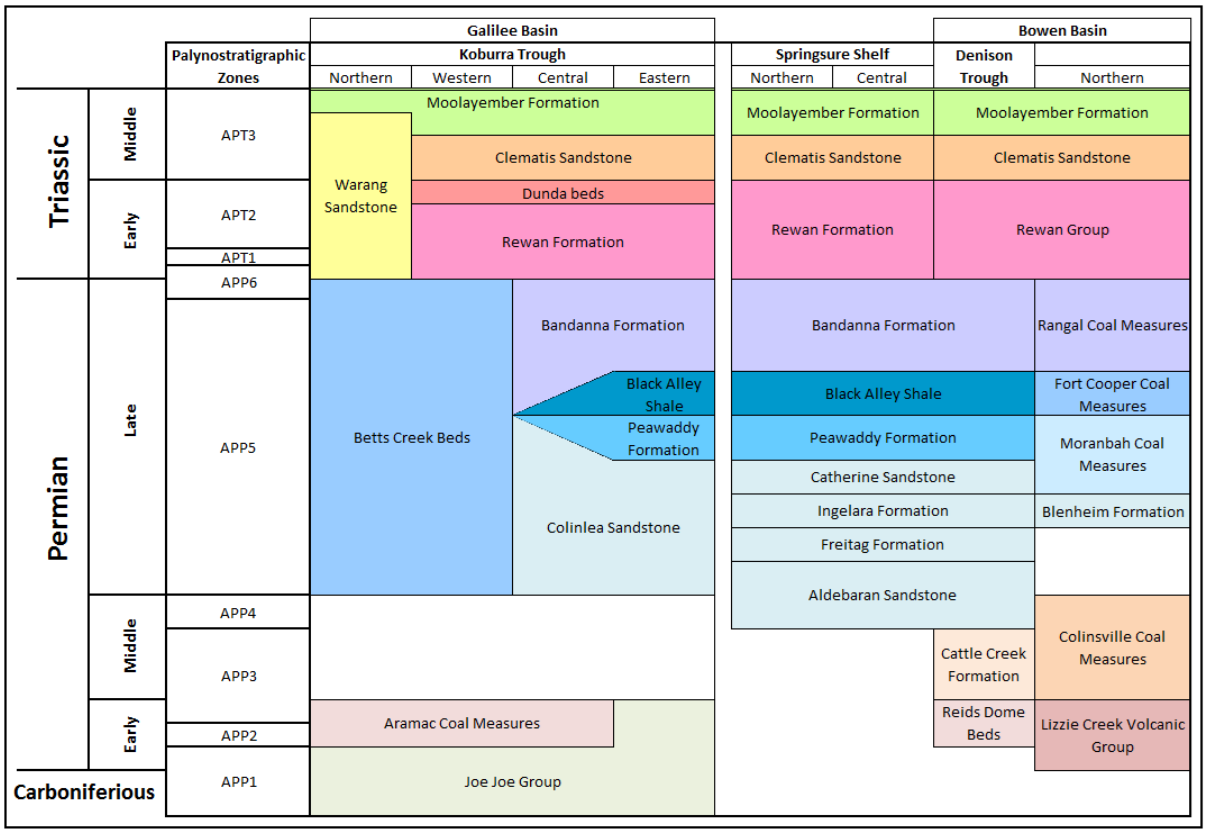

Figure 2. Current stratigraphic framework of the Galilee and Bowen Basins (after Scott et al., 1995, Allen and Fielding, 2007b and Draper 2012).

Definition of the Bandanna Formation and Colinlea Sandstone

Scott et al. (1995) mapped out the extent of the Bandanna Formation, the Peawaddy Formation, the Black Alley Shale and the Colinlea Sandstone. When combined these units make up the Betts Creek Beds.

The Bandanna Formation is typically laminated to thickly bedded labile sandstone, interbedded with mudstones and siltstones (Hawkins, 1978, Hawkins and Green, 1993, Allen and Fielding, 2007b, Grigorescu, 2012). It also contains major coal seams targeted by mining and CSG exploration companies. It contains sandstones that range from fine to coarse grained. The range of grain sizes and complex mineralogy has been interpreted to have been deposited on an alluvial to paralic system (Hawkins, 1978, Hawkins and Green, 1993, Allen and Fielding, 2007b, Grigorescu, 2012). The Peawaddy Formation and Black Alley Shale have been interpreted to have formed in a lacustrine/restricted marine environment.

The Colinlea Sandstone was first defined in 1952, referring to the stratigraphic interval between the Joe Joe Group and the Mantuan Productus Bed within the upper Peawaddy Formation (SQD, 1952) on the western Springsure 1:250,000 geological map (Mollan et al., 1969). Mollan et al. (1969) defined the Colinlea Sandstone in more detail and described the extent to which it was thought to exist across the western and eastern Springsure Sheet into the Galilee and Bowen basins, although its occurrence was sporadic.

Colinlea Sandstone was first described to consist of predominantly fine to medium grained quartz sandstone and various conglomerates with thin minor siltstone that occurs interbedded among the sandstones (Mollan et al., 1969). Hill (1957) suggested that it was a formation rather than a unit, because of its heterogeneity. Hawkins (1978), Hawkins and Green (1993), Grigorescu (2012) mention the presence of mudstone and coal in the formation. The sandstone is well sorted, but with angular to sub-angular grains. The mudstone is laminated and contains kaolinite with rare illite and minor chlorite (Hawkins and Carmichael, 1987).

Both Mollan et al. (1969) and Scott et al. (1995) interpret the depositional environments of the Colinlea Sandstone as alluvial systems (rivers and their floodplains) that at times supported coal accumulation, but sediment dispersal patterns were variable. Palaeo-flow direction was to the south-east (Scott et al., 1995), and Mollan et al. (1969) suggested a south-westerly provenance for the lower part of the sandstone and a shift to towards the upper part of the Colinlea Sandstone, as the basin received sediment from north and east. Vine (1975) notes that the Colinlea Sandstone cannot

be observed north of 23oS (approximately 7450000N), however Scott and Hawkins (1992) and Allen and Fielding (2007b) suggested that the correlatives of the Colinlea Sandstone can be found further north along the basin margin. Towards the western side of the basin, it has been noted in various well completion reports that the Colinlea Sandstone is a section of coarse grained sandstone within the Betts Creek Beds between the coal seams found in the Rodney Sequence and the coal seams in the older Crossmore Sequence in the west of the Koburra Trough. This adds to the confusion of the applied stratigraphy as the Colinlea Sandstone is thought to be a lateral correlative of the lower Betts Creek Beds, not a unit within it.

Coal Seam Stratigraphy

Coal seam nomenclature is different from the west to the east of the basin. In this study all individually correlated coal seams have been given a uniform name, modelled on seam nomenclature suggested by Scott and Hawkins (1992), from west to east (Figure 3).

Coal seams in the Bandanna Formation are called the A and B seams (Scott and Hawkins, 1992), separated by 14m-61m of clastic strata attributed to the Black Alley Shale and Peawaddy Formations. The youngest coal seam, the A seam, is commonly used as the boundary between the Permian and coal void Triassic sediments in the basin, although the boundary is poorly defined. The coal seams within the Colinlea Sandstone are known as C, D, E, F, G, H and I seams (Scott and Hawkins, 1992) from younger to older respectively. The C seam is highly tuffaceous (Scott and Hawkins, 1992), whereas the other seams only sporadically contain tuffaceous material.

In the west of the basin, the coals are referred as the Thompson, Rodney, Crossmore and Glenaras sequences within the Betts Creek Beds. Seam names ‘J and K’ are proposed for the Crossmore and Glenaras Sequences respectively, as shown in Figure 3.

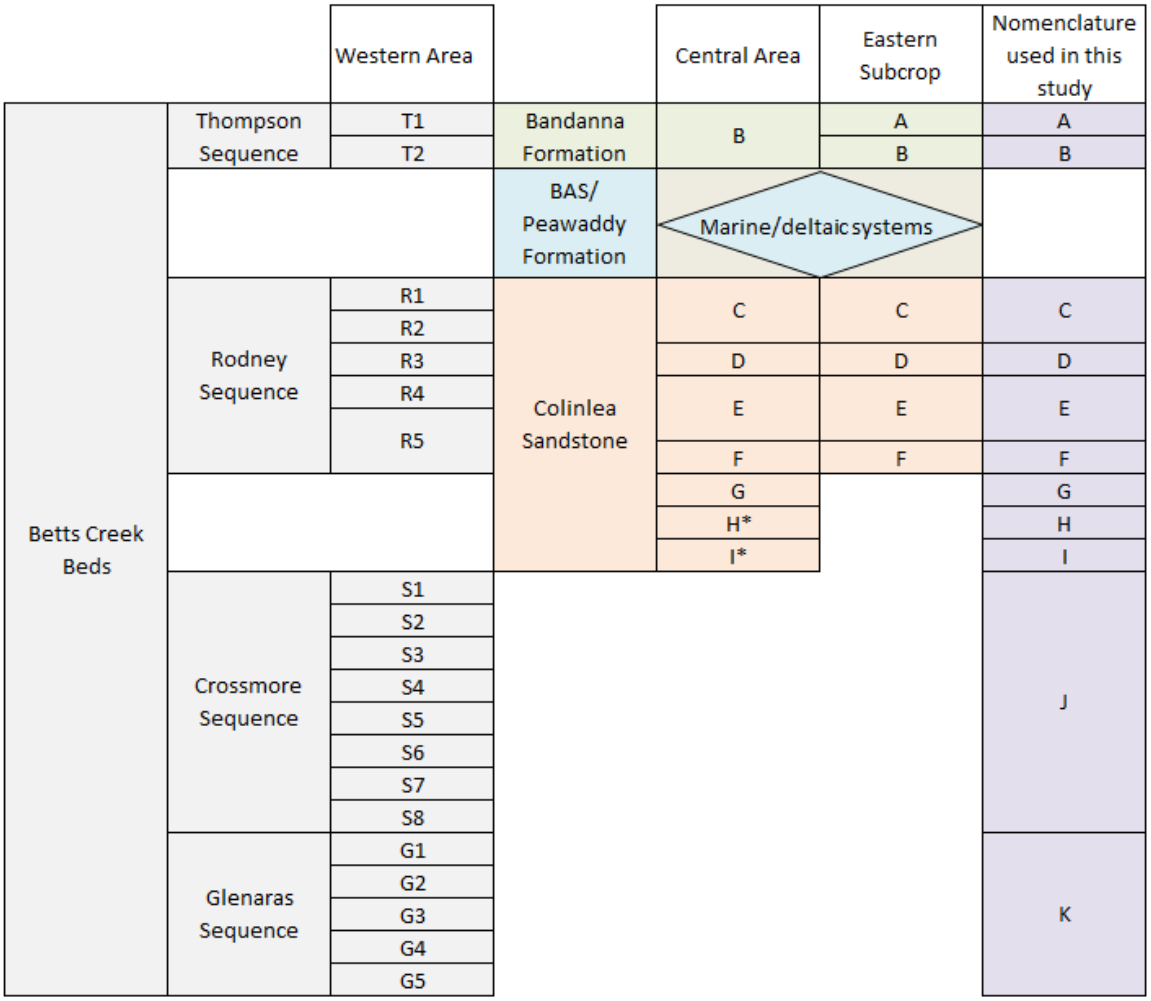

Figure 3. Late Permian coal seam nomenclature of the Galilee basin (Scott and Hawkins, 1992b, Scott et al., 1995, Galilee Energy Limited, 2001) and nomenclature used in this study. * denotes coal seams that do not occur across all parts of the region.

Methodology

Wireline logs were collated from the QDEX database and were analysed using Paradigm Geolog 7.1TM Software. Each wireline log underwent a quality control process where they were checked against English logs for anomalies. The gamma logs were normalised to define a consistent shale line for all logs used in the study.

For this study, a simple classification of sandstone, siltstone and coal was used. Some boreholes did not have density logs, so coal was identified using sonic or where able the gamma log, and verified by English log description. Forty boreholes from the central part of the basin were correlated. Twelve of these boreholes were selected from across the basin for use in the study (see Figure 1 for locations and names) and a new south-west to north-east correlation section was created (Figure 4).

Results

Displayed in the cross section, the low gamma lithologies, interpreted as sandstone, are coloured in yellow, grading down to the high gamma lithologies interpreted as finer grained heterolithic strata in the red colours.

The cross section has been flattened to the C seam, the youngest coal within the Colinlea Sandstone. Due to the tuffaceous nature of the C seam it can be easy distinguished from other coal seams and can be used as a marker horizon across the basin. From the SW-NE cross section (Figure 4) it becomes clear that the coal seams can be separated into four groups:

- the Bandanna Formation, A and B seams
- the Colinlea Sandstone, C to G seams (H and I where they exist) which are laterally consistent but taper to the west and split to the east of the basin
- Late Permian 'J and K' seams (Crossmore and Glenaras Sequences)
- the Early Permian Aramac Coal Measures.

Seams A and B are correlated within the Bandanna Formation. The B seam is thought to be continuous across the basin, however the A seam has not been correlated west of the Koburra Trough.

Situated between the B and C seams is a coal barren unit that displays a coarsening upward sequence (Figure 4). This can be found in the central part of the basin and across the Koburra Trough. This is thought to represent the Black Alley Shale and Peawaddy Formation equivalents (Figure 2).

There is a shift of coal seam geometry from west to east. Towards the east, the C to I coal seams open up to a series of thicker seams separated by heterolithic interburden that also increases in thickness. In the central and eastern part of the basin, the C seam is referred to as the youngest coal seam of the Colinlea Sandstone (Scott and Hawkins, 1992), and the G (or I where it exists) as the oldest coal seam within the Late Permian Coal Measures. Yet these coal seams are condensed on the western side of the basin above where the 'J and K' seams are correlated. Towards the west of the cross section shown in Figure 4, the electrofacies, and where available, core photos, show a coarse grained sandstone lithology situated below the coal seams of the Colinlea Sandstone (seams C to I). This section alone is referred to as the Colinlea Sandstone in various well completion reports for the western Koburra Trough area adding to the confusion of the stratigraphy.

The ‘J and K’ seams have only been correlated on the western side of the basin, and appear to thin and pinch towards the Koburra Trough and are not seen in the east (Figure 4). The ‘J and K’ seams show very distinct ‘blocky’ density characteristics. They also appear on the down thrown side of the Hulton-Rand Structure above where the Early Permian Aramac Coal Measures are located.

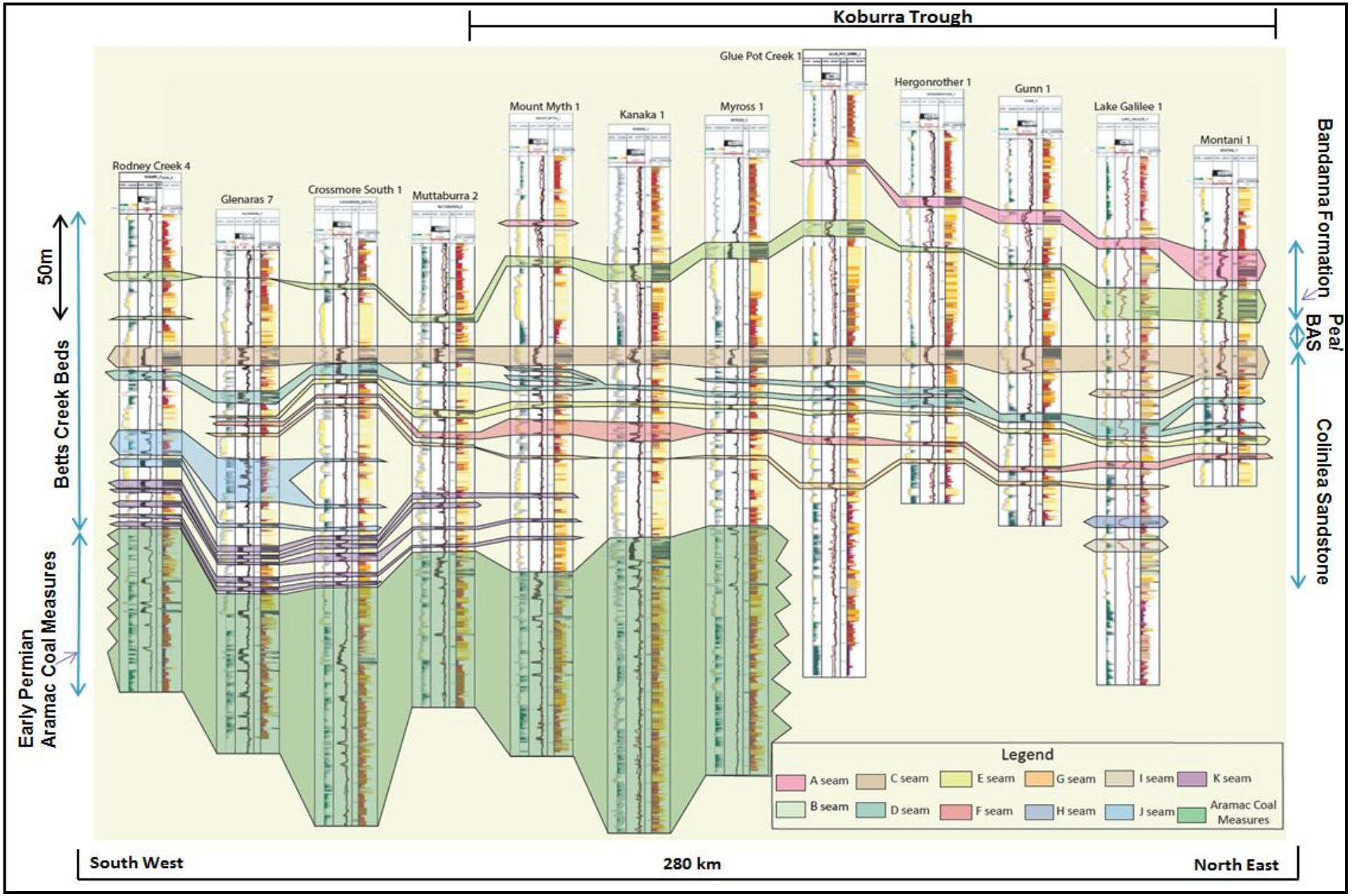
Koburra Trough
Rodney Creek 4
Glenaras 7
Crossmore South 1
Muttaburra 2
Mount Myth 1
Kanaka 1
Myross 1
Glue Pot Creek 1
Hergonrother 1
Gunn 1
Lake Galilee 1
Montani 1
50m
Betts Creek Beds
Early Permian
Aramac Coal Measures
Bandanna Formation
Peat
BAS
Colinlea Sandstone
Legend
A seam
B seam
C seam
D seam
E seam
F seam
G seam
H seam
I seam
J seam
K seam
Aramac Coal Measures
South West
280 km
North East

Figure 4. A correlation section of coal seams across the Galilee basin from the NE to SW. Main structural features are mentioned at top of figure. Gamma logs have been coloured in yellow >100API and green <100API. Where density (black wireline log) is not present Sonic (red wireline log) has been used. Yellow electrofacies represent coarser lithologies, grading into red electrofacies for finer grained lithologies. Coal is represented by the black and grey electrofacies.

Discussion

Regional correlation of coal seam packages has provided new insight into the currently used formation and coal seam nomenclature in the Galilee Basin. The Bandanna Formation, which includes the A and B seams, is present across the basin, however the A seam, the youngest coal seam is not. This may affect as to where the boundary between the Permian and Triassic lithological units is placed, as the appearance of the A seam is commonly used as the marker for the top of the Permian sediments.

Below the Bandanna Formation is a coarsening upwards sequence, often floored by a bioturbated mudstone. This unit is the correlatives of the Peawaddy and Black Alley Shale, and represents a prograding fluvial-deltaic system where thick in the eastern part of the basin (Blanco, 2010).

The highly tuffaceous C seam is useful as a marker horizon across the basin. Other lithostratigraphic units are dynamic and may only exist locally and not on a basin scale. The tuffaceous nature of the C seam is reminiscent of the Fort Cooper Coal Measures in the Bowen Basin (Anderson, 1985, Ayaz et al., In Press), in particular the Fairhill Formation. If this could be confirmed, e.g. by age dating, then it provides a key horizon for correlating between the basins.

The architecture of the C to I coal seams, thick and split in the east of the cross section and condensed towards the west, suggests that during deposition, tectonic subsidence in the Koburra Trough was higher in the east of the basin. The interburden between the C to I seams is heterolithic and displays both small scale fining up and coarsening upward sequences. These sequences may be attributed to alternating fluvial and lacustrine systems.

The presence of the ‘J and K’ seams (or Crossmore and Glenaras Sequence) provides a correlation issue of stratigraphic groups. In the west of the basin, they are persistent, and separated from the overlying C to I coals by a series of blocky sandstones that are not observed in the east where the succession consists of finer grained heteroliths. The apparent offset relationship between the C to I seams and the J seams, and their proximity to the Aramac Coal Measures suggest that the J seams to the west are older than the C to I seams, possibly much older and Early Permian in age, however current nomenclature places all seams in the Late Permian Betts Creek Beds .

The appearance of the ‘J and K’ seams in close proximity to the Early Permian Aramac Coal Measures to the west of the basin raises the idea of an Early Permian sub basin occurring adjacent to the Maneroo Platform, however the current nomenclature places the ‘J and K’ seams into the Late Permian Betts Creek Beds. They could be age equivalent and part of the Betts Creek Beds, but we propose that they are older than the coal seams correlated with the Colinlea Sandstone to the east of the basin. No palynological analysis has been found on the ‘J and K’ seams, however analysis on the older Aramac Coal Measures and the C to I seams have placed the coal measures in stage APP3 and APP5 respectively (Norvick, 1981).Using the correlations in this study (Figure 4), the J seams have a greater affinity with the Early Permian Aramac Co0al Measures. The mid-Permian hiatus (Figure 2), has not been identified in the geophysical logs, and so cannot help to further constrain the placement of the ‘J and K’ seams in the stratigraphic record.

Conclusions

An assessment of all current literature has shown that there are inconsistencies with the application of formation nomenclature across the Galilee Basin. When further studied it became apparent that no correlations of the coal seams had been conducted on a regional scale from west to east across the basin. The correlations presented in this study show that coal seams, in particular the highly tuffaceous C seam, can be used as a marker horizon across the basin and potentially across to the Bowen Basin.

The correlation suggests that the A and B seams, which are part of the Bandanna Formation, are the lateral equivalents to the Rangal Coal Measures in the Bowen Basin. The highly tuffaceous nature of the C seam and its stratigraphic relationship below the Black Alley Shale and Peawaddy Formation suggest that it may be a lateral correlative of the Fairhill Formation. This will be further tested through age dating of the volcanic tuff horizons. The ‘J and K’ seams to the west of the Basin are poorly constrained. Their regional appearance overlying the Early Permian Aramac Coal Measures suggest that they too may be Early Permian in age, possibly correlatives of the Bowen Basin Collinsville Coal Measures. However current literature places them in the Late Permian Betts Creek Beds.

Future Work

To further this study, tephrochronology will be conducted on volcanic tuffs and with biostratigraphic analysis, will help to corroborate or refute the correlations proposed in this study. Provenance analysis and sediment dispersal studies of the sandstones within the Permian sequence in the Galilee Basin will contribute to testing the proposed stratigraphy and aid in interpretation of depositional settings across the basin.

Acknowledgements

The authors of this study wish to thank ACARP for providing funding as part of a larger study on the Rangal Coal Measures. Thank you to Ms Syeda Areeba Ayaz for constructive comments to help improve the quality of the paper and to fellow colleagues at the University of Queensland who helped to improve this manuscript through thoughtful discussions.

References

ALLEN, J. P. & FIELDING, C. R. 2007a. Sedimentology and stratigraphic architecture of the Late Permian Betts Creek Beds, Queensland, Australia. Sedimentary Geology, 202, 5-34.

ALLEN, J. P. & FIELDING, C. R. 2007b. Sequence architecture within a low-accommodation setting: An example from the Permian of the Galilee and Bowen basins, Queensland, Australia. AAPG Bulletin, 91, 1503-1539.

ANDERSON, J. C. 1985. Geology of the Fort Cooper Coal Measures Interval. Bowen Basin Coal Symposium. Geological Society of Australia Abstracts.

AYAZ, S. A., ESTERLE, J. & MARTIN, M. In Press. Spatial Variation in Stratigraphic architecture of the fort cooper coal measures, Bowen Basin, Queensland, Australia. Australian Journal of Earth Sciences.

BAUER, J. A. & DIXON, O. 1981. Results of a seismic survey in the southern Denison Trough, Queensland, 1978-79. Journal of Australian Geology and Geophysics, 6, 213-222.

BLANCO, E. 2010. Coal lithotype response to changing depositional sequences in the Betts Creek Beds, Galilee Basin. Honours, University of Queensland.

DE CARITAT, P. & BRAUN, J. 1992. Cyclic development of sedimentary basins at convergent plate margins — 1. Structural and tectono-thermal evolution of some gondwana basins of eastern Australia. Journal of Geodynamics, 16, 241-282.

DRAPER, J. J. 2012. Bowen Basin. In: JELL, P. A. (ed.) Geology of Queensland. Queensland: Geological Survey of Queensland.

EVANS, P. R. & ROBERTS, J. 1980. Evolution of central eastern Australia during the late Palaeozoic and early Mesozoic. Journal of the Geological Society of Australia, 26, 325-340.

GALILEE ENERGY LIMITED 2001. Rodney Creek 5, Well Completion Report.

GRAY, A. R. G. & SWARBRICK, C. F. J. 1975. Nomenclature of Late Palaeozoic strata in the Northeastern Galilee Basin. Queensland Government Mining Journal, 76, 344-352.

GRIGORESCU, M. 2012. Mineralogy and petrography of the southern Galilee Basin, Queensland. Queensland Geological Record, 2012/13.

HAWKINS, P. J. 1978. Galilee Basin - Review of petroleum prospects. Queensland Government Mining Journal, 79, 96-112.

HAWKINS, P. J. & CARMICHAEL, D. C. 1987. Petrology and clay mineralogy of fine-grained rocks, Northern Galilee Basin. Queensland Government Mining Journal, 88, 426-435.

HAWKINS, P. J. & GREEN, P. M. 1993. Exploration results, hydrocarbon potential and future strategies for the Northern Galilee Basin. APEA Journal, 33, 280-296.

HILL, D. 1957. Explanatory notes on the Springsure 4-mile geological sheet. Bureau of Mineral Resources.

MOLLAN, R. G., DICKINS, J. M., EXON, N. F. & KIRKEGAARD, A. G. 1969. Geology of the Springsure 1:250000 sheet area, Queensland. Bureau of Mineral Resources, Geology and Geophysics, 123.

NORVICK, M. 1981. Permian and Late Carboniferous Palynostratigraphy of the Galilee Basin, Queensland. Bureau of Mineral Resources 219, 140-149.

PRICE, P. L. 1997. Permian to Jurassic palynostratigraphic nomenclature of the Bowen and Surat Basins. In: GREEN, P. M. (ed.) The Surat and Bowen Basins south-east Queensland, Queensland Minerals and Energy Review Series. Brisbane: Queensland Department of Mines and Energy.

SCOTT, S. G., BEESTON, J. W. & CARR, A. F. 1995. Galilee Basin. Special Publication of the Geological Society of Australia Coal Geology, 1, 341-352.

SCOTT, S. G. & HAWKINS, P. J. 1992. Coal geology of the northern Galilee Basin and its implications for coalbed methane investigations. Sympoisum on coalbed methane research and development in Australia. Townsville. Australia: James Cook University of North Queensland.

SWARBRICK, C. F. J. & WALLIN, C. I. 1976. QDM Aramac 1 and Hexam 1, Well Completion Report.

VAN HEESWIJCK, A. 2006. The structure, sedimentology, sequence stratigraphy and tectonics of the Northern Drummond and Galilee Basins, Central Queensland, Australia. Phd, James Cook University.

VAN HEESWIJCK, A. 2010. Late Paleozoic to Early Mesozoic deformation in the northeastern Galilee Basin, Australia. Australian Journal of Earth Sciences, 57, 431-451.

VEEVERS, J. J., JONES, J. G. & POWELL, C. M. 1982. Tectonic Framework of Austalias Sedimentary Basins. APEA Journal, 22, 283-300.

VINE, R. R. 1975. Galilee Basin. In: LESLIE, R. B., EVANS, H. J. & KNIGHT, C. L. (eds.) Economic Geology of Australia and Papua New Guinea. Victoria: The Australian Institue of Mining and Metallurgy.

VINE, R. R. & DOUTCH, H. F. 1972. Galilee(SF/55-10), Queensland, 1:250,000 geological series, explanatory notes. Bureau of Mineral Resources.

8.2. The Society of Organic Petrology conference (2014) abstract

Vertical trends in maceral composition in inertinite-rich coals: a case study from the Galilee Basin

L. J. Phillips[1], A. Roslin[1] and S. A. Ayaz[1]

[1] University of Queensland, School of Earth Sciences, Steele Building, St. Lucia Campus, Brisbane, 4072

The Permian Galilee Basin, located in central Queensland, is an intracratonic basin with studies performed by Hunt (1989) and Hunt and Smyth (1989) that discuss the origin of the high inertinite content of the coals. They attributed the abundant inertinite group macerals to the slow subsidence rates of the basin and the fluctuating water table causing a higher rate of sub-aerial and subaqueous oxidation (Hunt and Smyth, 1989). This study examines vertical and lateral trends in the maceral composition of the coal sequence from available open file data, and uses complementary analysis of wireline logs to develop a proxy for maceral composition. Three open file wells were used in this study to examine vertical trends in maceral composition and develop electrofacies, and preliminary results are presented here.

There are 5 main coal seams found in the Galilee Basin, located in the Bandana formation and Colinlea Sandstone and their stratigraphic equivalent, the Betts Creek Beds. Seams are generally referred as A through E, from top to bottom. Tuff banding of thicknesses 1cm-10cm is not uncommon, however one seam in particular, known as the C seam, sees a rise in tuff band frequency, with tuffaceous material occurring every 10cm-20cm. Despite being rich in inertinite (25.5 to 81.4% m.m.f., average of 59.6%), the C seam represents a vertical variation in vitrinite with, 31.4% m.m.f. at the base and increasing up to 48.6% m.m.f. at the top of the seam (average figures of the three wells). The numerous tuff bands found within the C seam could be beneficial to the preservation of vitrinite, providing either nutrients and stable ground for woody shrub growth, else pooling and/or sealing off the peat to prevent oxidation.

As well as the overall vertical increase in vitrinite through the C Seam it is seen that when splitting of the C seam occurs, the vitrinite content increases relative to the C seams that are coalesced elsewhere in the basin. The increase in accommodation leading to an influx in clastic sediments causing the seams to split (Wadsworth et al., 2002), reflects a relative increase in the subsidence

rate, which is preferable to the preservation of vitrinite as little oxidation can occur. This trend was corroborated by the electrofacies analysis.

REFERENCES

Hunt, J. W., 1989. Permian coals of eastern Australia: geological control of petrographic variation. International Journal of Coal Geology 12, 589-634.

Hunt, J. W., Smyth, M., 1989. Origin of inertinite-rich coals of Australian cratonic basins. International Journal of Coal Geology 11, 23-46.

Wadsworth, J., Boyd, R., Diessel, C., Leckie, D. and Zaitlin, B. A., 2002. Stratigraphic style of coal and non-marine strata in a tectonically influenced intermediate accommodation setting: the Mannville Group of the Western Canadian Sedimentary Basin, south-central Alberta. Bulletin of Canadian Petroleum Geology 50, 507-541

8.3. Australian Earth Sciences Convention (2016) abstract

Sedimentary trends in Late Permian coal measure strata, Galilee Basin

Phillips, Laura[1], Bianchi, Valeria[1], and Esterle, Joan[1]

[1]University of Queensland, St. Lucia, Australia

Three key wells, GSQ Tambo 1-1A, OCE Glue Pot Creek 1 and COI Montani 1, intersecting the Late Permian coal measures were chosen for sedimentary logging and facies analysis. These wells traverse the eastern margin of the Galilee Basin from south to north, respectively. Here the coal-bearing Bandanna Formation (BF) and underlying Colinlea Sandstone (CS) are separated by the Black Alley Shale (BAS)/Peawaddy Formations (PF). Regional trends in thickness and lithology of these formations were generated from 1000 coal exploration wells.

On the Springsure Shelf (southernmost area) the CS was only partly intersected by drilling and contains a coal seam capped by sequence that grades upward from wavy and flaser-bedded sandstone with horizontally bioturbated mud-drapes, to thick clean massive to low and high angle cross-bedded sandstone, interpreted as the drowning, rapid transgression and regression of lower and upper shorefaces deposits over the coastal or deltaic peats. These facies are occasionally interrupted by sandy matrix supported conglomerates hypothesised as storm events that rework fanglomerates sourced from the nearby Anakie Inlier.

Overlying the thick sandstone unit, ripple-laminated, horizontally burrowed mud-drapes and clean sandstone interbedded with minor conglomeratic units are observed again. These shoreface derived facies, representing a start of a transgression, are considered stratigraphically as PF, and are overlain by the dark carbonaceous siltstones of the BAS, which also contain tuff horizons that can be correlated northward into the basin.

Using the sequence of tuffs in the BAS as marker horizons, the marine shoreface deposits of the PF either pinch or interfinger northward into the increasingly coal-bearing CS. It is comprised of a series of fining-upward sequences capped by coal seams, with each cycle becoming thinner upwards, ascribed as avulsing fluvial channels. Northwards, two fining-upwards cycles are observed in the lower CS, however the cycles above have the addition of coarsening-up sequences and periods of silt dominated interburden, suggesting sedimentation in ponded areas. Northerly and

southerly, it is overlain by fine-grained siltstone representing the transgression of the BAS. The youngest coal in the CS is recognised regionally as the C seam by its tuffaceous nature, and in the centre of the basin it is overlain by an intensely bioturbated black siltstone that coarsens upward until capped by fine grained, flat to cross laminated clean sandstones that are capped by the BF Coal Measures. These coarsening-upward sequences pinch to the north, where the correlative is a grey siltstone with siderite. Based on regionally correlated siltstone intervals within the coarsening-upwards sequence it is interpreted as a southerly prograding deltaic sequence, capped by wave to tide dominated top set beds that are overlain by the terrestrial coal measures.

The ‘BF’ contains a second tuffaceous horizon persistent across the basin that is correlative southward with another tuffaceous horizon above the coarsening-upwards sequence of the BAS on the Springsure Shelf. This suggests that possibly the BF is misplaced stratigraphically, as they could be correlated with the younger tuffaceous rich Burngrove Member of the Fort Cooper Coal Measures belonging to the Bowen Basin.

8.4. Australian Exploration Geoscience Conference (2018) abstract

Detrital zircon analysis from the Galilee Basin, Queensland

Laura Phillips[1], Charlie Verdel[2], Charlotte Allen[3] and Joan Esterle[4]*

School of Earth and Environmental Sciences, University of Queensland, l.phillips3@uq.edu.au[1]*
School of Earth and Environmental Sciences, University of Queensland, c.verdel@uq.edu.au[2]
School of Earth, Environmental and Biological Sciences, Queensland University of Technology, cm.allen@qut.edu.au[3]
School of Earth and Environmental Sciences, University of Queensland, j.esterle@uq.edu.au[4]

Little is written about the effects of the Permian onset of the Hunter-Bowen Orogeny on sedimentation patterns in the Galilee Basin of Queensland. Through a comparison of age populations of detrital zircon grains in sandstone of the Galilee Basin, a potential shift in sediment provenance has been recognised. One key well (OEC Glue Pot Creek 1) was selected from the Galilee Basin for detrital zircon analysis. The well intersected both Cisuralian (early Permian) and Lopingian (late Permian) strata. Nine sandstone samples were collected (three from the Cisuralian and six from Lopingian) and zircon grains were extracted. U-Pb isotopic data was gathered using the Laser Ablation – Inductively Coupled Plasma Mass Spectrometer (LA-ICPMS) technique.

A total of 271 concordant ages were obtained from the nine samples. The Cisuralian samples have a varied age population range, with multiple peaks between 300 and 1200 Ma, suggesting numerous sources and orogenic recycling. In contrast, the Lopingian samples have a dominant peak of 250 to 300 Ma zircons, with a singular minor peak of 1500 Ma zircons, suggesting a transition in provenance between the Cisuralian and Lopingian. This transition corresponds with the onset of the Hunter-Bowen Orogeny and may mark a change in the tectonic setting of the Galilee Basin from an earlier back-arc (extensional) setting to a subsequent foreland basin position.

8.5. Dates and sample numbers from previous studies shown in Figure 12b

Age (Ma)	**Sample Number**	**Formation**	**Locality**	**Original study**	**Analysis type**
252.54 ± 0.04	GA2122750	Kaloola Member	Meeleebee 5 - Southern Bowen Basin	Metcalfe et al (2015)	CA-IDTIMS
252.58 ± 0.23		Boundary between the overlying Rangal Coal Measures and underlying Burngrove Formation	Peat 1 - Burunga Anticline, south eastern Bowen Basin	Ayaz et al (2016)	CA-IDTIMS
252.69 ± 0.16		Boundary between the overlying Rangal Coal Measures and underlying Burngrove Formation	Duckworth 11 - Northern Taroom Trough, central eastern Bowen Basin	Ayaz et al (2016)	CA-IDTIMS
252.85 ± 0.07	POI-1	Boundary between the overlying Rangal Coal Measures and underlying Burngrove Formation	Bowen Basin	Esterle et al (2017)	CA-IDTIMS
252.87 ± 0.07	NEW-1	Boundary between the overlying Rangal Coal Measures and underlying Burngrove Formation	Bowen Basin	Esterle et al (2017)	CA-IDTIMS
252.87 ± 0.07	POI-4	Boundary between the overlying Rangal Coal Measures and underlying Burngrove Formation	Bowen Basin	Esterle et al (2017)	CA-IDTIMS
252.91 ± 0.07	Daw-2	Boundary between the overlying Rangal Coal Measures and underlying Burngrove Formation	Bowen Basin	Esterle et al (2017)	CA-IDTIMS
252.92 ± 0.07	FOX-1	Boundary between the overlying Rangal Coal Measures and underlying Burngrove Formation	Bowen Basin	Esterle et al (2017)	CA-IDTIMS
253.07 ± 0.22		Boundary between the overlying Rangal Coal Measures and underlying Burngrove Formation	Crocker Gully 2 - Southern Taroom Trough, central eastern Bowen Basin	Ayaz et al (2016)	CA-IDTIMS
254.1 ± 0.05	GA2122742	Boundary between the overlying Kaloola Member and underlying Black Alley Shale	Meeleebee 5 - Southern Bowen Basin	Metcalfe et al (2015)	CA-IDTIMS
254.34 ± 0.08	GA2122738	Black Alley Shale	Meeleebee 5 - Southern Bowen Basin	Metcalfe et al (2015)	CA-IDTIMS
256.01 ± 0.07	GA2122736	Tinowon Formation	Meeleebee 5 - Southern Bowen Basin	Metcalfe et al (2015)	CA-IDTIMS
256.01 ± 0.07	2122736	Tinowon Formation	Meeleebee 5 - Southern Bowen Basin	Smith and Mantle (2013)	CA-IDTIMS
257.0 ± 1.5		Wallabella Tuff	Myall Creek 3 - Southern Bowen Basin	Collins (2009)	SHRIMP
258.09 ± 2.7	WB1	Playtpus Tuff	West Broadmeadow 1 - Northern Bowen Basin	Michaelsen et al (2001)	SHRIMP

8.6. Summary table of all tuff samples sent for CA-IDTIMS analysis

Well	Sample Name/#	from	to	thickness	Picked for CA-IDTIMS (1)
COE Montani 1	MON_15	895.36	895.44	0.08	
COE Montani 1	MON_28	852.17	852.32	0.15	
COE Montani 1	MON_31	851.47	851.60	0.13	x
COE Montani 1	MON_34	849.30	849.52	0.22	
COE Montani 1	MON_37	843.12	843.42	0.30	
COE Montani 1	MON_39	842.48	842.69	0.21	
COE Montani 1	MON_45	829.19	829.29	0.10	x
COE Montani 1	MON_48	821.25	821.81	0.56	x
COE Montani 1	MON_51	817.02	817.34	0.32	
COE Montani 1	MON_55	804.38	804.46	0.08	
COE Montani 1	MON_57	800.06	800.22	0.16	
COE Montani 1	MON_60	796.77	796.90	0.13	x

Well	Sample Name/#	from	to	thickness	Picked for CA-IDTIMS (1)
GSQ Tambo 1-1A	TAM_21	826.66	826.73	0.07	
GSQ Tambo 1-1A	TAM_22	826.38	826.63	0.25	
GSQ Tambo 1-1A	TAM_26	813.07	813.33	0.26	
GSQ Tambo 1-1A	TAM_29	810.25	810.46	0.21	x
GSQ Tambo 1-1A	TAM_40	732.47	732.57	0.10	

Well	Sample Name/#	from	to	thickness	Picked for CA-IDTIMS (1)
OEC Glue Pot Creek 1	GPC_37	824.60	824.80	0.20	x
OEC Glue Pot Creek 1	GPC_20	726.59	726.89	0.30	
OEC Glue Pot Creek 1	GPC_28	653.32	653.50	0.18	

Well	Sample Name/#	from	to	thickness	Picked for CA-IDTIMS (1)
GSQ Muttaburra 1	MUT_37	982.98	983.03	0.05	
GSQ Muttaburra 1	MUT_39	982.21	982.27	0.06	
GSQ Muttaburra 1	MUT_44	975.72	975.78	0.06	
GSQ Muttaburra 1	MUT_45	975.12	975.19	0.07	

(1) Samples not picked for CA-IDTIMS either contained no zircons or yielded a poor amount not sufficient for CA-IDTIMS analysis.

8.7. LA-ICPMS data (Boise State University)

Analysis	CL image (dark or light)	Notes	U ppm	Th ppm	Pb* ppm	Th/U	206Pb / 204Pb
MON_48 S 17 6/4/2016 1:29:45 PM (Run: 1)	Light		121.55	75.281	12.252	0.6194	261.5185185
MON_48 M 9 6/4/2016 1:05:40 PM (Run: 1)	Dark	high U signal variance	533.45	325.15	37.345	0.6095	774.0588851
MON_48 S 28 6/4/2016 1:59:01 PM (Run: 1)	Light	high U signal variance	61.761	26.223	3.7618	0.4246	85.30547337
MON_48 S 33 6/4/2016 2:18:05 PM (Run: 1)	Dark		320.74	155.22	19.38	0.4839	510.1564103
MON_48 M 8 6/4/2016 1:03:58 PM (Run: 1)	Light	high U signal variance	57.552	45.788	3.4019	0.7956	89.44495504
MON_48 M 10 6/4/2016 1:07:22 PM (Run: 1)	Dark		368.56	130.83	19.418	0.355	328.1269939
MON_48 L 1 6/4/2016 12:52:00 PM (Run: 1)	Light	high U signal variance	57.031	54.579	3.3946	0.957	140.6415712
MON_48 M 6 6/4/2016 1:00:34 PM (Run: 1)	Dark		138.18	151.57	8.3056	1.0969	125.1555427
MON_48 M 7 6/4/2016 1:02:16 PM (Run: 1)	Light		139.76	112.09	8.0015	0.802	57.69691781
MON_48 S 15 6/4/2016 1:26:21 PM (Run: 1)	Light	high U signal variance	174.71	173.62	10.51	0.9938	172.7808858
MON_48 S 13 6/4/2016 1:22:58 PM (Run: 1)	Light		40.561	51.762	2.5872	1.2762	35.75088757
MON_48 M 4 6/4/2016 12:57:10 PM (Run: 1)	Light		76.835	50.982	3.9222	0.6635	244.0955199
MON_48 M 2 6/4/2016 12:53:47 PM (Run: 1)	Dark		557.42	227.81	28.502	0.4087	1751.490385
MON_48 M 12 6/4/2016 1:21:12 PM (Run: 1)	Dark	high U signal variance	135.65	84.159	7.0307	0.6204	548.7361933
MON_48 M 11 6/4/2016 1:19:30 PM (Run: 1)	Light		99.316	56.937	4.9698	0.5733	280.745842
MON_48 S 32 6/4/2016 2:16:23 PM (Run: 1)	Light		256.8	208.86	13.565	0.8133	639.078042
MON_48 M 3 6/4/2016 12:55:29 PM (Run: 1)	Light		256.1	201.32	13.651	0.7861	
MON_48 S 30 6/4/2016 2:02:25 PM (Run: 1)	Light		114.82	80.328	5.6567	0.6996	82.10992908
MON_48 S 31 6/4/2016 2:14:41 PM (Run: 1)	Dark		133.69	157.05	7.6316	1.1747	185.6300518

	Corrected isotope ratios										
Analysis	208Pb* / 232Th	±2s (%)	206Pb* / 207Pb*	±2s (%)	207Pb* / 235U*	±2s (%)	206Pb* / 238U	±2s (%)	error corr.	207Pb* / 206Pb*	±2s (%)
MON_48 S 17 6/4/2016 1:29:45 PM (Run: 1)	0.02794308	7.08215936	17.59160408	6.22114	0.63394	7.62	0.08088	4.40	0.55	0.05685	6.22
MON_48 M 9 6/4/2016 1:05:40 PM (Run: 1)	0.019417944	3.349856323	18.71981988	2.833557	0.40253	4.10	0.05465	2.96	0.65	0.05342	2.83
MON_48 S 28 6/4/2016 1:59:01 PM (Run: 1)	0.016472862	12.64623652	19.45655044	8.085754	0.37559	10.19	0.05300	6.20	0.59	0.05140	8.09
MON_48 S 33 6/4/2016 2:18:05 PM (Run: 1)	0.022698965	15.61580401	15.36218741	9.311556	0.42208	9.82	0.04703	3.13	0.29	0.06509	9.31
MON_48 M 8 6/4/2016 1:03:58 PM (Run: 1)	0.015941861	15.26348276	18.90874206	12.10247	0.33263	13.17	0.04562	5.18	0.38	0.05289	12.10
MON_48 M 10 6/4/2016 1:07:22 PM (Run: 1)	0.016538948	7.730187124	19.67917809	3.822849	0.31610	5.50	0.04512	3.95	0.68	0.05082	3.82
MON_48 L 1 6/4/2016 12:52:00 PM (Run: 1)	0.016270374	7.173625166	21.43749547	11.4577	0.27946	12.49	0.04345	4.97	0.38	0.04665	11.46
MON_48 M 6 6/4/2016 1:00:34 PM (Run: 1)	0.014824979	6.963877003	18.765471	7.340909	0.31486	8.99	0.04285	5.19	0.56	0.05329	7.34
MON_48 M 7 6/4/2016 1:02:16 PM (Run: 1)	0.016616351	10.72222779	17.30511597	6.79398	0.34054	8.26	0.04274	4.70	0.55	0.05779	6.79
MON_48 S 15 6/4/2016 1:26:21 PM (Run: 1)	0.016362208	22.24323969	17.78038317	14.36252	0.33124	15.14	0.04272	4.80	0.31	0.05624	14.36
MON_48 S 13 6/4/2016 1:22:58 PM (Run: 1)	0.016226046	12.56302529	16.02740303	15.92422	0.36145	16.57	0.04202	4.60	0.27	0.06239	15.92
MON_48 M 4 6/4/2016 12:57:10 PM (Run: 1)	0.013245606	14.66064965	19.7331803	8.477297	0.29055	9.84	0.04158	5.00	0.49	0.05068	8.48
MON_48 M 2 6/4/2016 12:53:47 PM (Run: 1)	0.017647007	8.897947099	16.12259198	8.758462	0.35469	9.65	0.04148	4.06	0.40	0.06202	8.76
MON_48 M 12 6/4/2016 1:21:12 PM (Run: 1)	0.015551801	6.603562624	18.56846065	7.84148	0.30622	8.95	0.04124	4.32	0.46	0.05385	7.84
MON_48 M 11 6/4/2016 1:19:30 PM (Run: 1)	0.015100798	13.82161713	20.21644366	10.38599	0.27771	11.14	0.04072	4.04	0.34	0.04946	10.39
MON_48 S 32 6/4/2016 2:16:23 PM (Run: 1)	0.013911403	4.806939085	20.23352616	6.139254	0.27557	6.74	0.04044	2.78	0.36	0.04942	6.14
MON_48 M 3 6/4/2016 12:55:29 PM (Run: 1)	0.015109474	7.069207173	18.37381505	4.630403	0.30163	5.82	0.04020	3.53	0.56	0.05443	4.63
MON_48 S 30 6/4/2016 2:02:25 PM (Run: 1)	0.011935678	9.331064809	19.63110708	12.00481	0.28211	12.51	0.04017	3.50	0.26	0.05094	12.00
MON_48 S 31 6/4/2016 2:14:41 PM (Run: 1)	0.013301397	8.881809338	15.37158721	6.895248	0.35989	7.41	0.04012	2.70	0.32	0.06506	6.90

											Common Pb corrected Ages			
					Dates (Ma)						207-corrected		208-corrected	
	208Pb*	±2s	207Pb*	±2s	207Pb*	±2s	206Pb*	±2s	%		206Pb*	±2s	206Pb*	±2s
Analysis	232Th	(Ma)	206Pb*	(Ma)	235U	(Ma)	238U*	(Ma)	disc.		238U*	(Ma)	238U*	(Ma)
MON_48 S 17 6/4/2016 1:29:45 PM (Run: 1)	557	39	486	137	499	30	501	21	-3		37.71846	0.8668	0.001	0.475966
MON_48 M 9 6/4/2016 1:05:40 PM (Run: 1)	389	13	347	64	343	12	343	10	1		37.99506	0.8567	0.001	0.478868
MON_48 S 28 6/4/2016 1:59:01 PM (Run: 1)	330	41	259	186	324	28	333	20	-29		38.04138	0.855071	0.001	0.479342
MON_48 S 33 6/4/2016 2:18:05 PM (Run: 1)	454	70	777	196	358	30	296	9	62		38.09871	0.85308	0.001	0.479924
MON_48 M 8 6/4/2016 1:03:58 PM (Run: 1)	320	48	324	275	292	33	288	15	11		38.12617	0.852136	0.001	0.4802
MON_48 M 10 6/4/2016 1:07:22 PM (Run: 1)	332	25	232	88	279	13	284	11	-22		38.12075	0.852322	0.001	0.480146
MON_48 L 1 6/4/2016 12:52:00 PM (Run: 1)	326	23	31	275	250	28	274	13	-778		38.15107	0.851287	0.001	0.48045
MON_48 M 6 6/4/2016 1:00:34 PM (Run: 1)	297	21	341	166	278	22	**270**	**14**	21		38.1554	0.85114	0.001	0.480494
MON_48 M 7 6/4/2016 1:02:16 PM (Run: 1)	333	35	522	149	298	21	**270**	**12**	48		38.15661	0.851099	0.001	0.480506
MON_48 S 15 6/4/2016 1:26:21 PM (Run: 1)	328	72	462	318	291	38	**270**	**13**	42		38.1562	0.851113	0.001	0.480502
MON_48 S 13 6/4/2016 1:22:58 PM (Run: 1)	325	41	688	340	313	45	**265**	**12**	61		38.16818	0.850706	0.001	0.480622
MON_48 M 4 6/4/2016 12:57:10 PM (Run: 1)	266	39	226	196	259	22	**263**	**13**	-16		38.17208	0.850574	0.001	0.480661
MON_48 M 2 6/4/2016 12:53:47 PM (Run: 1)	354	31	675	187	308	26	**262**	**10**	61		38.15863	0.85103	0.001	0.480526
MON_48 M 12 6/4/2016 1:21:12 PM (Run: 1)	312	20	365	177	271	21	**261**	**11**	29		38.17438	0.850497	0.001	0.480684
MON_48 M 11 6/4/2016 1:19:30 PM (Run: 1)	303	42	170	243	249	25	**257**	**10**	-51		38.18144	0.850258	0.001	0.480754
MON_48 S 32 6/4/2016 2:16:23 PM (Run: 1)	279	13	168	143	247	15	**256**	**7**	-52		38.18	0.850307	0.001	0.48074
MON_48 M 3 6/4/2016 12:55:29 PM (Run: 1)	303	21	389	104	268	14	**254**	**9**	35		38.18313	0.850201	0.001	0.480771
MON_48 S 30 6/4/2016 2:02:25 PM (Run: 1)	240	22	238	277	252	28	**254**	**9**	-7		38.18737	0.850059	0.001	0.480813
MON_48 S 31 6/4/2016 2:14:41 PM (Run: 1)	267	24	776	145	312	20	**254**	**7**	67		38.18746	0.850055	0.001	0.480814

	Concentrations (ppm)										
	1.0	2.00	0	2.00	2.00	2.00	2.00	2.00	2.00	2.00	2.00
Analysis	P	Ti	Y	Nb	La	Ce	Pr	Nd	Sm	Eu	Gd
MON_48 S 17 6/4/2016 1:29:45 PM (Run: 1)	158.4	2.94	493	0.54		4.89		0.35	0.95	0.40	8.11
MON_48 M 9 6/4/2016 1:05:40 PM (Run: 1)	254.2	6.19	1467	1.87		10.53	0.17	3.55	5.91	1.07	29.03
MON_48 S 28 6/4/2016 1:59:01 PM (Run: 1)	190.4	6.32	534	0.53	0.02	2.57		0.24	1.20	0.28	8.74
MON_48 S 33 6/4/2016 2:18:05 PM (Run: 1)	1309.3	17.67	3473	1.47	0.23	2.25	0.37	5.48	14.10	0.44	74.04
MON_48 M 8 6/4/2016 1:03:58 PM (Run: 1)	449.4	27.48	1204	0.57		1.18	0.11	3.07	6.05	0.36	33.16
MON_48 M 10 6/4/2016 1:07:22 PM (Run: 1)	875.6	5.74	2407	2.20		2.21	0.09	2.39	9.71	0.56	71.56
MON_48 L 1 6/4/2016 12:52:00 PM (Run: 1)	184.2	11.34	954	0.46		6.46	0.05	1.28	4.30	0.78	21.49
MON_48 M 6 6/4/2016 1:00:34 PM (Run: 1)	231.3	6.78	1271	0.66		12.69	0.14	3.48	5.75	1.69	33.85
MON_48 M 7 6/4/2016 1:02:16 PM (Run: 1)	747.5	3.62	2385	2.95		9.77	0.04	0.48	3.22	0.88	29.96
MON_48 S 15 6/4/2016 1:26:21 PM (Run: 1)	342.7	9.43	2307	1.16		8.81	0.18	2.95	9.13	1.91	47.82
MON_48 S 13 6/4/2016 1:22:58 PM (Run: 1)	275.3	23.26	1680	0.29	0.09	6.23	0.25	4.07	10.38	5.31	54.68
MON_48 M 4 6/4/2016 12:57:10 PM (Run: 1)	288.2	7.16	816	1.24	0.27	7.38	0.09	1.09	2.56	0.37	12.79
MON_48 M 2 6/4/2016 12:53:47 PM (Run: 1)	313.4	3.65	1308	1.08	0.02	6.77	0.10	2.60	5.29	1.18	29.67
MON_48 M 12 6/4/2016 1:21:12 PM (Run: 1)	300.4	4.57	786	0.80		6.76	0.02	0.31	1.55	0.54	10.58
MON_48 M 11 6/4/2016 1:19:30 PM (Run: 1)	217.8	8.08	739	0.79		5.28		1.22	1.92	0.35	14.61
MON_48 S 32 6/4/2016 2:16:23 PM (Run: 1)	270.6	4.77	1466	2.46	0.23	11.60	0.11	1.69	4.50	0.94	29.55
MON_48 M 3 6/4/2016 12:55:29 PM (Run: 1)	337.6	12.32	2283	5.19		9.70		1.74	5.72	2.37	43.16
MON_48 S 30 6/4/2016 2:02:25 PM (Run: 1)	234.8	8.24	807	1.03	0.05	5.95	0.01	0.83	1.74	0.55	13.52

	Concentrations (ppm)											
	2.00	1.0	2.00	1.0	1.0	1.0	1.0	0	2.00	1.0	0	Ti-in-zircon
Analysis	Tb	Dy	Ho	Er	Tm	Yb	Lu	Hf	Ta	Th	U	T(°C)
MON_48 S 17 6/4/2016 1:29:45 PM (Run: 1)	2.80	37.7	15.47	80.968836	23.2	263.4	46.8	9363	0.17	75.3	122	660
MON_48 M 9 6/4/2016 1:05:40 PM (Run: 1)	11.17	137.6	51.26	228.68545	58.6	625.5	91.1	9557	1.30	325.2	533	722
MON_48 S 28 6/4/2016 1:59:01 PM (Run: 1)	3.64	46.8	18.49	89.342689	22.9	229.7	34.9	9959	0.46	26.2	62	724
MON_48 S 33 6/4/2016 2:18:05 PM (Run: 1)	28.91	358.2	134.62	558.16188	128.5	1229.2	159.2	11162	0.95	155.2	321	826
MON_48 M 8 6/4/2016 1:03:58 PM (Run: 1)	10.68	131.3	43.50	187.71005	42.4	416.4	53.8	9937	0.20	45.8	58	877
MON_48 M 10 6/4/2016 1:07:22 PM (Run: 1)	26.02	278.0	84.50	293.94765	59.9	518.3	63.6	11872	1.39	130.8	369	716
MON_48 L 1 6/4/2016 12:52:00 PM (Run: 1)	7.84	96.8	34.84	148.46338	35.7	375.3	43.8	8713	0.27	54.6	57	780
MON_48 M 6 6/4/2016 1:00:34 PM (Run: 1)	10.73	124.9	45.16	197.80956	48.6	519.3	71.0	9226	0.64	151.6	138	731
MON_48 M 7 6/4/2016 1:02:16 PM (Run: 1)	13.87	207.2	87.71	396.33298	105.8	1097.8	163.6	11195	1.26	112.1	140	676
MON_48 S 15 6/4/2016 1:26:21 PM (Run: 1)	17.44	220.6	86.05	368.6768	85.6	886.7	117.3	8990	0.59	173.6	175	762
MON_48 S 13 6/4/2016 1:22:58 PM (Run: 1)	16.90	188.5	64.24	263.1309	60.5	575.6	78.0	6589	0.08	51.8	41	857
MON_48 M 4 6/4/2016 12:57:10 PM (Run: 1)	4.94	74.4	29.63	138.07381	33.4	344.1	48.9	9497	0.69	51.0	77	736
MON_48 M 2 6/4/2016 12:53:47 PM (Run: 1)	9.51	118.6	46.62	209.42912	55.2	595.7	85.8	8840	0.63	227.8	557	677
MON_48 M 12 6/4/2016 1:21:12 PM (Run: 1)	4.59	61.3	26.29	139.28142	39.8	465.0	75.2	9316	0.68	84.2	136	696
MON_48 M 11 6/4/2016 1:19:30 PM (Run: 1)	5.40	72.1	27.68	120.27534	31.3	319.6	47.2	9340	0.39	56.9	99	747
MON_48 S 32 6/4/2016 2:16:23 PM (Run: 1)	10.39	135.6	51.01	242.79006	61.4	635.1	87.9	10233	0.98	208.9	257	700
MON_48 M 3 6/4/2016 12:55:29 PM (Run: 1)	16.24	222.5	87.61	378.9944	92.4	915.7	124.5	7433	1.47	201.3	256	788
MON_48 S 30 6/4/2016 2:02:25 PM (Run: 1)	5.41	73.7	29.34	137.95738	33.2	354.4	50.6	9308	0.56	80.3	115	749

8.8. LA-ICPMS data (QUT)

Sample GPC_A

	DateTime	Combined Sample	Individual sample	Duration(s)	207_235	207_235_Prop2SE*	206_238	206_238_Prop2SE	207_206	207_206_Prop2SE	208_232	208_232_Prop2SE	Age207_235	Age207_235_Prop2SE	Age206_238	Age206_238_Prop2SE	error corel
smpl1_0	08/12/2016 (5) 11:13:58.91	GPC_A	2	20.912	0.565	0.052	0.0694	0.003	0.0589	0.0043	0.02068	0.0023	453	33	432.3	18	0.496233312
smpl1_1	08/12/2016 (5) 11:15:01.86	GPC_A	2	24.077	0.556	0.05	0.0699	0.0031	0.0575	0.0039	0.0203	0.0022	447	32	435.4	18	0.500088295
smpl1_2	08/12/2016 (5) 11:18:10.34	GPC_A	2	20.913	0.335	0.04	0.0482	0.0022	0.0503	0.0054	0.01405	0.0016	290	31	303.4	13	0.372057582
smpl1_3	08/12/2016 (5) 11:20:22.92	GPC_A	2	21.265	3.727	0.32	0.2737	0.012	0.0982	0.0062	0.0601	0.0068	1574	70	1559	61	0.660548796
smpl1_4	08/12/2016 (5) 11:22:35.85	GPC_A	2	16.693	0.313	0.077	0.0463	0.0023	0.049	0.012	0.01352	0.0017	270	57	291.9	14	0.221541307
smpl1_5	08/12/2016 (5) 11:23:59.54	GPC_A	2	22.32	2.26	0.27	0.2003	0.0096	0.0821	0.0091	0.0564	0.0062	1186	80	1176	52	0.54823385
smpl1_6	08/12/2016 (5) 11:25:57.35	GPC_A	2	21.968	0.374	0.043	0.0511	0.0023	0.0526	0.005	0.01561	0.0018	319	31	320.9	14	0.409559563
smpl1_7	08/12/2016 (5) 11:27:31.59	GPC_A	2	21.968	0.401	0.068	0.0489	0.0024	0.0597	0.0098	0.01527	0.0018	328	49	307.7	15	0.310219448
smpl1_8	08/12/2016 (5) 11:29:22.36	GPC_A	2	21.968	0.404	0.049	0.0501	0.0023	0.058	0.006	0.01482	0.0017	339	35	315	14	0.395396852
smpl1_9	08/12/2016 (5) 11:30:34.46	GPC_A	2	23.022	0.725	0.07	0.0823	0.0036	0.0632	0.0048	0.025	0.0031	550	41	510	21	0.483508881
smpl1_10	08/12/2016 (5) 11:31:55.69	GPC_A	2	21.968	0.645	0.063	0.0823	0.0036	0.0566	0.0046	0.0237	0.0027	502	39	509.5	21	0.468662709
smpl1_11	08/12/2016 (5) 11:42:20.24	GPC_A	2	21.616	3.98	0.44	0.2194	0.01	0.132	0.012	0.0521	0.0061	1602	95	1278	53	0.573095353
smpl1_12	08/12/2016 (5) 11:43:37.60	GPC_A	2	23.021	0.459	0.041	0.05961	0.0025	0.0555	0.0038	0.01718	0.0019	383	29	373.2	15	0.46886162
smpl1_13	08/12/2016 (5) 11:45:06.22	GPC_A	2	17.998	0.476	0.063	0.04843	0.0021	0.0708	0.0083	0.016	0.0019	388	43	304.8	13	0.359169937
smpl1_14	08/12/2016 (5) 11:46:39.06	GPC_A	2	19.154	0.31	0.13	0.0495	0.0025	0.043	0.019	0.0131	0.0019	235	100	311.6	15	0.112408816
smpl1_15	08/12/2016 (5) 11:47:46.22	GPC_A	2	21.967	0.423	0.06	0.0584	0.0026	0.0523	0.0067	0.01715	0.0019	349	43	366.1	16	0.334304697
smpl1_16	08/12/2016 (5) 11:49:03.94	GPC_A	2	23.024	0.407	0.045	0.0499	0.0022	0.059	0.0054	0.01506	0.0016	352	32	313.9	13	0.41456728
smpl1_17	08/12/2016 (5) 11:50:35.47	GPC_A	2	16.616	0.512	0.095	0.062	0.0031	0.0577	0.01	0.017	0.0022	403	62	388	19	0.303305025
smpl1_18	08/12/2016 (5) 11:51:42.54	GPC_A	2	23.022	0.497	0.084	0.0615	0.0029	0.0585	0.0094	0.0181	0.0022	408	59	384.7	17	0.292246046
smpl1_19	08/12/2016 (5) 11:53:07.64	GPC_A	2	20.21	1.335	0.12	0.1386	0.0072	0.07	0.0044	0.0255	0.0033	858	52	836	41	0.629051096

smpl1_20	08/12/2016 (5) 11:54:48.92	GPC_A	2	21.968	1.805	0.16	0.1759	0.0075	0.0742	0.0046	0.0495	0.0053	1048	60	1044	41	0.565661384
smpl1_21	08/12/2016 (5) 12:00:58.51	GPC_A	2	23.726	0.461	0.046	0.0627	0.0027	0.054	0.0045	0.01842	0.002	385	34	391.7	17	0.441062549
smpl1_22	08/12/2016 (5) 12:02:44.01	GPC_A	2	16.673	0.352	0.053	0.049	0.0023	0.0521	0.007	0.0144	0.0019	300	39	308.6	14	0.32948438
smpl1_23	08/12/2016 (5) 12:04:11.22	GPC_A	2	18.803	0.546	0.079	0.0699	0.0032	0.0576	0.0083	0.0194	0.0023	430	52	435.4	19	0.339429653
smpl1_24	08/12/2016 (5) 12:05:30.69	GPC_A	2	20.209	1.305	0.14	0.1277	0.0086	0.074	0.0047	0.0339	0.0041	839	59	773	49	0.669546695
smpl1_25	08/12/2016 (5) 12:06:50.87	GPC_A	2	23.023	0.502	0.061	0.0693	0.0031	0.0527	0.0055	0.01937	0.0022	406	42	432.1	18	0.373536445
smpl1_26	08/12/2016 (5) 12:08:02.96	GPC_A	2	23.023	2.277	0.2	0.2047	0.0086	0.0816	0.0057	0.0573	0.0061	1205	68	1200	46	0.561907903
smpl1_27	08/12/2016 (5) 12:09:15.76	GPC_A	2	20.912	0.423	0.073	0.0508	0.0024	0.0606	0.0098	0.01471	0.0017	343	54	319.1	15	0.286101825
smpl1_28	08/12/2016 (5) 12:10:28.90	GPC_A	2	23.023	1.344	0.14	0.1422	0.0062	0.0693	0.0065	0.0423	0.0046	852	62	857	35	0.489414777
smpl1_29	08/12/2016 (5) 12:11:40.64	GPC_A	2	23.375	2.4	0.23	0.2065	0.0089	0.0839	0.0063	0.0558	0.006	1232	70	1210	48	0.57246139
smpl1_30	08/12/2016 (5) 12:13:12.42	GPC_A	2	23.023	0.705	0.066	0.0895	0.0038	0.0573	0.0042	0.0261	0.0028	539	39	552.5	22	0.482133346
smpl1_31	08/12/2016 (5) 12:19:26.94	GPC_A	2	23.022	4.418	0.38	0.2749	0.012	0.1169	0.0071	0.0677	0.0073	1714	70	1565	58	0.672010365
smpl1_32	08/12/2016 (5) 12:20:45.14	GPC_A	2	23.606	0.3	1.2	0.096	0.013	0.04	0.14	-0.093	0.092	1160	340	583	78	0.415247765
smpl1_33	08/12/2016 (5) 12:22:49.85	GPC_A	2	21.264	0.357	0.037	0.04968	0.0021	0.0525	0.0045	0.01448	0.0016	308	28	312.5	13	0.416103564
smpl1_34	08/12/2016 (5) 12:24:08.62	GPC_A	2	23.023	0.544	0.052	0.0719	0.0031	0.0558	0.0041	0.02141	0.0023	442	32	447.8	19	0.505624933
smpl1_35	08/12/2016 (5) 12:25:27.74	GPC_A	2	23.022	6.67	0.58	0.3884	0.017	0.1255	0.008	0.1012	0.011	2065	78	2114	80	0.707766255
smpl1_36	08/12/2016 (5) 12:26:35.61	GPC_A	2	23.023	1.111	0.096	0.1231	0.0053	0.0659	0.0041	0.0275	0.0041	758	46	748	30	0.551360942
smpl1_37	08/12/2016 (5) 12:27:49.81	GPC_A	2	23.023	0.731	0.11	0.04781	0.0021	0.11	0.014	0.0195	0.0028	538	57	301	13	0.377487182
smpl1_38	08/12/2016 (5) 12:29:14.91	GPC_A	2	23.022	0.71	0.1	0.0934	0.0042	0.0556	0.0073	0.0257	0.0034	525	60	575	25	0.355572828
smpl1_39	08/12/2016 (5) 12:30:54.08	GPC_A	2	21.265	0.481	0.092	0.0601	0.0029	0.059	0.011	0.01759	0.0021	386	66	375.9	17	0.255703408
smpl1_40	08/12/2016 (5) 12:32:11.45	GPC_A	2	23.375	1.16	0.17	0.1275	0.0062	0.0664	0.0086	0.0381	0.0044	772	77	773	36	0.423079633
smpl1_41	08/12/2016 (5) 12:42:34.59	GPC_A	2	23.022	0.344	0.032	0.04863	0.0021	0.0517	0.0037	0.01421	0.0015	301	25	306.1	13	0.455269926
smpl1_42	08/12/2016 (5) 12:43:59.69	GPC_A	2	23.726	0.427	0.064	0.0583	0.0026	0.0536	0.0073	0.01686	0.002	349	47	365.2	16	0.309365168
smpl1_43	08/12/2016 (5) 12:45:08.96	GPC_A	2	22.671	12.56	1.1	0.465	0.02	0.1973	0.012	0.0942	0.01	2645	81	2461	88	0.759526724
smpl1_44	08/12/2016 (5) 12:46:17.19	GPC_A	2	22.671	0.351	0.044	0.05046	0.0022	0.0501	0.0055	0.01471	0.0016	300	33	317.3	13	0.349036443
smpl1_45	08/12/2016 (5) 12:47:20.84	GPC_A	2	22.671	0.496	0.062	0.0699	0.0031	0.0522	0.0059	0.02001	0.0023	401	43	435.8	19	0.376636657

smpl1_46	08/12/2016 (5) 12:48:42.42	GPC_A	2	22.671	1.559	0.14	0.1611	0.0069	0.0706	0.0047	0.04472	0.0048	952	55	963	38	0.564012472
smpl1_47	08/12/2016 (5) 12:49:58.03	GPC_A	2	23.375	0.696	0.067	0.0877	0.0038	0.0581	0.0044	0.02491	0.0028	533	40	542.1	22	0.475671447
smpl1_48	08/12/2016 (5) 12:51:44.23	GPC_A	2	23.022	0.522	0.061	0.0675	0.0031	0.0565	0.0055	0.0194	0.0023	420	40	420.8	19	0.428390929
smpl1_49	08/12/2016 (5) 12:52:45.77	GPC_A	2	23.023	13.23	1.1	0.5248	0.022	0.1841	0.012	0.133	0.014	2693	82	2719	94	0.75042964
smpl1_50	08/12/2016 (5) 12:54:05.95	GPC_A	2	23.375	0.455	0.06	0.0618	0.0028	0.0541	0.0065	0.01779	0.002	379	39	386.2	17	0.393297416
smpl1_51	08/12/2016 (5) 13:01:11.45	GPC_A	2	20.562	0.397	0.04	0.05438	0.0024	0.0533	0.0045	0.01549	0.0017	337	29	341.3	14	0.430291106
smpl1_52	08/12/2016 (5) 13:05:19.37	GPC_A	3	23.023	0.384	0.042	0.04991	0.0022	0.0559	0.0051	0.0144	0.0016	327	31	314	14	0.425591081
smpl1_53	08/12/2016 (5) 13:07:50.24	GPC_A	3	23.023	0.326	0.039	0.04791	0.0021	0.0496	0.0051	0.01388	0.0015	283	30	301.7	13	0.376555492
smpl1_54	08/12/2016 (5) 13:10:03.87	GPC_A	3	7.9417	0.621	0.092	0.0805	0.0038	0.0585	0.0088	0.024	0.0036	502	67	499	23	0.326429782
smpl1_55	08/12/2016 (5) 13:11:34.24	GPC_A	3	21.616	0.361	0.05	0.05	0.0023	0.0528	0.0066	0.01471	0.0018	306	37	314.2	14	0.345773432
smpl1_56	08/12/2016 (5) 13:12:38.60	GPC_A	3	23.023	0.644	0.063	0.0822	0.0035	0.0571	0.0044	0.0239	0.0026	501	39	509.4	21	0.46800544
smpl1_57	08/12/2016 (5) 13:13:53.85	GPC_A	3	22.671	0.36	0.039	0.04657	0.0021	0.0553	0.0051	0.01278	0.0014	309	29	293.4	13	0.426923748
smpl1_58	08/12/2016 (5) 13:15:04.18	GPC_A	3	23.021	0.351	0.049	0.04736	0.0021	0.0541	0.0068	0.01355	0.0017	299	36	298.2	13	0.340450162
smpl1_59	08/12/2016 (5) 13:16:08.19	GPC_A	3	20.912	0.335	0.041	0.04805	0.0022	0.0498	0.0053	0.0137	0.0017	289	31	302.5	13	0.371902633
smpl1_60	08/12/2016 (5) 13:17:41.38	GPC_A	3	18.451	0.61	0.058	0.0785	0.0035	0.0562	0.0043	0.0181	0.0029	481	37	487.2	21	0.488832356
smpl1_61	08/12/2016 (5) 13:24:00.46	GPC_A	3	24.078	0.81	0.072	0.102	0.0044	0.0582	0.0039	0.02949	0.0032	603	42	626.1	26	0.512098744
smpl1_62	08/12/2016 (5) 13:25:16.42	GPC_A	3	20.21	0.372	0.036	0.04415	0.0019	0.0611	0.0048	0.01362	0.0015	320	27	278.5	12	0.454801142
smpl1_63	08/12/2016 (5) 13:26:33.08	GPC_A	3	22.319	0.323	0.037	0.04571	0.002	0.0511	0.0049	0.01339	0.0015	281	28	288.1	12	0.385670898
smpl1_64	08/12/2016 (5) 13:28:11.90	GPC_A	3	11.137	0.398	0.052	0.0536	0.0029	0.0534	0.0058	0.0157	0.0021	337	38	336	18	0.429126077
smpl1_65	08/12/2016 (5) 13:29:08.52	GPC_A	3	23.727	2.44	0.27	0.2066	0.0092	0.0858	0.008	0.0581	0.0064	1233	79	1210	49	0.534273437
smpl1_66	08/12/2016 (5) 13:30:09.00	GPC_A	3	22.319	0.519	0.05	0.0663	0.0029	0.0567	0.0044	0.01936	0.0021	422	34	413.5	18	0.475349488
smpl1_67	08/12/2016 (5) 13:31:08.43	GPC_A	3	21.969	0.346	0.036	0.04591	0.0019	0.0547	0.0046	0.01316	0.0014	300	27	289.4	12	0.418447761
smpl1_68	08/12/2016 (5) 13:32:30.37	GPC_A	3	23.727	0.399	0.045	0.0524	0.0024	0.0563	0.0056	0.0148	0.0017	341	34	329	14	0.392529574
smpl1_69	08/12/2016 (5) 13:33:40.70	GPC_A	3	23.726	0.37	0.036	0.0488	0.0021	0.055	0.0044	0.01479	0.0016	318	27	307.2	13	0.44607377
smpl1_70	08/12/2016 (5) 13:34:45.76	GPC_A	3	20.914	0.325	0.066	0.0465	0.0022	0.0517	0.01	0.01434	0.0017	270	51	292.9	13	0.228742922
smpl1_71	08/12/2016 (5) 13:44:16.15	GPC_A	6	10.604	0.32	0.14	0.049	0.0033	0.044	0.018	0.0169	0.0032	240	110	308	20	0.140275677

smpl1_72	08/12/2016 (5) 13:45:06.09	GPC_A	6	23.726	0.335	0.037	0.04649	0.002	0.0522	0.0051	0.01356	0.0015	294	27	292.9	12	0.407410963
smpl1_73	08/12/2016 (5) 13:46:42.44	GPC_A	6	20.561	0.349	0.031	0.04711	0.0021	0.0534	0.0036	0.01326	0.0014	303	24	296.7	13	0.48404577
smpl1_74	08/12/2016 (5) 13:48:07.54	GPC_A	6	21.265	0.338	0.056	0.0463	0.0022	0.0531	0.0085	0.01341	0.0015	285	43	291.5	13	0.283460482
smpl1_75	08/12/2016 (5) 13:50:36.29	GPC_A	6	20.562	0.348	0.043	0.0482	0.0022	0.0525	0.006	0.01433	0.0016	299	32	303.4	13	0.371677521
smpl1_76	08/12/2016 (5) 13:51:37.13	GPC_A	6	23.023	0.335	0.035	0.04732	0.002	0.0509	0.0043	0.01329	0.0014	291	26	298	12	0.410893009
smpl1_77	08/12/2016 (5) 13:52:44.65	GPC_A	6	19.154	0.353	0.055	0.04783	0.0021	0.0532	0.0078	0.01383	0.0016	299	41	301.2	13	0.300235901
smpl1_78	08/12/2016 (5) 13:54:02.20	GPC_A	6	12.634	0.334	0.039	0.0484	0.0022	0.0483	0.0045	0.01384	0.0015	291	29	305	14	0.418354758
smpl1_79	08/12/2016 (5) 13:54:50.89	GPC_A	6	24.077	2.069	0.19	0.1995	0.0088	0.075	0.0054	0.0575	0.0062	1132	63	1172	47	0.584609201
smpl1_80	08/12/2016 (5) 13:55:48.92	GPC_A	6	24.078	17.46	1.5	0.5927	0.026	0.2127	0.013	0.1519	0.017	2957	83	2999	100	0.765030405
smpl1_81	08/12/2016 (5) 14:03:10.60	GPC_A	6	16.582	0.339	0.04	0.0489	0.0023	0.0499	0.0049	0.01448	0.0017	294	30	307.8	14	0.407129405
smpl1_82	08/12/2016 (5) 14:04:12.49	GPC_A	6	23.727	0.499	0.057	0.0485	0.0022	0.0744	0.0073	0.01549	0.0017	410	36	305.5	14	0.462687213
smpl1_83	08/12/2016 (5) 14:05:36.54	GPC_A	6	12.443	0.395	0.043	0.0516	0.0024	0.0551	0.0051	0.01512	0.0017	336	31	324.3	15	0.448163022
smpl1_84	08/12/2016 (5) 14:06:36.67	GPC_A	6	21.969	0.363	0.035	0.0498	0.0022	0.0524	0.004	0.01492	0.0016	313	26	313.3	13	0.446870914
smpl1_85	08/12/2016 (5) 14:07:36.46	GPC_A	6	23.726	0.342	0.039	0.04899	0.0022	0.0505	0.005	0.01427	0.0016	295	29	308.3	14	0.419353062
smpl1_86	08/12/2016 (5) 14:08:49.60	GPC_A	6	21.616	0.437	0.052	0.0643	0.0029	0.0484	0.0049	0.01803	0.002	363	35	401.5	18	0.421622178
smpl1_87	08/12/2016 (5) 14:10:05.91	GPC_A	6	18.1	0.367	0.041	0.049	0.0022	0.054	0.0051	0.01408	0.0015	315	31	308.3	14	0.418975034
smpl1_88	08/12/2016 (5) 14:11:01.82	GPC_A	6	22.672	1.2	0.2	0.1338	0.0072	0.0648	0.0099	0.0433	0.0052	766	92	808	41	0.389179095
smpl1_89	08/12/2016 (5) 14:12:23.06	GPC_A	6	19.507	0.343	0.034	0.04691	0.0021	0.0525	0.0041	0.01409	0.0015	298	26	295.5	13	0.45023274
smpl1_90	08/12/2016 (5) 14:13:25.65	GPC_A	6	23.024	4.68	0.41	0.3064	0.013	0.1092	0.0068	0.082	0.0088	1760	71	1722	65	0.683239525
smpl1_91	08/12/2016 (5) 14:22:46.39	GPC_A	6	4.6121	0.355	0.1	0.0639	0.0041	0.04	0.011	0.0196	0.0026	301	78	399	25	0.235018067
smpl1_92	08/12/2016 (5) 14:23:48.09	GPC_A	6	23.728	0.379	0.05	0.0524	0.0024	0.0516	0.0057	0.01561	0.0018	325	34	329.4	15	0.399112254
smpl1_93	08/12/2016 (5) 14:25:17.76	GPC_A	6	23.374	0.464	0.053	0.0598	0.0028	0.0561	0.0056	0.01936	0.0021	382	37	374.1	17	0.424739669
smpl1_94	08/12/2016 (5) 14:26:34.07	GPC_A	6	19.506	3.4	0.33	0.2492	0.011	0.0976	0.0068	0.0735	0.0082	1495	74	1434	59	0.639221591
smpl1_95	08/12/2016 (5) 14:27:36.67	GPC_A	6	22.671	0.345	0.045	0.048	0.0022	0.052	0.0062	0.01538	0.0017	300	36	302.1	14	0.360254757
smpl1_96	08/12/2016 (5) 14:28:45.24	GPC_A	6	21.617	0.344	0.04	0.04817	0.0021	0.0516	0.0053	0.01499	0.0017	297	30	303.2	13	0.390729162
smpl1_97	08/12/2016 (5)	GPC_A	6	23.727	3.21	0.29	0.2457	0.012	0.0937	0.0059	0.0598	0.0089	1453	72	1415	61	0.656354519

	14:29:52.41															
smpl1_98	08/12/2016 (5) 14:31:25.60	GPC_A	6	23.374	0.348	0.04	0.0494	0.0023	0.0499	0.0047	0.01509	0.0017	300	30	310.7	14	0.410816073
smpl1_99	08/12/2016 (5) 14:32:36.63	GPC_A	6	23.022	1.22	0.15	0.1287	0.0088	0.0669	0.0051	0.0451	0.0053	791	65	778	50	0.616052029
smpl1_100	08/12/2016 (5) 14:33:36.06	GPC_A	6	23.023	0.326	0.045	0.0475	0.0022	0.0498	0.0065	0.01481	0.0017	280	35	299.3	14	0.350471795

	Combined Sample	Individual sample	Age208_232	Age208_232_Prop2SE	Age207_206	Age207_206_Prop2SE	Th(ppm)	U(ppm)	calc208/206	PERCENT 206 THAT IS COMMON	overall best concordant age	2 s.e. uncert	age type**
smpl1_0	GPC_A	2	414	45	524	160	351	723	0.14840511	-0.349146521	432	18	unc'd 6/38
smpl1_1	GPC_A	2	406	44	496	150	214	465	0.13710985	-0.510373464	435	18	unc'd 6/38
smpl1_2	GPC_A	2	282	32	140	210	132.9	256	0.155239871	-0.615825193	303	13	unc'd 6/38
smpl1_3	GPC_A	2	1179	130	1579	120	70.2	409	0.038663614	-0.595276955	1579	120	7/6
smpl1_4	GPC_A	2	271	34			314	136	0.691632531	-3.849842505			
smpl1_5	GPC_A	2	1109	120	1130	210	86.6	36.3	0.689125616	-3.007149176			
smpl1_6	GPC_A	2	313	35	230	190	160.3	319	0.157475797	-0.214437235	321	14	unc'd 6/38
smpl1_7	GPC_A	2	306	36	310	320	113.4	100.4	0.361824934	-0.099928559	308	15	unc'd 6/38
smpl1_8	GPC_A	2	297	33	410	210	194	215.4	0.273309974	-0.910167003	315	14	unc'd 6/38
smpl1_9	GPC_A	2	499	60	660	160	164	424	0.120533325	-0.131813478	510	21	unc'd 6/38
smpl1_10	GPC_A	2	474	54	420	170	86.6	277.9	0.092059122	-0.355491298	510	21	unc'd 6/38
smpl1_11	GPC_A	2	1026	120	2030	190	75	46.4	0.393761595	-5.88261917			
smpl1_12	GPC_A	2	344.3	37	419	160	309.1	874	0.104563613	-0.445700521	373	15	unc'd 6/38
smpl1_13	GPC_A	2	320	39	790	250	178.6	273.1	0.221643112	0.588003093			
smpl1_14	GPC_A	2	263	38			74	67.6	0.297194038	-3.151661966			
smpl1_15	GPC_A	2	344	37	170	250	193.7	156.7	0.372392455	-1.420208031	366	16	unc'd 6/38
smpl1_16	GPC_A	2	302	33	540	180	424	388	0.338335469	-0.76028937			
smpl1_17	GPC_A	2	340	43	350	340	76.2	89.5	0.239484903	-1.82149187	388	19	unc'd 6/38
smpl1_18	GPC_A	2	362	43	400	310	85.5	93.1	0.27727382	-0.945031705	385	17	unc'd 6/38
smpl1_19	GPC_A	2	509	65	916	130	235	980	0.045259287	-1.438144086	836	41	unc'd 6/38
smpl1_20	GPC_A	2	976	100	1039	120	243.2	479	0.146573814	-0.521806622	1039	120	7/6
smpl1_21	GPC_A	2	369	40	320	180	221.1	204.5	0.325841568	-1.171098439	392	17	unc'd 6/38
smpl1_22	GPC_A	2	288	37	170	270	91.8	192.3	0.143919215	-0.500078099	309	14	unc'd 6/38
smpl1_23	GPC_A	2	388	46	320	280	79.8	105.1	0.216179099	-1.422316472	435	19	unc'd 6/38
smpl1_24	GPC_A	2	674	80	1030	130	409	626	0.177929004	-1.405505378	773	49	unc'd 6/38
smpl1_25	GPC_A	2	388	43	230	220	146.7	169.9	0.247583725	-1.554594746	432	18	unc'd 6/38
smpl1_26	GPC_A	2	1125	120	1207	140	140.4	189.4	0.212869228	-0.740638974	1207	140	7/6
smpl1_27	GPC_A	2	295	34	370	340	115	109.9	0.310840845	-1.460952935	319	15	unc'd 6/38
smpl1_28	GPC_A	2	838	88	790	200	133.2	101	0.402450614	-0.55774075	857	35	unc'd 6/38
smpl1_29	GPC_A	2	1097	110	1278	150	167.4	78.1	0.594165642	-4.117378367			
smpl1_30	GPC_A	2	521	55	462	160	241.8	367.2	0.196997207	-0.638626821	553	22	unc'd 6/38
smpl1_31	GPC_A	2	1323	140	1904	110	121.8	407	0.075605916	-0.671242316			
smpl1_32	GPC_A	2	-2700	2400			0.822	5.85	-0.139642186	-8.867896947			
smpl1_33	GPC_A	2	290.5	31	260	180	247.1	370.4	0.199470058	-0.806524642	313	13	unc'd 6/38
smpl1_34	GPC_A	2	428	46	403	160	201.7	305.8	0.201486135	-0.48609432	448	19	unc'd 6/38
smpl1_35	GPC_A	2	1947	200	2025	120	122.8	121.8	0.269489186	-1.207801716	2025	120	7/6
smpl1_36	GPC_A	2	547	80	793	130	31.5	1019	0.00708435	-0.123816664	748	30	unc'd 6/38
smpl1_37	GPC_A	2	389	55	1600	210	352	421	0.349836732	4.404634634			
smpl1_38	GPC_A	2	513	68	260	260	46.4	78.4	0.167061793	-1.07218041	582	25	cor'd 6/38)
smpl1_39	GPC_A	2	352	42	300	360	86.5	97	0.267747061	-1.003128085	376	17	unc'd 6/38

smpl1_40	GPC_A	2	755	86	670	260	52.5	53.1	0.303087863	-0.398731279	773	36	unc'd 6/38
smpl1_41	GPC_A	2	285.2	30	261	160	816	887	0.275768921	-1.129559911	306	13	unc'd 6/38
smpl1_42	GPC_A	2	338	40	200	280	95.8	139	0.204469576	-0.886504474	365	16	unc'd 6/38
smpl1_43	GPC_A	2	1819	190	2800	100	81.3	311.1	0.054309707	-0.885451958			
smpl1_44	GPC_A	2	295.1	32	150	230	276	225.8	0.365543902	-1.622215156	317	13	unc'd 6/38
smpl1_45	GPC_A	2	400	45	200	230	121.7	165.4	0.216079695	-1.021108127	440	19	cor'd 6/38)
smpl1_46	GPC_A	2	884	92	927	130	140.5	319.6	0.125188599	-0.564167657	927	38	cor'd 6/38)
smpl1_47	GPC_A	2	497	55	480	170	134.1	265	0.147450419	-0.684574885	542	22	unc'd 6/38
smpl1_48	GPC_A	2	388	45	380	210	150	231	0.191454778	-0.857473009	421	19	unc'd 6/38
smpl1_49	GPC_A	2	2523	260	2683	100	84.1	126.2	0.173254063	-0.640182745	2683	100	7/6
smpl1_50	GPC_A	2	356	39	290	220	177.2	154.8	0.338040867	-1.660507361	386	17	unc'd 6/38
smpl1_51	GPC_A	2	311	34	290	180	290.9	397.2	0.214010789	-1.141080542	341	14	unc'd 6/38
smpl1_52	GPC_A	3	289	32	370	200	279	278	0.297045722	-1.456326396	314	14	unc'd 6/38
smpl1_53	GPC_A	3	278.5	31	120	210	216.5	260.2	0.247287905	-1.125847821	302	13	unc'd 6/38
smpl1_54	GPC_A	3	479	70	440	270	137.9	259.5	0.16252914	-0.348374733	499	23	unc'd 6/38
smpl1_55	GPC_A	3	295	35	200	250	121.9	181.2	0.203037919	-0.712818008	314	14	unc'd 6/38
smpl1_56	GPC_A	3	477	51	450	170	265	314	0.251727859	-0.920720148	509	21	unc'd 6/38
smpl1_57	GPC_A	3	256.6	28	370	190	676	338.5	0.562213942	-5.571097893			
smpl1_58	GPC_A	3	272	33	230	250	112.1	169.2	0.194456215	-1.002645052	298	13	unc'd 6/38
smpl1_59	GPC_A	3	275	33	160	220	129.3	224.1	0.168761282	-0.888723953	303	13	unc'd 6/38
smpl1_60	GPC_A	3	361	57	448	150	165	470	0.083039357	-1.442634241	487	21	unc'd 6/38
smpl1_61	GPC_A	3	587	63	513	140	138.4	425	0.096585233	-0.319358622	628	26	cor'd 6/38)
smpl1_62	GPC_A	3	273.3	29	590	170	690	633	0.344969542	-0.369014386			
smpl1_63	GPC_A	3	268.7	29	190	200	251.2	331.8	0.227510571	-0.886256937	288	12	unc'd 6/38
smpl1_64	GPC_A	3	315	42	290	230	138	357	0.116154143	-0.408682584	336	18	unc'd 6/38
smpl1_65	GPC_A	3	1140	120	1220	190	78.8	57.5	0.395360393	-1.401434662	1220	190	7/6
smpl1_66	GPC_A	3	387	42	430	170	461	397	0.347849365	-1.371519003	414	18	unc'd 6/38
smpl1_67	GPC_A	3	264.2	28	370	170	470	455	0.303755416	-1.645941816	289	12	unc'd 6/38
smpl1_68	GPC_A	3	297	34	360	210	179.8	200.1	0.260352648	-1.574846902			
smpl1_69	GPC_A	3	296.8	32	370	170	563	533	0.328411616	-0.65895351	307	13	unc'd 6/38
smpl1_70	GPC_A	3	288	34	0	370	119.3	143.4	0.26319429	-0.262365861	294	13	cor'd 6/38)
smpl1_71	GPC_A	6	338	64			37.1	52.3	0.250987341	1.210604763			
smpl1_72	GPC_A	6	272.3	30	250	190	322	310	0.310801634	-1.349305484	293	12	unc'd 6/38
smpl1_73	GPC_A	6	266.3	29	326	150	1810	1189	0.439557923	-3.153065727			
smpl1_74	GPC_A	6	269	31	140	320	143.2	128.2	0.331888154	-1.608332454	292	13	unc'd 6/38
smpl1_75	GPC_A	6	287.6	31	210	230	259	231	0.341960473	-1.094000519	303	13	unc'd 6/38
smpl1_76	GPC_A	6	266.8	29	190	180	345	499	0.199199281	-1.250159195	298	12	unc'd 6/38
smpl1_77	GPC_A	6	278	31	170	280	209	197.8	0.313422933	-1.523587013	301	13	unc'd 6/38
smpl1_78	GPC_A	6	278	31	180	240	418	373	0.328735912	-1.841981523	305	14	unc'd 6/38
smpl1_79	GPC_A	6	1130	120	1029	140	110.6	147.2	0.22215763	-0.443088046	1029	140	7/6
smpl1_80	GPC_A	6	2855	290	2918	100	59.6	54.4	0.288044229	-0.702309427	2918	100	7/6
smpl1_81	GPC_A	6	291	34	190	220	172.3	266	0.196767023	-0.6201222	310	14	cor'd 6/38)
smpl1_82	GPC_A	6	311	34	960	190	180.8	187.7	0.315596955	0.307939344			

smpl1_83	GPC_A	6	303	33	400	220	404	408	0.29765437	-1.166176013	324	15	unc'd 6/38
smpl1_84	GPC_A	6	299	33	270	170	351	501	0.215326679	-0.53955696	313	13	unc'd 6/38
smpl1_85	GPC_A	6	286	31	180	210	170.7	274.5	0.185821807	-0.754641459	308	14	unc'd 6/38
smpl1_86	GPC_A	6	361	40	90	200	162.6	182.2	0.256711837	-1.59818987	402	18	unc'd 6/38
smpl1_87	GPC_A	6	282.6	30	310	210	307	325	0.278452141	-1.425059399	308	14	unc'd 6/38
smpl1_88	GPC_A	6	855	100	480	310	51.5	68.6	0.249232038	0.734645454	808	41	unc'd 6/38
smpl1_89	GPC_A	6	282.7	30	280	180	550	505	0.335587552	-0.869768023	296	13	unc'd 6/38
smpl1_90	GPC_A	6	1593	160	1779	110	119.8	507	0.064872842	-0.253860868	1779	110	7/6
smpl1_91	GPC_A	6	392	52			758	755	0.31591223	-0.317894502			
smpl1_92	GPC_A	6	313	36	210	210	202.2	215.1	0.287277312	-0.830893214	329	15	unc'd 6/38
smpl1_93	GPC_A	6	388	43	360	210	348	349	0.331166927	0.635471556	374	17	unc'd 6/38
smpl1_94	GPC_A	6	1432	150	1556	130	103.9	374	0.084056677	-0.002390686	1556	130	7/6
smpl1_95	GPC_A	6	308	34	200	240	204	198	0.338664011	0.391951224	302	14	unc'd 6/38
smpl1_96	GPC_A	6	301	33	190	200	228.9	329	0.222107822	-0.100967516			
smpl1_97	GPC_A	6	1170	170	1491	120	64.4	1125	0.014292834	-0.13957137	1491	120	7/6
smpl1_98	GPC_A	6	303	34	160	200	348.6	352	0.310338733	-0.470592149	312	14	cor'd 6/38)
smpl1_99	GPC_A	6	892	100	780	170	56.4	249	0.081426679	0.500016979	778	50	unc'd 6/38
smpl1_100	GPC_A	6	297	34	80	250	294	264	0.356199926	-0.139050812	300	14	cor'd 6/38)

* Propagated 2se uncertainties are about 1.5 to twice that of 2se using the calculations as given in Paton et al. (2010)
**three age types are allowed. Best age for grains >950 Ma is 207/206. For those younger, 206/238 is used, but if a 208Pb based common Pb correction makes the point more concordant it is used.
+dwell time=0.35 seconds

Sample GPC_B

	DateTime	Combined Sample	Individual sample	Duration(s)	207_235	207_235_Prop 2SE*	206_238	206_238_Prop 2SE	207_206	207_206_Prop 2SE	208_232	208_232_Prop 2SE	Age207_235	Age207_235_Prop2SE	Age206_238	Age206_238_Prop2SE	error corel
smpl2_0	08/12/2016 (5) 15:32:09.66	GPC_B	8	23.374	0.348	0.039	0.0487	0.0023	0.0522	0.0049	0.01502	0.0017	304	31	306.7	14	0.408570445
smpl2_1	08/12/2016 (5) 15:33:21.40	GPC_B	8	19.858	0.325	0.039	0.0473	0.0023	0.0495	0.0051	0.01437	0.0018	282	30	297.9	14	0.40408618
smpl2_2	08/12/2016 (5) 15:34:42.90	GPC_B	8	13.746	0.327	0.04	0.0449	0.0026	0.0514	0.0048	0.0113	0.0017	285	30	283	16	0.473171381
smpl2_3	08/12/2016 (5) 15:36:01.40	GPC_B	8	20.913	0.33	0.032	0.04713	0.0021	0.0505	0.0038	0.01551	0.0017	288	24	296.8	13	0.465254685
smpl2_4	08/12/2016 (5) 15:37:19.82	GPC_B	8	21.616	0.335	0.031	0.0461	0.002	0.0524	0.0037	0.01441	0.0016	292.4	23	290.5	13	0.494490531
smpl2_5	08/12/2016 (5) 15:38:20.31	GPC_B	8	24.078	0.347	0.035	0.04733	0.0021	0.0526	0.0041	0.01553	0.0017	300	26	298.1	13	0.44948956
smpl2_6	08/12/2016 (5) 15:39:26.77	GPC_B	8	23.023	0.314	0.037	0.04644	0.0021	0.0491	0.0051	0.01531	0.0017	274	28	292.6	13	0.398717925
smpl2_7	08/12/2016 (5) 15:40:35.34	GPC_B	8	19.507	0.328	0.047	0.0478	0.0022	0.0493	0.0065	0.01574	0.0018	282	36	301.2	14	0.342127114
smpl2_8	08/12/2016 (5) 15:41:32.67	GPC_B	8	24.078	0.334	0.034	0.047	0.0022	0.0514	0.0043	0.01506	0.0016	291	26	295.9	13	0.441259604
smpl2_9	08/12/2016 (5) 15:42:49.13	GPC_B	8	16.651	0.295	0.027	0.0396	0.0019	0.0531	0.0037	0.01203	0.0013	261.6	21	250.3	12	0.512743627
smpl2_10	08/12/2016 (5) 15:49:22.13	GPC_B	9	17.467	0.39	0.051	0.0461	0.0023	0.0613	0.0074	0.01195	0.0013	329	37	290.2	14	0.394227105
smpl2_11	08/12/2016 (5) 15:50:16.64	GPC_B	9	21.616	0.407	0.059	0.0477	0.0023	0.0593	0.0062	0.01549	0.0018	339	37	300.2	14	0.392917886
smpl2_12	08/12/2016 (5) 15:51:20.99	GPC_B	9	23.374	0.324	0.029	0.0433	0.0018	0.0537	0.0037	0.01203	0.0013	284.2	23	273.2	11	0.445434507
smpl2_13	08/12/2016 (5) 15:52:31.67	GPC_B	9	19.858	0.334	0.05	0.0453	0.0021	0.0529	0.0073	0.01428	0.0016	286	38	285.4	13	0.324296673
smpl2_14	08/12/2016 (5) 15:53:29.35	GPC_B	9	14.995	0.358	0.043	0.0454	0.0021	0.0566	0.006	0.01476	0.0018	308	32	285.9	13	0.400936496
smpl2_15	08/12/2016 (5) 15:54:29.83	GPC_B	9	23.022	0.353	0.036	0.0469	0.0022	0.0538	0.0043	0.01428	0.0016	305	27	295.1	13	0.445518363
smpl2_16	08/12/2016 (5) 15:55:35.59	GPC_B	9	16.412	0.331	0.036	0.0437	0.002	0.0533	0.0044	0.01267	0.0014	289	27	275.6	13	0.450703527
smpl2_17	08/12/2016 (5) 15:56:39.59	GPC_B	9	12.986	0.497	0.058	0.0598	0.0028	0.0591	0.0055	0.0192	0.0023	407	39	374.3	17	0.428303734
smpl2_18	08/12/2016 (5) 15:57:43.95	GPC_B	9	23.023	0.331	0.037	0.0449	0.0021	0.053	0.0052	0.01427	0.0016	288	28	283.4	13	0.426710143
smpl2_19	08/12/2016 (5) 15:58:47.95	GPC_B	9	23.726	0.329	0.044	0.0453	0.0021	0.0519	0.0062	0.01439	0.0016	283	34	285.3	13	0.354621689
smpl2_20	08/12/2016 (5) 16:03:59.52	GPC_B	9	22.672	0.309	0.031	0.04425	0.0019	0.0496	0.0041	0.01435	0.0016	272	24	279.1	12	0.438042842
smpl2_21	08/12/2016 (5) 16:04:54.73	GPC_B	9	9.459	0.314	0.034	0.0449	0.0021	0.0495	0.0045	0.01384	0.0015	276	26	283.1	13	0.438173385

smpl2_22	08/12/2016 (5) 16:05:47.48	GPC_B	9	13.678	0.392	0.043	0.0444	0.0021	0.0633	0.0061	0.01336	0.0015	334	31	279.8	13	0.44763417
smpl2_23	08/12/2016 (5) 16:07:03.44	GPC_B	9	21.968	0.331	0.034	0.04387	0.0019	0.0545	0.0047	0.01223	0.0014	292	28	276.8	12	0.411959655
smpl2_24	08/12/2016 (5) 16:08:03.92	GPC_B	9	22.671	0.325	0.032	0.04362	0.0019	0.053	0.0041	0.01397	0.0015	287	26	275.2	12	0.43370354
smpl2_25	08/12/2016 (5) 16:09:04.06	GPC_B	9	21.616	0.329	0.033	0.04317	0.0019	0.0544	0.0044	0.01355	0.0015	287	25	272.4	12	0.451297331
smpl2_26	08/12/2016 (5) 16:09:52.58	GPC_B	9	23.375	0.34	0.034	0.0448	0.0019	0.0544	0.0045	0.01353	0.0015	295	26	282.5	12	0.434165905
smpl2_27	08/12/2016 (5) 16:10:52.72	GPC_B	9	20.913	0.374	0.037	0.04352	0.0019	0.0614	0.0048	0.01248	0.0014	321	27	274.6	11	0.429976121
smpl2_28	08/12/2016 (5) 16:11:51.45	GPC_B	9	16.693	0.334	0.031	0.04454	0.002	0.0538	0.0039	0.01295	0.0014	292	23	280.9	12	0.476751636
smpl2_29	08/12/2016 (5) 16:12:50.53	GPC_B	9	18.451	0.334	0.037	0.04253	0.0019	0.0562	0.0053	0.01324	0.0014	291	28	268.5	12	0.421260165
smpl2_30	08/12/2016 (5) 16:17:36.07	GPC_B	9	15.638	0.309	0.053	0.0431	0.0021	0.0519	0.0085	0.01344	0.0015	266	41	272.1	13	0.296068229
smpl2_31	08/12/2016 (5) 16:19:15.24	GPC_B	9	20.561	0.336	0.031	0.04403	0.0019	0.0547	0.0039	0.01367	0.0015	294	24	277.7	12	0.467843851
smpl2_32	08/12/2016 (5) 16:20:14.67	GPC_B	9	19.506	0.321	0.031	0.04416	0.0019	0.0522	0.0041	0.01387	0.0015	282	24	278.6	12	0.451563802
smpl2_33	08/12/2016 (5) 16:21:10.23	GPC_B	9	21.617	0.35	0.035	0.04432	0.002	0.0568	0.0047	0.01416	0.0015	303	26	279.5	12	0.447459706
smpl2_34	08/12/2016 (5) 16:22:08.61	GPC_B	9	19.506	0.312	0.031	0.04318	0.0019	0.0519	0.0043	0.01386	0.0015	274	24	272.5	11	0.418547349
smpl2_35	08/12/2016 (5) 16:23:03.47	GPC_B	9	20.561	0.342	0.032	0.04298	0.0019	0.0574	0.0042	0.01402	0.0015	298	24	271.3	12	0.481385366
smpl2_36	08/12/2016 (5) 16:24:03.10	GPC_B	9	14.734	0.492	0.059	0.0578	0.0028	0.0611	0.0063	0.01851	0.0021	402	41	362.2	17	0.418052425
smpl2_37	08/12/2016 (5) 16:24:49.67	GPC_B	9	22.671	1.753	0.17	0.0484	0.0025	0.261	0.02	0.02122	0.0024	1020	62	304.8	15	0.629246498
smpl2_38	08/12/2016 (5) 16:25:47.69	GPC_B	9	8.0335	0.411	0.071	0.0446	0.0023	0.0655	0.01	0.0146	0.0018	344	51	281.4	14	0.31814152
smpl2_39	08/12/2016 (5) 16:31:52.71	GPC_B	9	14.231	0.317	0.048	0.045	0.0022	0.0504	0.0067	0.01517	0.0018	275	36	283.8	14	0.352624577
smpl2_40	08/12/2016 (5) 16:32:52.50	GPC_B	9	17.748	0.385	0.036	0.0492	0.0023	0.0564	0.0042	0.01656	0.0018	330	26	309.8	14	0.497539289
smpl2_41	08/12/2016 (5) 16:35:14.92	GPC_B	9	17.396	0.344	0.038	0.04456	0.002	0.0554	0.0051	0.01328	0.0015	298	29	281	12	0.401838398
smpl2_42	08/12/2016 (5) 16:38:08.64	GPC_B	9	21.968	0.368	0.037	0.04425	0.0019	0.0593	0.0049	0.01266	0.0014	317	27	279.1	12	0.450636288
smpl2_43	08/12/2016 (5) 16:39:02.79	GPC_B	9	22.319	0.347	0.035	0.0465	0.0022	0.054	0.0046	0.01471	0.0016	301	26	293	13	0.456902077
smpl2_44	08/12/2016 (5) 16:40:05.39	GPC_B	9	23.726	0.36	0.036	0.04748	0.0021	0.0545	0.0044	0.01357	0.0015	310	27	299	13	0.446637197
smpl2_45	08/12/2016 (5) 16:41:06.42	GPC_B	9	19.315	0.401	0.05	0.0489	0.0023	0.0577	0.0059	0.0152	0.0017	337	35	307.7	14	0.401271648
smpl2_46	08/12/2016 (5) 16:42:13.04	GPC_B	9	23.023	0.352	0.038	0.04862	0.0021	0.0528	0.0048	0.01421	0.0016	307	30	306	13	0.398700541
smpl2_47	08/12/2016 (5) 16:43:47.99	GPC_B	9	10.162	0.368	0.038	0.0478	0.0022	0.0553	0.0049	0.01356	0.0015	317	28	301	14	0.465928156

smpl2_48	08/12/2016 (5) 16:44:44.96	GPC_B	9	21.968	0.36	0.042	0.04888	0.0022	0.0533	0.0054	0.014	0.0016	309	32	307.6	13	0.377845987
smpl2_49	08/12/2016 (5) 16:49:36.83	GPC_B	9	16.141	0.343	0.034	0.04601	0.0021	0.0535	0.0042	0.01383	0.0015	298	26	290	13	0.457001466
smpl2_50	08/12/2016 (5) 16:50:35.91	GPC_B	9	23.726	0.379	0.039	0.04834	0.0022	0.0567	0.0049	0.01495	0.0017	324	29	304.3	13	0.430747191
smpl2_51	08/12/2016 (5) 16:51:30.77	GPC_B	9	23.726	0.336	0.047	0.0463	0.0022	0.0524	0.0065	0.0142	0.0016	287	36	291.7	13	0.334789794
smpl2_52	08/12/2016 (5) 16:52:37.23	GPC_B	9	20.913	0.304	0.054	0.0471	0.0023	0.047	0.0078	0.01403	0.0017	277	43	296.8	14	0.290735578
smpl2_53	08/12/2016 (5) 16:55:51.70	GPC_B	9	23.022	0.35	0.032	0.04515	0.0019	0.056	0.004	0.01384	0.0015	304	24	284.7	12	0.470974164
smpl2_54	08/12/2016 (5) 16:56:53.59	GPC_B	9	23.023	0.327	0.033	0.0456	0.002	0.0519	0.0044	0.01367	0.0015	286	25	287.4	13	0.45958096
smpl2_55	08/12/2016 (5) 16:58:03.57	GPC_B	9	23.726	0.353	0.032	0.04775	0.0021	0.0534	0.0038	0.01426	0.0015	306	24	300.7	13	0.482734691
smpl2_56	08/12/2016 (5) 16:59:06.87	GPC_B	9	24.43	0.351	0.033	0.04479	0.0019	0.0566	0.0041	0.01336	0.0014	304	25	282.4	12	0.459053159
smpl2_57	08/12/2016 (5) 17:00:04.35	GPC_B	9	19.474	0.381	0.039	0.04427	0.002	0.0625	0.0054	0.01095	0.0013	326	28	279.2	13	0.47658453
smpl2_58	08/12/2016 (5) 17:01:01.16	GPC_B	9	18.451	0.347	0.039	0.04516	0.002	0.0554	0.0053	0.0132	0.0014	300	29	284.7	12	0.399688045
smpl2_59	08/12/2016 (5) 17:07:36.08	GPC_B	9	24.078	0.35	0.032	0.04558	0.0019	0.0551	0.0038	0.0126	0.0014	303.6	24	287.3	12	0.467166429
smpl2_60	08/12/2016 (5) 17:08:30.58	GPC_B	9	22.671	0.379	0.072	0.049	0.0025	0.0564	0.01	0.01469	0.0018	308	55	308	15	0.263117406
smpl2_61	08/12/2016 (5) 17:09:26.50	GPC_B	9	20.913	7.63	1.1	0.0965	0.0081	0.537	0.05	0.0749	0.011	2080	170	592	48	0.704279519
smpl2_62	08/12/2016 (5) 17:10:35.60	GPC_B	9	12.905	0.369	0.04	0.04401	0.002	0.0607	0.0055	0.01146	0.0013	317	30	277.6	12	0.41548097
smpl2_63	08/12/2016 (5) 17:11:32.39	GPC_B	9	22.32	0.364	0.036	0.04732	0.002	0.0555	0.0045	0.01407	0.0015	313	27	298	12	0.422996437
smpl2_64	08/12/2016 (5) 17:12:21.97	GPC_B	9	29.704	0.338	0.03	0.04473	0.0019	0.0547	0.0037	0.01271	0.0013	295.2	23	282	12	0.479329876
smpl2_65	08/12/2016 (5) 17:13:31.95	GPC_B	9	24.078	0.337	0.034	0.04542	0.002	0.0538	0.0044	0.01396	0.0015	293	26	286.3	13	0.455527383
smpl2_66	08/12/2016 (5) 17:14:32.44	GPC_B	9	23.022	0.324	0.039	0.04469	0.002	0.0528	0.0056	0.01356	0.0015	282	29	281.8	13	0.4092976
smpl2_67	08/12/2016 (5) 17:16:20.75	GPC_B	9	23.022	0.367	0.034	0.04644	0.002	0.0573	0.0041	0.01328	0.0014	317	25	292.6	12	0.461371831
smpl2_68	08/12/2016 (5) 17:17:22.99	GPC_B	9	19.506	0.339	0.032	0.04401	0.0019	0.0557	0.004	0.01349	0.0015	295	24	277.6	12	0.469217248
smpl2_69	08/12/2016 (5) 17:18:14.34	GPC_B	9	22.671	0.342	0.034	0.04503	0.0019	0.0549	0.0043	0.01323	0.0014	297	25	283.9	12	0.448749058
smpl2_70	08/12/2016 (5) 17:24:20.41	GPC_B	9	17.818	0.328	0.047	0.0453	0.0021	0.0527	0.0071	0.01375	0.0016	282	36	285.5	13	0.335953222
smpl2_71	08/12/2016 (5) 17:25:45.52	GPC_B	9	22.32	0.338	0.034	0.04445	0.002	0.0551	0.0045	0.01348	0.0015	294	26	280.3	12	0.435725559
smpl2_72	08/12/2016 (5) 17:26:58.31	GPC_B	9	23.374	2.118	0.18	0.1943	0.0083	0.0789	0.0049	0.0553	0.0059	1153	60	1145	45	0.602672866
smpl2_73	08/12/2016 (5) 17:29:36.20	GPC_B	9	10.785	0.372	0.044	0.0463	0.0022	0.0574	0.0059	0.01403	0.0016	319	33	291.9	14	0.420621177

smpl2_74	08/12/2016 (5) 17:30:19.46	GPC_B	9	22.671	0.313	0.037	0.04455	0.002	0.051	0.0054	0.01332	0.0015	273	29	281	12	0.372999839
smpl2_75	08/12/2016 (5) 17:31:38.23	GPC_B	9	19.507	0.331	0.03	0.04151	0.0018	0.0586	0.0043	0.00965	0.0011	293	28	262.2	11	0.40197527
smpl2_76	08/12/2016 (5) 17:32:37.66	GPC_B	9	23.726	0.317	0.031	0.04446	0.0019	0.0516	0.004	0.01356	0.0015	278	24	280.4	12	0.4441435
smpl2_77	08/12/2016 (5) 17:33:37.44	GPC_B	9	23.023	0.327	0.036	0.04528	0.002	0.0526	0.0051	0.01354	0.0015	285	27	285.4	12	0.405662973
smpl2_78	08/12/2016 (5) 17:34:35.82	GPC_B	9	15.357	1.16	0.22	0.0509	0.0029	0.157	0.025	0.0208	0.0029	733	100	320	18	0.381182781
smpl2_79	08/12/2016 (5) 17:35:50.72	GPC_B	9	19.506	0.331	0.035	0.045	0.0021	0.0535	0.0048	0.01425	0.0016	288	27	283.6	13	0.439255583
smpl2_80	08/12/2016 (5) 17:41:00.18	GPC_B	9	23.375	0.357	0.035	0.04818	0.0021	0.0536	0.0042	0.01427	0.0016	308	26	303.3	13	0.452731915
smpl2_81	08/12/2016 (5) 17:42:16.19	GPC_B	9	8.2042	0.61	0.1	0.0483	0.0028	0.092	0.015	0.01712	0.002	475	64	304	17	0.383334121
smpl2_82	08/12/2016 (5) 17:43:14.51	GPC_B	9	22.672	0.348	0.033	0.04782	0.0021	0.0527	0.004	0.01425	0.0015	302	25	301.1	13	0.462437187
smpl2_83	08/12/2016 (5) 17:44:09.37	GPC_B	9	23.375	0.364	0.034	0.05008	0.0022	0.0526	0.0038	0.01536	0.0016	314	25	315	13	0.460198693
smpl2_84	08/12/2016 (5) 17:45:21.81	GPC_B	9	23.727	0.431	0.052	0.0581	0.0027	0.0542	0.0059	0.0162	0.0019	358	37	363.7	16	0.391651238
smpl2_85	08/12/2016 (5) 17:46:22.58	GPC_B	9	5.1956	0.45	0.11	0.0372	0.0035	0.1	0.027	0.0111	0.0036	420	120	235	21	0.298506233
smpl2_86	08/12/2016 (5) 17:47:21.73	GPC_B	9	22.319	0.341	0.038	0.04906	0.0021	0.0502	0.0048	0.01364	0.0015	295	29	308.7	13	0.393771826
smpl2_87	08/12/2016 (5) 17:48:22.57	GPC_B	9	24.079	0.35	0.041	0.04672	0.0021	0.0553	0.0058	0.01403	0.0015	301	31	294.3	13	0.39417581
smpl2_88	08/12/2016 (5) 17:49:43.10	GPC_B	9	25.483	0.342	0.043	0.0493	0.0022	0.0508	0.006	0.01489	0.0017	294	32	310.3	14	0.382923631
smpl2_89	08/12/2016 (5) 17:51:03.27	GPC_B	9	22.671	0.426	0.041	0.055	0.0025	0.0553	0.0042	0.01645	0.0018	358	29	345.2	15	0.47270501
smpl2_90	08/12/2016 (5) 17:55:55.85	GPC_B	9	23.727	0.369	0.067	0.0509	0.0023	0.0507	0.0084	0.0155	0.0017	303	48	319.7	14	0.266438573
smpl2_91	08/12/2016 (5) 17:57:01.62	GPC_B	9	19.858	0.496	0.074	0.04763	0.0021	0.076	0.011	0.01483	0.0016	398	47	299.9	13	0.34459063
smpl2_92	08/12/2016 (5) 17:57:55.42	GPC_B	9	22.319	0.355	0.04	0.04789	0.0021	0.0537	0.0052	0.01521	0.0017	305	30	301.5	13	0.401482707
smpl2_93	08/12/2016 (5) 17:58:52.74	GPC_B	9	11.119	0.388	0.044	0.0472	0.0022	0.0592	0.0057	0.01478	0.0017	331	32	297	14	0.438263378
smpl2_94	08/12/2016 (5) 18:00:12.92	GPC_B	9	21.266	0.328	0.032	0.0471	0.0021	0.0503	0.0038	0.01475	0.0016	287	24	296.6	13	0.464232939
smpl2_95	08/12/2016 (5) 18:01:19.38	GPC_B	9	19.152	0.378	0.05	0.0472	0.0023	0.0581	0.0069	0.0141	0.0019	320	37	297.1	14	0.377404725
smpl2_96	08/12/2016 (5) 18:02:16.35	GPC_B	9	23.022	0.356	0.033	0.04672	0.002	0.0551	0.004	0.01474	0.0016	308	25	294.3	12	0.448888856
smpl2_97	08/12/2016 (5) 18:03:16.84	GPC_B	9	21.969	0.356	0.033	0.04665	0.0021	0.0547	0.0039	0.01498	0.0017	308	25	293.9	13	0.478508795
smpl2_98	08/12/2016 (5) 18:04:09.94	GPC_B	9	23.022	0.369	0.037	0.04696	0.0021	0.0567	0.0045	0.01679	0.0019	317	27	295.8	13	0.458544849
smpl2_99	08/12/2016 (5) 18:06:10.20	GPC_B	9	21.267	0.621	0.058	0.04663	0.0021	0.0964	0.0071	0.01623	0.0017	489	37	293.7	13	0.504935908

smpl2_100	08/12/2016 (5) 18:07:02.25	GPC_B	9	24.077	0.323	0.034	0.04556	0.002	0.0513	0.0045	0.01453	0.0016	282	26	287.2	12	0.412773386
smpl2_101	08/12/2016 (5) 18:12:20.85	GPC_B	9	22.319	0.327	0.032	0.04553	0.0021	0.0525	0.0043	0.01439	0.0015	288	25	287	13	0.462616679
smpl2_102	08/12/2016 (5) 18:13:09.38	GPC_B	9	23.726	0.414	0.041	0.05529	0.0024	0.0541	0.0043	0.01751	0.0019	350	29	346.9	15	0.462652741
smpl2_103	08/12/2016 (5) 18:14:11.98	GPC_B	9	20.912	0.303	0.029	0.04315	0.0019	0.0506	0.0037	0.01307	0.0014	268	22	272.3	11	0.441537126
smpl2_104	08/12/2016 (5) 18:15:33.56	GPC_B	9	19.857	0.373	0.038	0.04776	0.0021	0.0561	0.0046	0.01541	0.0017	320	29	300.7	13	0.430564239
smpl2_105	08/12/2016 (5) 18:16:35.45	GPC_B	9	13.576	0.354	0.051	0.0458	0.0021	0.0557	0.0076	0.01466	0.0017	303	37	288.4	13	0.346297666
smpl2_106	08/12/2016 (5) 18:17:34.53	GPC_B	9	20.914	0.306	0.032	0.04464	0.0019	0.0494	0.0043	0.01506	0.0016	269	25	281.5	12	0.416919308
smpl2_107	08/12/2016 (5) 18:18:57.88	GPC_B	9	23.374	0.366	0.061	0.054	0.0027	0.0493	0.0076	0.01927	0.0022	304	46	339	17	0.314583762
smpl2_108	08/12/2016 (5) 18:19:52.03	GPC_B	9	23.021	0.309	0.03	0.04489	0.002	0.0499	0.004	0.0147	0.0016	272	23	283	12	0.448257027
smpl2_109	08/12/2016 (5) 18:20:54.98	GPC_B	9	20.911	0.3	0.036	0.04469	0.002	0.0483	0.005	0.01422	0.0016	264	28	281.8	12	0.372590807
smpl2_110	08/12/2016 (5) 18:22:05.31	GPC_B	9	19.155	0.313	0.033	0.0447	0.0021	0.0508	0.0047	0.01456	0.0017	275	26	281.6	13	0.438769386
smpl2_111	08/12/2016 (5) 18:27:37.63	GPC_B	9	12.182	1.144	0.1	0.1235	0.0057	0.0666	0.0047	0.0365	0.0043	773	50	751	33	0.561933376
smpl2_112	08/12/2016 (5) 18:28:37.76	GPC_B	9	22.319	0.317	0.05	0.04373	0.002	0.052	0.0076	0.0143	0.0017	271	39	275.9	12	0.289303629
smpl2_113	08/12/2016 (5) 18:29:48.80	GPC_B	9	21.616	0.337	0.031	0.04418	0.002	0.055	0.0039	0.01428	0.0015	294	24	278.6	12	0.466662058
smpl2_114	08/12/2016 (5) 18:30:42.25	GPC_B	9	23.375	0.3	0.03	0.04372	0.0019	0.0495	0.0041	0.01399	0.0015	265	23	275.8	12	0.448149109
smpl2_115	08/12/2016 (5) 18:32:03.83	GPC_B	9	23.022	0.316	0.031	0.0445	0.002	0.0506	0.0039	0.01477	0.0016	280	23	280.6	12	0.461788013
smpl2_116	08/12/2016 (5) 18:33:08.19	GPC_B	9	19.153	0.31	0.028	0.04391	0.0019	0.0508	0.0033	0.01512	0.0016	273.9	22	277	12	0.474706043
smpl2_117	08/12/2016 (5) 18:34:09.38	GPC_B	9	18.802	0.331	0.033	0.0451	0.002	0.0531	0.0045	0.01482	0.0016	289	25	284.3	12	0.438518298
smpl2_118	08/12/2016 (5) 18:35:05.99	GPC_B	9	18.182	0.366	0.04	0.04348	0.0019	0.0608	0.0057	0.01429	0.0016	315	30	274.4	12	0.41729322
smpl2_119	08/12/2016 (5) 18:36:19.84	GPC_B	9	23.024	0.332	0.031	0.04777	0.002	0.0502	0.0037	0.01589	0.0017	290	23	300.8	12	0.449360974
smpl2_120	08/12/2016 (5) 18:37:25.25	GPC_B	9	23.727	0.359	0.036	0.04773	0.0021	0.0542	0.0044	0.01573	0.0018	309	27	300.5	13	0.443697679
smpl2_121	08/12/2016 (5) 18:42:36.47	GPC_B	9	24.078	0.982	0.12	0.117	0.0055	0.0605	0.0065	0.0354	0.0044	685	62	713	32	0.444244103
smpl2_122	08/12/2016 (5) 18:43:41.52	GPC_B	9	18.101	0.381	0.052	0.0483	0.0024	0.0578	0.0074	0.01571	0.0019	322	38	303.9	15	0.385857313
smpl2_123	08/12/2016 (5) 18:44:30.40	GPC_B	9	22.319	0.326	0.038	0.04612	0.002	0.0511	0.0053	0.014	0.0015	283	30	290.6	13	0.388798627
smpl2_124	08/12/2016 (5) 18:45:30.19	GPC_B	9	21.265	0.324	0.035	0.04385	0.002	0.0535	0.0049	0.01016	0.0011	283	27	276.6	12	0.413940693
smpl2_125	08/12/2016 (5) 18:46:35.36	GPC_B	9	13.057	0.326	0.042	0.0488	0.0023	0.0484	0.0055	0.01548	0.0018	284	32	307.2	14	0.374951974

smpl2_126	08/12/2016 (5) 18:47:20.26	GPC_B	9	25.483	0.324	0.033	0.04754	0.0022	0.0497	0.0044	0.01461	0.0016	283	26	299.3	13	0.427411038
smpl2_127	08/12/2016 (5) 18:48:28.48	GPC_B	9	12.11	0.315	0.03	0.04499	0.002	0.0505	0.0039	0.0149	0.0016	277	23	283.7	12	0.453914121
smpl2_128	08/12/2016 (5) 18:49:32.48	GPC_B	9	23.022	0.368	0.036	0.04866	0.0021	0.0545	0.0042	0.01486	0.0016	317	26	306.3	13	0.459580674
smpl2_129	08/12/2016 (5) 18:50:31.56	GPC_B	9	23.727	0.321	0.031	0.04697	0.0021	0.0493	0.0038	0.01483	0.0016	281	24	295.9	13	0.45742214
smpl2_130	08/12/2016 (5) 18:51:43.65	GPC_B	9	21.968	0.332	0.054	0.0455	0.0022	0.0534	0.0085	0.0141	0.0019	281	43	286.5	14	0.304197695
smpl2_131	08/12/2016 (5) 18:58:47.05	GPC_B	9	23.727	0.331	0.032	0.04727	0.0021	0.0507	0.0039	0.01496	0.0016	289	24	297.7	13	0.465414533
smpl2_132	08/12/2016 (5) 18:59:44.37	GPC_B	9	23.727	0.738	0.074	0.0917	0.0041	0.0581	0.0046	0.02803	0.003	556	43	565.2	24	0.481282287
smpl2_133	08/12/2016 (5) 19:00:37.47	GPC_B	9	24.078	0.334	0.035	0.04588	0.002	0.0526	0.0046	0.01233	0.0013	290	27	289.1	12	0.407193453
smpl2_134	08/12/2016 (5) 19:01:28.46	GPC_B	9	22.671	0.303	0.028	0.0448	0.0019	0.0489	0.0034	0.01418	0.0015	268.3	22	282.5	12	0.459980177
smpl2_135	08/12/2016 (5) 19:02:19.10	GPC_B	9	21.264	0.326	0.03	0.04542	0.0019	0.0518	0.0036	0.01463	0.0016	286	23	286.3	12	0.462184888
smpl2_136	08/12/2016 (5) 19:03:13.25	GPC_B	9	12.925	0.309	0.033	0.0447	0.0021	0.0498	0.0045	0.01373	0.0016	272	26	282.1	13	0.4342668
smpl2_137	08/12/2016 (5) 19:04:10.22	GPC_B	9	22.319	0.308	0.029	0.04532	0.002	0.0492	0.0037	0.01409	0.0015	272	23	285.7	12	0.44486235
smpl2_138	08/12/2016 (5) 19:05:04.73	GPC_B	9	24.078	0.312	0.037	0.04599	0.0021	0.0499	0.0052	0.01335	0.0015	276	30	289.8	13	0.381487655
smpl2_139	08/12/2016 (5) 19:06:00.64	GPC_B	9	23.022	0.347	0.035	0.04851	0.0021	0.0512	0.0041	0.01487	0.0016	301	26	305.3	13	0.442153278
smpl2_140	08/12/2016 (5) 19:07:49.31	GPC_B	9	21.968	0.329	0.033	0.04479	0.0019	0.0529	0.0041	0.01324	0.0014	287	25	282.5	12	0.438308287
smpl2_141	08/12/2016 (5) 19:13:01.93	GPC_B	9	23.726	0.319	0.03	0.0444	0.0019	0.0521	0.004	0.01374	0.0015	280	23	280	12	0.462566007
smpl2_142	08/12/2016 (5) 19:13:57.14	GPC_B	9	21.265	0.365	0.034	0.05075	0.0022	0.052	0.0038	0.01559	0.0017	315	26	319.1	14	0.469357018
smpl2_143	08/12/2016 (5) 19:14:55.87	GPC_B	9	21.615	0.355	0.047	0.0459	0.0021	0.0558	0.0064	0.0147	0.0017	303	34	289.2	13	0.371869173
smpl2_144	08/12/2016 (5) 19:15:46.16	GPC_B	9	23.022	0.294	0.033	0.04439	0.002	0.0482	0.0047	0.0133	0.0015	259	26	279.9	12	0.392756819
smpl2_145	08/12/2016 (5) 19:16:52.97	GPC_B	9	21.264	0.304	0.036	0.04326	0.002	0.051	0.0053	0.0137	0.0015	267	28	272.9	12	0.386688269
smpl2_146	08/12/2016 (5) 19:17:48.88	GPC_B	9	23.374	0.333	0.032	0.04622	0.0021	0.0525	0.0038	0.01411	0.0015	293	26	291.2	13	0.44942099
smpl2_147	08/12/2016 (5) 19:19:25.24	GPC_B	9	21.968	0.319	0.032	0.04459	0.0019	0.0515	0.0041	0.01399	0.0015	280	24	281.2	12	0.44568488
smpl2_148	08/12/2016 (5) 19:20:37.33	GPC_B	9	23.375	0.31	0.029	0.04348	0.0019	0.0521	0.004	0.01371	0.0015	275	24	274.4	12	0.44799538
smpl2_149	08/12/2016 (5) 19:21:50.83	GPC_B	9	17.747	0.304	0.03	0.04162	0.0018	0.0527	0.0042	0.01182	0.0013	268	24	262.8	11	0.423432665
smpl2_150	08/12/2016 (5) 19:22:48.15	GPC_B	9	15.637	0.299	0.029	0.04363	0.0019	0.0495	0.0038	0.01378	0.0015	265	23	275.3	12	0.448799214

	Combined Sample	Individual sample	Age208_232	Age208_232_Prop2SE	Age207_206	Age207_206_Prop2SE	Th(ppm)	U(ppm)	calc208/206	PERCENT 206 THAT IS COMMON	overall best concordant age	2 s.e. uncert	age type**
smpl2_0	GPC_B	8	301	34	230	190	129.7	187.7	0.218627932	-0.202580204	307	14	unc'd 6/38
smpl2_1	GPC_B	8	288	36	120	210	151	243	0.193666843	-0.339907462	299	14	cor'd 6/38)
smpl2_2	GPC_B	8	226	33	250	210	407	610	0.172260478	-2.272218947			
smpl2_3	GPC_B	8	311.1	34	193	160	545	1027	0.179155188	0.427448135	297	13	unc'd 6/38
smpl2_4	GPC_B	8	289.1	31	279	150	917	847	0.347166613	-0.093569385	291	13	unc'd 6/38
smpl2_5	GPC_B	8	311	35	270	170	329.6	490	0.226420136	0.520255046	298	13	unc'd 6/38
smpl2_6	GPC_B	8	307	33	90	210	244	334	0.247067324	0.629494769	293	13	unc'd 6/38
smpl2_7	GPC_B	8	316	36	70	260	119.8	161	0.251360334	0.632579979	301	14	unc'd 6/38
smpl2_8	GPC_B	8	302.1	33	210	170	452	351	0.423299158	0.506723107	296	13	unc'd 6/38
smpl2_9	GPC_B	8	241.6	27	330	160	1620	1870	0.269980764	-0.535458882	250	12	unc'd 6/38
smpl2_10	GPC_B	9	240.1	27	510	250	282	229	0.327468536	-4.070860185			
smpl2_11	GPC_B	9	311	36	530	210	430	583	0.245709479	0.440726058	299	14	cor'd 6/38)
smpl2_12	GPC_B	9	241.7	26	332	150	621	862	0.205329352	-1.447009741	273	11	unc'd 6/38
smpl2_13	GPC_B	9	287	33	190	270	144.5	161	0.290242462	0.055517471	285	13	unc'd 6/38
smpl2_14	GPC_B	9	296	35	390	230	246	276	0.29726618	0.554222463			
smpl2_15	GPC_B	9	287	32	310	170	391	368	0.331874035	-0.589482784	295	13	unc'd 6/38
smpl2_16	GPC_B	9	254	29	320	180	350	721	0.144383289	-0.625341205	276	13	unc'd 6/38
smpl2_17	GPC_B	9	384	46	510	200	214.3	421	0.167659857	0.226376601	374	17	cor'd 6/38)
smpl2_18	GPC_B	9	286	32	280	210	221.7	256	0.282352952	0.177920501	283	13	cor'd 6/38)
smpl2_19	GPC_B	9	289	32	170	240	316.6	145.8	0.707627905	0.560287164	285	13	unc'd 6/38
smpl2_20	GPC_B	9	287.9	31	160	180	248.7	424.8	0.19476857	0.316086835	279	12	unc'd 6/38
smpl2_21	GPC_B	9	278	31	150	200	267.1	514	0.164319646	-0.163990841	284	13	cor'd 6/38)
smpl2_22	GPC_B	9	268	30	640	200	340	479	0.219106804	-0.519486345			
smpl2_23	GPC_B	9	246	28	360	160	313.4	327	0.274093688	-1.951795928	277	12	unc'd 6/38
smpl2_24	GPC_B	9	280.4	30	310	170	271	544	0.163670387	0.157096374			
smpl2_25	GPC_B	9	272	29	340	170	258	411	0.202126894	-0.016430901	272	12	cor'd 6/38)
smpl2_26	GPC_B	9	271.5	29	330	180	221.1	357	0.191879811	-0.407648884	283	12	unc'd 6/38
smpl2_27	GPC_B	9	250.7	28	600	170	453	655	0.203456502	-1.043054244			
smpl2_28	GPC_B	9	260.1	28	337	160	728	883	0.245911707	-1.08328488	281	12	unc'd 6/38
smpl2_29	GPC_B	9	265.9	28	390	200	401	397	0.322578517	-0.182208499	269	12	unc'd 6/38
smpl2_30	GPC_B	9	270	31	130	320	134.8	128.3	0.336104407	-0.15513261	272	13	unc'd 6/38
smpl2_31	GPC_B	9	274.5	29	371	160	618	903	0.217976425	-0.142129909	278	12	unc'd 6/38
smpl2_32	GPC_B	9	278.3	30	260	170	323.4	504	0.206750157	-0.005911016	279	12	cor'd 6/38)
smpl2_33	GPC_B	9	284.2	31	420	180	296	345	0.281206328	0.253947251	279	12	cor'd 6/38)
smpl2_34	GPC_B	9	278.1	30	240	170	281.7	351.6	0.263819896	0.296094944	273	11	unc'd 6/38
smpl2_35	GPC_B	9	281.3	30	470	170	322	553	0.194850406	0.369800721	270	12	cor'd 6/38)
smpl2_36	GPC_B	9	371	41	550	230	223.5	198.3	0.370273274	0.490222861			
smpl2_37	GPC_B	9	424	47	3220	120	282	166.4	0.762227786	13.94011156			
smpl2_38	GPC_B	9	293	35	660	340	144.9	160.3	0.303558105	0.674782699	279	14	cor'd 6/38)
smpl2_39	GPC_B	9	304	35	120	250	113.4	150.9	0.259887777	0.953025142	284	14	unc'd 6/38

smpl2_40	GPC_B	9	331.9	35	450	170	566	676	0.289103891	1.072286032	310	14	unc'd 6/38
smpl2_41	GPC_B	9	267	30	360	200	201.3	293	0.210047743	-0.608075641	281	12	unc'd 6/38
smpl2_42	GPC_B	9	254.2	28	530	190	191.6	277	0.203013603	-1.065237701			
smpl2_43	GPC_B	9	295	31	310	180	339	292	0.376760651	0.160913712	293	13	cor'd 6/38)
smpl2_44	GPC_B	9	272.4	30	340	170	215.2	372.7	0.169293773	-0.870205903	299	13	unc'd 6/38
smpl2_45	GPC_B	9	305	34	450	230	137.3	224.8	0.194759177	-0.096419674	308	14	unc'd 6/38
smpl2_46	GPC_B	9	285	31	250	190	239	273	0.262484311	-1.06357413	306	13	unc'd 6/38
smpl2_47	GPC_B	9	272	31	390	190	272	434	0.182389545	-1.023135697			
smpl2_48	GPC_B	9	281	32	260	210	143.5	225	0.187393789	-0.944598319	308	13	unc'd 6/38
smpl2_49	GPC_B	9	277.6	30	320	170	415	619	0.206736123	-0.492363087	290	13	unc'd 6/38
smpl2_50	GPC_B	9	300	34	420	190	147.7	267	0.175506317	-0.134570476	304	13	unc'd 6/38
smpl2_51	GPC_B	9	285	32	190	250	142	202	0.221173607	-0.282718479	292	13	unc'd 6/38
smpl2_52	GPC_B	9	282	34	60	300	82.7	97.4	0.25946112	-0.766866954	299	14	cor'd 6/38)
smpl2_53	GPC_B	9	277.7	30	417	160	321.5	529	0.191114049	-0.249700856	285	12	unc'd 6/38
smpl2_54	GPC_B	9	274.5	29	250	180	291	281	0.318477909	-0.862483562	287	13	unc'd 6/38
smpl2_55	GPC_B	9	286.2	31	315	160	476	458	0.318402593	-0.921093631	301	13	unc'd 6/38
smpl2_56	GPC_B	9	268.3	29	432	160	693	493	0.43013094	-1.394760812	282	12	unc'd 6/38
smpl2_57	GPC_B	9	220	26	650	190	433	360	0.30519609	-4.827060559			
smpl2_58	GPC_B	9	265.1	29	350	200	268	329.7	0.243738883	-0.992654892	285	12	unc'd 6/38
smpl2_59	GPC_B	9	253	28	399	160	237.1	659	0.10203081	-0.701373731	287	12	unc'd 6/38
smpl2_60	GPC_B	9	295	36	190	360	64.3	62.2	0.317932757	-0.838130289	308	15	unc'd 6/38
smpl2_61	GPC_B	9	1450	210	4290	160	272	149	1.45353707	56.66496211			
smpl2_62	GPC_B	9	230.4	26	570	200	417.5	489	0.228070882	-2.589314701			
smpl2_63	GPC_B	9	282.3	30	380	180	338.5	474	0.217830488	-0.650318882	298	12	unc'd 6/38
smpl2_64	GPC_B	9	255.2	27	371	140	946	984	0.280240993	-1.657333038	282	12	unc'd 6/38
smpl2_65	GPC_B	9	280.2	30	310	170	284	399	0.22442576	-0.264589771			
smpl2_66	GPC_B	9	272	31	220	210	125.9	164.8	0.237797251	-0.456144454	282	13	unc'd 6/38
smpl2_67	GPC_B	9	266.7	28	467	160	560	492	0.333901031	-1.891555493			
smpl2_68	GPC_B	9	270.8	29	407	170	347	520	0.209833915	-0.281836298	278	12	unc'd 6/38
smpl2_69	GPC_B	9	265.6	28	360	170	281.6	582	0.145833244	-0.520382799	284	12	unc'd 6/38
smpl2_70	GPC_B	9	276	31	190	270	120	189	0.197702841	-0.364848465	286	13	unc'd 6/38
smpl2_71	GPC_B	9	270.6	30	360	180	175.1	383	0.142231068	-0.26364006	280	12	unc'd 6/38
smpl2_72	GPC_B	9	1089	110	1160	130	181.2	353.3	0.149746217	-0.397628264	1160	130	7/6
smpl2_73	GPC_B	9	281	32	450	230	208.8	323	0.200952597	-0.38615721	292	14	unc'd 6/38
smpl2_74	GPC_B	9	267.5	29	170	220	150.4	188.9	0.244208832	-0.675358892	281	12	unc'd 6/38
smpl2_75	GPC_B	9	194.2	21	541	160	1427	904	0.376460223	-8.371773265			
smpl2_76	GPC_B	9	272.3	29	230	160	303	427	0.22202095	-0.35952824	280	12	unc'd 6/38
smpl2_77	GPC_B	9	272	31	230	190	139.2	241.3	0.176963269	-0.467676395	285	12	unc'd 6/38
smpl2_78	GPC_B	9	416	57	2130	330	261.4	200	0.547911117	7.586658616			
smpl2_79	GPC_B	9	286	32	300	190	143.5	295	0.158023329	0.064146746	284	13	unc'd 6/38
smpl2_80	GPC_B	9	286.4	31	310	170	201.5	342.7	0.178651676	-0.557629045	303	13	unc'd 6/38
smpl2_81	GPC_B	9	343	39	1310	330	178	187	0.34611785	2.212084188			
smpl2_82	GPC_B	9	286.1	31	280	160	472	506	0.285158122	-0.844955781	301	13	unc'd 6/38

smpl2_83	GPC_B	9	308.1	33	281	160	350	533	0.206612552	-0.247319942	315	13	unc'd 6/38
smpl2_84	GPC_B	9	325	38	270	220	121	161	0.214974699	-1.407108784	364	16	unc'd 6/38
smpl2_85	GPC_B	9	223	72	1420	400	738	770	0.293382799	-0.914375498			
smpl2_86	GPC_B	9	274	30	150	190	188.9	226.8	0.23755529	-1.666211005	309	13	unc'd 6/38
smpl2_87	GPC_B	9	281.6	30	310	210	250.4	223.4	0.345298717	-0.905930504	294	13	unc'd 6/38
smpl2_88	GPC_B	9	299	34	150	220	101.2	157	0.199718185	-0.408615593	311	14	cor'd 6/38)
smpl2_89	GPC_B	9	330	36	400	170	319	348	0.281257184	-0.73058541	345	15	unc'd 6/38
smpl2_90	GPC_B	9	311	35	60	300	200.6	103.4	0.60605673	-1.219366038	320	14	unc'd 6/38
smpl2_91	GPC_B	9	297.4	32	850	250	553	489	0.361215031	-0.169801218			
smpl2_92	GPC_B	9	305	34	270	200	162.7	200	0.265051891	0.169475563	301	13	cor'd 6/38)
smpl2_93	GPC_B	9	296	33	520	200	506	503	0.323149836	-0.04715089			
smpl2_94	GPC_B	9	295.9	32	180	160	315.6	486	0.208622339	-0.027841611			
smpl2_95	GPC_B	9	283	37	400	250	66.5	117.3	0.17373596	-0.461741705	297	14	unc'd 6/38
smpl2_96	GPC_B	9	295.7	31	377	160	428	599	0.231260025	0.059020188	294	12	cor'd 6/38)
smpl2_97	GPC_B	9	301	33	385	160	216.2	378	0.188413938	0.218074712	293	13	cor'd 6/38)
smpl2_98	GPC_B	9	336	37	420	170	295.2	381	0.284186182	1.872554764	296	13	unc'd 6/38
smpl2_99	GPC_B	9	325.5	35	1520	150	364.2	204.1	0.637146077	4.0906247			
smpl2_100	GPC_B	9	291.5	31	200	180	196.3	319.5	0.201011224	0.159503244	287	12	unc'd 6/38
smpl2_101	GPC_B	9	288.8	31	260	170	309	361	0.277525819	0.093523551	287	13	unc'd 6/38
smpl2_102	GPC_B	9	350.9	37	330	170	254.2	288.2	0.28655639	0.178160734	347	15	unc'd 6/38
smpl2_103	GPC_B	9	262.5	28	202	160	462.9	588	0.244620931	-0.502225355	272	11	unc'd 6/38
smpl2_104	GPC_B	9	309	34	440	170	222.5	353	0.208632808	0.299033426	300	13	cor'd 6/38)
smpl2_105	GPC_B	9	294	34	360	280	138.9	166.8	0.273441019	0.279905078	288	13	cor'd 6/38)
smpl2_106	GPC_B	9	302.1	33	130	180	218.9	337	0.22480482	0.817126489	282	12	unc'd 6/38
smpl2_107	GPC_B	9	386	44	20	280	176	121	0.532481133	3.980212154			
smpl2_108	GPC_B	9	294.9	31	180	170	336	394	0.286483594	0.637506061	283	12	unc'd 6/38
smpl2_109	GPC_B	9	285	31	60	200	158.2	250.1	0.206476677	0.136717182	282	12	unc'd 6/38
smpl2_110	GPC_B	9	292	33	180	190	142	251.5	0.188665799	0.348328885	282	13	unc'd 6/38
smpl2_111	GPC_B	9	725	83	806	150	135	570	0.071808159	-0.127592661			
smpl2_112	GPC_B	9	287	33	130	280	90.1	102.4	0.295168744	0.632315628	276	12	unc'd 6/38
smpl2_113	GPC_B	9	286.6	31	376	160	266.5	484	0.182575845	0.263809476	278	12	cor'd 6/38)
smpl2_114	GPC_B	9	281	31	140	170	212	459	0.151617632	0.138330341	276	12	unc'd 6/38
smpl2_115	GPC_B	9	296.4	32	230	160	183	324	0.192316052	0.53497262	281	12	unc'd 6/38
smpl2_116	GPC_B	9	303.3	33	220	150	412	1385	0.105081138	0.458251672	277	12	unc'd 6/38
smpl2_117	GPC_B	9	297.3	32	290	180	337	470	0.241708919	0.569026487	284	12	unc'd 6/38
smpl2_118	GPC_B	9	286.7	31	550	200	256	255	0.338478783	0.832134565	272	12	cor'd 6/38)
smpl2_119	GPC_B	9	318.7	34	177	150	326.3	723	0.154005562	0.444309731	301	12	unc'd 6/38
smpl2_120	GPC_B	9	315	36	320	170	157.9	289	0.184718566	0.456746857	301	13	unc'd 6/38
smpl2_121	GPC_B	9	703	86	530	220	27.2	55.3	0.152668748	-0.113316382	714	32	cor'd 6/38)
smpl2_122	GPC_B	9	315	38	380	260	88.5	110	0.268453217	0.512433102	303	15	cor'd 6/38)
smpl2_123	GPC_B	9	281	30	170	210	262	218	0.374259219	-0.756266323	291	13	unc'd 6/38
smpl2_124	GPC_B	9	204.4	23	280	190	274	311.7	0.208942527	-4.105296758			
smpl2_125	GPC_B	9	311	36	90	230	184	285	0.210093719	0.120322423	307	14	unc'd 6/38

smpl2_126	GPC_B	9	293	32	140	180	278	393	0.223014066	-0.255448543	300	13	cor'd 6/38)
smpl2_127	GPC_B	9	298.9	32	190	170	466	959	0.165092201	0.436868904	284	12	unc'd 6/38
smpl2_128	GPC_B	9	298.1	32	350	170	328	382	0.268996208	-0.406100177			
smpl2_129	GPC_B	9	297.5	32	140	160	423	404	0.339131839	0.107811108	296	13	unc'd 6/38
smpl2_130	GPC_B	9	283	37	150	310	60.7	103	0.187347609	-0.134077238	287	14	unc'd 6/38
smpl2_131	GPC_B	9	300	32	200	170	296	390	0.246412121	0.106831487	298	13	unc'd 6/38
smpl2_132	GPC_B	9	559	59	500	160	741	195.6	1.187933396	-1.607245911	565	24	unc'd 6/38
smpl2_133	GPC_B	9	247.7	26	250	180	406	335	0.334125688	-3.299887719			
smpl2_134	GPC_B	9	284.7	30	143	160	846	938	0.292856396	0.119192474	283	12	unc'd 6/38
smpl2_135	GPC_B	9	293.4	32	253	150	415	842	0.162862904	0.208006904	286	12	unc'd 6/38
smpl2_136	GPC_B	9	276	31	160	190	254.9	343	0.234168084	-0.288683215	283	13	cor'd 6/38)
smpl2_137	GPC_B	9	282.8	30	140	160	356.3	528	0.215224627	-0.119094756	286	12	cor'd 6/38)
smpl2_138	GPC_B	9	268	30	110	210	126	189	0.198525167	-0.863574976	290	13	unc'd 6/38
smpl2_139	GPC_B	9	298	33	230	170	192.2	307.9	0.196296412	-0.245280626	306	13	cor'd 6/38)
smpl2_140	GPC_B	9	265.8	28	290	170	707	506	0.423706173	-1.617002444	283	12	unc'd 6/38
smpl2_141	GPC_B	9	275.9	29	250	160	376	468	0.25505552	-0.21388563	280	12	unc'd 6/38
smpl2_142	GPC_B	9	312.7	33	255	160	580.8	393.9	0.464664686	-0.593755948	319	14	unc'd 6/38
smpl2_143	GPC_B	9	295	33	320	230	209.9	194.3	0.354922277	0.391517051	288	13	cor'd 6/38)
smpl2_144	GPC_B	9	266.9	29	90	200	155.2	175.9	0.271194792	-0.729535344	282	12	cor'd 6/38)
smpl2_145	GPC_B	9	274.9	30	170	220	223.1	218.1	0.332327996	0.138889761	273	12	unc'd 6/38
smpl2_146	GPC_B	9	283.2	30	276	160	542	711	0.2387348	-0.369877004	291	13	unc'd 6/38
smpl2_147	GPC_B	9	280.8	30	230	170	340.4	447	0.245104476	-0.01956305	281	12	cor'd 6/38)
smpl2_148	GPC_B	9	275.1	29	254	160	345	292.6	0.381400857	0.069877514	274	12	unc'd 6/38
smpl2_149	GPC_B	9	237.6	26	280	170	664	608	0.318177066	-1.960465873			
smpl2_150	GPC_B	9	276.7	30	150	170	273.5	486	0.182336678	0.046023147	275	12	unc'd 6/38

* Propagated 2se uncertainties are about 1.5 to twice that of 2se using the calculations as given in Paton et al. (2010)
**three age types are allowed. Best age for grains >950 Ma is 207/206. For those younger, 206/238 is used, but if a 208Pb based common Pb correction makes the point more concordant it is used.

+dwell time=0.35 seconds

Sample GPC_C

	DateTime	Combined Sample	Individual sample	Duration(s)	207_235	207_235_Prop2SE*	206_238	206_238_Prop2SE	207_206	207_206_Prop2SE	208_232	208_232_Prop2SE	Age207_235	Age207_235_Prop2SE	Age206_238	Age206_238_Prop2SE	error corel
Output_1_0	09/12/2016 (6) 10:22:20.60	GPC_C	29	23.374	0.333	0.06	0.0418	0.0025	0.058	0.011	0.0109	0.0013	278	47	264	16	0.337451148
Output_1_1	09/12/2016 (6) 10:23:32.36	GPC_C	29	13.152	0.404	0.045	0.0442	0.0024	0.0674	0.0062	0.01378	0.00074	342	32	278.9	15	0.498342629
Output_1_2	09/12/2016 (6) 10:24:19.46	GPC_C	29	24.43	0.273	0.038	0.04109	0.0021	0.0486	0.0059	0.01294	0.00086	240	30	259.6	13	0.371883839
Output_1_3	09/12/2016 (6) 10:25:17.83	GPC_C	29	11.533	0.329	0.03	0.04238	0.0021	0.0556	0.0038	0.00942	0.00058	288	23	267.5	13	0.519845632
Output_1_4	09/12/2016 (6) 10:26:18.67	GPC_C	29	23.374	0.292	0.063	0.0415	0.0024	0.049	0.01	0.0128	0.0016	252	47	262	15	0.29345297
Output_1_5	09/12/2016 (6) 10:27:20.91	GPC_C	29	24.429	0.289	0.049	0.03835	0.002	0.0552	0.0088	0.0126	0.0011	248	39	242.5	12	0.300160969
Output_1_6	09/12/2016 (6) 10:29:20.48	GPC_C	29	24.429	0.27	0.029	0.03934	0.0019	0.0505	0.0044	0.01167	0.00052	240	23	248.7	12	0.449703969
Output_1_7	09/12/2016 (6) 10:30:22.02	GPC_C	29	24.781	0.29	0.037	0.03908	0.0019	0.0546	0.006	0.01162	0.00076	254	29	247.1	12	0.391411731
Output_1_8	09/12/2016 (6) 10:31:22.85	GPC_C	29	24.43	0.289	0.045	0.0416	0.0022	0.0516	0.0076	0.01243	0.0009	250	35	262.5	13	0.333490962
Output_1_9	09/12/2016 (6) 10:32:28.61	GPC_C	29	16.342	0.252	0.084	0.0398	0.0023	0.045	0.015	0.0115	0.0019	204	66	251.8	14	0.169370695
Output_1_10	09/12/2016 (6) 10:36:55.17	GPC_C	29	23.726	0.276	0.051	0.0393	0.0021	0.0514	0.0092	0.0121	0.0015	236	43	248.3	13	0.276173663
Output_1_11	09/12/2016 (6) 10:37:58.82	GPC_C	29	23.375	0.303	0.075	0.0412	0.0023	0.051	0.013	0.0121	0.0019	243	60	260.1	14	0.212991043
Output_1_12	09/12/2016 (6) 10:38:54.38	GPC_C	29	24.078	0.278	0.047	0.0405	0.0021	0.0527	0.0086	0.0119	0.00091	246	39	256	13	0.305045676
Output_1_13	09/12/2016 (6) 10:42:28.19	GPC_C	29	18.803	0.264	0.068	0.0392	0.0022	0.05	0.013	0.01	0.0014	219	57	247.7	14	0.212209816
Output_1_14	09/12/2016 (6) 10:43:36.93	GPC_C	29	11.253	0.341	0.037	0.0467	0.0024	0.0525	0.0041	0.01422	0.00088	297	28	294.3	15	0.475577319
Output_1_15	09/12/2016 (6) 10:47:00.02	GPC_C	29	14.934	3.51	0.33	0.2709	0.014	0.0945	0.006	0.0775	0.0044	1531	80	1545	69	0.6497134
Output_1_16	09/12/2016 (6) 10:47:56.64	GPC_C	29	23.726	0.318	0.029	0.04382	0.0022	0.0533	0.0032	0.01085	0.00065	280	22	276.4	13	0.513615665
Output_1_17	09/12/2016 (6) 10:48:53.26	GPC_C	29	24.078	0.27	0.059	0.0372	0.0021	0.053	0.011	0.0109	0.0013	227	47	235.1	13	0.258022897
Output_1_18	09/12/2016 (6) 10:49:49.52	GPC_C	29	24.43	0.466	0.055	0.0597	0.003	0.0576	0.0058	0.0189	0.0014	392	39	373.6	18	0.435851528
Output_1_19	09/12/2016 (6) 10:50:52.35	GPC_C	30	6.0595	0.22	0.11	0.0385	0.0028	0.04	0.02	0.0111	0.0023	180	110	243	17	0.113735276
Output_1_20	09/12/2016 (6) 12:01:27.77	GPC_C	30	8.7242	0.293	0.077	0.0386	0.0023	0.053	0.014	0.0122	0.0023	251	61	244.4	14	0.229419224
Output_1_21	09/12/2016 (6) 12:02:26.23	GPC_C	30	24.077	0.286	0.033	0.03976	0.0019	0.0529	0.0051	0.01183	0.00067	253	26	251.3	12	0.421391038
Output_1_22	09/12/2016 (6) 12:03:25.66	GPC_C	30	23.375	0.4	0.12	0.036	0.0025	0.093	0.027	0.009	0.0022	353	87	228	15	0.257908203

Output_1_23	09/12/2016 (6) 12:04:22.98	GPC_C	30	24.077	0.45	0.04	0.0558	0.0027	0.0595	0.0037	0.01879	0.00087	379	30	349.8	17	0.523222683
Output_1_24	09/12/2016 (6) 12:05:21.71	GPC_C	30	23.022	0.285	0.062	0.0389	0.0021	0.053	0.011	0.01205	0.00098	247	48	245.8	13	0.2626039
Output_1_25	09/12/2016 (6) 12:06:23.60	GPC_C	30	17.396	0.292	0.048	0.037	0.0021	0.0574	0.0083	0.01234	0.00094	254	37	233.9	13	0.356478335
Output_1_26	09/12/2016 (6) 12:07:25.14	GPC_C	30	23.022	0.275	0.027	0.03863	0.0019	0.0521	0.0039	0.01215	0.00059	246	22	244.3	12	0.48141409
Output_1_27	09/12/2016 (6) 12:08:40.39	GPC_C	30	24.078	0.266	0.031	0.03965	0.002	0.0489	0.0048	0.01244	0.00071	240	27	250.6	12	0.391643353
Output_1_28	09/12/2016 (6) 12:09:38.77	GPC_C	30	24.078	0.285	0.035	0.0388	0.002	0.0532	0.0057	0.01204	0.00067	251	27	245.5	13	0.441655531
Output_1_29	09/12/2016 (6) 12:10:59.30	GPC_C	30	24.078	0.251	0.058	0.0386	0.0021	0.049	0.011	0.01215	0.0009	211	48	244.3	13	0.227768222
Output_1_30	09/12/2016 (6) 12:15:31.38	GPC_C	30	23.992	0.223	0.077	0.0389	0.0022	0.044	0.014	0.0131	0.0032	170	69	245.9	14	0.138911506
Output_1_31	09/12/2016 (6) 12:16:31.27	GPC_C	30	24.077	0.327	0.056	0.0509	0.0026	0.0468	0.0074	0.01633	0.0011	283	46	320	16	0.294012843
Output_1_32	09/12/2016 (6) 12:17:35.56	GPC_C	30	18.157	0.257	0.085	0.0375	0.0024	0.052	0.017	0.0128	0.0017	205	67	237	15	0.190119949
Output_1_33	09/12/2016 (6) 12:18:27.66	GPC_C	30	24.078	0.383	0.035	0.0511	0.0024	0.0548	0.0036	0.01605	0.00069	328	26	321.2	15	0.507597129
Output_1_34	09/12/2016 (6) 12:19:23.67	GPC_C	30	4.3621	0.36	0.18	0.0411	0.0034	0.06	0.028	0.0119	0.0022	290	130	260	21	0.177322215
Output_1_35	09/12/2016 (6) 12:20:51.85	GPC_C	30	23.726	0.288	0.039	0.03849	0.0019	0.0534	0.0064	0.01237	0.00077	256	29	243.4	12	0.399058584
Output_1_36	09/12/2016 (6) 12:21:53.74	GPC_C	30	20.21	0.365	0.044	0.0471	0.0024	0.0559	0.0057	0.01495	0.00083	312	32	296.7	15	0.442127587
Output_1_37	09/12/2016 (6) 12:22:53.17	GPC_C	30	18.1	3.85	0.36	0.2867	0.015	0.0961	0.0058	0.088	0.0048	1593	73	1624	74	0.705100171
Output_1_38	09/12/2016 (6) 12:24:12.99	GPC_C	30	20.561	0.241	0.096	0.0421	0.0028	0.039	0.016	0.0146	0.0021	176	80	266	17	0.139232015
Output_1_39	09/12/2016 (6) 12:25:35.28	GPC_C	30	24.078	0.352	0.039	0.0499	0.0025	0.0507	0.0045	0.01689	0.001	306	32	314	16	0.43802875
Output_1_40	09/12/2016 (6) 12:33:34.94	GPC_C	30	23.024	0.261	0.064	0.0382	0.0022	0.048	0.011	0.0131	0.0014	226	50	241.6	14	0.253373666
Output_1_41	09/12/2016 (6) 12:34:34.38	GPC_C	30	23.726	0.257	0.025	0.02548	0.0014	0.0727	0.0044	0.00872	0.00047	232	20	162.2	8.7	0.528285115
Output_1_42	09/12/2016 (6) 12:35:32.05	GPC_C	30	24.078	0.281	0.043	0.0394	0.0021	0.0512	0.007	0.01248	0.00094	244	34	248.9	13	0.350980351
Output_1_43	09/12/2016 (6) 12:36:35.35	GPC_C	30	23.726	0.236	0.035	0.03904	0.002	0.0444	0.0063	0.01134	0.0008	215	31	246.8	12	0.319540136
Output_1_44	09/12/2016 (6) 12:38:18.38	GPC_C	30	12.478	0.249	0.057	0.038	0.0022	0.047	0.01	0.012	0.0014	217	47	240.4	13	0.242236587
Output_1_45	09/12/2016 (6) 12:39:30.82	GPC_C	30	7.9371	0.366	0.051	0.0484	0.0028	0.0531	0.0059	0.0154	0.0014	314	37	304	17	0.42874223
Output_1_46	09/12/2016 (6) 12:40:26.03	GPC_C	30	21.266	0.27	0.033	0.0395	0.0021	0.0493	0.0052	0.01405	0.0011	239	26	249.6	13	0.431826273
Output_1_47	09/12/2016 (6) 12:41:56.06	GPC_C	30	23.021	0.303	0.051	0.0397	0.0021	0.0554	0.0087	0.01291	0.0009	280	38	250.9	13	0.356673266
Output_1_48	09/12/2016 (6) 12:43:16.86	GPC_C	30	4.8223	0.341	0.083	0.033	0.0039	0.075	0.015	0.013	0.0028	293	59	209	25	0.510717555

Output_1_49	09/12/2016 (6) 12:44:02.66	GPC_C	30	24.079	0.368	0.054	0.0502	0.0027	0.0531	0.0071	0.0161	0.0012	309	40	315.6	17	0.384179127
Output_1_50	09/12/2016 (6) 12:48:42.93	GPC_C	30	19.508	0.373	0.041	0.048	0.0025	0.0556	0.0046	0.01607	0.00094	319	30	302	15	0.467013054
Output_1_51	09/12/2016 (6) 12:49:36.03	GPC_C	30	24.077	0.2788	0.024	0.03927	0.0019	0.0512	0.0029	0.01262	0.0005	250.7	20	248.3	12	0.518138336
Output_1_52	09/12/2016 (6) 12:50:38.62	GPC_C	30	8.5286	0.246	0.056	0.0364	0.0022	0.048	0.011	0.0114	0.0011	218	46	230.5	14	0.276611919
Output_1_53	09/12/2016 (6) 12:51:37.73	GPC_C	30	16.317	0.268	0.028	0.03879	0.0019	0.0504	0.0043	0.012	0.00049	240	23	245.3	12	0.454655666
Output_1_54	09/12/2016 (6) 12:52:28.69	GPC_C	30	24.076	2.96	0.27	0.2268	0.013	0.094	0.005	0.0794	0.0036	1388	68	1316	66	0.715335512
Output_1_55	09/12/2016 (6) 12:53:24.96	GPC_C	30	16.883	0.29	0.046	0.0393	0.0021	0.0527	0.0073	0.0125	0.0011	260	33	248.3	13	0.38133249
Output_1_56	09/12/2016 (6) 12:54:21.22	GPC_C	30	24.077	0.231	0.065	0.0381	0.0021	0.044	0.012	0.01206	0.00087	188	56	241	13	0.178192456
Output_1_57	09/12/2016 (6) 12:55:40.35	GPC_C	30	18.804	0.297	0.059	0.0407	0.0024	0.0493	0.0085	0.0119	0.0022	254	43	257.4	15	0.325485143
Output_1_58	09/12/2016 (6) 12:56:35.21	GPC_C	30	10.987	0.488	0.048	0.0643	0.0032	0.0539	0.0042	0.01675	0.00093	402	33	401.9	19	0.499057678
Output_1_59	09/12/2016 (6) 12:57:40.61	GPC_C	30	17.396	0.332	0.037	0.04716	0.0023	0.0498	0.0045	0.01409	0.00068	289	28	297.1	14	0.437379721
Output_1_60	09/12/2016 (6) 13:02:21.94	GPC_C	30	22.671	0.29	0.066	0.0392	0.0021	0.054	0.012	0.012	0.0016	240	52	247.7	13	0.235420343
Output_1_61	09/12/2016 (6) 13:03:18.56	GPC_C	30	24.076	0.275	0.043	0.0386	0.002	0.0516	0.0077	0.01223	0.0009	239	35	244.3	13	0.341522411
Output_1_62	09/12/2016 (6) 13:04:32.41	GPC_C	30	26.891	0.276	0.036	0.03988	0.002	0.0506	0.0058	0.01294	0.00079	242	29	252.1	12	0.369158417
Output_1_63	09/12/2016 (6) 13:05:30.78	GPC_C	30	24.43	0.284	0.05	0.0384	0.0021	0.0525	0.0087	0.0128	0.0013	244	39	242.7	13	0.317751
Output_1_64	09/12/2016 (6) 13:06:29.16	GPC_C	30	24.078	0.3	0.039	0.04361	0.0022	0.0511	0.006	0.01272	0.00066	266	32	275.1	13	0.365615735
Output_1_65	09/12/2016 (6) 13:07:29.29	GPC_C	30	24.781	0.283	0.059	0.0388	0.0021	0.053	0.011	0.0112	0.0013	243	49	245.3	13	0.254186334
Output_1_66	09/12/2016 (6) 13:08:31.89	GPC_C	30	18.451	0.228	0.068	0.0392	0.0023	0.046	0.014	0.0116	0.0011	201	59	248.1	14	0.188783943
Output_1_67	09/12/2016 (6) 13:09:26.04	GPC_C	30	20.912	0.298	0.089	0.0373	0.0024	0.058	0.017	0.0134	0.0024	246	65	236	15	0.233876326
Output_1_68	09/12/2016 (6) 13:10:18.97	GPC_C	30	22.489	3.22	0.29	0.2535	0.013	0.0923	0.0057	0.0719	0.0038	1459	76	1456	64	0.644911283
Output_1_69	09/12/2016 (6) 13:11:17.87	GPC_C	30	23.374	0.251	0.051	0.0379	0.002	0.0481	0.0097	0.012	0.0012	216	41	239.5	12	0.255222663
Output_1_70	09/12/2016 (6) 13:18:43.42	GPC_C	30	23.726	0.275	0.044	0.039	0.0021	0.0501	0.0069	0.01188	0.00074	239	35	246.3	13	0.339069173
Output_1_71	09/12/2016 (6) 13:19:43.56	GPC_C	30	23.024	0.328	0.046	0.04652	0.0023	0.0516	0.0065	0.01342	0.00069	281	36	293.1	14	0.349343865
Output_1_72	09/12/2016 (6) 13:20:38.77	GPC_C	30	23.727	0.293	0.046	0.03899	0.002	0.0547	0.0079	0.01111	0.0008	252	37	246.5	13	0.338045222
Output_1_73	09/12/2016 (6) 13:21:40.60	GPC_C	30	6.8401	0.319	0.062	0.0383	0.0021	0.0587	0.01	0.0123	0.0013	277	48	242.3	13	0.295767247
Output_1_74	09/12/2016 (6) 13:22:46.51	GPC_C	30	8.7242	1.23	0.44	0.0409	0.0044	0.189	0.051	0.047	0.016	710	180	258	27	0.381560543

Output_1_75	09/12/2016 (6) 13:23:46.94	GPC_C	30	18.413	0.375	0.041	0.05619	0.0027	0.0497	0.0045	0.01647	0.00081	325	32	352.4	17	0.439974663
Output_1_76	09/12/2016 (6) 13:24:38.95	GPC_C	30	23.726	0.234	0.06	0.0398	0.0023	0.043	0.01	0.0121	0.0012	204	48	251.8	14	0.229965555
Output_1_77	09/12/2016 (6) 13:25:36.62	GPC_C	30	24.076	0.33	0.047	0.0463	0.0023	0.0519	0.0067	0.01454	0.00076	282	37	291.9	14	0.343326176
Output_1_78	09/12/2016 (6) 13:26:32.54	GPC_C	30	23.727	0.234	0.073	0.0388	0.0022	0.047	0.015	0.0117	0.0022	195	63	245.3	14	0.173960909
Output_1_79	09/12/2016 (6) 13:27:28.45	GPC_C	30	24.077	0.36	0.047	0.0497	0.0025	0.0531	0.0058	0.01558	0.00094	314	31	312.3	15	0.437479116
Output_1_80	09/12/2016 (6) 13:32:02.39	GPC_C	30	4.581	0.409	0.056	0.0539	0.0033	0.0543	0.0076	0.0163	0.0012	346	40	338	20	0.455621422
Output_1_81	09/12/2016 (6) 13:33:02.17	GPC_C	30	14.64	0.546	0.048	0.0695	0.0034	0.0562	0.0033	0.02101	0.00093	441	32	433.1	20	0.536897549
Output_1_82	09/12/2016 (6) 13:34:05.12	GPC_C	31	20.558	0.343	0.044	0.04107	0.0021	0.0623	0.0074	0.01298	0.00075	300	34	259.4	13	0.404421284
Output_1_83	09/12/2016 (6) 13:37:02.71	GPC_C	31	13.879	0.266	0.073	0.0413	0.0029	0.048	0.014	0.012	0.0021	223	61	261	18	0.244469749
Output_1_84	09/12/2016 (6) 13:37:50.18	GPC_C	31	24.429	0.261	0.044	0.0396	0.0022	0.0492	0.0078	0.01242	0.00096	239	31	250.3	13	0.371728951
Output_1_85	09/12/2016 (6) 13:39:02.54	GPC_C	31	8.3389	3.58	0.31	0.2651	0.013	0.0988	0.0058	0.0743	0.0034	1543	69	1516	66	0.697570046
Output_1_86	09/12/2016 (6) 13:39:44.12	GPC_C	31	23.726	3.602	0.29	0.2781	0.013	0.0941	0.0047	0.0785	0.0033	1548	65	1581	66	0.705043883
Output_1_87	09/12/2016 (6) 13:40:40.74	GPC_C	31	23.375	0.277	0.034	0.03813	0.0019	0.0528	0.0053	0.01148	0.00079	245	26	241.2	12	0.424478265
Output_1_88	09/12/2016 (6) 13:41:39.11	GPC_C	31	23.023	0.282	0.06	0.0401	0.0023	0.052	0.011	0.0121	0.001	236	48	253.5	14	0.262043494
Output_1_89	09/12/2016 (6) 13:42:36.79	GPC_C	31	23.374	0.313	0.055	0.0393	0.0022	0.0558	0.0089	0.01151	0.00097	266	41	248.3	14	0.343540851
Output_1_90	09/12/2016 (6) 13:49:14.51	GPC_C	31	21.617	0.463	0.043	0.06133	0.0029	0.0549	0.0037	0.01722	0.00076	384	30	383.7	18	0.514791446
Output_1_91	09/12/2016 (6) 13:50:38.91	GPC_C	31	20.644													
Output_1_92	09/12/2016 (6) 13:52:01.90	GPC_C	31	21.265	0.36	0.041	0.0507	0.0026	0.0515	0.0049	0.01505	0.00074	308	31	319	16	0.446018504
Output_1_93	09/12/2016 (6) 13:53:15.04	GPC_C	31	8.044	0.35	0.11	0.0442	0.003	0.056	0.016	0.0138	0.0016	288	80	279	19	0.238110008
Output_1_94			31														
Output_1_95	09/12/2016 (6) 13:56:52.37	GPC_C	31	24.076	0.294	0.042	0.04156	0.0021	0.052	0.0068	0.01156	0.00074	255	34	262.5	13	0.34818653
Output_1_96	09/12/2016 (6) 13:57:51.10	GPC_C	31	23.725	0.32	0.057	0.04103	0.0021	0.0561	0.0089	0.0111	0.0011	270	44	259.1	13	0.294253147
Output_1_97	09/12/2016 (6) 13:59:16.90	GPC_C	31	23.373	0.323	0.049	0.0439	0.0022	0.0539	0.0074	0.0135	0.0011	276	37	276.6	14	0.353220304
Output_1_98	09/12/2016 (6) 14:00:16.33	GPC_C	31	23.023	0.395	0.039	0.05249	0.0025	0.0547	0.0039	0.01522	0.00071	336	28	329.8	15	0.479075887
Output_1_99	09/12/2016 (6) 14:01:17.17	GPC_C	31	24.078	0.258	0.068	0.0409	0.0023	0.044	0.012	0.0134	0.0018	210	56	258.2	14	0.199253557
Output_1_100	09/12/2016 (6) 14:12:33.76	GPC_C	31	21.616	0.252	0.049	0.0394	0.0023	0.047	0.0088	0.0139	0.0014	218	39	249.2	14	0.299605021
Output_1_101	09/12/2016 (6)	GPC_C	31	23.727	0.305	0.039	0.03927	0.002	0.0562	0.006	0.0133	0.0012	266	30	248.2	12	0.394008682

	14:13:26.51																
Output_1_102	09/12/2016 (6) 14:14:22.42	GPC_C	31	22.319	0.254	0.053	0.0387	0.0023	0.0458	0.0087	0.0123	0.0014	218	42	244.4	14	0.284996239
Output_1_103	09/12/2016 (6) 14:15:24.32	GPC_C	32	15.989	0.272	0.026	0.0357	0.0019	0.0548	0.0039	0.00958	0.00062	244	20	226.1	12	0.543512939
Output_1_104	09/12/2016 (6) 14:16:10.38	GPC_C	32	24.781	0.245	0.064	0.0389	0.0022	0.046	0.012	0.0124	0.0017	201	53	245.8	13	0.196660309
Output_1_105	09/12/2016 (6) 14:17:08.06	GPC_C	32	22.32	0.251	0.044	0.0385	0.002	0.047	0.0076	0.0113	0.0015	220	35	243.8	13	0.317794082
Output_1_106	09/12/2016 (6) 14:18:13.82	GPC_C	32	16.186	0.404	0.046	0.0461	0.0024	0.0627	0.0059	0.01372	0.00076	341	34	290.6	15	0.459738315
Output_1_107	09/12/2016 (6) 14:19:08.32	GPC_C	32	24.077	0.335	0.031	0.04827	0.0023	0.0509	0.0033	0.01439	0.00055	293	24	303.8	14	0.4903248
Output_1_108	09/12/2016 (6) 14:20:03.53	GPC_C	32	24.078	0.34	0.035	0.0488	0.0024	0.0514	0.0042	0.01443	0.00068	298	28	306.9	15	0.461477555
Output_1_109	09/12/2016 (6) 14:20:58.04	GPC_C	32	14.831	0.514	0.058	0.0676	0.0033	0.0548	0.0053	0.01961	0.0011	417	39	421.6	20	0.452361132
Output_1_110	09/12/2016 (6) 14:25:21.08	GPC_C	32	26.892	0.272	0.037	0.03784	0.0019	0.052	0.0061	0.01154	0.00091	239	30	239.4	12	0.370855547
Output_1_111	09/12/2016 (6) 14:26:22.97	GPC_C	32	22.319	0.336	0.039	0.04624	0.0023	0.0529	0.005	0.01404	0.00063	290	30	291.4	14	0.421214942
Output_1_112	09/12/2016 (6) 14:27:14.32	GPC_C	32	25.133	0.333	0.031	0.04692	0.0022	0.0516	0.0036	0.01446	0.0006	290	24	295.6	14	0.496697456
Output_1_113	09/12/2016 (6) 14:28:11.29	GPC_C	32	23.375	0.287	0.037	0.0388	0.002	0.0538	0.0061	0.01214	0.00088	252	29	245.4	12	0.391079845
Output_1_114	09/12/2016 (6) 14:29:06.85	GPC_C	32	23.725	0.247	0.026	0.03895	0.0019	0.046	0.0039	0.01158	0.00071	222	21	246.3	12	0.457886203
Output_1_115	09/12/2016 (6) 14:29:59.95	GPC_C	32	23.726	0.296	0.027	0.0412	0.0023	0.0528	0.0033	0.01005	0.00074	262	21	259.9	14	0.557791561
Output_1_116	09/12/2016 (6) 14:30:57.27	GPC_C	32	15.285	2.78	0.36	0.214	0.023	0.0924	0.005	0.0595	0.0056	1309	120	1240	130	0.752793145
Output_1_117	09/12/2016 (6) 14:31:54.94	GPC_C	32	8.2067	0.33	0.033	0.0445	0.0023	0.053	0.0045	0.01387	0.00064	289	25	280.4	14	0.499886448
Output_1_118	09/12/2016 (6) 14:32:53.32	GPC_C	32	18.1	0.286	0.056	0.0387	0.0022	0.0508	0.0089	0.0125	0.0012	246	43	245	13	0.290471208
Output_1_119	09/12/2016 (6) 14:33:47.47	GPC_C	32	21.966	0.279	0.026	0.03875	0.0019	0.0523	0.0036	0.01155	0.00049	251	20	245.1	12	0.52351545
Output_1_120	09/12/2016 (6) 14:39:27.95	GPC_C	32	8.5275	0.312	0.034	0.0435	0.0023	0.0525	0.0042	0.01173	0.00053	274	26	274.5	14	0.473429947
Output_1_121	09/12/2016 (6) 14:40:10.78	GPC_C	32	18.803	0.287	0.068	0.0395	0.0024	0.053	0.012	0.0122	0.0012	239	54	250	15	0.256659917
Output_1_122	09/12/2016 (6) 14:41:02.12	GPC_C	32	21.616	0.269	0.059	0.0397	0.0023	0.0476	0.01	0.0118	0.0011	227	47	250.8	14	0.260310679
Output_1_123	09/12/2016 (6) 14:41:59.47	GPC_C	32														
Output_1_124	09/12/2016 (6) 14:42:52.89	GPC_C	32	22.319	0.338	0.031	0.04776	0.0023	0.0515	0.0035	0.0142	0.00056	295	24	300.7	14	0.496693165
Output_1_125	09/12/2016 (6) 14:43:51.62	GPC_C	32	17.696	0.268	0.028	0.04016	0.0019	0.0482	0.0039	0.01214	0.00054	239	22	253.8	12	0.456898721
Output_1_126	09/12/2016 (6) 14:44:42.61	GPC_C	32	8.9959	0.88	0.19	0.0557	0.0039	0.112	0.02	0.0322	0.0051	650	110	349	24	0.376461194
Output_1_127	09/12/2016 (6)	GPC_C	32	14.479	0.269	0.04	0.0386	0.002	0.0502	0.0067	0.01172	0.00082	238	32	243.9	13	0.368522085

14:45:42.74

	Combined Sample	Individual sample	Age208_232	Age208_232_Prop2SE	Age207_206	Age207_206_Prop2SE	Th(ppm)	U(ppm)	calc208/206	PERCENT 206 THAT IS COMMON	overall best concordant age	2 s.e. uncert	age type**
Output_1_0	GPC_C	29	220	26	270	350	146	120.1	0.325198877	-3.931497912			
Output_1_1	GPC_C	29	277	15	820	170	501	387	0.414040364	-0.196406438			
Output_1_2	GPC_C	29	260	17	30	230	76.9	149.6	0.166066432	0.009425796	260	13	cor'd 6/38)
Output_1_3	GPC_C	29	189.5	12	410	150	566	757	0.170490221	-3.809433603			
Output_1_4	GPC_C	29	256	32	30	350	38.03	73.8	0.163050002	-0.167044408	263	15	cor'd 6/38)
Output_1_5	GPC_C	29	252	22	180	310	62.6	94.6	0.223037221	0.494065777	241	12	cor'd 6/38)
Output_1_6	GPC_C	29	234.5	10	160	170	237	278.3	0.259155609	-0.869094068	249	12	unc'd 6/38
Output_1_7	GPC_C	29	233	15	260	220	91.3	152.3	0.182856928	-0.564066743	247	12	unc'd 6/38
Output_1_8	GPC_C	29	250	18	80	270	76.6	110.8	0.211912112	-0.595333022	263	13	unc'd 6/38
Output_1_9	GPC_C	29	230	38			31.6	62.6	0.149629247	-0.690153515			
Output_1_10	GPC_C	29	244	30	30	340	37.4	65.8	0.17952606	-0.209656029	249	13	cor'd 6/38)
Output_1_11	GPC_C	29	243	37			28.76	64.6	0.134132337	-0.488251379			
Output_1_12	GPC_C	29	239	18	80	290	83.2	100.1	0.250536011	-0.970610682	256	13	unc'd 6/38
Output_1_13	GPC_C	29	200	28			31.78	64.8	0.128345839	-1.549786315			
Output_1_14	GPC_C	29	285	17	270	170	932	707	0.411782785	-0.766923683	294	15	unc'd 6/38
Output_1_15	GPC_C	29	1507	82	1494	120	66.5	286	0.068239727	-0.080027563	1494	120	7/6
Output_1_16	GPC_C	29	218	13	312	130	1547	1373	0.286197683	-4.444552371			
Output_1_17	GPC_C	29	219	26	60	390	45.7	80.4	0.170856963	-0.670512916			
Output_1_18	GPC_C	29	379	27	470	210	71.6	117.8	0.197398649	0.12792473	373	18	cor'd 6/38)
Output_1_19	GPC_C	30	222	47			39.7	100	0.117419906	-0.549532356			
Output_1_20	GPC_C	30	245	46	140	500	40.1	104.5	0.124419823	0.024640148			
Output_1_21	GPC_C	30	238	13	230	200	119.8	236.4	0.154680899	-0.462183409	251	12	unc'd 6/38
Output_1_22	GPC_C	30	189	46	600	600	21.12	43.19	0.125412172	-1.686932661			
Output_1_23	GPC_C	30	376	17	545	130	259	498	0.17966024	0.652444437	348	17	cor'd 6/38)
Output_1_24	GPC_C	30	242	19	140	380	59.1	80.6	0.233012305	-0.203828131	246	13	unc'd 6/38
Output_1_25	GPC_C	30	248	19	330	300	76	133	0.195507922	0.568121045	233	13	cor'd 6/38)
Output_1_26	GPC_C	30	244.1	12	270	150	240	315	0.245833594	-0.012999521			
Output_1_27	GPC_C	30	250	14	120	210	158.4	205.5	0.248090144	-0.041917784	251	12	cor'd 6/38)
Output_1_28	GPC_C	30	242	13	260	220	170	210	0.257699372	-0.203801685	246	13	unc'd 6/38
Output_1_29	GPC_C	30	244	18			70.7	70.6	0.323364737	-0.003658736			
Output_1_30	GPC_C	30	261	64			13	49.7	0.090364454	0.293005722			
Output_1_31	GPC_C	30	327	21	0	300	80.2	77.9	0.338839697	0.433502888	320	16	unc'd 6/38
Output_1_32	GPC_C	30	256	34			34.91	58.3	0.209676118	0.852357676			
Output_1_33	GPC_C	30	321.8	14	360	140	295	503	0.188971861	0.017262688			
Output_1_34	GPC_C	30	238	45	200	900	36.7	72.5	0.150356487	-0.672387665			
Output_1_35	GPC_C	30	248	15	290	230	91	154	0.194819055	0.208092278	243	12	cor'd 6/38)
Output_1_36	GPC_C	30	300	17	330	200	233	246	0.308411151	0.187289178	296	15	cor'd 6/38)
Output_1_37	GPC_C	30	1703	90	1527	110	195	4290	0.01431269	0.031326835	1527	110	7/6
Output_1_38	GPC_C	30	292	41			23.61	41.8	0.200946033	0.978351744			
Output_1_39	GPC_C	30	338	20	200	190	101.2	161	0.218259277	0.843009372	314	16	unc'd 6/38

Output_1_40	GPC_C	30	262	28			43.4	77.7	0.196501385	0.839672671			
Output_1_41	GPC_C	30	175.4	9.5	1005	140	2724	3680	0.259875488	1.068502755			
Output_1_42	GPC_C	30	251	19	100	270	77	162	0.154448269	0.050174964	249	13	cor'd 6/38)
Output_1_43	GPC_C	30	228	16			66.3	126.4	0.15629989	-0.679349869	249	12	cor'd 6/38)
Output_1_44	GPC_C	30	241	28			48	91.8	0.16938899	0.02490109			
Output_1_45	GPC_C	30	308	28	280	230	212	360	0.19221961	0.137660349	304	17	cor'd 6/38)
Output_1_46	GPC_C	30	282	21	90	210	105.3	160	0.240146681	1.468329372	250	13	unc'd 6/38
Output_1_47	GPC_C	30	259	18	380	290	74.9	93.2	0.268096172	0.470058255	250	13	cor'd 6/38)
Output_1_48	GPC_C	30	261	56	920	390	370	400	0.373817921	4.154510814			
Output_1_49	GPC_C	30	322	23	160	260	51.3	107.9	0.15642532	0.177360123	315	17	cor'd 6/38)
Output_1_50	GPC_C	30	322	19	370	180	247	304	0.279053183	0.949157027	302	15	unc'd 6/38
Output_1_51	GPC_C	30	253.6	10	244	130	488	1084	0.148415058	0.156345198	248	12	unc'd 6/38
Output_1_52	GPC_C	30	229	21			91.8	133.1	0.221593525	-0.070877209			
Output_1_53	GPC_C	30	241.1	9.8	170	180	349	406	0.272803433	-0.264646569	245	12	unc'd 6/38
Output_1_54	GPC_C	30	1544	68	1492	100	89.6	283	0.113707209	0.820718382	1492	100	7/6
Output_1_55	GPC_C	30	250	22	270	260	87.3	159	0.179152781	0.096994757	248	13	cor'd 6/38)
Output_1_56	GPC_C	30	242	17			62.4	61.8	0.327874332	0.096631535			
Output_1_57	GPC_C	30	238	44	50	320	66	119	0.166356011	-0.659628195	257	15	unc'd 6/38
Output_1_58	GPC_C	30	336	19	330	170	183.2	457	0.107127774	-1.074359981	402	19	unc'd 6/38
Output_1_59	GPC_C	30	283	14	170	190	271	239	0.347534208	-1.018003941	297	14	unc'd 6/38
Output_1_60	GPC_C	30	240	33			28.6	58.9	0.152487727	-0.222264131			
Output_1_61	GPC_C	30	246	18	90	290	53.2	83.4	0.207335518	0.069602413	244	13	cor'd 6/38)
Output_1_62	GPC_C	30	260	16	110	230	109.5	154	0.236679965	0.3820262	252	12	unc'd 6/38
Output_1_63	GPC_C	30	258	26	120	310	63.5	138.1	0.157234471	0.447723914	243	13	unc'd 6/38
Output_1_64	GPC_C	30	255	13	130	220	131.9	177	0.222977749	-0.931802513	275	13	unc'd 6/38
Output_1_65	GPC_C	30	225	26	70	380	43.45	72	0.178703292	-0.851966996			
Output_1_66	GPC_C	30	233	22			54.7	72.8	0.228095565	-0.784069289			
Output_1_67	GPC_C	30	268	47	20	500	22.8	41	0.20494434	1.319133537			
Output_1_68	GPC_C	30	1403	73	1455	130	26.8	159	0.049043061	-0.089068284	1455	130	7/6
Output_1_69	GPC_C	30	240	24			46.9	87.9	0.17330655	0.048749166	240	12	cor'd 6/38)
Output_1_70	GPC_C	30	239	15	100	280	76	113.3	0.209616028	-0.372897715	246	13	unc'd 6/38
Output_1_71	GPC_C	30	269	14	140	250	143.4	141.4	0.300124551	-1.499020449	293	14	unc'd 6/38
Output_1_72	GPC_C	30	223	16	200	290	71.7	110.3	0.19001743	-1.055667383	247	13	unc'd 6/38
Output_1_73	GPC_C	30	248	25	430	380	177	293	0.19902194	0.205010098	242	13	cor'd 6/38)
Output_1_74	GPC_C	30	910	300	2290	480	604	1240	0.574220609	21.50631781			
Output_1_75	GPC_C	30	330	16	140	180	185	312	0.17829562	-0.633009465	355	17	cor'd 6/38)
Output_1_76	GPC_C	30	243	23			38.33	60.8	0.196619465	-0.365156728			
Output_1_77	GPC_C	30	292	15	140	260	114.6	129.2	0.28575543	0.000340775	292	14	cor'd 6/38)
Output_1_78	GPC_C	30	235	43			25.32	58.8	0.133207747	-0.299582054			
Output_1_79	GPC_C	30	312	19	320	220	126	152.3	0.266054543	-0.009694369	312	15	unc'd 6/38
Output_1_80	GPC_C	30	327	24	330	290	393	524	0.232674653	-0.448457118	338	20	unc'd 6/38
Output_1_81	GPC_C	30	420	18	440	130	456	979	0.144448279	-0.228298276	433	20	unc'd 6/38
Output_1_82	GPC_C	31	261	15	510	230	207.5	194.7	0.345534257	0.091649241	259	13	unc'd 6/38

Output_1_83	GPC_C	31	240	42			44.5	73	0.181701	-0.7897914			
Output_1_84	GPC_C	31	249	19			66.7	100.3	0.21396379	-0.03964039	250	13	cor'd 6/38)
Output_1_85	GPC_C	31	1448	63	1592	120	125.7	210.6	0.17161094	-0.405510645	1592	120	7/6
Output_1_86	GPC_C	31	1526	61	1502	95	56.3	527	0.030935377	-0.052141627	1502	95	7/6
Output_1_87	GPC_C	31	231	16	220	200	97.6	173.1	0.174147324	-0.417484303	241	12	unc'd 6/38
Output_1_88	GPC_C	31	243	21			57.8	73.6	0.243097221	-0.565397609			
Output_1_89	GPC_C	31	231	19	270	320	69.9	78.3	0.26821753	-1.109115261	248	14	unc'd 6/38
Output_1_90	GPC_C	31	345	15	370	150	219.3	332.7	0.18986066	-1.132220241	384	18	unc'd 6/38
Output_1_91	GPC_C	31											
Output_1_92	GPC_C	31	302	15	190	190	158.2	162.3	0.296828414	-0.936273573	319	16	unc'd 6/38
Output_1_93	GPC_C	31	278	32	160	550	60.7	72	0.270023762	-0.096197112			
Output_1_94		31			0	0							
Output_1_95	GPC_C	31	232	15	140	260	94.2	125.6	0.214009243	-1.508968313	263	13	unc'd 6/38
Output_1_96	GPC_C	31	222	22	200	310	50.8	83	0.16986193	-1.456531774	259	13	unc'd 6/38
Output_1_97	GPC_C	31	270	22	190	270	65.1	96.9	0.211941221	-0.248103883	277	14	unc'd 6/38
Output_1_98	GPC_C	31	305	14	340	150	207.7	318.7	0.193856999	-0.828169614	330	15	unc'd 6/38
Output_1_99	GPC_C	31	268	35			22.64	48.6	0.156570744	0.320035671			
Output_1_100	GPC_C	31	278	27			52.2	104.1	0.181479396	1.012063755	249	14	unc'd 6/38
Output_1_101	GPC_C	31	267	24	320	220	61.3	131.9	0.161471318	0.586107161	247	12	cor'd 6/38)
Output_1_102	GPC_C	31	246	27			29.26	72.1	0.13231899	0.063612002	245	14	cor'd 6/38)
Output_1_103	GPC_C	32	193	12	360	160	990	811	0.336047451	-3.448005603			
Output_1_104	GPC_C	32	248	35			21.87	53.3	0.134178407	0.084949236			
Output_1_105	GPC_C	32	227	30	10	310	34.6	97.1	0.107291065	-0.393805382	244	13	cor'd 6/38)
Output_1_106	GPC_C	32	275	15	600	210	405	272	0.454598792	-1.551125889			
Output_1_107	GPC_C	32	288.8	11	210	140	617	460	0.410203914	-1.296790939	304	14	unc'd 6/38
Output_1_108	GPC_C	32	289.5	14	200	170	150.9	178.4	0.256584177	-0.858624424	307	15	unc'd 6/38
Output_1_109	GPC_C	32	392	21	340	210	128.7	138.7	0.276135317	-1.143944074	422	20	unc'd 6/38
Output_1_110	GPC_C	32	232	18	160	240	59.2	135.6	0.136585838	-0.227935734	239	12	unc'd 6/38
Output_1_111	GPC_C	32	281.8	13	250	190	213.1	195.9	0.338834223	-0.664306566	291	14	unc'd 6/38
Output_1_112	GPC_C	32	290.2	12	220	140	308	338	0.288093379	-0.299569219	296	14	unc'd 6/38
Output_1_113	GPC_C	32	244	18	230	220	54.9	153.8	0.114575548	-0.035598919	245	12	unc'd 6/38
Output_1_114	GPC_C	32	233	14			104.3	278.5	0.114221847	-0.34036515	247	12	cor'd 6/38)
Output_1_115	GPC_C	32	202	15	282	130	1560	634	0.615734033	-13.69066081			
Output_1_116	GPC_C	32	1170	110	1463	100	187	392	0.1360654	-0.485996559	1463	100	7/6
Output_1_117	GPC_C	32	278.4	13	300	180	624	833	0.23952178	-0.105119024	280	14	unc'd 6/38
Output_1_118	GPC_C	32	250	24	110	340	56.2	91.2	0.204187662	0.272670917	245	13	unc'd 6/38
Output_1_119	GPC_C	32	232.1	9.8	280	140	334	441	0.231583241	-0.703275989	245	12	unc'd 6/38
Output_1_120	GPC_C	32	235.8	11	280	170	641	649	0.273219102	-2.544091776			
Output_1_121	GPC_C	32	244	23			51.4	75.5	0.215708806	-0.218680954			
Output_1_122	GPC_C	32	237	21			49.1	67.2	0.22278846	-0.704956738			
Output_1_123	GPC_C	32											
Output_1_124	GPC_C	32	285	11	230	140	409	311.8	0.400092302	-1.329181005	301	14	unc'd 6/38
Output_1_125	GPC_C	32	243.9	11	90	170	371.7	438	0.263167591	-0.591526507	255	12	cor'd 6/38)

Output_1_126	GPC_C	32	639	99	1680	420	53.6	75.3	0.422142874	10.32460069			
Output_1_127	GPC_C	32	236	16	110	260	118.8	204	0.181390924	-0.351146761	244	13	unc'd 6/38

* Propagated 2se uncertainties are about 1.5 to twice that of 2se using the calculations as given in Paton et al. (2010)
**three age types are allowed. Best age for grains >950 Ma is 207/206. For those younger, 206/238 is used, but if a 208Pb based common Pb correction makes the point more concordant it is used.

+dwell time=0.35 seconds

Reference Materials

	DateTime	Sample type	Duration(s)	207_235	207_235_Prop2SE*	206_238	206_238_Prop2SE	207_206	207_206_Prop2SE	208_232	208_232_Prop2SE	Age207_235	Age207_235_Prop2SE	Age206_238	Age206_238_Prop2SE	error corel
Z_Temora2_0	08/12/2016 (5) 11:12:50.69	std	22.671	0.523	0.054	0.06683	0.0028	0.0562	0.0047	0.02088	0.0023	424	36	417	17	0.432840388
Z_Temora2_1	08/12/2016 (5) 11:36:41.59	std	21.968	0.493	0.05	0.0671	0.0029	0.0536	0.0045	0.02079	0.0023	408	36	418.4	18	0.43825432
Z_Temora2_2	08/12/2016 (5) 11:59:03.17	std	20.913	0.487	0.055	0.0658	0.003	0.0538	0.0053	0.021	0.0025	403	40	410.5	18	0.404100981
Z_Temora2_3	08/12/2016 (5) 12:17:29.49	std	24.078	0.509	0.05	0.0671	0.003	0.0556	0.0044	0.02071	0.0022	416	33	418.4	18	0.476731022
Z_Temora2_4	08/12/2016 (5) 12:40:53.31	std	23.727	0.518	0.049	0.0667	0.0029	0.0563	0.0042	0.02121	0.0024	421	33	415.9	18	0.483358574
Z_Temora2_5	08/12/2016 (5) 12:58:55.36	std	22.67	0.511	0.054	0.067	0.0031	0.055	0.0046	0.02078	0.0023	415	36	418.1	18	0.444555005
Z_Temora2_6	08/12/2016 (5) 13:22:03.36	std	21.265	0.49	0.052	0.0665	0.003	0.0536	0.0047	0.0212	0.0025	402	35	414.7	18	0.446165084
Z_Temora2_7	08/12/2016 (5) 13:38:49.81	std	23.375	0.526	0.049	0.0677	0.003	0.056	0.0041	0.02056	0.0022	428	33	422.2	18	0.483898063
Z_Temora2_8	08/12/2016 (5) 13:59:56.49	std	23.726	0.503	0.045	0.0661	0.0029	0.0549	0.0037	0.02115	0.0023	412	30	412.7	18	0.513853661
Z_Temora2_9	08/12/2016 (5) 14:21:18.99	std	23.374	0.479	0.066	0.0671	0.0034	0.0517	0.0063	0.0199	0.0024	387	46	419	20	0.372652098
Z_Temora2_10	08/12/2016 (5) 15:30:50.18	std	18.289	0.504	0.045	0.0659	0.003	0.0556	0.0037	0.02086	0.0023	414	30	411.2	18	0.517064807
Z_Temora2_11	08/12/2016 (5) 15:47:04.28	std	24.078	0.52	0.048	0.0663	0.0029	0.0567	0.0043	0.02043	0.0023	424	32	414	17	0.477922755
Z_Temora2_12	08/12/2016 (5) 16:02:41.10	std	20.913	0.52	0.05	0.0688	0.003	0.0541	0.0041	0.02118	0.0023	423	33	428.6	18	0.474008494
Z_Temora2_13	08/12/2016 (5) 16:16:26.79	std	24.781	0.499	0.046	0.06634	0.0029	0.0539	0.0038	0.02062	0.0022	409	31	414	17	0.476349358
Z_Temora2_14	08/12/2016 (5) 16:30:13.55	std	23.374	0.504	0.045	0.0659	0.0029	0.0558	0.0038	0.02109	0.0023	416	32	411.5	18	0.494317875
Z_Temora2_15	08/12/2016 (5) 16:48:19.82	std	24.429	0.512	0.048	0.06721	0.0029	0.0549	0.004	0.02062	0.0022	418	32	419.3	17	0.468019654
Z_Temora2_16	08/12/2016 (5) 17:06:14.49	std	24.43	0.515	0.046	0.0671	0.003	0.0555	0.0037	0.0205	0.0022	421	31	418.7	18	0.504194076
Z_Temora2_17	08/12/2016 (5) 17:22:46.87	std	24.43	0.502	0.044	0.066	0.003	0.055	0.0036	0.021	0.0022	413	30	411.8	18	0.515138386
Z_Temora2_18	08/12/2016 (5) 17:39:42.46	std	24.429	0.503	0.044	0.06692	0.0028	0.0542	0.0036	0.02092	0.0022	413	30	417.5	17	0.488794244
Z_Temora2_19	08/12/2016 (5) 17:54:44.12	std	24.078	0.493	0.046	0.0661	0.0029	0.0544	0.0039	0.02117	0.0023	408	33	412.7	18	0.474632745
Z_Temora2_20	08/12/2016 (5) 18:11:10.87	std	23.375	0.552	0.05	0.06756	0.0029	0.0588	0.004	0.01979	0.0022	445	33	421.4	17	0.477868416
Z_Temora2_21	08/12/2016 (5) 18:25:51.78	std	10.073	0.481	0.045	0.0651	0.0034	0.0531	0.0039	0.02084	0.0023	398	31	406	20	0.534518391
Z_Temora2_22	08/12/2016 (5)	std	23.726	0.511	0.049	0.0667	0.0029	0.0554	0.0043	0.02137	0.0023	417	33	416.4	18	0.479383642

	18:57:33.55														
Z_Temora2_23	08/12/2016 (5) 19:11:35.07	std	23.727	0.506	0.046	0.0669	0.0029	0.0548	0.0038	0.02069	0.0022	414	31	417.2	18	0.499246795
Z_Plesovice_0	08/12/2016 (5) 11:11:04.49	std	23.374	0.439	0.056	0.0561	0.0025	0.0566	0.0063	0.0196	0.0048	362	40	351.8	15	0.360000681
Z_Plesovice_1	08/12/2016 (5) 11:35:06.64	std	22.319	0.383	0.051	0.05719	0.0025	0.0482	0.0057	0.0176	0.0044	322	38	358.5	15	0.334166022
Z_Plesovice_2	08/12/2016 (5) 11:43:41.29	std	18.255	0.461	0.042	0.0596	0.0025	0.0562	0.004	0.01753	0.0019	384	29	373.2	15	0.469815866
Z_Plesovice_3	08/12/2016 (5) 11:57:45.45	std	23.023	0.393	0.054	0.0556	0.0025	0.0502	0.0062	0.0144	0.0046	329	40	348.5	15	0.333721959
Z_Plesovice_4	08/12/2016 (5) 12:16:07.20	std	23.023	0.417	0.057	0.0553	0.0025	0.0543	0.0063	0.0215	0.0057	346	40	347.2	15	0.350058819
Z_Plesovice_5	08/12/2016 (5) 12:57:37.99	std	23.726	0.406	0.036	0.05519	0.0024	0.0538	0.0036	0.0169	0.0021	345	26	346.3	14	0.473143795
Z_Plesovice_6	08/12/2016 (5) 13:20:47.40	std	23.375	0.379	0.036	0.05277	0.0023	0.052	0.0039	0.0173	0.0021	325	26	331.5	14	0.466845555
Z_Plesovice_7	08/12/2016 (5) 13:37:26.82	std	23.376	0.389	0.036	0.05327	0.0023	0.0531	0.0038	0.0163	0.0022	332	26	334.6	14	0.471236409
Z_Plesovice_8	08/12/2016 (5) 13:58:37.71	std	23.726	0.382	0.035	0.05299	0.0023	0.0518	0.0037	0.0174	0.0022	327	26	332.8	14	0.467656783
Z_Plesovice_9	08/12/2016 (5) 14:19:50.02	std	22.671	0.425	0.038	0.05469	0.0023	0.0558	0.0038	0.0186	0.0022	359	27	343.2	14	0.47677447
Z_Plesovice_10	08/12/2016 (5) 15:29:30.01	std	23.023	0.407	0.042	0.0574	0.0025	0.0506	0.0042	0.0157	0.0026	344	30	359.7	15	0.431393373
Z_Plesovice_11	08/12/2016 (5) 15:45:52.89	std	23.726	0.41	0.042	0.05482	0.0024	0.0538	0.0044	0.0194	0.004	347	30	344	15	0.450325527
Z_Plesovice_12	08/12/2016 (5) 16:01:18.46	std	23.726	0.404	0.042	0.05234	0.0023	0.0553	0.0047	0.0158	0.0028	342	31	328.8	14	0.425170862
Z_Plesovice_13	08/12/2016 (5) 16:15:14.35	std	24.078	0.402	0.042	0.0539	0.0024	0.0532	0.0045	0.0165	0.0029	341	30	338.5	15	0.449850067
Z_Plesovice_14	08/12/2016 (5) 16:29:01.10	std	23.023	0.392	0.036	0.05327	0.0023	0.0528	0.0037	0.0167	0.002	334	26	334.6	14	0.473440364
Z_Plesovice_15	08/12/2016 (5) 16:47:13.36	std	23.726	0.418	0.04	0.05357	0.0024	0.0562	0.0041	0.0177	0.0022	353	28	336.4	14	0.464606892
Z_Plesovice_16	08/12/2016 (5) 17:04:42.71	std	23.726	0.413	0.039	0.05553	0.0024	0.0539	0.0041	0.0167	0.0026	350	28	348.4	15	0.473903873
Z_Plesovice_17	08/12/2016 (5) 17:21:15.79	std	23.374	0.431	0.047	0.05517	0.0024	0.0566	0.0053	0.0155	0.0031	360	33	346.1	15	0.427433961
Z_Plesovice_18	08/12/2016 (5) 17:38:26.86	std	23.023	0.4	0.046	0.0549	0.0025	0.0528	0.0053	0.0158	0.0034	342	36	344.8	15	0.381949296
Z_Plesovice_19	08/12/2016 (5) 17:53:26.40	std	24.431	0.394	0.036	0.0548	0.0024	0.0521	0.0037	0.01659	0.002	336	26	343.9	14	0.465591411
Z_Plesovice_20	08/12/2016 (5) 18:09:36.63	std	24.078	0.397	0.037	0.0549	0.0024	0.0523	0.0039	0.0183	0.0023	338	26	344.7	15	0.492381715
Z_Plesovice_21	08/12/2016 (5) 18:24:39.34	std	24.077	0.391	0.036	0.05386	0.0023	0.0521	0.0037	0.0179	0.0022	334	26	338.2	14	0.469516387
Z_Plesovice_22	08/12/2016 (5) 18:39:52.60	std	22.67	0.385	0.036	0.05312	0.0024	0.0523	0.0039	0.0181	0.0022	329	27	333.6	14	0.455292878
Z_Plesovice_23	08/12/2016 (5) 18:56:16.89	std	22.319	0.379	0.035	0.05268	0.0024	0.052	0.0037	0.01686	0.002	325	26	330.9	14	0.467507173

Z_Plesovice_24	08/12/2016 (5) 19:10:39.72	std	17.454	0.385	0.034	0.0529	0.0024	0.0527	0.0037	0.0168	0.0021	330	25	332.4	15	0.512099738
G_NIST610_0	08/12/2016 (5) 11:09:37.98	std	22.672	30.52	2.6	0.2377	0.01	0.926	0.057	0.4995	0.053	3501	83	1374	53	0.85195424
G_NIST610_1	08/12/2016 (5) 11:33:31.34	std	21.616	31.05	2.6	0.2415	0.01	0.926	0.056	0.4986	0.052	3519	83	1394	53	0.849764603
G_NIST610_2	08/12/2016 (5) 11:56:27.38	std	12.473	32.2	2.8	0.2464	0.011	0.944	0.057	0.5122	0.054	3554	84	1419	57	0.861873836
G_NIST610_3	08/12/2016 (5) 12:14:48.43	std	23.375	29.95	2.5	0.2395	0.01	0.916	0.056	0.5022	0.053	3483	84	1384	53	0.846177032
G_NIST610_4	08/12/2016 (5) 12:38:13.30	std	24.077	29.43	2.5	0.238	0.01	0.905	0.055	0.5081	0.054	3466	82	1376	53	0.85209886
G_NIST610_5	08/12/2016 (5) 12:56:09.03	std	23.726	29.05	2.5	0.2352	0.01	0.897	0.055	0.502	0.053	3453	83	1361	52	0.84642573
G_NIST610_6	08/12/2016 (5) 13:19:00.50	std	22.319	28.99	2.5	0.2346	0.01	0.897	0.055	0.5003	0.053	3450	83	1358	53	0.851261335
G_NIST610_7	08/12/2016 (5) 13:36:08.68	std	7.855	31.22	2.7	0.242	0.011	0.93	0.061	0.518	0.055	3524	86	1397	56	0.854160942
G_NIST610_8	08/12/2016 (5) 13:57:20.35	std	23.375	29.72	2.5	0.2363	0.01	0.908	0.056	0.4975	0.053	3475	83	1367	54	0.855735599
G_NIST610_9	08/12/2016 (5) 14:18:26.67	std	23.374	30.58	2.6	0.2437	0.011	0.9	0.055	0.512	0.054	3507	79	1405	57	0.874268655
G_NIST610_10	08/12/2016 (5) 15:25:51.27	std	23.023	30.05	2.6	0.2391	0.01	0.905	0.057	0.523	0.056	3483	85	1382	54	0.848162937
G_NIST610_11	08/12/2016 (5) 15:44:30.60	std	23.375	29.31	2.5	0.2369	0.01	0.892	0.055	0.5164	0.055	3462	84	1370	53	0.847164632
G_NIST610_12	08/12/2016 (5) 16:00:09.18	std	15.638	29.95	2.6	0.2336	0.011	0.917	0.057	0.5068	0.054	3483	83	1352	56	0.866784527
G_NIST610_13	08/12/2016 (5) 16:14:11.05	std	23.726	29.74	2.5	0.2318	0.01	0.922	0.056	0.5006	0.053	3476	80	1344	52	0.85944013
G_NIST610_14	08/12/2016 (5) 16:27:50.07	std	23.374	30.28	2.7	0.231	0.01	0.935	0.058	0.504	0.054	3489	85	1339	54	0.855942938
G_NIST610_15	08/12/2016 (5) 16:45:54.94	std	23.024	29.95	2.6	0.2301	0.0099	0.934	0.057	0.5024	0.053	3486	89	1335	52	0.836354125
G_NIST610_16	08/12/2016 (5) 17:03:05.30	std	24.429	30.37	2.6	0.2385	0.011	0.925	0.057	0.4945	0.052	3494	83	1378	55	0.859318246
G_NIST610_17	08/12/2016 (5) 17:19:56.32	std	23.726	29.85	2.6	0.2324	0.01	0.931	0.058	0.5006	0.053	3479	83	1347	53	0.855092357
G_NIST610_18	08/12/2016 (5) 17:37:14.42	std	22.671	29.72	2.6	0.2371	0.011	0.901	0.055	0.501	0.053	3473	84	1371	55	0.856393205
G_NIST610_19	08/12/2016 (5) 17:52:15.36	std	12.122	31.26	2.7	0.2465	0.013	0.917	0.06	0.524	0.057	3524	87	1419	66	0.883284416
G_NIST610_20	08/12/2016 (5) 18:08:24.18	std	23.375	28.65	2.5	0.2362	0.01	0.876	0.054	0.531	0.056	3438	83	1366	54	0.853437246
G_NIST610_21	08/12/2016 (5) 18:23:19.16	std	23.375	28.08	2.4	0.2315	0.0099	0.867	0.053	0.5398	0.057	3418	83	1346	57	0.867496304
G_NIST610_22	08/12/2016 (5) 18:38:43.32	std	20.914	27.93	2.4	0.2293	0.01	0.873	0.053	0.542	0.058	3414	85	1330	53	0.848079922
G_NIST610_23	08/12/2016 (5) 18:55:05.50	std	20.21	28.24	2.4	0.2299	0.011	0.881	0.055	0.5182	0.055	3424	85	1333	55	0.856863979
G_NIST610_24	08/12/2016 (5)	std	23.374	27.76	2.4	0.229	0.01	0.876	0.054	0.5099	0.054	3407	83	1329	53	0.853370022

	19:09:16.87														
Z_Temora2_0	09/12/2016 (6) 10:20:25.96	std	19.506	0.506	0.046	0.0669	0.0033	0.055	0.0034	0.02129	0.00099	414	31	417.2	20	0.539180823
Z_Temora2_1	09/12/2016 (6) 10:35:45.54	std	22.672	0.518	0.052	0.0667	0.0033	0.0569	0.0043	0.02043	0.00097	420	35	416.5	20	0.499272154
Z_Temora2_2	09/12/2016 (6) 12:00:03.81	std	21.264	0.497	0.044	0.0667	0.0032	0.0542	0.0033	0.02047	0.00095	408	30	416.2	19	0.527464484
Z_Temora2_3	09/12/2016 (6) 12:47:26.27	std	23.727	0.521	0.044	0.0671	0.0032	0.0561	0.0031	0.02146	0.00087	425	29	418.5	19	0.553940095
Z_Temora2_4	09/12/2016 (6) 13:00:58.60	std	26.541	0.522	0.051	0.0667	0.0032	0.0566	0.0042	0.02022	0.00091	422	35	416.2	19	0.482202687
Z_Temora2_5	09/12/2016 (6) 13:17:35.20	std	24.43	0.489	0.043	0.06679	0.0032	0.0532	0.0031	0.02042	0.00085	403	29	416.7	19	0.535232171
Z_Temora2_6	09/12/2016 (6) 13:30:51.71	std	23.726	0.503	0.045	0.0664	0.0032	0.0553	0.0036	0.02105	0.00087	412	30	414.5	19	0.532742872
Z_Temora2_7	09/12/2016 (6) 13:47:56.09	std	23.728	0.504	0.042	0.0674	0.0033	0.0545	0.003	0.02103	0.00084	414	28	420.2	20	0.575516821
Z_Temora2_8	09/12/2016 (6) 14:07:46.10	std	21.616	0.51	0.046	0.0658	0.0033	0.0563	0.0035	0.0211	0.00092	417	31	410.7	20	0.547959203
Z_Temora2_9	09/12/2016 (6) 14:24:11.10	std	24.079	0.528	0.05	0.0676	0.0033	0.0566	0.0039	0.02083	0.0011	428	33	421.9	20	0.52375054
Z_Temora2_10	09/12/2016 (6) 14:38:07.70	std	22.672	0.503	0.05	0.0663	0.0033	0.0551	0.004	0.0199	0.0012	411	33	414	20	0.515546827
Z_Plesovice_0	09/12/2016 (6) 10:15:50.61	std	24.077	0.38	0.034	0.05342	0.0026	0.0518	0.0033	0.0176	0.0013	326	25	335.5	16	0.52809102
Z_Plesovice_1	09/12/2016 (6) 10:34:42.25	std	23.023	0.37	0.033	0.05414	0.0026	0.0498	0.003	0.0168	0.0014	318	25	339.9	16	0.513716024
Z_Plesovice_2	09/12/2016 (6) 11:58:57.70	std	20.209	0.418	0.037	0.05426	0.0026	0.056	0.0033	0.0179	0.0012	354	27	340.6	16	0.524419738
Z_Plesovice_3	09/12/2016 (6) 12:13:17.15	std	24.78	0.386	0.033	0.05281	0.0025	0.0536	0.0032	0.01791	0.001	330.5	24	331.7	16	0.553308584
Z_Plesovice_4	09/12/2016 (6) 12:27:52.78	std	24.429	0.383	0.034	0.05083	0.0025	0.0543	0.0033	0.01781	0.00094	328	25	319.6	15	0.524335249
Z_Plesovice_5	09/12/2016 (6) 12:46:24.73	std	24.078	0.395	0.035	0.05269	0.0025	0.0544	0.0034	0.0169	0.0013	339	27	331	16	0.518835847
Z_Plesovice_6	09/12/2016 (6) 12:59:59.87	std	23.727	0.39	0.035	0.05325	0.0026	0.0529	0.0033	0.017	0.0013	333	25	334.4	16	0.537449749
Z_Plesovice_7	09/12/2016 (6) 13:16:35.77	std	20.562	0.398	0.034	0.0549	0.0027	0.0526	0.0029	0.0178	0.0013	339.8	24	344.7	17	0.572506794
Z_Plesovice_8	09/12/2016 (6) 13:29:50.17	std	23.726	0.396	0.034	0.05357	0.0026	0.0537	0.0029	0.01781	0.00092	338.1	24	336.4	16	0.556636338
G_NIST610_0	09/12/2016 (6) 10:14:40.98	std	22.671	27.6	2.4	0.2284	0.011	0.878	0.047	0.511	0.023	3396	85	1325	59	0.871723757
G_NIST610_1	09/12/2016 (6) 10:33:33.67	std	20.561	27.81	2.3	0.2278	0.011	0.887	0.043	0.514	0.021	3408	80	1322	60	0.888227423
G_NIST610_2	09/12/2016 (6) 11:57:45.25	std	24.078	27.84	2.3	0.2224	0.011	0.914	0.044	0.506	0.021	3410	78	1294	56	0.884102591
G_NIST610_3	09/12/2016 (6)	std	24.431	28.26	2.3	0.2237	0.011	0.919	0.044	0.508	0.02	3426	77	1301	56	0.886436593

	12:12:07.52															
G_NIST610_4	09/12/2016 (6) 12:26:53.35	std	21.616	28.31	2.3	0.2241	0.011	0.919	0.044	0.51	0.021	3435	89	1303	59	0.867950715
G_NIST610_5	09/12/2016 (6) 12:45:21.08	std	23.374	28.46	2.4	0.2257	0.011	0.909	0.046	0.546	0.044	3429	82	1315	54	0.864151388
G_NIST610_6	09/12/2016 (6) 12:58:53.41	std	22.319	28.55	2.3	0.226	0.011	0.91	0.044	0.504	0.019	3435	78	1313	57	0.886101644
G_NIST610_7	09/12/2016 (6) 13:15:22.98	std	13.528	29.6	2.6	0.2351	0.013	0.902	0.049	0.516	0.024	3467	85	1360	66	0.892564326
G_NIST610_8	09/12/2016 (6) 13:28:44.41	std	22.671	28.41	2.3	0.2283	0.011	0.903	0.044	0.499	0.019	3430	79	1325	57	0.881597254
G_NIST610_9	09/12/2016 (6) 13:43:52.74	std	17.045	30.08	2.6	0.2346	0.012	0.923	0.047	0.51	0.02	3484	82	1358	62	0.888841924
G_NIST610_10	09/12/2016 (6) 14:05:43.02	std	24.077	28.77	2.5	0.2326	0.012	0.898	0.047	0.504	0.022	3437	86	1347	60	0.871858567
G_NIST610_11	09/12/2016 (6) 14:22:04.15	std	24.077	28.06	2.3	0.2287	0.011	0.89	0.044	0.508	0.02	3416	80	1327	59	0.884765813
G_NIST610_12	09/12/2016 (6) 14:36:04.27	std	21.968	27.96	2.3	0.228	0.011	0.89	0.045	0.509	0.022	3412	80	1324	57	0.878203255

	Combined Sample	Age208_232	Age208_232_Prop2SE	Age207_206	Age207_206_Prop2SE	Th(ppm)	U(ppm)
Z_Temora2_0	std	418	45	400	180	159.2	255.2
Z_Temora2_1	std	416	46	300	180	156.2	321.7
Z_Temora2_2	std	420	49	310	220	92.2	220.4
Z_Temora2_3	std	414	44	380	170	243.5	366
Z_Temora2_4	std	424	47	440	170	117	296.4
Z_Temora2_5	std	416	45	380	190	184	297.9
Z_Temora2_6	std	424	49	300	180	91.4	278
Z_Temora2_7	std	411	44	418	160	250.2	456
Z_Temora2_8	std	423.1	45	383	150	438	826
Z_Temora2_9	std	399	47	160	250	166.6	286
Z_Temora2_10	std	417	45	419	150	438	741
Z_Temora2_11	std	409	45	430	160	168.4	448
Z_Temora2_12	std	424	45	330	160	227.9	365
Z_Temora2_13	std	412	44	334	160	196.8	488
Z_Temora2_14	std	421.8	45	415	150	420	657
Z_Temora2_15	std	413	44	368	160	177.1	398
Z_Temora2_16	std	410	44	421	160	225.7	470
Z_Temora2_17	std	420.1	44	402	150	441	730
Z_Temora2_18	std	418.5	44	359	140	819	1049
Z_Temora2_19	std	423.5	45	350	150	322	510
Z_Temora2_20	std	396	43	530	150	725	1330
Z_Temora2_21	std	417	45	315	160	727	1068
Z_Temora2_22	std	427	46	380	170	167.9	266.7
Z_Temora2_23	std	414	44	387	160	235	444
				0	0		
Z_Plesovice_0	std	390	95	350	240	16.13	187.2
Z_Plesovice_1	std	351	87	40	230	16.34	190.7
Z_Plesovice_2	std	351.1	38	430	160	309.7	876
Z_Plesovice_3	std	287	92	140	250	16.12	193
Z_Plesovice_4	std	430	110	260	230	15.92	190.3
Z_Plesovice_5	std	339	42	339	150	73.9	686
Z_Plesovice_6	std	346	43	250	160	79.7	723
Z_Plesovice_7	std	332	45	303	160	55.1	610
Z_Plesovice_8	std	349	43	249	160	62.8	674
Z_Plesovice_9	std	373	44	417	150	92.7	744
Z_Plesovice_10	std	314	52	200	180	25.54	314
Z_Plesovice_11	std	386	79	310	180	16.5	201.7
Z_Plesovice_12	std	316	55	360	180	20.26	241.2
Z_Plesovice_13	std	330	58	280	180	19.37	231.6
Z_Plesovice_14	std	335	41	292	150	53.2	643

Z_Plesovice_15	std	355	44	420	160	47.9	591
Z_Plesovice_16	std	334	52	330	160	27.79	340
Z_Plesovice_17	std	319	59	390	200	15.19	190.2
Z_Plesovice_18	std	328	72	270	220	15.2	189.1
Z_Plesovice_19	std	332	40	265	160	52.5	590
Z_Plesovice_20	std	366	46	264	160	42.01	509
Z_Plesovice_21	std	359	44	261	160	49.9	590
Z_Plesovice_22	std	362	44	265	160	47.3	576
Z_Plesovice_23	std	338	39	257	160	72.1	732
Z_Plesovice_24	std	336	43	293	150	60	675
				0	0		
G_NIST610_0	std	8185	710	5248	130	457.9	462.7
G_NIST610_1	std	8174	710	5247	130	457.1	459.4
G_NIST610_2	std	8360	730	5287	130	449	462
G_NIST610_3	std	8220	710	5223	130	463.9	465
G_NIST610_4	std	8300	720	5198	120	452.5	457.5
G_NIST610_5	std	8220	710	5180	120	460	465.3
G_NIST610_6	std	8200	710	5182	120	455.7	456.6
G_NIST610_7	std	8430	730	5256	140	452	472
G_NIST610_8	std	8160	710	5205	130	458.1	461
G_NIST610_9	std	8350	720	5188	130	462	468
G_NIST610_10	std	8490	740	5199	130	452.9	455
G_NIST610_11	std	8410	730	5169	120	459.8	462.8
G_NIST610_12	std	8280	720	5226	130	450	460
G_NIST610_13	std	8200	710	5238	130	461	462.3
G_NIST610_14	std	8240	720	5267	130	454.1	463
G_NIST610_15	std	8220	720	5265	130	457	464
G_NIST610_16	std	8120	710	5244	130	458.6	457.3
G_NIST610_17	std	8200	710	5258	130	455	468
G_NIST610_18	std	8200	710	5189	120	458	462
G_NIST610_19	std	8510	760	5225	130	438	451
G_NIST610_20	std	8600	740	5133	120	463.7	463
G_NIST610_21	std	8720	750	5114	120	460.3	465
G_NIST610_22	std	8750	760	5126	120	450	457
G_NIST610_23	std	8430	730	5146	120	456.3	462
G_NIST610_24	std	8320	720	5134	120	459	462
Z_Temora2_0	std	426	20	378	130	360	447
Z_Temora2_1	std	409	19	430	170	124.2	208.9
Z_Temora2_2	std	409	19	347	130	128.9	348
Z_Temora2_3	std	429	17	433	130	248.9	411
Z_Temora2_4	std	405	18	410	160	104.9	231.5
Z_Temora2_5	std	408	17	321	130	286	386

Z_Temora2_6	std	421	17	379	140	228.7	330
Z_Temora2_7	std	420.7	17	371	120	456	826
Z_Temora2_8	std	422	18	425	130	342.6	439
Z_Temora2_9	std	417	22	430	150	90.6	254
Z_Temora2_10	std	399	25	360	160	70.6	198.9
				0	0		
Z_Plesovice_0	std	356	27	241	140	47.1	563
Z_Plesovice_1	std	337	28	170	130	49.4	592
Z_Plesovice_2	std	359	23	426	130	47.2	537
Z_Plesovice_3	std	359	20	326	130	79.4	713
Z_Plesovice_4	std	357	19	352	130	81.8	727
Z_Plesovice_5	std	339	25	356	140	47.7	567
Z_Plesovice_6	std	341	25	293	130	49.65	589
Z_Plesovice_7	std	357	26	292	130	48.2	586
Z_Plesovice_8	std	357	18	342	120	77.4	715
				0	0		
G_NIST610_0	std	8330	310	5138	110	459	454
G_NIST610_1	std	8370	280	5157	98	458	463
G_NIST610_2	std	8270	280	5219	99	449	462
G_NIST610_3	std	8290	270	5231	100	455.2	466.4
G_NIST610_4	std	8320	280	5231	100	461.6	470
G_NIST610_5	std	8710	520	5208	100	400	418
G_NIST610_6	std	8240	260	5211	99	462.7	465
G_NIST610_7	std	8400	310	5193	110	459	476
G_NIST610_8	std	8200	280	5194	99	457	458.7
G_NIST610_9	std	8320	270	5241	110	469	477
G_NIST610_10	std	8230	290	5182	110	460.2	461
G_NIST610_11	std	8300	270	5164	99	449	457
G_NIST610_12	std	8300	290	5166	100	453.8	455

* Propagated 2se uncertainties are about 1.5 to twice that of 2se using the calculations as given in Paton et al. (2010)
**three age types are allowed. Best age for grains >950 Ma is 207/206. For those younger, 206/238 is used, but if a 208Pb based common Pb correction makes the point more concordant it is used.

+dwell time=0.35 seconds

8.9. Palynological data conditions

*1: DIVERSITY	
V. High	30+ species
High	20-29 species
Moderate	10-19 species
Low	5-9 species
Very Low	1-4 species

*2: ENVIRONMENT	DINOFLAGELLATE CONTENT %		DINOFLAGELLATE DIVERSITY	FRESHWATER ALGAE CONTENT %
Offshore Marine	67 to 100		Very High	Low
Shelfal Marine	34 to 66		High	"
Nearshore Marine	11 to 33		Moderate	"
Very Nearshore Marine	5 to 10		Moderate-Low	"
Marginal Marine	<1 to 4		Low-Very Low	"
Brackish	0, Spiny Acritarchs only		Extremely Low	"
Non-Marine (undiff.)	0, no Spiny Acritarchs		Nil	Low <3
Non-Marine (lacustrine)	0, no Spiny Acritarchs		Nil	Moderate 3-10+

*The spore-pollen colour is related to hydrocarbon potential assuming that regional thermal maturity has increased with depth over a similar time frame. However other factors such as volcanic intrusions or localised movements of hot fluids may also greatly affect spore-pollen colour.

8.10. Well names and locations used in this study

Well name	Easting	Northing	GDA 94 Zone
ABERFOYLE_1A	315191	7617653	55
ARAMAC_1	324187	7461274	55
BALLYNEETY_1	366706	7491774	55
BELLARA_1	322349	7438456	55
BULLOCK_1	270364	7694816	55
CARMICHAEL_1	400358	7571695	55
CAROLINA_1	362851	7524004	55
CERNAN_1	410126	7521861	55
COREENA_1	335344	7420886	55
CROSSMORE_1	250949	7464703	55
CROSSMORE_2	250949	7464703	55
CROSSMORE_SOUTH_1	256715	7461057	55
DINGONOSE_14	720193	7381606	55
DUCKWORTH_11	710315	7398699	55
EEA_RODNEY_CREEK_1	271282	7447454	55
EEA_RODNEY_CREEK_2	266915	7446309	55
EMERALD_3	644880	7413910	55
FLEETWOOD_1	381552	7554866	55
FLINDERS_RIVER_1	206890	7688727	55
GLENARAS_1	266894	7444001	55
GLENARAS_2	267184	7445176	55
GLENARAS_3	267602	7445134	55
GLENARAS_4	267411	7444978	55
GLENARAS_5	267203	7444701	55
GLENARAS_6	267671	7444723	55
GLENARAS_7	264505	7452485	55
GLUE_POT_CREEK_1	392175	7478085	55
GUNN_1	383464	7526088	55
HERGENROTHER_1	383823	7509589	55
HEXHAM_1	392579	7477725	55
HUGHENDEN_7	207033	7690204	55
HUGHES_1	274343	7427713	55
HULTON_1	287763	7411910	55
JERICHO_1	406627	7370721	55
KANAKA_1	304148	7488326	55
KOBURRA_1	323940	7644233	55
LAKE_GALILEE_1	394509	7545672	55
LONGREACH_1-1B	254142	7442073	55
MARCHMONT_1	268670	7435935	55
MONTANI_1	402353	7571404	55
MOUNT_MYTH_1	286388	7483939	55
MUTTABURRA_1	242900	7485275	55
MUTTABURRA_2	252857	7485862	55

Well name	Easting	Northing	GDA 94 Zone
MYROSS_1	336394	7480959	55
NORRIS_1	234408	7458418	55
OPHIR_3	368516	7544983	55
PENTLAND_1	303172	7704612	55
RAND_1	266454	7441193	55
RODNEY_CREEK_1	271282	7447454	55
RODNEY_CREEK_2	266915	7446309	55
RODNEY_CREEK_3	271282	7447454	55
RODNEY_CREEK_4	270992	7447818	55
RODNEY_CREEK_5	270559	7448181	55
RODNEY_CREEK_6	271184	7448252	55
RODNEY_CREEK_7	270657	7447382	55
RODNEY_CREEK_8	266708	7445376	55
ROLLESTON_1	664399	7282464	55
SALTERN_CREEK_1	289517	7416582	55
SCHMITT_1	398062	7518014	55
SHOEMAKER_1	421644	7559670	55
SKIFF_1	300159	7669232	55
SOLOMON_1A	250913	7660318	55
SOLOMON_3	283164	7614185	55
SPLITTERS_CREEK_1	349305	7458179	55
SPRINGSURE_11	598041	7288388	55
SPRINGSURE_13	517030	7316401	55
SPRINGSURE_14	618053	7339298	55
STAINBURN_DOWNS_1	306508	7471452	55
STOCKHOLM_1	270380	7507485	55
TAMBO_1-1A	459598	7286828	55
TAMBO_3	496731	7310875	55
VERA_PARK_1	273220	7458222	55
WARRINILLA_NORTH	654609	7247439	55
WYUNA_1	642921	7413572	55
YAMALA_2	640809	7393154	55
ZEROGEN_1	653036	7342203	55

8.11. Seam picks

Well name	Coal seam	Depth (m)
ABERFOYLE_1A	B0	1325.392
ABERFOYLE_1A	B1	1333.892
ABERFOYLE_1A	C	1357.978
ABERFOYLE_1A	C0	1363.711
ABERFOYLE_1A	C1	1377.919
ABERFOYLE_1A	D	1389.219
ABERFOYLE_1A	D0	1396.428
ABERFOYLE_1A	D1	1404.713
ABERFOYLE_1A	D11	1412.576
ABERFOYLE_1A	D12	1421.828
ABERFOYLE_1A	D13	1427.252
ABERFOYLE_1A	D2	1438.047
ABERFOYLE_1A	E	1445.852
ABERFOYLE_1A	F	1453.802
BALLYNEETY_1	A2	826.6859
BALLYNEETY_1	B	833.421
BALLYNEETY_1	C	886.5646
BALLYNEETY_1	C0	891.706
BALLYNEETY_1	D	907.4126
BALLYNEETY_1	D1	913.1373
BALLYNEETY_1	D2	923.9405
BALLYNEETY_1	D3	940.3245
BALLYNEETY_1	E	955.762
BULLOCK_1	A2	1128.448
BULLOCK_1	B1	1148.953
BULLOCK_1	C	1152.128
BULLOCK_1	C00	1156.229
BULLOCK_1	C1	1161.231
BULLOCK_1	D	1163.876
BULLOCK_1	D0	1171.417
BULLOCK_1	D1	1172.395
BULLOCK_1	D11	1179.539
BULLOCK_1	D2	1192.055
BULLOCK_1	E	1200.706
BULLOCK_1	F	1212.031
CARMICHAEL_1	B	791.46
CARMICHAEL_1	B1	798.869
CARMICHAEL_1	C	822.152
CARMICHAEL_1	C0	833.662
CARMICHAEL_1	C1	857.871
CARMICHAEL_1	D	865.279
CARMICHAEL_1	D0	869.909
CARMICHAEL_1	D1	876.789
CARMICHAEL_1	D11	891.605

Well name	Coal seam	Depth (m)
CARMICHAEL_1	D13	903.879
CARMICHAEL_1	D2	910.92
CARMICHAEL_1	E	922.165
CAROLINA_1	A	836.07
CAROLINA_1	B	847.315
CAROLINA_1	B1	850.887
CAROLINA_1	C	898.174
CAROLINA_1	C0	907.434
CAROLINA_1	D	916.768
CAROLINA_1	D0	919.943
CAROLINA_1	D1	933.893
CAROLINA_1	D12	954.581
CAROLINA_1	D13	963.048
CAROLINA_1	D2	972.703
CAROLINA_1	D3	974.771
CAROLINA_1	E	980.929
CAROLINA_1	F	987.206
CROSSMORE_1	J2	819.949
CROSSMORE_1	J4	845.084
CROSSMORE_1	K1	854.609
CROSSMORE_1	K2	859.24
CROSSMORE_1	K3	861.753
CROSSMORE_1	K4	867.706
CROSSMORE_1	K6	876.702
CROSSMORE_1	AM1	911.759
CROSSMORE_1	AM2	919.035
CROSSMORE_1	AM1	922.27
CROSSMORE_SOUTH_1	B	1008.684
CROSSMORE_SOUTH_1	C	1043.399
CROSSMORE_SOUTH_1	C0	1046.123
CROSSMORE_SOUTH_1	D	1051.15
CROSSMORE_SOUTH_1	D1	1060.278
CROSSMORE_SOUTH_1	D2	1069.671
CROSSMORE_SOUTH_1	D3	1074.036
CROSSMORE_SOUTH_1	E	1077.53
CROSSMORE_SOUTH_1	J1	1103.537
CROSSMORE_SOUTH_1	J2	1111.514
CROSSMORE_SOUTH_1	J4	1128.805
CROSSMORE_SOUTH_1	K1	1141.108
CROSSMORE_SOUTH_1	K2	1145.474
CROSSMORE_SOUTH_1	K3	1149.575
CROSSMORE_SOUTH_1	K4	1154.205
CROSSMORE_SOUTH_1	K5	1164.921
CROSSMORE_SOUTH_1	K6	1169.683

Well name	Coal seam	Depth (m)
CROSSMORE_SOUTH_1	AM1	1195.652
CROSSMORE_SOUTH_1	AM2	1203.947
CROSSMORE_SOUTH_1	AM21	1210.297
CROSSMORE_SOUTH_1	AM22	1213.644
CROSSMORE_SOUTH_1	AM3	1217.705
CROSSMORE_SOUTH_1	AM4	1231.86
CROSSMORE_SOUTH_1	AM5	1248.794
CROSSMORE_SOUTH_1	AM6	1256.863
FLEETWOOD_1	A	1038.97
FLEETWOOD_1	A2	1049.422
FLEETWOOD_1	B	1066.222
FLEETWOOD_1	B1	1076.93
FLEETWOOD_1	C	1119.471
FLEETWOOD_1	C0	1130.681
FLEETWOOD_1	C1	1141.529
FLEETWOOD_1	D	1146.465
FLEETWOOD_1	D0	1151.133
FLEETWOOD_1	D1	1156.588
FLEETWOOD_1	D11	1166.888
FLEETWOOD_1	D12	1175.396
FLEETWOOD_1	D13	1181.613
FLEETWOOD_1	D2	1190.863
FLEETWOOD_1	D3	1193.123
FLEETWOOD_1	E	1199.715
FLEETWOOD_1	F	1209.221
FLINDERS_RIVER_1	BHCA	194.3823
FLINDERS_RIVER_1	C	874.2644
FLINDERS_RIVER_1	C0	882.4313
FLINDERS_RIVER_1	C00	886.0383
FLINDERS_RIVER_1	C1	889.3104
FLINDERS_RIVER_1	D	893.4115
FLINDERS_RIVER_1	D0	900.0261
FLINDERS_RIVER_1	D1	902.9365
FLINDERS_RIVER_1	D11	909.8156
FLINDERS_RIVER_1	D2	912.7261
FLINDERS_RIVER_1	E	919.7023
GLENARAS_2	A	866.3703
GLENARAS_2	BL	889.5214
GLENARAS_2	C	913.2016
GLENARAS_2	C0	914.6568
GLENARAS_2	D	916.6412
GLENARAS_2	D1	923.9172
GLENARAS_2	D2	926.8276
GLENARAS_2	D3	931.0609
GLENARAS_2	E	936.6172
GLENARAS_2	J2	956.8578
GLENARAS_2	J3	963.6047

Well name	Coal seam	Depth (m)
GLENARAS_2	J4	968.2349
GLENARAS_2	K1	978.5537
GLENARAS_2	K2	981.9932
GLENARAS_2	K3	985.8297
GLENARAS_2	K4	992.8412
GLENARAS_2	K5	996.6776
GLENARAS_2	K6	1011.681
GLENARAS_2	AM1	1032.396
GLENARAS_2	AM2	1042.583
GLENARAS_2	AM21	1045.361
GLENARAS_2	AM3	1051.976
GLENARAS_2	AM4	1062.691
GLENARAS_3	A	871.432
GLENARAS_3	BL	894.4507
GLENARAS_3	C	910.458
GLENARAS_3	C0	912.5747
GLENARAS_3	D	914.9559
GLENARAS_3	D1	921.0414
GLENARAS_3	D2	924.7455
GLENARAS_3	D3	928.7143
GLENARAS_3	E	935.7257
GLENARAS_3	J2	954.2466
GLENARAS_3	J3	961.5226
GLENARAS_3	J4	966.682
GLENARAS_3	K1	975.1487
GLENARAS_3	K2	978.5882
GLENARAS_3	K3	982.9539
GLENARAS_3	K4	990.2299
GLENARAS_3	K5	995.257
GLENARAS_3	K6	1006.424
GLENARAS_3	AM1	1027.933
GLENARAS_3	AM2	1037.59
GLENARAS_3	AM21	1040.104
GLENARAS_3	AM3	1048.438
GLENARAS_4	A	872.953
GLENARAS_4	BL	894.7812
GLENARAS_4	C	913.6989
GLENARAS_4	C0	915.2864
GLENARAS_4	D	917.403
GLENARAS_4	D1	922.2978
GLENARAS_4	D2	927.4572
GLENARAS_4	D3	930.8968
GLENARAS_4	E	936.453
GLENARAS_4	J2	957.3551
GLENARAS_4	J3	964.2343
GLENARAS_4	J4	967.6739
GLENARAS_4	K1	977.3312

Well name	Coal seam	Depth (m)
GLENARAS_4	K2	981.9614
GLENARAS_4	K3	987.1207
GLENARAS_4	K4	994.3968
GLENARAS_4	K5	998.7624
GLENARAS_4	K6	1011.781
GLENARAS_4	AM1	1034.349
GLENARAS_4	AM2	1040.963
GLENARAS_4	AM21	1045.726
GLENARAS_4	AM3	1050.092
GLENARAS_4	AM4	1061.469
GLENARAS_5	A	868.5609
GLENARAS_5	BL	890.6537
GLENARAS_5	C	912.2172
GLENARAS_5	C0	914.0693
GLENARAS_5	D	915.3922
GLENARAS_5	D1	920.5516
GLENARAS_5	D2	923.9912
GLENARAS_5	D3	925.9755
GLENARAS_5	E	934.0453
GLENARAS_5	J2	951.9047
GLENARAS_5	J3	957.9901
GLENARAS_5	J4	962.8849
GLENARAS_5	K1	973.6005
GLENARAS_5	K2	977.5693
GLENARAS_5	K3	983.1255
GLENARAS_5	K4	990.0047
GLENARAS_5	K5	996.2224
GLENARAS_5	K6	1007.919
GLENARAS_5	AM1	1033.396
GLENARAS_5	AM2	1042.789
GLENARAS_5	AM21	1046.283
GLENARAS_5	AM4	1061.761
GLENARAS_6	A	869.5372
GLENARAS_6	BL	893.6143
GLENARAS_6	C	909.4893
GLENARAS_6	C0	911.4737
GLENARAS_6	D	913.458
GLENARAS_6	D1	917.4268
GLENARAS_6	D2	921.2632
GLENARAS_6	D3	923.7768
GLENARAS_6	E	932.7726
GLENARAS_6	J2	948.6476
GLENARAS_6	J3	955.7914
GLENARAS_6	J4	959.6278
GLENARAS_6	K1	968.4914
GLENARAS_6	K2	972.857
GLENARAS_6	K3	976.5612

Well name	Coal seam	Depth (m)
GLENARAS_6	K4	983.5726
GLENARAS_6	K5	989.5257
GLENARAS_6	K6	1000.031
GLENARAS_6	AM1	1022.466
GLENARAS_6	AM21	1035.299
GLENARAS_6	AM3	1040.723
GLENARAS_6	AM4	1051.438
GLENARAS_7	C	988.0431
GLENARAS_7	C0	989.1792
GLENARAS_7	D	994.8678
GLENARAS_7	D1	998.8365
GLENARAS_7	D2	1006.906
GLENARAS_7	D3	1012.992
GLENARAS_7	D30	1017.357
GLENARAS_7	E	1025.295
GLENARAS_7	F	1029.528
GLENARAS_7	J1	1048.578
GLENARAS_7	J2	1056.814
GLENARAS_7	J3	1063.164
GLENARAS_7	J4	1070.97
GLENARAS_7	K1	1084.032
GLENARAS_7	K2	1096.203
GLENARAS_7	K3	1100.701
GLENARAS_7	K4	1104.273
GLENARAS_7	K5	1112.078
GLENARAS_7	K6	1118.031
GLENARAS_7	AM1	1130.864
GLENARAS_7	AM2	1150.972
GLENARAS_7	AM21	1155.47
GLENARAS_7	AM3	1163.407
GLENARAS_7	AM4	1175.446
GLENARAS_7	AM5	1187.749
GLENARAS_7	AM6	1194.496
GLUE_POT_CREEK_1	A	617.6368
GLUE_POT_CREEK_1	A2	650.5958
GLUE_POT_CREEK_1	B	654.017
GLUE_POT_CREEK_1	B1	656.4392
GLUE_POT_CREEK_1	C	719.8034
GLUE_POT_CREEK_1	C0	727.1059
GLUE_POT_CREEK_1	D	737.4246
GLUE_POT_CREEK_1	D1	746.4105
GLUE_POT_CREEK_1	D2	754.5761
GLUE_POT_CREEK_1	D3	768.2257
GLUE_POT_CREEK_1	E	785.6882
GLUE_POT_CREEK_1	F	793.758
GUNN_1	A	842.4366
GUNN_1	B	871.4085

Well name	Coal seam	Depth (m)
GUNN_1	B1	877.8023
GUNN_1	C	914.9028
GUNN_1	C0	925.2215
GUNN_1	D	936.989
GUNN_1	D1	947.3607
GUNN_1	D2	950.548
GUNN_1	D3	960.5994
GUNN_1	E	979.2165
GUNN_1	F	987.4021
HERGENROTHER_1	A	744.1277
HERGENROTHER_1	A2	750.7904
HERGENROTHER_1	B	771.909
HERGENROTHER_1	B1	782.0954
HERGENROTHER_1	C	826.5157
HERGENROTHER_1	C0	832.3366
HERGENROTHER_1	D	840.6381
HERGENROTHER_1	D1	849.1376
HERGENROTHER_1	D2	853.4561
HERGENROTHER_1	D3	862.8197
HERGENROTHER_1	E	877.9178
HERGENROTHER_1	F	886.9766
KANAKA_1	A2	987.6834
KANAKA_1	B	992.0491
KANAKA_1	C	1033.775
KANAKA_1	C0	1037.083
KANAKA_1	D1	1053.884
KANAKA_1	D2	1061.689
KANAKA_1	D3	1073.938
KANAKA_1	D30	1079.626
KANAKA_1	E	1082.591
KANAKA_1	F	1092.778
KANAKA_1	K3	1136.075
KANAKA_1	K4	1138.893
KANAKA_1	K5	1143.258
KANAKA_1	K6	1147.492
KANAKA_1	AM1	1151.99
KANAKA_1	AM2	1157.281
KANAKA_1	AM21	1160.986
KANAKA_1	AM22	1163.234
KANAKA_1	AM3	1180.829
MONTANI_1	B	793.0182
MONTANI_1	B1	800.9044
MONTANI_1	C	814.7686
MONTANI_1	C0	827.3098
MONTANI_1	C1	845.6969
MONTANI_1	D	853.2125
MONTANI_1	D0	859.3402

Well name	Coal seam	Depth (m)
MONTANI_1	D1	868.1615
MONTANI_1	D11	873.3386
MONTANI_1	D13	887.2292
MONTANI_1	D2	893.6938
MONTANI_1	E	903.3511
MOUNT_MYTH_1	A	1037.171
MOUNT_MYTH_1	A2	1058.205
MOUNT_MYTH_1	B	1060.719
MOUNT_MYTH_1	C	1105.884
MOUNT_MYTH_1	C0	1109.324
MOUNT_MYTH_1	D	1117.339
MOUNT_MYTH_1	D1	1120.911
MOUNT_MYTH_1	D10	1127.129
MOUNT_MYTH_1	D2	1130.833
MOUNT_MYTH_1	D3	1137.183
MOUNT_MYTH_1	D30	1145.253
MOUNT_MYTH_1	E	1152.132
MOUNT_MYTH_1	F	1164.964
MOUNT_MYTH_1	J1	1185.337
MOUNT_MYTH_1	J4	1198.699
MOUNT_MYTH_1	K3	1209.282
MOUNT_MYTH_1	K4	1227.671
MOUNT_MYTH_1	K5	1236.005
MOUNT_MYTH_1	K6	1240.503
MOUNT_MYTH_1	AM1	1251.483
MOUNT_MYTH_1	AM2	1269.078
MOUNT_MYTH_1	AM21	1272.253
MOUNT_MYTH_1	AM22	1276.089
MOUNT_MYTH_1	AM3	1282.704
MOUNT_MYTH_1	AM4	1287.334
MOUNT_MYTH_1	AM5	1301.093
MUTTABURRA_1	B	963.7225
MUTTABURRA_1	C	974.7969
MUTTABURRA_1	C0	980.7881
MUTTABURRA_1	D3	998.7962
MUTTABURRA_1	D30	1008.872
MUTTABURRA_1	E	1015.845
MUTTABURRA_1	F	1029.207
MUTTABURRA_1	J1	1041.642
MUTTABURRA_1	J2	1049.051
MUTTABURRA_1	J4	1059.688
MUTTABURRA_1	K1	1064.455
MUTTABURRA_1	K3	1074.77
MUTTABURRA_1	K4	1078.871
MUTTABURRA_1	K5	1089.057
MUTTABURRA_1	AM1	1094.217
MUTTABURRA_1	AM2	1106.123

Well name	Coal seam	Depth (m)
MUTTABURRA_1	AM21	1117.368
MUTTABURRA_2	B	870.76
MUTTABURRA_2	C	888.4093
MUTTABURRA_2	C0	892.059
MUTTABURRA_2	D1	906.3465
MUTTABURRA_2	D3	921.56
MUTTABURRA_2	D30	926.5871
MUTTABURRA_2	E	935.9798
MUTTABURRA_2	F	940.3454
MUTTABURRA_2	J1	966.5937
MUTTABURRA_2	J2	972.2822
MUTTABURRA_2	J4	976.9902
MUTTABURRA_2	K1	985.6982
MUTTABURRA_2	K3	995.1268
MUTTABURRA_2	K4	1002.006
MUTTABURRA_2	K5	1007.153
MUTTABURRA_2	K6	1010.605
MUTTABURRA_2	AM1	1026.444
MUTTABURRA_2	AM2	1043.136
MUTTABURRA_2	AM21	1052
MUTTABURRA_2	AM22	1055.571
MUTTABURRA_2	AM3	1059.143
MUTTABURRA_2	AM4	1070.256
MUTTABURRA_2	AM5	1075.018
MYROSS_1	A2	805.0605
MYROSS_1	B	807.971
MYROSS_1	C	863.4557
MYROSS_1	C0	867.5567
MYROSS_1	D	880.4668
MYROSS_1	D1	887.665
MYROSS_1	D2	893.3536
MYROSS_1	D3	907.1897
MYROSS_1	D30	914.4658
MYROSS_1	E	921.5317
MYROSS_1	F	930.3952
MYROSS_1	AM22	990.798
OPHIR_3	C	1096.83
OPHIR_3	C0	1109.38
OPHIR_3	D0	1130.547
OPHIR_3	D1	1141.33
OPHIR_3	D11	1148.473
OPHIR_3	D12	1156.676
OPHIR_3	D13	1165.142
OPHIR_3	D2	1173.477
OPHIR_3	D3	1177.181
RODNEY_CREEK_1	B	942.8741
RODNEY_CREEK_1	BL	968.8032

Well name	Coal seam	Depth (m)
RODNEY_CREEK_1	C	981.6355
RODNEY_CREEK_1	C0	984.1491
RODNEY_CREEK_1	D	987.4564
RODNEY_CREEK_1	D1	991.5574
RODNEY_CREEK_1	D2	995.1293
RODNEY_CREEK_1	D3	997.3782
RODNEY_CREEK_1	E	1007.829
RODNEY_CREEK_1	J1	1024.895
RODNEY_CREEK_1	J2	1032.832
RODNEY_CREEK_1	J3	1041.167
RODNEY_CREEK_1	J4	1046.723
RODNEY_CREEK_1	K1	1056.116
RODNEY_CREEK_1	K2	1060.614
RODNEY_CREEK_1	K3	1066.831
RODNEY_CREEK_1	K4	1074.372
RODNEY_CREEK_1	K5	1079.002
RODNEY_CREEK_1	K6	1091.57
RODNEY_CREEK_1	AM1	1106.783
RODNEY_CREEK_1	AM2	1122.658
RODNEY_CREEK_1	AM21	1126.098
RODNEY_CREEK_1	AM3	1134.697
RODNEY_CREEK_1	AM4	1147.926
RODNEY_CREEK_1	AM5	1157.583
RODNEY_CREEK_2	BL	919.4562
RODNEY_CREEK_2	C	931.8916
RODNEY_CREEK_2	C0	934.4051
RODNEY_CREEK_2	D	936.1249
RODNEY_CREEK_2	D1	943.0041
RODNEY_CREEK_2	D2	947.1051
RODNEY_CREEK_2	D3	950.9416
RODNEY_CREEK_2	J1	977.3999
RODNEY_CREEK_2	J2	987.9832
RODNEY_CREEK_2	J3	994.4655
RODNEY_CREEK_2	J4	999.3603
RODNEY_CREEK_2	K1	1010.473
RODNEY_CREEK_2	K2	1014.309
RODNEY_CREEK_2	K3	1019.072
RODNEY_CREEK_2	K4	1027.671
RODNEY_CREEK_2	K5	1035.873
RODNEY_CREEK_2	K6	1048.23
RODNEY_CREEK_2	AM1	1064.712
RODNEY_CREEK_2	AM2	1078.603
RODNEY_CREEK_2	AM21	1080.455
RODNEY_CREEK_2	AM3	1086.144
RODNEY_CREEK_2	AM4	1099.241
RODNEY_CREEK_4	A	917.9955
RODNEY_CREEK_4	BL	941.1466

Well name	Coal seam	Depth (m)
RODNEY_CREEK_4	C	958.3445
RODNEY_CREEK_4	C0	960.9903
RODNEY_CREEK_4	D	962.8424
RODNEY_CREEK_4	D1	966.8111
RODNEY_CREEK_4	D2	971.8382
RODNEY_CREEK_4	D3	974.8809
RODNEY_CREEK_4	E	984.6705
RODNEY_CREEK_4	J1	1003.588
RODNEY_CREEK_4	J2	1008.086
RODNEY_CREEK_4	J3	1014.304
RODNEY_CREEK_4	J4	1019.596
RODNEY_CREEK_4	K1	1031.105
RODNEY_CREEK_4	K2	1035.471
RODNEY_CREEK_4	K3	1041.953
RODNEY_CREEK_4	K4	1048.7
RODNEY_CREEK_4	K5	1053.065
RODNEY_CREEK_4	K6	1066.824
RODNEY_CREEK_4	AM1	1083.492
RODNEY_CREEK_4	AM2	1096.854
RODNEY_CREEK_4	AM21	1099.632
RODNEY_CREEK_4	AM3	1108.496
RODNEY_CREEK_4	AM4	1121.063
RODNEY_CREEK_4	AM5	1132.043
RODNEY_CREEK_5	A	907.1608
RODNEY_CREEK_5	BL	927.4014
RODNEY_CREEK_5	C	942.4826
RODNEY_CREEK_5	C0	944.2024
RODNEY_CREEK_5	D	946.0545
RODNEY_CREEK_5	D1	954.3889
RODNEY_CREEK_5	D2	962.8555
RODNEY_CREEK_5	D3	965.2368
RODNEY_CREEK_5	E	972.9097
RODNEY_CREEK_5	J1	992.4889
RODNEY_CREEK_5	J2	997.3837
RODNEY_CREEK_5	J3	1003.601
RODNEY_CREEK_5	J4	1010.216
RODNEY_CREEK_5	K1	1019.609
RODNEY_CREEK_5	K2	1024.239
RODNEY_CREEK_5	K3	1031.383
RODNEY_CREEK_5	K4	1036.542
RODNEY_CREEK_5	K5	1041.172
RODNEY_CREEK_5	K6	1053.343
RODNEY_CREEK_5	AM1	1071.202
RODNEY_CREEK_5	AM2	1083.902
RODNEY_CREEK_5	AM21	1085.887
RODNEY_CREEK_5	AM3	1095.147
RODNEY_CREEK_5	AM4	1107.186

Well name	Coal seam	Depth (m)
RODNEY_CREEK_5	AM5	1116.578
RODNEY_CREEK_6	A	923.9074
RODNEY_CREEK_6	BL	950.6303
RODNEY_CREEK_6	C	955.922
RODNEY_CREEK_6	C0	958.5678
RODNEY_CREEK_6	D	961.2137
RODNEY_CREEK_6	D1	968.8866
RODNEY_CREEK_6	D2	973.7814
RODNEY_CREEK_6	D3	979.2053
RODNEY_CREEK_6	E	988.4657
RODNEY_CREEK_6	F	991.1116
RODNEY_CREEK_6	J2	1018.761
RODNEY_CREEK_6	J3	1024.846
RODNEY_CREEK_6	J4	1029.344
RODNEY_CREEK_6	K1	1034.636
RODNEY_CREEK_6	K2	1039.663
RODNEY_CREEK_6	K3	1043.102
RODNEY_CREEK_6	K4	1049.849
RODNEY_CREEK_6	K5	1054.215
RODNEY_CREEK_6	K6	1068.37
RODNEY_CREEK_6	AM1	1089.404
RODNEY_CREEK_6	AM2	1100.517
RODNEY_CREEK_6	AM21	1102.237
RODNEY_CREEK_6	AM3	1111.762
RODNEY_CREEK_7	A	919.8715
RODNEY_CREEK_7	BL	945.8007
RODNEY_CREEK_7	C	958.2361
RODNEY_CREEK_7	C0	960.0882
RODNEY_CREEK_7	D	962.8663
RODNEY_CREEK_7	D1	967.4965
RODNEY_CREEK_7	D2	971.333
RODNEY_CREEK_7	D3	973.9788
RODNEY_CREEK_7	E	983.107
RODNEY_CREEK_7	J1	1000.834
RODNEY_CREEK_7	J2	1004.67
RODNEY_CREEK_7	J3	1010.756
RODNEY_CREEK_7	J4	1016.631
RODNEY_CREEK_7	K1	1027.16
RODNEY_CREEK_7	K2	1031.79
RODNEY_CREEK_7	K3	1041.58
RODNEY_CREEK_7	K4	1047.798
RODNEY_CREEK_7	K5	1050.84
RODNEY_CREEK_7	K6	1066.451
RODNEY_CREEK_7	AM1	1078.754
RODNEY_CREEK_7	AM2	1092.777
RODNEY_CREEK_7	AM21	1096.481
RODNEY_CREEK_7	AM3	1104.815

Well name	Coal seam	Depth (m)
RODNEY_CREEK_7	AM4	1117.515
RODNEY_CREEK_8	BL	890.7426
RODNEY_CREEK_8	C	909.1312
RODNEY_CREEK_8	C0	910.3218
RODNEY_CREEK_8	D	912.5707
RODNEY_CREEK_8	D2	926.1968
RODNEY_CREEK_8	D3	929.1072
RODNEY_CREEK_8	E	937.0447
RODNEY_CREEK_8	J2	959.402
RODNEY_CREEK_8	J3	966.1489
RODNEY_CREEK_8	J4	971.9697
RODNEY_CREEK_8	K1	984.1405
RODNEY_CREEK_8	K2	987.5801
RODNEY_CREEK_8	K3	991.5489
RODNEY_CREEK_8	K4	1000.28
RODNEY_CREEK_8	K5	1004.646
RODNEY_CREEK_8	K6	1018.855
RODNEY_CREEK_8	AM1	1041.423
RODNEY_CREEK_8	AM2	1050.816
RODNEY_CREEK_8	AM21	1054.784
RODNEY_CREEK_8	AM3	1061.002
RODNEY_CREEK_8	AM4	1071.321
SCHMITT_1	C	875.2417
SCHMITT_1	D	892.6862
SCHMITT_1	D1	895.7289
SCHMITT_1	D2	897.3164
SCHMITT_1	D3	907.6352
SCHMITT_1	E	921.7904
SCHMITT_1	F	931.7122
SKIFF_1	A	1360.965
SKIFF_1	C	1396.683
SKIFF_1	C0	1399.858
SHOEMAKER_1	A	530.8417
SHOEMAKER_1	A2	537.9854
SHOEMAKER_1	C	589.8967
SHOEMAKER_1	C0	598.284
SHOEMAKER_1	C1	604.981
SHOEMAKER_1	D	617.0844
SHOEMAKER_1	D0	623.6342
SHOEMAKER_1	D1	630.6319
SHOEMAKER_1	D11	641.2289
SHOEMAKER_1	D2	647.1683
SOLOMON_1A	C	1191.01
SOLOMON_1A	C0	1195.257
SOLOMON_1A	C1	1203.939
SOLOMON_1A	D	1209.491
SOLOMON_1A	D0	1216.242

Well name	Coal seam	Depth (m)
SOLOMON_1A	D1	1217.535
SOLOMON_1A	D11	1226.693
SOLOMON_1A	D2	1235.474
SOLOMON_1A	E	1249.456
SOLOMON_1A	F	1268.903
SOLOMON_3	BHCA	501
SOLOMON_3	B0	1195.122
SOLOMON_3	C	1212.752
SOLOMON_3	D	1259.827
SOLOMON_3	D0	1267.973
SOLOMON_3	D1	1276.781
SOLOMON_3	D11	1286.835
SOLOMON_3	D12	1292.488
SOLOMON_3	D13	1298.805
SOLOMON_3	D2	1302.975
SOLOMON_3	E	1313.558
SOLOMON_3	F	1331.043
SPLITTERS_CREEK_1	A	756.394
SPLITTERS_CREEK_1	A2	766.316
SPLITTERS_CREEK_1	B	772.005
SPLITTERS_CREEK_1	C	832.197
SPLITTERS_CREEK_1	D	852.703
SPLITTERS_CREEK_1	D1	862.625
SPLITTERS_CREEK_1	D2	866.726
SPLITTERS_CREEK_1	D3	874.795
SPLITTERS_CREEK_1	E	894.242
SPLITTERS_CREEK_1	F	909.588
STAINBURN_DOWNS_1	C	960.426
STAINBURN_DOWNS_1	D1	986.091
STAINBURN_DOWNS_1	D3	1000.246
STAINBURN_DOWNS_1	E	1016.65
STAINBURN_DOWNS_1	F	1021.667
STAINBURN_DOWNS_1	J2	1049.062
STAINBURN_DOWNS_1	J4	1054.618
STAINBURN_DOWNS_1	K4	1072.874
STAINBURN_DOWNS_1	K5	1082.399
STAINBURN_DOWNS_1	K6	1085.839
STOCKHOLM_1	A2	954.4
STOCKHOLM_1	B1	964.719
STOCKHOLM_1	C	993.823
STOCKHOLM_1	C0	996.866
STOCKHOLM_1	D1	1009.963
STOCKHOLM_1	D2	1016.18
STOCKHOLM_1	D3	1019.884
STOCKHOLM_1	D30	1031.791
STOCKHOLM_1	E	1046.21
STOCKHOLM_1	F	1053.222

Well name	Coal seam	Depth (m)
VERA_PARK_1	C	990.918
VERA_PARK_1	C0	993.0346
VERA_PARK_1	D	996.4742
VERA_PARK_1	D1	1003.883
VERA_PARK_1	D2	1007.587
VERA_PARK_1	D3	1014.334
VERA_PARK_1	E	1025.711
VERA_PARK_1	F	1028.092
VERA_PARK_1	J1	1046.877
VERA_PARK_1	J2	1054.683
VERA_PARK_1	J4	1064.075

Well name	Coal seam	Depth (m)
VERA_PARK_1	K1	1069.499
VERA_PARK_1	K3	1080.215
VERA_PARK_1	K4	1085.771
VERA_PARK_1	K5	1093.631
VERA_PARK_1	AM1	1114.004
VERA_PARK_1	AM2	1118.712
VERA_PARK_1	AM21	1125.194
VERA_PARK_1	AM3	1134.851
VERA_PARK_1	AM4	1142.392
VERA_PARK_1	AM5	1155.146

8.12. Formation picks

Well name	Formation	top depth (m)
ABERFOYLE_1A	Bandanna Formation	1279.627
ABERFOYLE_1A	'Burngrove Formation equivalent'	1325.392
ABERFOYLE_1A	Black Alley Shale	1354.371
ABERFOYLE_1A	'Fair Hill Formation equivalent'	1357.978
ABERFOYLE_1A	'Colinlea Sandstone equivalent'	1389.032
BALLYNEETY_1	Bandanna Formation	826.6859
BALLYNEETY_1	'Burngrove Formation equivalent'	833.421
BALLYNEETY_1	Black Alley Shale	861.732
BALLYNEETY_1	'Fair Hill Formation equivalent'	886.5646
BALLYNEETY_1	'Colinlea Sandstone equivalent'	907.4126
BULLOCK_1	Bandanna Formation	1128.455
BULLOCK_1	'Fort Cooper Coal 'Measures equivalent'	1148.953
BULLOCK_1	Colinlea Sandstone equivalent'	1163.876
CARMICHAEL_1	Bandanna Formation	761.317
CARMICHAEL_1	'Burngrove Formation equivalent'	790.289
CARMICHAEL_1	Black Alley Shale	803.518
CARMICHAEL_1	'Fair Hill Formation equivalent'	822.0152
CARMICHAEL_1	'Colinlea Sandstone equivalent'	865.279
CAROLINA_1	Bandanna Formation	836.07
CAROLINA_1	'Burngrove Formation equivalent'	847.315
CAROLINA_1	Black Alley Shale	888.555
CAROLINA_1	'Fair Hill Formation equivalent'	898.174
CAROLINA_1	'Colinlea Sandstone equivalent'	916.768
CROSSMORE_1	'J' Seams	819.949
CROSSMORE_1	'K' Seams	854.609
CROSSMORE_1	Aramac Coal Measures	911.759
CROSSMORE_SOUTH_1	'Fort Cooper Coal Measures equivalent'	1008.684
CROSSMORE_SOUTH_1	'Colinlea Sandstone equivalent'	1051.15
CROSSMORE_SOUTH_1	'Rodney Creek Sandstone'	1082.199
CROSSMORE_SOUTH_1	'J' Seams	1103.567
CROSSMORE_SOUTH_1	'K 'Seams	1141.108
CROSSMORE_SOUTH_1	Aramac Coal Measures	1195.652
DINGONOSE_14	Rangal Coal Measures	524.871
DINGONOSE_14	Fort Cooper Coal Measures	767.582
DUCKWORTH_11	Rangal Coal Measures	460.61
DUCKWORTH_11	Fort Cooper Coal Measures	626.768
EMERALD_3	Rangal Coal Measures	200.669
EMERALD_3	Burngrove Formation	235.947
EMERALD_3	Black Alley Shale	343.191
EMERALD_3	Fair Hill Formation	396.108
EMERALD_3	MacMillian Formation	521.344
EMERALD_3	German Creek Formation	554.858
FLEETWOOD_1	Bandanna Formation	1038.97
FLEETWOOD_1	'Burngrove Formation equivalent'	1066.222
FLEETWOOD_1	Black Alley Shale	1117.32
FLEETWOOD_1	'Fair Hill Formation equivalent'	1119.471
FLEETWOOD_1	'Colinlea Sandstone equivalent'	1146.465
FLINDERS_RIVER_1	'Fort Cooper Coal Measures equivalent'	874.097
FLINDERS_RIVER_1	'Colinlea Sandstone equivalent'	893.941
GLENARAS_2	Bandanna Formation	866.3703
GLENARAS_2	'Fort Cooper Coal Measures equivalent'	889.5214
GLENARAS_2	'Colinlea Sandstone equivalent'	916.6412
GLENARAS_2	'Rodney Creek Sandstone'	941.037
GLENARAS_2	'J' Seams	956.8578
GLENARAS_2	'K' Seams	978.5537
GLENARAS_2	Aramac Coal Measures	1032.396
GLENARAS_3	Bandanna Formation	871.432
GLENARAS_3	'Fort Cooper Coal Measures equivalent'	894.4507
GLENARAS_3	'Colinlea Sandstone equivalent'	914.9559
GLENARAS_3	'Rodney Creek Sandstone'	940.543
GLENARAS_3	'J' Seams	954.2466
GLENARAS_3	'K' Seams	975.1487
GLENARAS_3	Aramac Coal Measures	1027.933
GLENARAS_4	Bandanna Formation	872.953
GLENARAS_4	'Fort Cooper Coal Measures equivalent'	894.7812
GLENARAS_4	'Colinlea Sandstone equivalent'	917.403
GLENARAS_4	'Rodney Creek Sandstone'	938.756
GLENARAS_4	'J' Seams	957.3551
GLENARAS_4	'K' Seams	977.3312
GLENARAS_4	Aramac Coal Measures	1034.349
GLENARAS_6	Bandanna Formation	868.5609
GLENARAS_6	'Fort Cooper Coal Measures equivalent'	890.6537
GLENARAS_6	'Colinlea Sandstone equivalent'	915.3992
GLENARAS_6	'Rodney Creek Sandstone'	937.407
GLENARAS_6	'J' Seams	951.9047
GLENARAS_6	'K' Seams	973.6005
GLENARAS_6	Aramac Coal Measures	1033.396
GLENARAS_6	Bandanna Formation	869.5372
GLENARAS_6	'Fort Cooper Coal Measures equivalent'	893.6143
GLENARAS_6	'Colinlea Sandstone equivalent'	913.458
GLENARAS_6	'Rodney Creek Sandstone'	938.648

GLENARAS_6	'J' Seams	948.6476
GLENARAS_6	'K' Seams	968.4914
GLENARAS_6	Aramac Coal Measures	1022.466
GLENARAS_7	'Fort Cooper Coal Measures equivalent'	954.611
GLENARAS_7	'Colinlea Sandstone equivalent'	944.8678
GLENARAS_7	'Rodney Creek Sandstone'	1036.765
GLENARAS_7	'J' Seams	1048.578
GLENARAS_7	'K' Seams	1084.032
GLENARAS_7	Aramac Coal Measures	1130.864
GLUE_POT_CREEK_1	Bandanna Formation	617.6368
GLUE_POT_CREEK_1	'Burngrove Formation equivalent'	654.017
GLUE_POT_CREEK_1	Black Alley Shale	711.169
GLUE_POT_CREEK_1	'Fair Hill Formation equivalent'	719.8034
GLUE_POT_CREEK_1	'Colinlea Sandstone equivalent'	729.822
GLUE_POT_CREEK_1	Edie Tuff Member	803.979
GLUE_POT_CREEK_1	Jochmus Formation	835.729
GUNN_1	Bandanna Formation	842.4366
GUNN_1	'Burngrove Formation equivalent'	871.4085
GUNN_1	Black Alley Shale	909.708
GUNN_1	'Fair Hill Formation equivalent'	914.9028
GUNN_1	'Colinlea Sandstone equivalent'	936.989
HERGENROTHER_1	Bandanna Formation	744.1277
HERGENROTHER_1	'Burngrove Formation equivalent'	771.909
HERGENROTHER_1	Black Alley Shale	819.337
HERGENROTHER_1	'Fair Hill Formation equivalent'	826.5157
HERGENROTHER_1	'Colinlea Sandstone equivalent'	840.6381
JERICHO_1	Bandanna Formation	393.962
JERICHO_1	'Burngrove Formation equivalent'	420.156
JERICHO_1	Black Alley Shale	460.505
JERICHO_1	'Fair Hill Formation equivalent'	486.434
JERICHO_1	'Colinlea Sandstone equivalent'	517.919
KANAKA_1	Bandanna Formation	969.123
KANAKA_1	'Burngrove Formation equivalent'	992.0491
KANAKA_1	Black Alley Shale	1013.97
KANAKA_1	'Fair Hill Formation equivalent'	1033.775
KANAKA_1	'Colinlea Sandstone equivalent'	1053.884
KANAKA_1	'Rodney Creek Sandstone'	1095.726
KANAKA_1	'J' Seams	1107.235
KANAKA_1	'K' Seams	1136.075
KANAKA_1	Aramac Coal Measures	1151.99
MONTANI_1	Bandanna Formation	771.415
MONTANI_1	'Burngrove Formation equivalent'	793.0182
MONTANI_1	Black Alley Shale	807.795
MONTANI_1	'Fair Hill Formation equivalent'	814.7686
MONTANI_1	'Colinlea Sandstone equivalent'	853.2125
MOUNT_MYTH_1	Bandanna Formation	1025.357
MOUNT_MYTH_1	'Burngrove Formation equivalent'	1060.719
MOUNT_MYTH_1	Black Alley Shale	1091.371
MOUNT_MYTH_1	'Fair Hill Formation equivalent'	1105.884
MOUNT_MYTH_1	'Colinlea Sandstone equivalent'	1117.339
MOUNT_MYTH_1	'Rodney Creek Sandstone'	1168.232
MOUNT_MYTH_1	'J' Seams	1185.337
MOUNT_MYTH_1	'K' Seams	1209.282
MOUNT_MYTH_1	Aramac Coal Measures	1251.483
MUTTABURRA_1	'Fort Cooper Coal Measures equivalent'	963.59
MUTTABURRA_1	'Colinlea Sandstone equivalent'	988.461
MUTTABURRA_1	'Rodney Creek Sandstone'	1035.425
MUTTABURRA_1	'J' Seams	1041.51
MUTTABURRA_1	'K' Seams	1064.455
MUTTABURRA_1	Aramac Coal Measures	1084.217
MUTTABURRA_1	Jochmus Formation	1212.248
MUTTABURRA_1	Edie Tuff Member	1254.485
MUTTABURRA_2	'Fort Cooper Coal Measures equivalent'	844.527
MUTTABURRA_2	'Colinlea Sandstone equivalent'	906.3465
MUTTABURRA_2	'Rodney Creek Sandstone'	943.613
MUTTABURRA_2	'J' Seams	966.5937
MUTTABURRA_2	'K' Seams	985.6982
MUTTABURRA_2	Aramac Coal Measures	1026.444
MYROSS_1	Bandanna Formation	797.745
MYROSS_1	'Burngrove Formation equivalent'	807.971
MYROSS_1	Black Alley Shale	834.845
MYROSS_1	'Fair Hill Formation equivalent'	863.4557
MYROSS_1	'Colinlea Sandstone equivalent'	880.4668
MYROSS_1	Aramac Coal Measures	990.798
RODNEY_CREEK_1	'Fort Cooper Coal Measures equivalent'	942.8741
RODNEY_CREEK_1	'Colinlea Sandstone equivalent'	987.4564
RODNEY_CREEK_1	'Rodney Creek Sandstone'	1011.059
RODNEY_CREEK_1	'J' Seams	1024.895
RODNEY_CREEK_1	'K' Seams	1056.116
RODNEY_CREEK_1	Aramac Coal Measures	1106.783
RODNEY_CREEK_2	'Fort Cooper Coal Measures equivalent'	919.4562
RODNEY_CREEK_2	'Colinlea Sandstone equivalent'	936.1249
RODNEY_CREEK_2	'Rodney Creek Sandstone'	966.077
RODNEY_CREEK_2	'J' Seams	977.3999
RODNEY_CREEK_2	'K' Seams	1010.473
RODNEY_CREEK_2	Aramac Coal Measures	1046.712

RODNEY_CREEK_4	Bandanna Formation	917.9955
RODNEY_CREEK_4	'Fort Cooper Coal Measures equivalent'	941.1466
RODNEY_CREEK_4	'Colinlea Sandstone equivalent'	958.3445
RODNEY_CREEK_4	'Rodney Creek Sandstone'	989.487
RODNEY_CREEK_4	'J' Seams	1003.588
RODNEY_CREEK_4	'K' Seams	1031.105
RODNEY_CREEK_4	Aramac Coal Measures	1083.492
RODNEY_CREEK_5	Bandanna Formation	907.1608
RODNEY_CREEK_5	'Fort Cooper Coal Measures equivalent'	927.401
RODNEY_CREEK_5	'Colinlea Sandstone equivalent'	946.0545
RODNEY_CREEK_5	'Rodney Creek Sandstone'	979.843
RODNEY_CREEK_5	'J' Seams	992.4889
RODNEY_CREEK_5	'K' Seams	1019.609
RODNEY_CREEK_5	Aramac Coal Measures	1071.202
RODNEY_CREEK_6	Bandanna Formation	923.9074
RODNEY_CREEK_6	'Fort Cooper Coal Measures equivalent'	950.6303
RODNEY_CREEK_6	'Colinlea Sandstone equivalent'	961.2137
RODNEY_CREEK_6	'Rodney Creek Sandstone'	994.738
RODNEY_CREEK_6	'J' Seams	1006.512
RODNEY_CREEK_6	'K' Seams	1034.636
RODNEY_CREEK_6	Aramac Coal Measures	1089.404
RODNEY_CREEK_7	Bandanna Formation	919.8715
RODNEY_CREEK_7	'Fort Cooper Coal Measures equivalent'	945.8007
RODNEY_CREEK_7	'Colinlea Sandstone equivalent'	962.8663
RODNEY_CREEK_7	'Rodney Creek Sandstone'	988.85
RODNEY_CREEK_7	'J' Seams	1000.834
RODNEY_CREEK_7	'K' Seams	1027.16
RODNEY_CREEK_7	Aramac Coal Measures	1078.754
RODNEY_CREEK_8	'Fort Cooper Coal Measures equivalent'	890.7426
RODNEY_CREEK_8	'Colinlea Sandstone equivalent'	912.5707
RODNEY_CREEK_8	'Rodney Creek Sandstone'	940.274
RODNEY_CREEK_8	'J' Seams	959.402
RODNEY_CREEK_8	'K' Seams	984.1405
RODNEY_CREEK_8	Aramac Coal Measures	1041.423
ROLLESTON_1	Bandanna Formation	233.609
ROLLESTON_1	Burngrove Formation	331.681
ROLLESTON_1	Black Alley Shale	422.698
ROLLESTON_1	Fair Hill Formation	546.876
ROLLESTON_1	Peawaddy Formation	591.679
ROLLESTON_1	German Creek Formation	716.562
ROLLESTON_1	Flat Top Formation	732.084
SCHMITT_1	'Fair Hill Formation equivalent'	875.2417
SCHMITT_1	'Colinlea Sandstone equivalent'	892.6862
SHOEMAKER_1	Bandanna Formation	530.8417
SHOEMAKER_1	'Burngrove Formation equivalent'	541.137
SHOEMAKER_1	'Fair Hill Formation equivalent'	589.284
SHOEMAKER_1	'Colinlea Sandstone equivalent'	617.0844
SKIFF_1	Bandanna Formation	1360.965
SKIFF_1	'Fort Cooper Coal Measures equivalent'	1383.19
SOLOMON_1A	'Fort Cooper Coal Measures equivalent'	1191.01
SOLOMON_1A	'Colinlea Sandstone equivalent'	1209.491
SOLOMON_3	'Fort Cooper Coal Measures equivalent'	1195.122
SOLOMON_3	'Colinlea Sandstone equivalent'	1259.827
SPLITTERS_CREEK_1	Bandanna Formation	756.394
SPLITTERS_CREEK_1	'Burngrove Formation equivalent'	772.005
SPLITTERS_CREEK_1	Black Alley Shale	818.996
SPLITTERS_CREEK_1	'Fair Hill Formation equivalent'	832.197
SPLITTERS_CREEK_1	'Colinlea Sandstone equivalent'	852.703
SPRINGSURE_11	Bandanna Formation	7.075
SPRINGSURE_11	'Burngrove Formation equivalent'	70.45
SPRINGSURE_11	Black Alley Shale	181.303
SPRINGSURE_11	'Fair Hill Formation equivalent'	212.656
SPRINGSURE_11	Peawaddy Formation	257.238
SPRINGSURE_11	Catherine Sandstone	271.526
SPRINGSURE_11	Ingelara Formation	307.112
SPRINGSURE_11	Freitag Formation	377.227
SPRINGSURE_11	upper Aldebaran Sandstone	426.307
STAINBURN_DOWNS_1	'Fort Cooper Coal Measures equivalent'	927.959
STAINBURN_DOWNS_1	'Colinlea Sandstone equivalent'	986.091
STAINBURN_DOWNS_1	'Rodney Creek Sandstone'	1026.649
STAINBURN_DOWNS_1	'J' Seams	1049.062
STAINBURN_DOWNS_1	'K' Seams	1072.874
STOCKHOLM_1	Bandanna Formation	954.4
STOCKHOLM_1	'Burngrove Formation equivalent'	964.719
STOCKHOLM_1	Black Alley Shale	975.519
STOCKHOLM_1	'Fair Hill Formation equivalent'	933.823
STOCKHOLM_1	'Colinlea Sandstone equivalent'	1009.963
TAMBO_1-1A	Bandanna Formation	701.5
TAMBO_1-1A	'Burngrove Formation equivalent'	728.65
TAMBO_1-1A	Black Alley Shale	773.1
TAMBO_1-1A	Peawaddy Formation	830.41
TAMBO_1-1A	Catherine Sandstone	850.49
TAMBO_1-1A	Ingelara Formation	870.64
TAMBO_1-1A	Freitag Formation	885.74
TAMBO_3	Bandanna Formation	54.832
TAMBO_3	'Burngrove Formation equivalent'	88.17
TAMBO_3	Black Alley Shale	137.779

TAMBO_3	'Fair Hill Formation equivalent'	160.798
TAMBO_3	'Colinlea Sandstone equivalent'	183.287
TAMBO_3	Catherine Sandstone	224.033
TAMBO_3	Ingelara Formation	250.492
TAMBO_3	Freitag Formation	253.42
TAMBO_3	upper Aldebaran Sandstone	296.264
VERA_PARK_1	'Fort Cooper Coal Measures equivalent'	975.494
VERA_PARK_1	'Colinlea Sandstone equivalent'	996.4742
VERA_PARK_1	'Rodney Creek Sandstone'	1033.967
VERA_PARK_1	'J' Seams	1046.877
VERA_PARK_1	'K' Seams	1069.499
VERA_PARK_1	Aramac Coal Measures	1114.004
WARRINILLA_NORTH	Bandanna Formation	630.255
WARRINILLA_NORTH	Burngrove Formation	748.524
WARRINILLA_NORTH	Black Alley Shale	795.355
WARRINILLA_NORTH	Fair Hill Formation	893.78
WARRINILLA_NORTH	Peawaddy Formation	941.14
WARRINILLA_NORTH	Catherine Sandstone	1015.224
WYUNA_1	Rangal Coal Measures	230.899
WYUNA_1	Burngrove Formation	302.16
WYUNA_1	Black Alley Shale	407.993
WYUNA_1	Fair Hill Formation	467.613
WYUNA_1	MacMillian Formation	599.904
WYUNA_1	German Creek Formation	633.418
YAMALA_2	Bandanna Formation	197.941
YAMALA_2	Burngrove Formation	247.683
YAMALA_2	Black Alley Shale	369.744
YAMALA_2	Fair Hill Formation	428.305
YAMALA_2	MacMillian Formation	503.094
YAMALA_2	German Creek Formation	540.136
YAMALA_2	Flat Top Formation	649.144
ZEROGEN_1	Bandanna Formation	347.811
ZEROGEN_1	Burngrove Formation	495.272
ZEROGEN_1	Black Alley Shale	546.072
ZEROGEN_1	Fair Hill Formation	624.389
ZEROGEN_1	Peawaddy Formation	733.75
ZEROGEN_1	German Creek Formation	748.92
ZEROGEN_1	Flat Top Formation	777.142